INFLUENCE OF SURFACE TOPOGRAPHY AND CURING CHEMISTRY ON FOULING-RELEASE PERFORMANCE OF SELF-STRATIFIED SILOXANE-POLYURETHANE COATINGS

A Dissertation
Submitted to the Graduate Faculty
of the
North Dakota State University
of Agriculture and Applied Science

By

Madhura Mangesh Pade

In Partial Fulfillment of the Requirements
for the Degree of
DOCTOR OF PHILOSOPHY

Major Department:
Coatings and Polymeric Materials

December 2017

Fargo, North Dakota

North Dakota State University
Graduate School

Title

INFLUENCE OF SURFACE TOPOGRAPHY AND CURING CHEMISTRY ON FOULING-RELEASE PERFORMANCE OF SELF-STRATIFIED SILOXANE-POLYURETHANE COATINGS

By

Madhura Mangesh Pade

The Supervisory Committee certifies that this ***disquisition*** complies with North Dakota State University's regulations and meets the accepted standards for the degree of

DOCTOR OF PHILOSOPHY

SUPERVISORY COMMITTEE:

Dr. Dean Webster
Chair

Dr. Andriy Voronov

Dr. Mohiuddin Quadir

Dr. Kalpana Katti

Approved:

12/05/2017
Date

Dr. Dean Webster
Department Chair

ABSTRACT

Biofouling, the attachment and growth of microorganisms and aquatic animals on submerged surfaces, poses many economic and environmental challenges like increase in frictional drag, fuel consumption, and cost of maintenance of ships. Coatings containing harmful biocides, called anti-fouling (AF) coatings, are used to combat fouling. But, the biocides proved toxic to the aquatic environment, which led to replacement of AF coatings by non-toxic fouling-release (FR) coatings. FR coatings do not contain toxic biocides and allow formation of a weak bond between the surface and the organisms, which can be easily broken through light grooming or hydrodynamic forces. Current research is aimed at developing robust coatings that can exhibit similar or superior FR performance as compared to commercial FR coatings.

Previously, self-stratified FR coating systems were developed using siloxane and polyurethane (SiPU) in the Webster research group. Although the SiPU coatings exhibited comparable FR performance to the commercial standards, previous experiments did not show effect of surface grooming or cleaning on the FR performance. In the first part of the work, an SiPU formulation was abraded using two different Scotch Brite pads with varying roughness. Surface analysis experiments showed retention of hydrophobicity even after abrasions. The abraded coatings were characterized for FR performance against common fouling organisms. Improvement in FR performance of the abraded coatings compared to the smooth SiPU coating and the commercial standards against macrofoulants, like barnacles, was attributed to dimensions of the features formed on the coatings after abrasions.

Recent concerns regarding hazards associated with using isocyanates to make polyurethanes necessitated the need to find “safer” alternatives in FR marine applications. Therefore, novel isocyanate-free glycidyl carbamate (GC) technologies were explored as potential substitutes for regular polyurethanes to make FR marine coatings. GC resins were modified using siloxanes and polyethylene glycols to make hydrophobic and amphiphilic coatings with varying surface chemistries. The resultant coatings were characterized for mechanical properties, thermal behavior, and finally, FR performance against common fouling organisms. Although GC coatings showed subpar overall FR performance as compared to the commercial standards, GC technologies show potential for use in marine applications.

ACKNOWLEDGMENTS

I am extremely grateful for everyone who, directly or indirectly, encouraged and motivated me to pursue my goals. I cannot thank you enough for your support.

First and foremost, I would like to thank my advisor, Dr. Dean Webster, for guiding me through graduate studies at NDSU. I feel privileged to have been your student for the past 5 years. Thank you for including me and making me feel at home in your research group. Your scientific insights, creative ideas, and encouragement have helped me become the scientist I always wished to be. I wish you luck for your future endeavors and look forward to a chance to work with you again.

To my present and past Ph.D. committee members, Dr. Andriy Voronov, Dr. Kalpana Katti, Dr. Mohiuddin Quadir, and Dr. Andrew Mara, I am thankful for your inputs and patience the past 5 years. I feel lucky to have professors like you, who shared their immense knowledge and experience with us. I will always remember and utilize those lessons in my professional life.

To my parents and my grandparents, none of this would have been possible without your love, support, and encouragement. Thank you for allowing your only child to move thousands of miles away from home to pursue her dreams. You have taught me the importance of hard work and determination and provided me with unforgettable personal and professional advice. To my best friends, who are like family, thank you for celebrating my achievements with me and patiently listening to my complaints, even when I was half way across the globe.

To Dr. Teluka Galhenage, thank you for welcoming me into Lab 228, helping me overcome initial research roadblocks and being a great lab partner for 4 years. To Dr. Teluka Galhenage, Alison Rohly, Dr. Arvin Yu, Eric Krall, Jackson Benda, Ryan Burgett, Raul Setien, and AliReza Rahimi, I am so grateful to have found friends like you. I have thoroughly enjoyed our conversations and banter about everything, from science to politics to culture to TV shows/Harry Potter movie marathons. I will surely miss our group lunch sessions at all-you-can-eat Indian/Chinese/Japanese buffets, random potlucks, summer grill-out picnics at Island Park. It was a pleasure exploring new places and cultures and sharing travel stories and experiences from domestic and international conferences with all of you. I have wonderful memories of our time together and I will take up every chance I get to work with you again. To the undergraduates, Dylan Hoffman, Augusto Moreira, Jackson Benda, Ryan Burgett, and SURE students, Kunyu Zheng and

Dat Nguyen, thank you for your assistance and contribution in my research. I am confident you will make amazing researchers and I wish you luck for the future.

To James Bahr, Shane Stafslien, Lyndsi Vanderwal, Gregory Strommen, Chunju Gu, Scott Payne, Jayma Moore, Justin Daniels, Justin Hoey, and Heidi Docktor, thank you for all your help and patience with testing samples, operating characterization equipments or training students to use the equipments. To our collaborators at Newcastle University, UK, Dr. John Finlay and Dr. Tony Clare, thank you for conducting fouling-release tests with our samples. To Janice Hanson, Lynn Stadum, Katherine Backen-Andersen, Jacinda Wollan, and Carol, thank you for taking care of the overwhelming administrative work for me. Further, I would like to thank the Office of Naval Research for providing us with financial support to conduct research at NDSU. Lastly, I am grateful to receive awards, scholarships, and travel grants from The Society for Protective Coatings (SSPC), American Coatings Association (ACA), and NDSU College of Science and Mathematics throughout my graduate career at NDSU.

DEDICATION

I would like to dedicate this dissertation to my parents, Mrs. Aarti M. Pade and Mr. Mangesh D. Pade, and my grandparents, late Mrs. Jayashree S. Mate and Mr. Shridhar V. Mate. I am eternally grateful for your love, trust, support, and encouragement that motivated me to achieve my goals.

TABLE OF CONTENTS

LIST OF TABLES

LIST OF FIGURES

CHAPTER 1. INTRODUCTION TO MARINE BIOFOULING

Marine Biofouling— Process and Impact

Marine biofouling, or simply biofouling, is the dynamic process of settlement, attachment, growth, and eventual metamorphosis of aquatic organisms like algae, barnacles, and tubeworms on surfaces submerged in natural water bodies.[1] Biofouling is an inevitable, typically fast, and extremely complex phenomenon.[2] Over 4000 different marine organisms have been identified as fouling organisms, all exhibiting different attachment mechanisms.[3] As soon as a material surface is immersed in water, a conditioning layer is formed on the surface due to adsorption of organic molecules like proteins and polysaccharides.[1] The extent of formation of the conditioning layer depends on the type and colonization, adhesion mechanism, availability of nutrients, and ability of the species to explore the underlying surface.[2] Unicellular organisms like bacteria attach onto the surface through electrostatic and then covalent interactions.[4] Then, soft foulants like diatoms and microalgae settle onto the surface forming biofilms.[3] Finally, the biofilm provides nutrients that attract macrofoulants like barnacles and mussels, leading to their attachment and growth onto the substrates.[1, 3, 5] Although biofouling can be explained in four main stages, the dynamic nature of the process allows attachment of hard foulants onto the surfaces as soon as the substrate is immersed in water.[2, 3]

Biofouling is extremely disadvantageous for marine ships and vessels. Attachment of marine organisms on ship hulls increases the roughness of the surface.[2] Roughening of the hulls in turn increases the frictional drag, while making movement of the ships difficult.[6] Damage to the underlying hull surfaces increases the rate of corrosion of the ship hulls.[4] More fuel is required to increase or maintain top speed and range of the vessels.[2] Higher fuel consumption may increase emission of greenhouse gases, increasing pollution.[2] Moreover, the aquatic species attached to the surface move to a non-native environment with the moving vessel.[2] This transfer of aquatic animals to unfamiliar and unsuitable zones leads to an imbalance in the biodiversity of the aquatic culture.[1, 2] Not just structurally and environmentally, economic impact of biofouling cannot be ignored either. For example, based on the type of marine coatings, the current hull cleaning practices and the level of fouling, the estimated overall cost of cleaning ship hulls of the Arleigh Burke DDG-51 destroyers (30% of the ships in the US Navy fleet) is ~$56 million US dollars annually.[2, 7] For the entire naval fleet, the costs can increase up to ~$220 million

per year.[7] Complexity of the biofouling phenomenon makes it difficult to identify a single practical solution to combat attachment of aquatic species.

Combating Biofouling

Historically, lead, tar, wax, asphalt and copper were used to prevent fouling on ship hulls, which were typically made of wood.[1, 3] Eventually, the wood substrates were replaced with iron. Iron surfaces were covered in copper or lead sheathing as antifouling layers.[1] Accelerated deterioration of the ship hulls due to corrosion necessitated a requirement for more practical technologies.[1] The efforts to find replacements for lead sheathings led to the introduction of antifouling (AF) coatings.

Initially, AF coatings contained toxins, called biocides, dispersed in binders such as linseed oil or rosin.[1, 8] Since the 1960s, more sophisticated AF coating systems have been developed. Tributyltin (TBT) was determined to be an effective biocide, which was widely used self-polishing AF paints. TBT was bound to polymeric binders *via* ester linkages.[3, 8] Upon immersion in water, hydrolysis of esters led to release of the biocide into water.[9] As the organisms approached the substrate, the toxic TBT completely stopped the attachment of the organisms by killing them, which in turn proved the TBT based AF coatings to be highly effective in combating biofouling.[3, 9] Although effective in preventing biofouling, the biocidal leachates posed a threat to non-target organisms like oysters, fishes, and ducks.[1, 10] High fat solubility of TBT leads to penetration of toxins into cell membranes, causing accumulation of toxins, disruption of cellular functions and mutation.[10] Therefore, use of TBT was banned in 2003 and the use of TBT AF paints was completely stopped by 2008.[2, 10] Apart from TBT, research was conducted to explore AF coatings containing copper oxide biocides.[8, 10] Accumulation of copper oxide may not be as detrimental as TBT, but the long-term effects of copper cannot be overlooked.[3] In general, leaching of biocides have detrimental effects on ecosystems. Extensive testing and research is required to find biocides that can be used to make AF coatings. Therefore, newer non-toxic fouling-release coatings have been introduced as replacement for the toxic AF coatings.

Non-Toxic Fouling-Release Marine Coatings

Fouling-release (FR) coatings were first introduced in the 1970s.[1, 8] But, initial results with FR coatings indicated subpar performance of the coatings as compared to the TBT AF coatings.[1, 5, 8] Since the 2000s, research to develop novel FR coatings, that reduce interactions between the surface and the

organism, has gained momentum.[8] FR coatings are made using low surface energy, “slippery” materials and do not contain toxic biocides.[3, 5] “Slippery” nature of the coatings causes the fouling organism to slip from the surface.[1, 3] FR coatings may also allow the organism to attach to the coating, but hydrodynamic forces can easily overcome the weak interactions between the organisms and the surface.[2] Generally, FR coatings are made using low surface energy and low modulus materials.[11] Fracture mechanics showed that the combination of low surface energy and low modulus facilitated release of the foulants from the surface.[12] Low surface energy of the coatings will minimize interfacial bond between the foulants and the surface.[13] Further, materials with low modulus values contain “mobile” chains in the bulk, that disallow bioadhesives from sticking onto the surface, thereby, reducing attachment.[11-13] Baier showed that materials with surface energy values between 20-30 mN/m are recommended for minimal bioadhesion.[13, 14]

(a) (b)

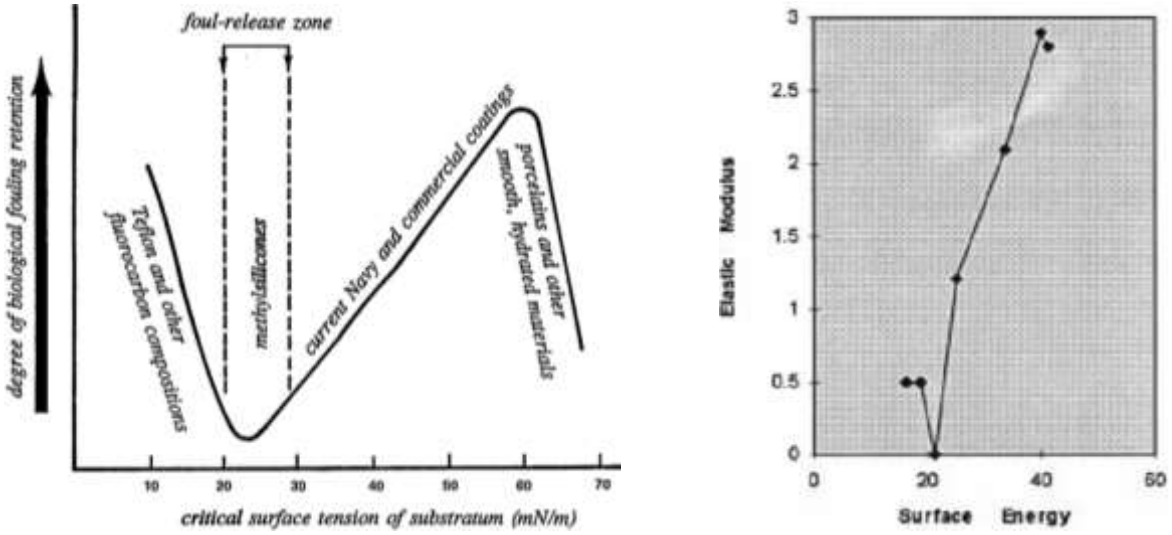

Figure 1.1. (a) The Baier curve, which shows the relationship between surface free energy and attachment of fouling (reproduced from Baier, **2006**).[14] (b) Relationship between surface free energy and elastic modulus of the surface (reproduced from Brady, **1999**).[13]

Commercially available FR coatings are typically based on polydimethylsiloxane (PDMS), which possesses surface tension of ~22 mN/m and modulus of ~5 MPa.[12, 13] One of the biggest advantages of PDMS is its non-toxic nature. Moreover, flexibility of Si-O bonds in PDMS, familiar curing chemistry, and stability makes it favorable for use in marine applications.[13] However, PDMS elastomers are more expensive compared to the previously developed marine paints. PDMS is susceptible to damage due to

its low modulus and low strength. Although useful for removal of foulants, non-wetting nature of PDMS makes adhesion of PDMS onto substrates difficult. Even if a tie coat is applied prior to application of PDMS, adhesion of PDMS to the tie coat may not be ideal for practical applications. The disadvantages of elastomeric PDMS based coatings led to further research to make tougher, more viable coatings for long term use in marine applications.

Self-Stratified Siloxane-Polyurethane FR Coatings

In an attempt to overcome the shortcomings of the commercial FR coatings, a novel one-pot siloxane-polyurethane (SiPU) coating system was developed at NDSU.[15-18] The hybrid SiPU system comprised of an acrylic polyol, polyisocyanate, amine terminated PDMS, catalyst, and a pot-life extender into a single coating system.[17-20] Incompatibility of PDMS with PU and surface energy minimization leads to stratification of PDMS to form the outer surface layer.[17, 20] The outer PDMS layer imparts FR properties to the coatings, while the underlying PU matrix provides the required strength and adhesion to substrates. Moreover, the crosslinking of functional PDMS into the PU matrix increases the stability and the durability of PDMS in marine environment.

Over the years, the self-stratified SiPU system has been optimized using combinatorial methods, involving different isocyanates, polyols, and siloxanes.[16, 19, 21-25] Previous laboratory experiments and field tests have shown the SiPU systems show comparable performance to the commercial standards.[16] Versatility of the SiPU coating system allows tuning of coating formulations as per requirements.[16, 18, 21, 26] The formulation flexibility of the SiPU system also facilitates modification of FR coatings to further enhance their FR performance. Over the years, focus has shifted towards developing methods to improve performance of FR coatings by tuning their surface chemistries. Among them, zwitterionic, amphiphilic, and bio-inspired FR coatings show promise to be used as viable FR coatings.

Surface Wetting

Difference in interfacial energies of a wetting liquid and a surface determines the extent of "wetting" of the surface by the liquid.[27] Upon contact with the surface, the liquid contact angle can be greater than or less than 90°. The extent of wetting is dependent on the chemical composition and the topography of the surface. A hydrophobic surface is characterized by a water contact angle > 90°, while angle < 90° indicates presence of a hydrophilic surface.[27] Increasing concentrations of hydrophobic

(hydrophilic) components on the surface increases hydrophobicity (hydrophilicity) of the surface. Apart from changing composition of the surfaces, increasing surfaces roughness enhances hydrophobic or hydrophilic character of the surfaces.[27] Introducing “textures” or features on the surfaces increases surface area, potentially increasing points of contact between the surface and the liquid.[27] Upon contact with a rough surface, the wetting liquid can show either Cassie Baxter or Wenzel wetting state (Figure 1.2).[28-32] In Cassie Baxter wetting state, liquid droplets remain suspended on top of the surface features due to presence of air pockets between the surface features.[28, 31] When the surface is tilted, the droplet rolls off of the surface, collecting dirt and surface impurities in the direction of flow.[27] On the other hand, in Wenzel state, the droplet penetrates the grooves, increasing contact between the liquid and the underlying substrate.[30, 32] Upon tilting, the droplet can either remain stationary or pass through the grooves.[27] In the direction of flow, each liquid droplet shows advancing contact angle and receding contact angle.[27] The difference between the two contact angles is called contact angle hysteresis (CAH). Rough hydrophobic surfaces, like Lotus leaf, typically show Cassie Baxter wetting state upon contact with water. CAH is extremely low due to similar advancing and receding water contact angles.[27] On the other hand, higher interactions between water droplets and hydrophobic surfaces during Wenzel wetting state result in higher CAH.[27] Wetting states of surfaces can be tuned per requirement. Yoshimitsu et al. showed that surfaces with higher actual surface roughness as compared to apparent surface area tended to show Wenzel wetting state.[27, 33] With increasing apparent area of the surfaces, the substrate transitioned from Wenzel to Cassie Baxter state.[33] Quéré et al. showed that area of substrate exposed to the wetting liquid also affects the wetting state of the surface— above a critical minimum area of exposure, Wenzel state was found to be thermodynamically stable.[34-36] Wetting states of substrates are believed to be reversible— slight increase in pressure with Cassie Baxter state causes transition to Wenzel state, while evaporation of liquid in Wenzel state increases tendency to form Cassie Baxter wetting state.[34, 35] In terms of bioadhesive attachment, Baier showed that more than the wetting state, CAH played an important role understanding FR behavior of surfaces; coatings with low CAH showed better FR properties.[27, 37, 38] Presence of air pockets on microtextured hydrophobic coating surface in Cassie Baxter wetting state imparts non-wetting character to the coating.[27] The non-wetting surface is believed to disallow spreading and adhesion of bioadhesives on the coatings, reducing attachment of foulants.[27] But, synthetic coatings

cannot retain or replenish air pockets over lifetime of the coating. Therefore, maintenance of the metastable Cassie Baxter wetting state is a big challenge in developing non-wetting surfaces in practical applications.

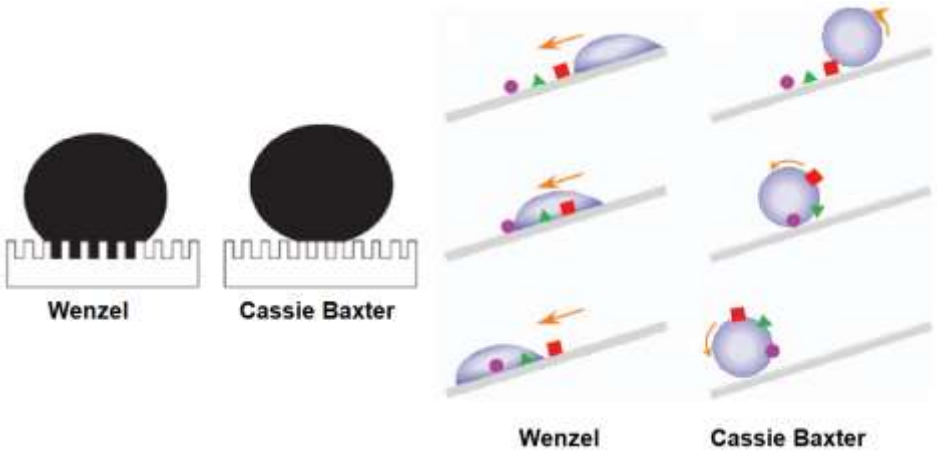

Figure 1.2. Left— Wenzel and Cassie Baxter wetting states (reproduced from Erbil et al., **2009**).[29] Right— Rolling of droplets in Wenzel and Cassie Baxter states when the surfaces are tilted (reproduced from Genzer et al., **2006**).[27]

Biomimetic Approaches for FR coatings

One of the biggest challenges in designing the optimum FR coating is the different attachment mechanism of the different fouling organisms.[2] Therefore, studying the surface chemistry alone is not sufficient to accurately identify coatings that can provide protection from all foulants. The phenomenon of biofouling is evident not only on submerged artificial surfaces, but also natural bodies of aquatic plants and animals.[39] Aquatic organisms have defense mechanisms that provide protection against attachment of fouling organisms.[39] For example, aquatic organisms like lotus leaves, corals, whales, and sharks exhibit inherent resistance to fouling due to the presence of hierarchical features on the outer layers of their skins, secretion of oils and self-replenishing skin layers.[39, 40] For naturally occurring surfaces, FR properties of the surfaces are a combination of physical, chemical, and mechanical attributes of the organisms. With such natural surfaces as inspiration, attempts have been made to incorporate these natural defense mechanisms into synthetic systems.

Biomimetic coatings with hierarchical microtopographies, similar to Lotus leaves and shark skin, have been widely studied to promote FR behavior of synthetic surfaces. Lotus leaves are made of waxy, slippery outer surface with nano-sized surface gradients.[39, 41] Water contact angle value of greater than

150° indicates superhydrophobic nature of the surfaces. Lotus leaves maintain Cassie Baxter wetting state due to presence of hierarchically arranged microtopographies on waxy surfaces.[27, 39, 42, 43] In nature, a Lotus leaf can self-replenish its waxy surface and self-heal whenever the surface is damaged.[42] This natural mechanism also allows air pockets on the leaf to be naturally regenerated.[39] Similar to the Lotus leaf, biomimetic/bioinspired coatings can be based on rice leaves and butterfly wings— surfaces of rice leaves are made of sinusoidal grooves and hierarchically arranged waxy fibrils and bumps that impart non-wetting character to the leaves.[44, 45] Similarly, wings made of roof shingle like scales with microgrooves impart water repellency and FR behavior to butterflies.[44, 45] Apart from Lotus leaves and butterflies, periostracum of blue mussels shows presence of regular, parallel 1-1.5 mm wide ripples, placed ~1-2 mm apart, significantly reduces settlement of barnacle larvae.[46] But the mussel-like topography did not show any particular effect on attachment of other foulants.[46] Efficiency of the surface disappears when the ripple-like microtopography is destroyed by damage or erosion.[46, 47] Therefore, the scale of this microtopography is substantially smaller than the artificial microtopographies tested so far.. Evenly distributed 200 mm diameter circular elevations on the carapace of crabs possess small, 2-2.5 mm long spicule-like structures between the elevations.[46, 48] Further, egg cases show presence of longitudinal ridges, with varying sizes and irregular spacing between 15-115 mm.[39, 46] Surface topographies on crabs and egg cases can successfully deter hard foulants like barnacles and microorganisms respectively.[46] Apart from ridges and ripples, surface of brittle star shows evenly distributed knob-like structures, 10 mm in diameter.[46]

Shark skin is another natural surface that shows excellent FR properties. FR behavior of the skin is attributed to presence of rib-like microstructures (~4 mm high, 4-16 mm in length, and ~2 mm wide).[39] Potential of making effective biomimetic FR surfaces inspired development of the Sharklet AF™ coatings by Hoipkemeier-Wilson et al. in 2005.[39, 49-51] Hierarchically arranged micro-sized ribs with different dimensions were introduced onto PDMS substrates.[50-53] FR performance of the Sharklet AF™ samples against *U.linza* spores showed that coatings with 3 µm high ribs spaced 2 µm apart reduced settlement of algal spores by 63%, while rib height of 40 µm spaced 20 µm apart resulted in 97% reduction in barnacle cyprid attachment.[52, 54] Apart from ribs, topographies such as pillars, channels, ridges, pits, and "honeycomb" textures have also been studied to develop potential "textured" FR surfaces. As compared

to rib-like Sharklet AF™ coatings, surfaces with ridges showed significant increase in spore settlement as compared to smooth surfaces.[39, 52] Schumacher et al. superimposed the optimum FR surface patterns for different organisms (barnacle cyprids— 40 µm high, 20 µm wide and microalgae— 3 µm high, 2 µm wide) on the same substrate.[53] Results obtained from the study showed that the barnacle cyprid attachment was successfully reduced due to presence of barnacle resistant topography.[39] But, the barnacle-specific pattern provided a conducive growth environment to the *Ulva* spores, despite the presence of the algal-specific pattern on the same surface.[54, 55] The results thus obtained showed that laboratory experiments are not sufficient to correctly identify the optimum FR topography. Performance of "textured" coatings in field applications is a synergistic effect of multiple "texture" patterns with different sizes and shapes, along with colonization of the organisms in the aquatic environment.[56, 57] Efimenko et al. attempted to study the durability and the efficiency of hierarchically textured coatings in field applications. Uniaxial strain was applied to PDMS substrates to create patterned surfaces.[58, 59] Field immersion studies with the uniaxially strained coatings showed that the strained coatings remained clean even after 1 year of immersion.[58] Any settlement that did occur could be easily removed from the surface of the coatings. The patterned surfaces successfully deterred barnacle attachment for 1 year after immersion.[58] But, the coatings were unsuccessful in reducing attachment of *U.linza* spores.[58] Settlement of algal spores was also studied on "honeycomb" textured surfaces made by hot embossing honeycomb structure onto poly(methyl methacrylate) surfaces.[60] Honeycomb with sizes less 2 µm showed significantly lower settlement of *U.linza* spores.[60] Barnacles of have shown tendency to preferentially settle in grooves of 1-10 mm in complex substrata and at the base of surface topographies of 3 mm height.[61, 62] Hills et al. showed that some barnacle cyprids responded to fine surface textures with 0.5–2 mm scale.[56, 63] Preferential settlement of organisms has been attributed to the need for refuge from shear forces that may be encountered during flow.[46] Mesh structures in the range 1–100 mm and riblets (30-45 mm high) significantly deter barnacle settlement.[64-66] Le Tourneux et al. proposed that roughness elements below 35 mm may interfere with the size of the barnacle antennules (40 mm), thereby preventing attachment of the antennular disc.[67] Unstable attachment of the barnacle causes the barnacle to avoid such textured surfaces.[67] Laboratory experiments showed that attachment of marine organisms was dependent on the size of the surface "textures". Since then, engineering models have been developed to better understand

the attachment behavior of the organisms on “textured” surfaces. Attachment point theory was developed to understand the effect of number of contact points between the organism and the surface on the FR performance.[54, 68-70] According to this theory, FR organisms can be easily deterred from attaching onto the surfaces if non-equilibrium is created in the organism by reducing the number of attachment points between the organism and the substrate. [68, 71] FR performance against *U.linza* spores showed that the spores did not attach onto surfaces with gradients less than the size of the organism.[68] Stresses generated within the organism due to lack of sufficient contact points on biomimetic surfaces forces the organism to explore other surfaces for attachment.[68] Engineered Roughness Index (ERI) was introduced to determine the effect of feature size, geometry, and wetting behavior of coatings on FR performance of the substrate.[51, 53, 72, 73] ERI is a dimensionless quantity that correlates Wenzel’s roughness factor with the degrees of freedom of movement and fraction of depressed surface.[53] According to ERI theory, continuous recessed grooves or channels tend to foul faster than isolated ridges, since degree of freedom is comparatively higher in case of a continuous network.[53, 74] Furthermore, similar to Wenzel wetting state, if the foulant can penetrate the microtextures, FR performance of the surface is significantly reduced.[52] As an improvement to ERI, a second generation ERI model, ERI_{II} model, was introduced, which correlated the attachment behavior of foulants with the ERI and the Reynolds number of the foulant.[75] The ERI_{II} model showed that attachment of microfoulants was a function of ERI (as determined from surface energy) x the Reynolds number of the organism.[75] Another theory, the surface energetic attachment (SEA) model, combines concepts of both the attachment point theory and the ERI. SEA model provides a good estimation of fouling attachment with respect to the number of attachment points, size, geometry and wetting state of the surface topography.[2, 72, 76] If the size of the feature is larger than the organism, the organism can insert itself between the features, exhibiting Wenzel wetting state.[76] But, topographies smaller than the organism create a non-wetting Cassie Baxter surface, reducing interactions between the surface and the organism and facilitating FR behavior. Brennan et al. showed that not only in the settling stage, but even in the larval stage of the organism, if the size of the features is less than the size of antennules that explore the surface, the coatings can successfully deter biofouling.[50, 51]

Further inspiration was drawn from whales, corals, and butterflies to make bioinspired FR systems. Whale skin-inspired coatings were made using polyelectrolytes, polyacrylic acid and

polyethylenimine through layer-by-layer assembly.[77] Changes in pH resulted in formation of textures, similar to whale skin, on the polyelectrolytes rich surfaces. FR performance against *U.linza* spores showed that feature size of 2 µm successfully reduced settlement of the spores. This study also further supported the hypothesis that FR performance is indeed dependent on size, roughness, and arrangement of surface features. FR behavior of aquatic organisms like corals and molluscs is attributed to presence of elastic and mobile hair-like fibrils called cilia.[39, 78, 79] Mobility of cilia also allows repulsion of the particles from the surfaces, reducing adhesion of organisms on the surface.[80, 81] Simulations have been made based on cilia to understand the possibility of using cilia-like surfaces in FR applications. Effectiveness of cilia is dependent on stimuli responsive nature of cilia and the movement of the fibrils.[82] So, for practical applications, developing surfaces that not only respond to stimulus, but also remain durable during use poses a big challenge.[39, 40] Epstein et al. developed pitcher plant-inspired slippery liquid infused surfaces (SLIPS) as non-toxic FR surfaces.[83]

Biomimetic and bioinspired surfaces provide promising strategies in development of non-toxic FR surfaces. Although lucrative, it is difficult to accurately predict FR performance of biomimetic/bioinspired coatings in practical applications due to different attachment behavior of target organisms and inability of the coatings to maintain their biomimetic characteristics.[27, 76, 84] For example, regeneration of slippery synthetic surfaces or maintenance of superhydrophobic character like Lotus leaf on synthetic coatings poses a big challenge. Wetting behavior of the surfaces is also extremely susceptible to environmental changes; slight increase in pressure can cause easy transition from non-wetting Cassie Baxter to Wenzel wetting state. Furthermore, complications in fabricating low cost, “textured” surfaces for large scale commercial use may not always possible.

Amphiphilic Coatings

Till date, thousands of fouling organisms have been identified that show different attachment behavior.[2, 3] For example, barnacles and mussels show affinity to hydrophilic surfaces, but can be easily removed from PDMS rich surfaces.[17, 85, 86] Conversely, diatoms *N.incerta* attach strongly onto hydrophobic coatings, but show weak adhesion to hydrophilic surfaces like polyethylene glycol (PEG).[87-89] Therefore, complex nature of adhesion processes of the different marine organisms has led to further research into developing viable “ambiguous” coatings containing hydrophobic and hydrophilic phases in the same

system.[2] The process of adhesion begins with release and spreading of proteinaceous adhesives on the surfaces.[1] Hydrophilic PEG chains have shown tendency to repel proteins and adhesives through hydrophilic interactions.[87] PEG chains bind water molecules to the chains through hydrogen bonding.[90] The bound water molecules form a hydration layer, which cannot be displaced by the incoming protein molecules.[90] Apart from that, presence of hydrophobic component in such amphiphilic coatings provides slippery character to the surfaces, reducing attachment of the organisms. Repulsion of proteins and release of foulants occur due to thermodynamic and kinetic instability caused due to surface ambiguity in the amphiphilic coatings.[2, 90] Combination of PDMS or fluoropolymers with PEG in an amphiphilic coating system is expected to reduce hydrogen bonding of organisms and increase repulsion of proteins and adhesives.[2, 91]

Previously, efforts have been made to design heterogeneous FR marine coatings through phase separation of polymer chains during or after crosslinking of the coatings.[2] Such heterogeneous coatings typically contain immiscible block polymers of opposite polarities in the coatings.[2] The first amphiphilic marine coating, based on self-assembly of hyperbranched fluoropolymers (HBFP) and PEG, was developed by Gudipati et al.[2, 88, 91] Gudipati et al. showed that adsorption of proteins and polysaccharides was reduced with 45-55% by weight PEG chains in the formulations.[88] Exposure of the HBFP-PEG coatings to aqueous environment caused swelling of PEG, leading to formation of heterogenous surfaces.[91] Furthermore, tunability of these coatings allowed convenient alteration of coating compositions with HBFP-PEG to successfully lower barnacle cyprid attachment and increase diatom removal compared to regular PDMS substrates.[92] Since then, different approaches involving amphiphilic prepolymers, amphiphilic additives, surface grafting, self-assembled layers, and nanocomposites have been explored to make amphiphilic coatings.[4, 24, 93-99] Martinelli et al. developed amphiphilic acrylic copolymers-PDMS systems by blending PEG-fluoroalkyl acrylate (PEGFA) and polysiloxane methacrylate (SMA) copolymer in PDMS coatings.[100] FR performance of the heterogeneous coating system was dependent on composition and concentration of the copolymer in coating formulations. Copolymer composition with 9:1 PEGFA: SMA ratio successfully lowered attachment and increased removal of *U.linza* spores; formulations with 1% and 4% by weight copolymer required low force of removal for barnacles.[100] In another study, amphiphilic formulations containing PDMS, silanol terminated

fluoropolymer (CF_3-PDMS), PEG modified trimethylsiloxane (TMS-PEG), and silica treated using hexamethyldisilazane were analyzed for FR performance.[24] This multicomponent system showed good FR performance against bacteria and barnacles due to presence of both CF_3-PDMS and TMS-PEG, but diatom removal remained unaffected by compositional variations in coating formulations.[24] Another approach to develop amphiphilic surfaces is by using surface active block copolymers (SABC).[89, 93, 97, 101, 102] In one attempt, SABC were modified by grafting fluoroalkyl side chains, which showed weak adhesion of diatoms *N.incerta* and microalgae *U.linza* as compared to regular SABC.[97] Similarly, SABC modified using PEG drastically reduced settlement of microalgae.[97] Surfaces that combined fluoroalkyl and PEG side chains on SABC in varying proportions showed that increasing amount of PEG chains reduced attachment and increased removal of microalgae and diatoms.[89] Studies conducted by making FR coatings by spraying or blending SABC with low and high modulus base coatings showed improvement in FR performance with decrease in modulus, supporting use of materials with low modulus in FR applications.[93] Studies have also been conducted to understand the effect of PDMS on efficiency of PDMS modified SABC, to replace fluorinated SABC due to environmental concerns and relative high cost of fluorinated compounds.[98, 103] Combination of SABC with PDMS showed similar FR performance to fluorinated SABC.[103, 104] Not just PEG-PDMS components, modifications with non-natural amino acids have also been explored for FR coatings, that showed opportunities for optimization of FR properties with components with different polarities and functionalities.[105] FR performance of a number of SABC modified using non-natural peptides through convenient thiol-ene click chemistry was evaluated.[105] SABC with peptides that hampered hydrogen bonding showed reduction in algal attachment.[105] Past research with SABC provided insights into development of cost effective technologies with convenient tunability of FR properties. Similar to SABC, amphiphilic additives containing blocks of hydrophobic and hydrophilic chains with different molecular weights, have been used to make amphiphilic coatings.[106-109] The additives can then be easily incorporated into coating formulations. Over time, the additives diffuse through the coating layer to impart heterogeneity to the outer surface of the coatings.[106] Grunlan et al. developed amphiphiles through hydrosilation reaction between oligodimethylsiloxanes and vinyl-terminated PEG and PDMS.[110] The MW of the oligodimethylsiloxanes and PEG were varied to make different additives.[110] The additives were then added to PDMS coatings and their FR performance was evaluated. FR results

obtained for the coatings showed that higher chain length of oligodimethylsiloxanes (13 repeating units) is anticipated to have increased mobilization of the PEG chains within the PDMS matrix, thereby increasing protein resistance of the coatings.[110] PEG chains with 8-16 repeating units showed the best FR performance.[111] Incorporation of 5-10% by weight additives showed drastic improvement of FR performance against biofilm, bacteria, and diatoms.[108] Among the different approaches, coatings made using hydrophobic and hydrophilic oligomers as resin modifiers, amphiphilic prepolymers, and amphiphilic additives appear to show potential for large scale marine applications. Galhenage et al. made several amphiphilic prepolymers by functionalizing isocyanurate of isophorone diisocyanate (IPDI trimer) with PEG and PDMS of varying MW, in varying amounts.[4] Then, formulations were made using additional IPDI trimer, the amphiphilic prepolymers and acrylic polyol to form self-stratified amphiphilic coatings.[4] Surface analysis experiments showed surface segregation of the polar and the non-polar phases.[4] Results obtained from FR experiments showed that FR performance of several amphiphilic formulations was comparable to or better than the commercially available marine coatings.[4] The prepolymer based amphiphilic coatings facilitated easy removal of microfoulants, like bacteria and algae, and macrofoulants, like barnacles and mussels.[4] Ability of amphiphilic systems to deter fouling by a variety of marine organisms with different attachment mechanisms has led to their popularity, not only in laboratory experiments, but also in practical applications. Commercially available Intersleek 1100SR and Hempasil X3 are two such popular amphiphilic marine coating.[112, 113]

Zwitterionic Coatings

Zwitterionic molecules possess both positive and negative moieties on the same molecule such that the overall charge of the molecule remains neutral.[2] Zwitterionic chains in the coatings are expected to electrostatically bind water molecules on the surface.[114] The tightly bound water molecules cannot be displaced by proteins and polysaccharides from bioadhesives secreted by the organisms.[115, 116] Therefore, the hydrophilic layer “camouflages” the substrates and does not allow bioadhesives to form strong bonds with the coating surface.[116] Polyphosphorylcholine, sulfobetaines (SB) and carboxybetaines (CB) are the most widely researched zwitterionic materials for FR applications.[117-122] Not just for good FR performance, SB and CB are also attractive candidates due to their low cost, superhydrophilicity, pH stability, high chemical stability, and resistance to protein adsorption.[2, 115] Zhang et al. showed that very

few algae *U.linza* spores attached to surfaces made by grafting poly(sulfobetaine methacrylate) (polySBMA) chains on glass surfaces.[2, 123] Another study, conducted to compare FR performances of polySBMA and poly(carboxybetaine methacrylate) (polyCBMA), showed successful inhibition of barnacle cyprid attachment.[119] The barnacle cyprids seemed to "explore" polySBMA rich surfaces for attachment, but interestingly, the cyprids left the polyCBMA coating soon after contact with the surface, without "exploring" potential sites for attachment.[119] The polyCBMA rich surfaces were believed to have provided an unfavorable surface for growth of the cyprids compared to the polySBMA rich surfaces, causing behavioral changes in the cyprids.[119] Bodkhe et al. synthesized ABA-type amine terminated amphiphilic block copolymers using PDMS and poly(SBMA), with varying chain lengths, using Atom Transfer Radical Polymerization (ATRP) technique.[114] The functional block copolymers were incorporated into self-stratified SiPU FR coating formulations. Pseudobarnacle adhesion experiments showed that the barnacle studs for coatings with PDMS MW = 5k g/mol and polySBMA MW between 2.5k-10k g/mol required force of < 10 N for detachment. Evaluation of FR performance of the coatings showed that the zwitterionic coatings successfully deterred fouling by bacterium *H.pacifica* and diatom *N.incerta*. But, the coatings showed higher attachment of bacteria *C.lytica* and microalgae *U.linza*. Biomimetic zwitterionic coatings have also been attempted for application as FR coatings.[124-126] Coatings modified using catechol functional groups, like 3,4-dihydroxyphenyl-L-alanine (DOPA), and SB have shown potential to reduce attachment of proteins and fibrogens.[127]

Antimicrobial Coatings for Biomedical Applications

Not just ships, biofilm formation on biomedical devices and implants poses big challenges. Biofilm growth on biomedical catheters, tubes, and implants begins with irreversible attachment of bacterial cells onto the substrates.[128] The cells, then, that colonize the substrates by producing extracellular polymers (EPS).[128] The highly hydrated EPS remains bound to the underlying surface even during flow.[128] Presence of "water channels" within the EPS allows transportation of essential nutrients and oxygen to the growing cells in the biofilm.[128] Further growth and cell division in the biofilm causes the cells to detach from the biofilm, resulting in systemic infection.[128] Therefore, surfaces of biomedical devices are physically or chemically altered to prevent or reduce attachment of the bacteria through functionalization derivatization, and surface modifications.

Antibacterial surfaces or coatings for biomedical applications are typically divided into two main types— 1. Bactericidal surfaces and 2. Antibiofouling surfaces.[129] Bactericidal coatings disrupt or rupture bacterial cells upon contact with the surface, causing cell death.[129] On the other hand, antibiofouling surfaces resist or prevent attachment of microorganisms through formation of unfavorable surface topographies or chemistries that repel and decrease proliferation of the bacteria.[129] Incorporation of silver ions on biomedical surfaces has shown tendency to damage the bacterial membranes and disrupt the function of the bacterial enzymes and nucleic acids, due to reaction of the silver ions with the negatively charged nitrogen, oxygen, and sulfur atoms from the proteins and DNA of the bacteria.[129, 130] The interaction of silver ions with thiol groups in the membranes is expected to provide bactericidal activity to the surfaces.[129, 131] Formation of hydroxyl radicals in the bacteria causes damage to the cellular DNA, thereby preventing the formation of the bacterial biofilm.[131] Bactericidal surfaces, incorporating covalently bonded antimicrobial agents, is another strategy used to reduce bacterial attachment onto biomedical devices. Requirements for successful use of antibacterial agents in coatings include presence of cationic groups, immobilized using PEG or oxazoline spacers, and apolar alkyl chains.[132] Cationic polymers are believed to disrupt net negative charge of the bacterial membranes, causing cell lysis and death.[129, 132] Antimicrobial peptides (AMPs) are extremely effective against bacterial adhesion.[129, 133, 134] Cationic nature of the AMPs allows electrostatic interactions with the negatively charged membranes.[129] Even at low concentration, AMPs disrupt the bilayer of the bacterial membranes by formation of pores, disintegration of the membranes, and damage to the metabolic functions of the cells.[133] Not just natural AMPs, synthetic mimics of AMPs (SMAPs) are amphiphilic polymers that cause disruption of cell membranes. SMAPs, polynorbornenes or poly(phenylene ethylene), derived from antimicrobial magainin or defensin peptides, exhibit antibacterial activity and low cytotoxicity.[129, 135] For non-natural peptide mimics, called peptoids, hydrophilic side chains (e.g. methoxyethyl) are desirable due to their similarity to PEG, absence of proton donors in the chains, and ability to make water soluble peptoids.[136, 137] Statz et al. synthesized a chimeric peptidomimetic polymer (PMP1) consisting of an N-substituted glycine (peptoid) oligomer coupled to a short functional peptide domain for surface adhesion.[137] This combination of the peptoid with the peptide resulted in excellent protein resistance of the polymer over extended periods of time.[137] Additionally, materials like polyethylene, polypropylene, nylon, poly(ethylene

terephthalate), and N-alkylated poly(ethyleneimines) (PEIs) are covalently immobilized onto cotton, wool, nylon, and polyester surfaces for antibacterial purposes; high molecular weight N-alkylated PEI chains exhibited higher antibacterial activity compared to low molecular weight PEI chains.[129, 138] Not just antibacterial polymers, enzymes such as subtilins, amylases, and lysozymes, exhibit antibacterial behavior by hydrolyzing bacterial proteins or degrading polysaccharide layers.[129, 139] Combination of the antibacterial N, N-dimethyldodecylammonium bromide (DDA) with hydrophilic cationic satellite, ethylenediamine (EDA), showed attraction of bacteria to the substrates and subsequent damage to the cells upon contact.[140] The positively charged nitrogen atom from DDA interacts with the negatively charged head groups of acidic phospholipids from the bacterial membranes, causing perturbations in the cellular bilayers.[140, 141] To combat these changes, the cells release potassium ions, which hampers physiological functions in the cells.[140] Quaternary ammonium cations (QACs) have also shown potential for use in antimicrobial coatings.[129, 142, 143] Effectiveness of the QACs is dependent on the length of the alkyl chains. For example, 14–16 carbons in the alkyl chains showed resistance to Gram-positive bacteria, whereas chain lengths of 12–14 carbons are more effective against Gram-negative bacterial cells.[144] Alkyl chains above and below 18 carbons and 4 carbons respectively are shown to be ineffective against bacterial adhesion.[129] In one attempt, well-defined PEGylated polymers with amines functionalities were synthesized using 2-(dimethylamino) ethyl methacrylate and oligo(ethylene glycol) methyl ether methacrylate monomers by reversible addition–fragmentation chain transfer polymerization (RAFT) technique.[132, 145] The tertiary amines in the polymers were converted to quaternary amines, using alkyl, primary alcohol, primary amine, and carboxylic acid, to introduce cationic character to the chains.[145] The length of the alkyl spacer and the chemical functionality present in the chains dictate antimicrobial activity of such polymers.[145] Brizzolara et al. compared performance of QACs on planar surfaces and particles.[132, 146] Results showed that QACs attached onto silica particles showed antibacterial character but QACs could not facilitate repulsion of bacteria.[146] This difference in performance was attributed to insufficient contact between the bacteria and the QAC on planar surfaces.[146] Biocides have incorporated into surface coatings to make bactericidal surfaces. N, N-dimethyldodecylammonium (DDA) combined with poly(2-methyl-2-oxazoline) acrylate (PMOXA) spacer showed tendency to kill incoming bacteria immediately upon contact due to long PMOXA chains and DDA biocide on the surfaces.[132, 147] The

PMOXA-DDA surfaces exhibited good bactericidal activity without leaching out, unlike low MW biocidal additives that must leach out of the coating matrix to become active.[147] Apart from DDA, bacterial tests conducted using cationic polyhexamethylene biguanides (PHMBs), with varying chain lengths, against *E.coli* showed inhibition of bacterial growth and bactericidal activity which increased with increasing chain length.[132, 148] Further, analysis of antimicrobial activity of polymethacrylate chains with guanide pendant groups indicated requirement of an optimal MW of 5×10^4-10^5 g/mol to allow diffusion of the chains through bacterial cell walls.[149] Although very effective as side chains or pendants, experiments with crosslinked polycations showed reduction in antibacterial character of the crosslinked polymers.[150] Long chain N-alkylated poly(4-vinylpyridine) attached onto glass substrates could kill more than 90% of deposited *S.aureus*, *S.epidermis*, *P.aeruginosa*, and *E.coli* bacterial cells in a dry state.[151] Contact active copolymeric emulsifiers, made using hydrophobic polystyrene block (PS) and hydrophilic block of antimicrobial polymer poly(4-vinyl-N-methylpyridinium iodide) (P4VMP), was designed by Fuchs et al.[152] Antimicrobial effect of the coatings was found to be dependent on the emulsifier loading in the formulations and PS content in the emulsifiers.[152]

"Textured" surfaces have also been explored as antibacterial surfaces. Inspiration was drawn from cicada wings that exhibit bactericidal effect due to presence of surface nanostructures instead of chemical composition of the surface.[129, 153] Bacterial cells can easily attach onto the wings, but the nanostructures cause cell membranes to stretch while suspended on the features.[154, 155] After a period of time after attachment, sufficient stretching of the suspended membranes causes the cells to rupture, decreasing bacterial cell growth.[154] The bactericidal insect wing nanostructures are believed to consistently rupture cell walls without encountering bacterial resistance, in contrast to the chemical based antibacterial mechanisms.[129] In one experiment, a "super surface" with nano-roughness gradients was created using a silicon wafer.[156] The surface exhibited superhydrophobicity and self-cleaning properties.[156] The surface also showed antibacterial character against both bacterial and mammalian cells.[156] Although useful in making antibacterial surfaces for biomedical instruments, packaging, and diagnostic tools, such surfaces are not useful for biomedical implants that require intimate contact with mammalian cells *in vivo*.[156] In-depth analysis of the bactericidal effect of "textured" surfaces showed that as weight of the bacterial cells on the "textures" increases, maximum membrane stretching of the bacteria

increases.[157] Comparison of different geometries on bactericidal performance of the surfaces showed that nanoridges cause most pronounced membrane stretching on Gram-positive bacteria.[157] Bacteria adsorbed onto nanopillars are much larger in size than those adsorbed onto nanoridges.[157] Surfaces with nanopillars of radius = 60 nm, height = 200 nm, and spacing = 170 nm imitate the surface of cicada wings, which make the surfaces immune to Gram-positive bacteria.[157] But, surfaces with nanopillars can successfully kill most Gram-negative bacteria.[157] The antibacterial properties of the nanopillars can be enhanced by sharpening the tips of the pillars or increasing the distance between the pillars.[157]

Antibiofouling or biopassive coatings do not actively kill bacterial cells, but resist adsorption and facilitate removal of bacterial proteins.[129, 132] Generally, hydrophilic polymers are used to make antibiofouling surfaces, used in different applications like medical implants, and diagnostic sensors.[132] The bioinert passive polymers increase resistance of biomedical devices to protein adsorption and thereby, reduce blood clot formation (thrombosis) or colonization of surfaces by bacteria.[128, 158] Formation of highly hydrated surfaces formed due to presence of the hydrophilic polymers and electrically neutral nature of the polymers are some of the advantages of the hydrophilic polymers.[132] For successful use as biopassive coatings, the polymers are required to possess sites for H-bond acceptors and no donors.[159] Presence of H-bond acceptor sites combined with the hydration layer are expected to prevent protein adsorption and ensuing biological events through excluded volume effects, steric hindrance, and entropic repulsion.[159, 160] The hydrophilic polymers can either be covalently immobilized or physisorbed on the surfaces. To this end, a variety of polymers, PEG, poly(2-methyl-2-oxazoline), zwitterionic phosphobetaine (PB), SB, and CB, phospholipid polymers containing a phosphorylcholine group and polysaccharides have been explored as potential biopassive coatings for application in biomedical devices, tools, and implants.[117, 132, 161-163] One of the most popular materials to reduce bacterial adhesion on biomedical surfaces is PEG.[164, 165] Unlike polymers with quaternary ammonium compounds, guanides, phosphonium salts, and antibiotics that kill bacteria upon contact, immobilization of PEG on the surfaces forms an interface between the bacteria and the substrate.[162, 163] Reducing contact between the substrate and the bacteria decreases protein adsorption on the biomaterials.[162] Studies have been conducted to understand the effect of PEG chain lengths, grafting density, and architecture on PEG-protein interactions.[93, 97, 101] Sofia et al. showed that grafting of PEG chains to form linear or star architectures

completely covers the underlying substrate, thereby preventing adsorption of proteins.[163] Such comb-like architectures can be made with high MW PEG side chains, PEG brushes, and dendritic structures.[163] But, low MW proteins and peptides can easily penetrate the hydrophilic brushes, thus reducing antibacterial efficiency of the surfaces.[132] Kingshott et al. demonstrated that higher stability and high surface coverage of grafted PEG chains can reduce the bacterial adhesion at least two orders magnitude better than physioadsorbed PEG chains.[166] Harbers et al. developed a crosslinked PEG-rich coating system, that combined both covalent bonding with the substrates and crosslinking chemistries, successfully inhibited protein, bacterial, and mammalian cell adsorption on the surface.[167] Although effective in lowering bacterial adhesion, PEG chains undergo oxidative degradation and chain cleavage in the long term, lowering its efficiency in practical applications.[132, 168] Studies conducted using poly(ethylene glycol) methyl ether methacrylate (POEGMEMA) brush-type graft polymers, synthesized using PEG and methyl methacrylate (MMA) using ATRP, showed more than 90% decrease in cell adhesion with brush thicknesses of greater than or equal to ~50 nm.[160] PMOXA has also shown potential for use as a bioinert polymer to decrease protein adsorption on surfaces.[169-171] Versatile nature of oxazolines allows exploration of different functional co-monomers, initiators, and controlled sequences in the chain for easy fabrication of protein resistant surfaces for biomedical applications.[170] Konradi et al. developed antibiofouling surface using PMOXA chains, grafted onto a poly(L-lysine) (PLL) backbone.[170] The comb-like PLL-PMOXA copolymer was allowed to self-assemble onto negatively charged niobium oxide (Nb_2O_5) surfaces.[170] Presence of PLL-PMOXA copolymers successfully deterred attachment of proteins and bacterial adhesion by *E.coli* on the surfaces, similar to PEG-rich surfaces.[170] Zwitterionic polymers, CB, SB, and PB, have shown potential for use in biomedical applications due to their long-term stability and biocompatibility.[120, 172-174] Polymer brushes of poly(CBMA) and poly(SBMA) reduced fibrinogen adsorption and deterred formation of *E.coli*, *S.epidermis*, and *P.aeruginosa* biofilms in short-term and long-term laboratory experiments.[120, 173, 175] Other monomers that have been used in antibiofouling biomedical applications include oligo(ethylene glycol) methacrylate, 2-hydroxyethyl methacrylate (HEMA), and acrylamide (AAm).[176-182] Chain orientation of grafted polyHEMA chains on silicon substrates successfully repelled bacterial proteins and prevented proteins from entering the brushes.[181] PolyAAm brushes with 20-80 nm thickness and grafting density between 0.6-0.8 nm^2 reduce adhesion of bacteria, *S. aureus*,

Streptococcus salivarius, and *Candida albicans*.[182] Not just hydrophilic, hydrophobic slippery liquid-infused porous surfaces (SLIPS), fabricated on a silicon substrates, prevented 99.6% of *P.aeruginosa*, *S.aureus*, and *E.coli* biofilm attachment in flow conditions.[83]

Hybrid surfaces, exhibiting simultaneous or reversible bactericidal and biopassive behavior, have also been studied for application in biomedical applications. Cheng et al. developed a reversible coating that could be easily converted from a bioactive cationic poly(N, N-dimethyl-N-(ethoxycarbonylmethyl)-N-(2'-(methacryloyloxy) ethyl)-ammoniumbromide) in dry state to a biopassive zwitterionic surface upon exposure to aqueous environment.[132, 183] In the cationic form, the coatings showed ability to kill bacteria after 1 hour of contact with the surface in air, while nonfouling zwitterionic character of the surface allowed the release of the dead bacterial cells from the coating surfaces.[183] Copolymerization of 2-(2-methoxyethoxy) ethyl methacrylate and hydroxyl-terminated oligo(ethylene glycol) methacrylate resulted in formation of coatings with simultaneous bactericidal-biopassive coatings.[132, 134] Reactive hydroxyl groups in the copolymers allowed immobilization of naturally occurring magainin I antimicrobial peptide.[134] Analysis of antibacterial performance showed that cell death occurred after 3 hours of contact with the dual performance surfaces.[134] Another dual performance coating, involving attachment of vancomycin biocide to anachelin chromophore through a PEG spacer, provided antibacterial character to the surfaces and exhibited retention of its dual performance in long-term bacterial adhesion and rinsing tests.[184]

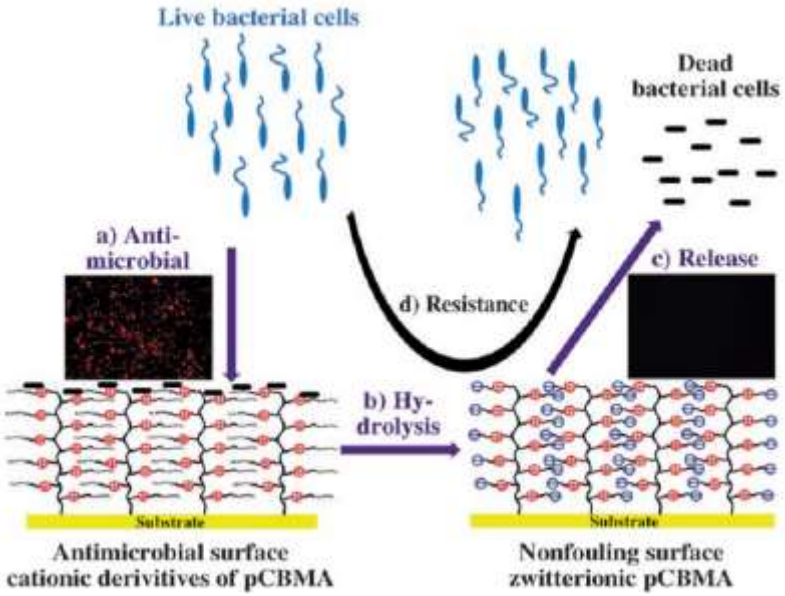

Figure 1.3. Representation of the reversible bactericidal-biopassive coating (reproduced from Cheng et al., **2008**).[183]

Non-Toxic Isocyanate-Free Polyurethane Technologies

As mentioned above, the self-stratified SiPU coatings show great potential for application as marine FR coatings. A typical SiPU formulation comprises of a polyisocyanate, acrylic polyol, and high molecular weight aminopropyl terminated PDMS (APT-PDMS).[17, 18, 20] In practical applications, coating formulations are sprayed onto the primed ship hulls using paint spray guns. SiPU formulations cure on the ship hulls, forming self-stratified FR coatings.[17] Reaction of the polyisocyanates with the polyols results in formation of urethane (-COO-NH-) linkages, which provides strength and adhesion to an otherwise soft PDMS layer.[20] Polyurethanes are one of the most widely used specialty polymers, with application areas like foams, adhesives, sealants and in biomedical applications.[185] The high mechanical strength, toughness, chemical and abrasion resistance of polyurethanes can be attributed to the presence of intermolecular bonds within the matrix.[185] In spite of the useful properties of urethanes, detrimental effects of prolonged exposure to unreacted isocyanates on the factory workers and personnel cannot be ignored. Depending of exposure to common isocyanate crosslinkers, like toluene diisocyanate (TDI) and methylene diisocyanate (MDI), factory workers have shown tendency to suffer from asthma within 5 years.[186-189] Moreover, previous studies have shown that long term effects of inhalation of isocyanate vapors and aerosols include inflammation, conjunctivitis, acute bronchitis, lung and breathing ailments.[186] Although the SiPU formulations are based on more stable polymeric cycloaliphatic isocyanates, concerns associated with spraying unreacted isocyanates has led to further research into finding suitable alternatives for conventional polyurethanes. As non-isocyanate routes to making polyurethanes, polycondensation, polyaddition, and ring-opening polymerization techniques have been explored that utilize carbamate and carbonate chemistries for polyurethanes synthesis.[190] Among all synthesis techniques, reaction of cyclic carbonates, which contain cyclo-carbonate and epoxy reactive groups, and diamines has been the most explored method of synthesizing urethanes (poly(hydroxyurethane)s).[190] The bulk of the poly(hydroxyurethane)s comprises of unreacted pendant hydroxyl groups, that form intra- and intermolecular hydrogen bonds. The hydroxyl groups are expected shield urethane linkages from hydrolysis, thereby increasing hydrolytic stability of polyurethanes as compared to conventional isocyanate based polyurethanes.[190] A drawback of this system is sluggish curing under ambient conditions.

In the past, glycidyl carbamate (GC) based coating technologies were introduced in the Webster group to make polyurethanes through an isocyanate-free approach.[191-199] GC resins can be easily synthesized using isocyanates and glycidol. The reaction between -NCO and -OH groups from isocyanates and glycidol respectively results in the formation of carbamate (urethane) linkages (-CO-NH-).[191] By the end of the synthesis reaction, all isocyanate functional groups are converted to epoxies, which are then available for crosslinking with a variety of diamine hardeners. Therefore, the synthesized GC resins combine properties of polyurethanes with convenience of epoxy-amine crosslinking chemistry.

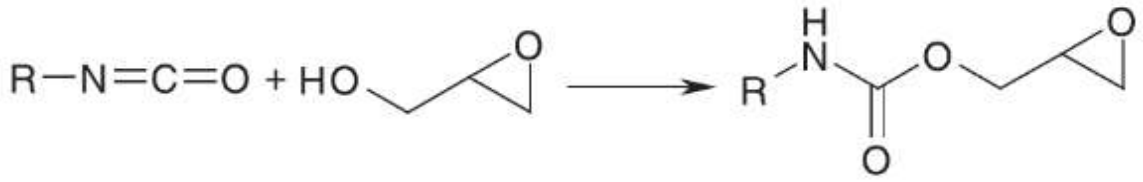

Figure 1.4. Reaction of isocyanate with glycidol to form carbamate linkages (reproduced from Edwards et al., **2005**).[191]

GC resins are extremely versatile in nature; the resins can be modified using a variety of functional compounds to develop coatings depending on the application. GC resins can undergo crosslinking with diamines or self-crosslinking at elevated temperatures.[192] Crosslinking with amine crosslinkers leads to formation of denser coating networks as compared to self-crosslinked GC coatings.[196] The type and stoichiometric ratio of amine crosslinkers, temperature of curing reactions, and structure of isocyanates directly affect the properties of the final coatings.[191] In decreasing order of reactions of diamines with GC resins— aliphatic > cycloaliphatic > aromatic.[191] GC coatings exhibit excellent corrosion protection; coatings containing H_{12}MDI show better corrosion resistance than HDI.[200] Hard, flexible, and thermally stable hybrid GC coatings have been made using amine functional silanes.[193-195] Inherent high viscosity of GC resins can be attributed to the presence of strong intermolecular hydrogen bonds between the polar carbamate groups.[196] High viscosity makes application of GC formulations difficult. But, highly functional nature of GC resins allows easy modification of the resins with different alcohols.[196] Past results have shown that viscosity of GC resins can be reduced significantly using ether alcohols as modifiers.[196] Further, water dispersible coatings can be easily made using PEG chains as modifiers.[197] Reaction of GC resins with acrylic acid introduces acrylate functional groups in the resins; the resultant acrylated resin can be easily cured using UV irradiation to give hard,

flexible and chemically resistant coatings.[198] High functionality, high reactivity, ease of synthesis, and versatility of GC resins makes the GC coatings viable for marine applications. A typical formulation with GC resin comprises of the modified GC resin and an amine crosslinker (Figure 1.5). Although isocyanates are used to synthesize the resin, lack of free isocyanate groups in the final coating formulation is expected to reduce health concerns associated with spraying unreacted isocyanates.

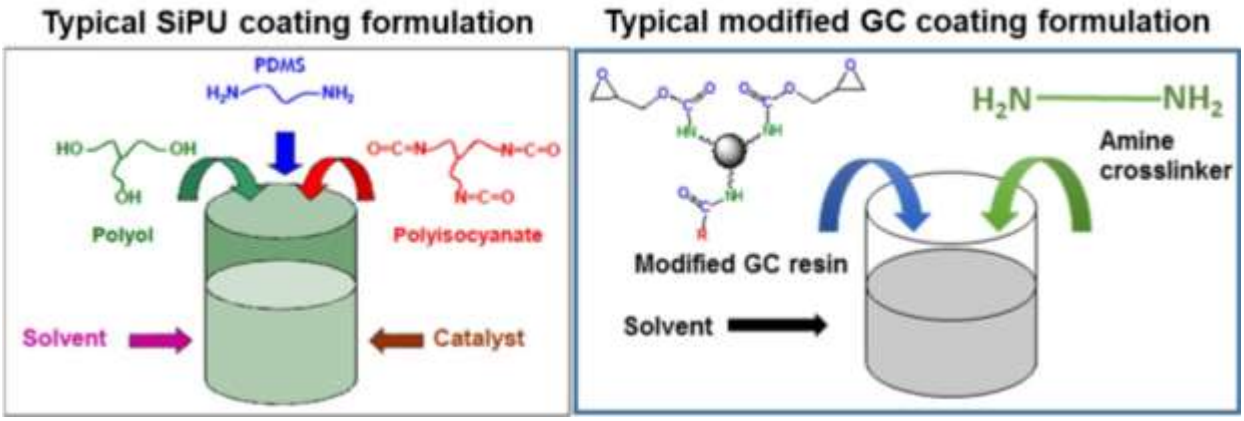

Figure 1.5. Comparison between SiPU and GC coating formulations.

Purpose of the Study

This study involves evaluation of FR performance of marine coating formulations made by changing topography of a previously introduced SiPU coating formulation and development of modified GC technologies with varying surface chemistries as potential FR surfaces. The objective of the first part of the project is to understand the effect of surface damage or “abrasions” on the FR performance of SiPU coatings. Over the course of development of self-stratified SiPU FR coatings, different formulations have been studied previously using different isocyanates, polyols, and APT-PDMS. Results from the extensive decade long research showed that the smooth SiPU coating systems exhibited FR performance comparable to the commercially available silicone elastomer based FR coatings. But, one important aspect of SiPU coatings that wasn’t evaluated was effect of surface damage, encountered during use, on the FR performance of these SiPU coatings. FR marine coatings are cleaned periodically to remove fouling organisms attached to ship hulls. The coating layer can be damaged even when the ship is held stationary in the docks. In this project, one SiPU formulation, with the best FR performance, was abraded to simulate surface damage. As previously mentioned, although forming engineered topographies is theoretically desirable, the process of introducing such topographies is not easy in

practical large scale applications. Therefore, this project hopes to demonstrate an effective and practical way to introduce surface “features” on the SiPU coating, using regular Scotch Brite pads, with varying roughness. Evaluation of FR performance of the abraded surfaces indicated dependence of the FR performance on the size of the features formed on the surface after abrasions. The results were also consistent with the basics of the previously introduced engineered surface models.

Recently, concerns have been raised about spraying SiPU formulations, containing free isocyanate groups, directly onto ship hulls. The second part of the study attempts to address these concerns by developing novel two-component isocyanate-free modified glycidyl carbamate (GC) systems as “safer” alternatives for isocyanate based polyurethanes to make self-stratified FR marine coatings. In this project, different hydrophobic and amphiphilic GC resins were synthesized by incorporating PDMS and PEG as modifiers. Consequently, GC coatings with different surface chemistries were made using the modified resins and different amine crosslinkers. Evaluation of mechanical and thermal properties of the coatings showed formation of hard, flexible and glossy coatings after curing. Preliminary results showed that the GC coatings exhibited subpar FR performance against hard foulants, like barnacles and mussels, as compared to the commercial standards. But, the GC coatings facilitated higher removal of diatoms from the surface as compared to the commercial standards. In spite of the poor FR performance of the GC coatings, it is anticipated that with future research into modification of GC resins, solvent selection and selection of curing agents, GC coatings can be successfully used in marine applications, as isocyanate-free replacements for both the commercial coatings and the previously developed SiPU FR coatings.

References

1. Yebra, D. M.; Kiil, S.; Dam-Johansen, K., Antifouling technology—past, present and future steps towards efficient and environmentally friendly antifouling coatings. *Progress in Organic Coatings* **2004,** *50* (2), 75-104.

2. Callow, J. A.; Callow, M. E., Trends in the development of environmentally friendly fouling-resistant marine coatings. *Nature Communications* **2011,** *2*, 244.

3. Lejars, M. n.; Margaillan, A.; Bressy, C., Fouling release coatings: a nontoxic alternative to biocidal antifouling coatings. *Chemical Reviews* **2012,** *112* (8), 4347-4390.

4. Galhenage, T. P.; Webster, D. C.; Moreira, A. M. S.; Burgett, R. J.; Stafslien, S. J.; Vanderwal, L.; Finlay, J. A.; Franco, S. C.; Clare, A. S., Poly (ethylene) glycol-modified, amphiphilic, siloxane–polyurethane coatings and their performance as fouling-release surfaces. *Journal of Coatings Technology and Research* **2016,** *2* (14), 307-322.

5. Magin, C. M.; Cooper, S. P.; Brennan, A. B., Non-toxic antifouling strategies. *Materials Today* **2010,** *13* (4), 36-44.

6. Schultz, M. P., Effects of coating roughness and biofouling on ship resistance and powering. *Biofouling* **2007,** *23* (5), 331-341.

7. Schultz, M. P.; Bendick, J. A.; Holm, E. R.; Hertel, W. M., Economic impact of biofouling on a naval surface ship. *Biofouling* **2011,** *27* (1), 87-98.

8. Ciriminna, R.; Bright, F. V.; Pagliaro, M., Ecofriendly antifouling marine coatings. *ACS Sustainable Chemistry & Engineering*, **2015,** *3*, 559-565.

9. Chambers, L. D.; Stokes, K. R.; Walsh, F. C.; Wood, R. J. K., Modern approaches to marine antifouling coatings. *Surface and Coatings Technology* **2006,** *201* (6), 3642-3652.

10. Dafforn, K. A.; Lewis, J. A.; Johnston, E. L., Antifouling strategies: history and regulation, ecological impacts and mitigation. *Marine Pollution Bulletin* **2011,** *62* (3), 453-465.

11. Brady, R. F., A fracture mechanical analysis of fouling release from nontoxic antifouling coatings. *Progress in Organic Coatings* **2001,** *43* (1), 188-192.

12. Brady Jr, R. F.; Singer, I. L., Mechanical factors favoring release from fouling release coatings. *Biofouling* **2000,** *15* (1-3), 73-81.

13. Brady, R. F., Properties which influence marine fouling resistance in polymers containing silicon and fluorine. *Progress in Organic Coatings* **1999,** *35* (1), 31-35.

14. Baier, R. E., Surface behaviour of biomaterials: the theta surface for biocompatibility. *Journal of Materials Science: Materials in Medicine* **2006,** *17* (11), 1057-1062.

15. Majumdar, P.; Ekin, A.; Webster, D. C., Thermoset Siloxane—Urethane Fouling Release Coatings. In *Smart Coatings;* ***March 13, 2007****, 61-75*.

16. Ekin, A.; Webster, D. C.; Daniels, J. W.; Stafslien, S. J.; Cassé, F.; Callow, J. A.; Callow, M. E., Synthesis, formulation, and characterization of siloxane–polyurethane coatings for underwater marine

applications using combinatorial high-throughput experimentation. *Journal of Coatings Technology and Research* **2007,** *4* (4), 435-451.

17. Bodkhe, R. B.; Thompson, S. E. M.; Yehle, C.; Cilz, N.; Daniels, J.; Stafslien, S. J.; Callow, M. E.; Callow, J. A.; Webster, D. C., The effect of formulation variables on fouling-release performance of stratified siloxane–polyurethane coatings. *Journal of Coatings Technology and Research* **2012,** *9* (3), 235-249.

18. Sommer, S.; Ekin, A.; Webster, D. C.; Stafslien, S. J.; Daniels, J.; VanderWal, L. J.; Thompson, S. E. M.; Callow, M. E.; Callow, J. A., A preliminary study on the properties and fouling-release performance of siloxane–polyurethane coatings prepared from poly (dimethylsiloxane)(PDMS) macromers. *Biofouling* **2010,** *26* (8), 961-972.

19. Pieper, R. J.; Ekin, A.; Webster, D. C.; Cassé, F.; Callow, J. A.; Callow, M. E., Combinatorial approach to study the effect of acrylic polyol composition on the properties of crosslinked siloxane-polyurethane fouling-release coatings. *Journal of Coatings Technology and Research* **2007,** *4* (4), 453-461.

20. Sommer, S. A.; Byrom, J. R.; Fischer, H. D.; Bodkhe, R. B.; Stafslien, S. J.; Daniels, J.; Yehle, C.; Webster, D. C., Effects of pigmentation on siloxane–polyurethane coatings and their performance as fouling-release marine coatings. *Journal of Coatings Technology and Research* **2011,** *8* (6), 661-670.

21. Ekin, A.; Webster, D. C., Combinatorial and High-Throughput Screening of the Effect of Siloxane Composition on the Surface Properties of Crosslinked Siloxane− Polyurethane Coatings. *Journal of Combinatorial Chemistry* **2007,** *9* (1), 178-188.

22. Majumdar, P.; Lee, E.; Patel, N.; Ward, K.; Stafslien, S. J.; Daniels, J.; Chisholm, B. J.; Boudjouk, P.; Callow, M. E.; Callow, J. A., Combinatorial materials research applied to the development of new surface coatings IX: an investigation of novel antifouling/fouling-release coatings containing quaternary ammonium salt groups. *Biofouling* **2008,** *24* (3), 185-200.

23. Kugel, A. J.; Jarabek, L. E.; Daniels, J. W.; Vander Wal, L. J.; Ebert, S. M.; Jepperson, M. J.; Stafslien, S. J.; Pieper, R. J.; Webster, D. C.; Bahr, J., Combinatorial materials research applied to the development of new surface coatings XII: Novel, environmentally friendly antimicrobial coatings derived

from biocide-functional acrylic polyols and isocyanates. *Journal of Coatings Technology and Research* **2009,** *6* (1), 107-121.

24. Stafslien, S. J.; Christianson, D.; Daniels, J.; VanderWal, L.; Chernykh, A.; Chisholm, B. J., Combinatorial materials research applied to the development of new surface coatings XVI: fouling-release properties of amphiphilic polysiloxane coatings. *Biofouling* **2015,** *31* (2), 135-149.

25. Majumdar, P.; Stafslien, S.; Daniels, J.; Webster, D. C., High throughput combinatorial characterization of thermosetting siloxane–urethane coatings having spontaneously formed microtopographical surfaces. *Journal of Coatings Technology and Research* **2007,** *4* (2), 131-138.

26. Ekin, A.; Webster, D. C., Library synthesis and characterization of 3-aminopropyl-terminated poly (dimethylsiloxane) s and poly (ϵ-caprolactone)-b-poly (dimethylsiloxane) s. *Journal of Polymer Science Part A: Polymer Chemistry* **2006,** *44* (16), 4880-4894.

27. Genzer, J.; Efimenko, K., Recent developments in superhydrophobic surfaces and their relevance to marine fouling: a review. *Biofouling* **2006,** *22* (5), 339-360.

28. Peters, A. M.; Pirat, C.; Sbragaglia, M.; Borkent, B. M.; Wessling, M.; Lohse, D.; Lammertink, R. G. H., Cassie-Baxter to Wenzel state wetting transition: Scaling of the front velocity. *The European Physical Journal E* **2009,** *29* (4), 391-397.

29. Erbil, H. Y.; Cansoy, C. E., Range of applicability of the Wenzel and Cassie− Baxter equations for superhydrophobic surfaces. *Langmuir* **2009,** *25* (24), 14135-14145.

30. Murakami, D.; Jinnai, H.; Takahara, A., Wetting transition from the Cassie–Baxter state to the Wenzel state on textured polymer surfaces. *Langmuir* **2014,** *30* (8), 2061-2067.

31. Cassie, A. B. D.; Baxter, S., Wettability of porous surfaces. *Transactions of the Faraday society* **1944,** *40*, 546-551.

32. Wenzel, R. N., Resistance of solid surfaces to wetting by water. *Industrial & Engineering Chemistry* **1936,** *28* (8), 988-994.

33. Yoshimitsu, Z.; Nakajima, A.; Watanabe, T.; Hashimoto, K., Effects of surface structure on the hydrophobicity and sliding behavior of water droplets. *Langmuir* **2002,** *18* (15), 5818-5822.

34. Lafuma, A.; Quéré, D., Superhydrophobic states. *Nature Materials* **2003,** *2* (7), 457-460.

35. Callies, M.; Quéré, D., On water repellency. *Soft matter* **2005,** *1* (1), 55-61.

36. Bico, J.; Tordeux, C.; Quéré, D., Rough wetting. *EPL (Europhysics Letters)* **2001,** *55* (2), 214.

37. Baier, R. E., Influence of the initial surface condition of materials on bioadhesion. In *Proceedings of the Third International Congress on Marine Corrosion and Fouling* **1973**, 633-639.

38. Schmidt, D. L.; Brady, R. F.; Lam, K.; Schmidt, D. C.; Chaudhury, M. K., Contact angle hysteresis, adhesion, and marine biofouling. *Langmuir* **2004,** *20* (7), 2830-2836.

39. Scardino, A. J.; de Nys, R., Mini review: biomimetic models and bioinspired surfaces for fouling control. *Biofouling* **2011,** *27* (1), 73-86.

40. Shivapooja, P.; Wang, Q.; Orihuela, B.; Rittschof, D.; López, G. P.; Zhao, X., Bioinspired surfaces with dynamic topography for active control of biofouling. *Advanced Materials* **2013,** *25* (10), 1430-1434.

41. Arnott, J.; Wu, A. H. F.; Vucko, M. J.; Lamb, R. N., Marine antifouling from thin air. *Biofouling* **2014,** *30* (9), 1045-1054.

42. Cheng, Y. T.; Rodak, D. E.; Wong, C. A.; Hayden, C. A., Effects of micro-and nano-structures on the self-cleaning behaviour of lotus leaves. *Nanotechnology* **2006,** *17* (5), 1359.

43. Patankar, N. A., Mimicking the lotus effect: influence of double roughness structures and slender pillars. *Langmuir* **2004,** *20* (19), 8209-8213.

44. Bixler, G. D.; Theiss, A.; Bhushan, B.; Lee, S. C., Anti-fouling properties of microstructured surfaces bio-inspired by rice leaves and butterfly wings. *Journal of Colloid and Interface Science* **2014,** *419*, 114-133.

45. Bixler, G. D.; Bhushan, B., Rice-and butterfly-wing effect inspired self-cleaning and low drag micro/nanopatterned surfaces in water, oil, and air flow. *Nanoscale* **2014,** *6* (1), 76-96.

46. Bers, A. V.; Wahl, M., The influence of natural surface microtopographies on fouling. *Biofouling* **2004,** *20* (1), 43-51.

47. Wahl, M.; Kröger, K.; Lenz, M., Non-toxic protection against epibiosis. *Biofouling* **1998,** *12* (1-3), 205-226.

48. Becker, K.; Wahl, M., Behaviour patterns as natural antifouling mechanisms of tropical marine crabs. *Journal of Experimental Marine Biology and Ecology* **1996,** *203* (2), 245-258.

49. Hoipkemeier-Wilson, L.; Schumacher, J. F.; Finlay, J. A.; Perry, R.; Callow, M. E.; Callow, J. A.; Brennan, A. B., Towards minimally fouling substrates: surface grafting and topography. *Polym. Prepr.* **2005,** *46*, 1312-1313.

50. Brennan, A. B.; Baney, R. H.; Carman, M. L.; Estes, T. G.; Feinberg, A. W.; Wilson, L. H.; Schumacher, J. F., Surface topography for non-toxic bioadhesion control. Google Patents: 2006.

51. Chung, K. K.; Schumacher, J. F.; Sampson, E. M.; Burne, R. A.; Antonelli, P. J.; Brennan, A. B., Impact of engineered surface microtopography on biofilm formation of Staphylococcus aureus. *Biointerphases* **2007,** *2* (2), 89-94.

52. Carman, M. L.; Estes, T. G.; Feinberg, A. W.; Schumacher, J. F.; Wilkerson, W.; Wilson, L. H.; Callow, M. E.; Callow, J. A.; Brennan, A. B., Engineered antifouling microtopographies–correlating wettability with cell attachment. *Biofouling* **2006,** *22* (1), 11-21.

53. Schumacher, J. F.; Carman, M. L.; Estes, T. G.; Feinberg, A. W.; Wilson, L. H.; Callow, M. E.; Callow, J. A.; Finlay, J. A.; Brennan, A. B., Engineered antifouling microtopographies–effect of feature size, geometry, and roughness on settlement of zoospores of the green alga Ulva. *Biofouling* **2007,** *23* (1), 55-62.

54. Schumacher, J. F.; Aldred, N.; Callow, M. E.; Finlay, J. A.; Callow, J. A.; Clare, A. S.; Brennan, A. B., Species-specific engineered antifouling topographies: correlations between the settlement of algal zoospores and barnacle cyprids. *Biofouling* **2007,** *23* (5), 307-317.

55. Callow, M. E.; Jennings, A. R.; Brennan, A. B.; Seegert, C. E.; Gibson, A.; Wilson, L.; Feinberg, A.; Baney, R.; Callow, J. A., Microtopographic cues for settlement of zoospores of the green fouling alga Enteromorpha. *Biofouling* **2002,** *18* (3), 229-236.

56. Hills, J. M.; Thomason, J. C., The effect of scales of surface roughness on the settlement of barnacle (Semibalanus balanoides) cyprids. *Biofouling* **1998,** *12* (1-3), 57-69.

57. Hills, J. M.; Thomason, J. C., On the effect of tile size and surface texture on recruitment pattern and density of the barnacle, Semibalanus balanoides. *Biofouling* **1998,** *13* (1), 31-50.

58. Efimenko, K.; Finlay, J.; Callow, M. E.; Callow, J. A.; Genzer, J., Development and testing of hierarchically wrinkled coatings for marine antifouling. *ACS Applied Materials & Interfaces* **2009,** *1* (5), 1031-1040.

59. Efimenko, K.; Rackaitis, M.; Manias, E.; Vaziri, A.; Mahadevan, L.; Genzer, J., Nested self-similar wrinkling patterns in skins. *Nature Materials* **2005,** *4* (4), 293-297.

60. Xiao, L.; Thompson, S. E. M.; Röhrig, M.; Callow, M. E.; Callow, J. A.; Grunze, M.; Rosenhahn, A., Hot embossed microtopographic gradients reveal morphological cues that guide the settlement of zoospores. *Langmuir* **2013,** *29* (4), 1093-1099.

61. Lemire, M.; Bourget, E., Substratum heterogeneity and complexity influence micro-habitat selection of Balanus sp. and Tubularia crocea larvae. *Marine Ecology Progress Series* **1996**, 77-87.

62. Walters, L. J., Field settlement locations on subtidal marine hard substrata: is active larval exploration involved? *Limnology and Oceanography* **1992,** *37* (5), 1101-1107.

63. Hills, J. M.; Thomason, J. C.; Milligan, J. L.; Richardson, M., Do barnacle larvae respond to multiple settlement cues over a range of spatial scales? In *Recruitment, Colonization and Physical-Chemical Forcing in Marine Biological Systems*, **1998,** 101-111.

64. Andersson, M.; Berntsson, K.; Jonsson, P.; Gatenholm, P., Microtextured surfaces: towards macrofouling resistant coatings. *Biofouling* **1999,** *14* (2), 167-178.

65. Berntsson, K. M.; Jonsson, P. R.; Lejhall, M.; Gatenholm, P., Analysis of behavioural rejection of micro-textured surfaces and implications for recruitment by the barnacle Balanus improvisus. *Journal of Experimental Marine Biology and Ecology* **2000,** *251* (1), 59-83.

66. Petronis, Š.; Berntsson, K.; Gold, J.; Gatenholm, P., Design and microstructuring of PDMS surfaces for improved marine biofouling resistance. *Journal of Biomaterials Science, Polymer Edition* **2000,** *11* (10), 1051-1072.

67. Le Tourneux, F.; Bourget, E., Importance of physical and biological settlement cues used at different spatial scales by the larvae of Semibalanus balanoides. *Marine Biology* **1988,** *97* (1), 57-66.

68. Schumacher, J. F.; Long, C. J.; Callow, M. E.; Finlay, J. A.; Callow, J. A.; Brennan, A. B., Engineered nanoforce gradients for inhibition of settlement (attachment) of swimming algal spores. *Langmuir* **2008,** *24* (9), 4931-4937.

69. Scardino, A. J.; Guenther, J.; De Nys, R., Attachment point theory revisited: the fouling response to a microtextured matrix. *Biofouling* **2008,** *24* (1), 45-53.

70. Scardino, A. J.; Harvey, E.; De Nys, R., Testing attachment point theory: diatom attachment on microtextured polyimide biomimics. *Biofouling* **2006,** *22* (1), 55-60.

71. Cooper, S. P.; Finlay, J. A.; Cone, G.; Callow, M. E.; Callow, J. A.; Brennan, A. B., Engineered antifouling microtopographies: kinetic analysis of the attachment of zoospores of the green alga Ulva to silicone elastomers. *Biofouling* **2011,** *27* (8), 881-892.

72. Long, C. J.; Finlay, J. A.; Callow, M. E.; Callow, J. A.; Brennan, A. B., Engineered antifouling microtopographies: mapping preferential and inhibitory microenvironments for zoospore attachment. *Biofouling* **2010,** *26* (8), 941-952.

73. Long, C. J.; Schumacher, J. F.; Robinson, P. A. C.; Finlay, J. A.; Callow, M. E.; Callow, J. A.; Brennan, A. B., A model that predicts the attachment behavior of Ulva linza zoospores on surface topography. *Biofouling* **2010,** *26* (4), 411-419.

74. Aldred, N.; Scardino, A.; Cavaco, A.; de Nys, R.; Clare, A. S., Attachment strength is a key factor in the selection of surfaces by barnacle cyprids (Balanus amphitrite) during settlement. *Biofouling* **2010,** *26* (3), 287-299.

75. Magin, C. M.; Long, C. J.; Cooper, S. P.; Ista, L. K.; López, G. P.; Brennan, A. B., Engineered antifouling microtopographies: the role of Reynolds number in a model that predicts attachment of zoospores of Ulva and cells of Cobetia marina. *Biofouling* **2010,** *26* (6), 719-727.

76. Decker, J. T.; Kirschner, C. M.; Long, C. J.; Finlay, J. A.; Callow, M. E.; Callow, J. A.; Brennan, A. B., Engineered antifouling microtopographies: an energetic model that predicts cell attachment. *Langmuir* **2013,** *29* (42), 13023-13030.

77. Cao, X.; Pettitt, M. E.; Wode, F.; Arpa Sancet, M. P.; Fu, J.; Ji, J.; Callow, M. E.; Callow, J. A.; Rosenhahn, A.; Grunze, M., Interaction of Zoospores of the Green Alga Ulva with Bioinspired Micro-and Nanostructured Surfaces Prepared by Polyelectrolyte Layer-by-Layer Self-Assembly. *Advanced Functional Materials* **2010,** *20* (12), 1984-1993.

78. Vrolijk, N. H.; Targett, N. M.; Baier, R. E.; Meyer, A. E., Surface characterisation of two gorgonian coral species: implications for a natural antifouling defence. *Biofouling* **1990,** *2* (1), 39-54.

79. Ghosh, R.; Buxton, G. A.; Usta, O. B.; Balazs, A. C.; Alexeev, A., Designing oscillating cilia that capture or release microscopic particles. *Langmuir* **2009,** *26* (4), 2963-2968.

80. Bhattacharya, A.; Buxton, G. A.; Usta, O. B.; Balazs, A. C., Propulsion and trapping of microparticles by active cilia arrays. *Langmuir* **2012,** *28* (6), 3217-3226.

81. Balazs, A. C.; Bhattacharya, A.; Tripathi, A.; Shum, H., Designing Bioinspired Artificial Cilia to Regulate Particle–Surface Interactions. *The Journal of Physical Chemistry Letters* **2014,** *5* (10), 1691-1700.

82. Kim, P.; Zarzar, L. D.; He, X.; Grinthal, A.; Aizenberg, J., Hydrogel-actuated integrated responsive systems (HAIRS): Moving towards adaptive materials. *Current Opinion in Solid State and Materials Science* **2011,** *15* (6), 236-245.

83. Epstein, A. K.; Wong, T.-S.; Belisle, R. A.; Boggs, E. M.; Aizenberg, J., Liquid-infused structured surfaces with exceptional anti-biofouling performance. *Proceedings of the National Academy of Sciences* **2012,** *109* (33), 13182-13187.

84. Wiegemann, M., Adhesion in blue mussels (Mytilus edulis) and barnacles (genus Balanus): mechanisms and technical applications. *Aquatic Sciences-Research Across Boundaries* **2005,** *67* (2), 166-176.

85. Crisp, D. J.; Walker, G.; Young, G. A.; Yule, A. B., Adhesion and substrate choice in mussels and barnacles. *Journal of Colloid and Interface Science* **1985,** *104* (1), 40-50.

86. Finlay, J. A.; Bennett, S. M.; Brewer, L. H.; Sokolova, A.; Clay, G.; Gunari, N.; Meyer, A. E.; Walker, G. C.; Wendt, D. E.; Callow, M. E., Barnacle settlement and the adhesion of protein and diatom microfouling to xerogel films with varying surface energy and water wettability. *Biofouling* **2010,** *26* (6), 657-666.

87. Holland, R.; Dugdale, T. M.; Wetherbee, R.; Brennan, A. B.; Finlay, J. A.; Callow, J. A.; Callow, M. E., Adhesion and motility of fouling diatoms on a silicone elastomer. *Biofouling* **2004,** *20* (6), 323-329.

88. Gudipati, C. S.; Finlay, J. A.; Callow, J. A.; Callow, M. E.; Wooley, K. L., The antifouling and fouling-release perfomance of hyperbranched fluoropolymer (HBFP)-poly (ethylene glycol)(PEG) composite coatings evaluated by adsorption of biomacromolecules and the green fouling alga ulva. *Langmuir* **2005,** *21* (7), 3044-3053.

89. Krishnan, S.; Wang, N.; Ober, C. K.; Finlay, J. A.; Callow, M. E.; Callow, J. A.; Hexemer, A.; Sohn, K. E.; Kramer, E. J.; Fischer, D. A., Comparison of the fouling release properties of hydrophobic

fluorinated and hydrophilic PEGylated block copolymer surfaces: attachment strength of the diatom Navicula and the green alga Ulva. *Biomacromolecules* **2006,** *7* (5), 1449-1462.

90. Chen, H.; Yuan, L.; Song, W.; Wu, Z.; Li, D., Biocompatible polymer materials: role of protein–surface interactions. *Progress in Polymer Science* **2008,** *33* (11), 1059-1087.

91. Gudipati, C. S.; Greenlief, C. M.; Johnson, J. A.; Prayongpan, P.; Wooley, K. L., Hyperbranched fluoropolymer and linear poly (ethylene glycol) based amphiphilic crosslinked networks as efficient antifouling coatings: an insight into the surface compositions, topographies, and morphologies. *Journal of Polymer Science Part A: Polymer Chemistry* **2004,** *42* (24), 6193-6208.

92. Imbesi, P. M.; Finlay, J. A.; Aldred, N.; Eller, M. J.; Felder, S. E.; Pollack, K. A.; Lonnecker, A. T.; Raymond, J. E.; Mackay, M. E.; Schweikert, E. A., Targeted surface nanocomplexity: two-dimensional control over the composition, physical properties and anti-biofouling performance of hyperbranched fluoropolymer–poly (ethylene glycol) amphiphilic crosslinked networks. *Polymer Chemistry* **2012,** *3* (11), 3121-3131.

93. Weinman, C. J.; Finlay, J. A.; Park, D.; Paik, M. Y.; Krishnan, S.; Sundaram, H. S.; Dimitriou, M.; Sohn, K. E.; Callow, M. E.; Callow, J. A., ABC triblock surface active block copolymer with grafted ethoxylated fluoroalkyl amphiphilic side chains for marine antifouling/fouling-release applications. *Langmuir* **2009,** *25* (20), 12266-12274.

94. Martinelli, E.; Suffredini, M.; Galli, G.; Glisenti, A.; Pettitt, M. E.; Callow, M. E.; Callow, J. A.; Williams, D.; Lyall, G., Amphiphilic block copolymer/poly (dimethylsiloxane)(PDMS) blends and nanocomposites for improved fouling-release. *Biofouling* **2011,** *27* (5), 529-541.

95. Park, D.; Weinman, C. J.; Finlay, J. A.; Fletcher, B. R.; Paik, M. Y.; Sundaram, H. S.; Dimitriou, M. D.; Sohn, K. E.; Callow, M. E.; Callow, J. A., Amphiphilic surface active triblock copolymers with mixed hydrophobic and hydrophilic side chains for tuned marine fouling-release properties. *Langmuir* **2010,** *26* (12), 9772-9781.

96. Bodkhe, R. B.; Stafslien, S. J.; Cilz, N.; Daniels, J.; Thompson, S. E. M.; Callow, M. E.; Callow, J. A.; Webster, D. C., Polyurethanes with amphiphilic surfaces made using telechelic functional PDMS having orthogonal acid functional groups. *Progress in Organic Coatings* **2012,** *75* (1), 38-48.

97. Krishnan, S.; Ayothi, R.; Hexemer, A.; Finlay, J. A.; Sohn, K. E.; Perry, R.; Ober, C. K.; Kramer, E. J.; Callow, M. E.; Callow, J. A., Anti-biofouling properties of comblike block copolymers with amphiphilic side chains. *Langmuir* **2006,** *22* (11), 5075-5086.

98. Sundaram, H. S.; Cho, Y.; Dimitriou, M. D.; Weinman, C. J.; Finlay, J. A.; Cone, G.; Callow, M. E.; Callow, J. A.; Kramer, E. J.; Ober, C. K., Fluorine-free mixed amphiphilic polymers based on PDMS and PEG side chains for fouling release applications. *Biofouling* **2011,** *27* (6), 589-602.

99. Wyszogrodzka, M.; Haag, R., Synthesis and characterization of glycerol dendrons, self-assembled monolayers on gold: a detailed study of their protein resistance. *Biomacromolecules* **2009,** *10* (5), 1043-1054.

100. Martinelli, E.; Sarvothaman, M. K.; Galli, G.; Pettitt, M. E.; Callow, M. E.; Callow, J. A.; Conlan, S. L.; Clare, A. S.; Sugiharto, A. B.; Davies, C., Poly (dimethyl siloxane)(PDMS) network blends of amphiphilic acrylic copolymers with poly (ethylene glycol)-fluoroalkyl side chains for fouling-release coatings. II. Laboratory assays and field immersion trials. *Biofouling* **2012,** *28* (6), 571-582.

101. Martinelli, E.; Menghetti, S.; Galli, G.; Glisenti, A.; Krishnan, S.; Paik, M. Y.; Ober, C. K.; Smilgies, D. M.; Fischer, D. A., Surface engineering of styrene/PEGylated-fluoroalkyl styrene block copolymer thin films. *Journal of Polymer Science Part A: Polymer Chemistry* **2009,** *47* (1), 267-284.

102. Martinelli, E.; Agostini, S.; Galli, G.; Chiellini, E.; Glisenti, A.; Pettitt, M. E.; Callow, M. E.; Callow, J. A.; Graf, K.; Bartels, F. W., Nanostructured films of amphiphilic fluorinated block copolymers for fouling release application. *Langmuir* **2008,** *24* (22), 13138-13147.

103. Sundaram, H. S.; Cho, Y.; Dimitriou, M. D.; Finlay, J. A.; Cone, G.; Williams, S.; Handlin, D.; Gatto, J.; Callow, M. E.; Callow, J. A., Fluorinated amphiphilic polymers and their blends for fouling-release applications: the benefits of a triblock copolymer surface. *ACS Applied Materials & Interfaces* **2011,** *3* (9), 3366-3374.

104. Zhou, Z.; Calabrese, D. R.; Taylor, W.; Finlay, J. A.; Callow, M. E.; Callow, J. A.; Fischer, D.; Kramer, E. J.; Ober, C. K., Amphiphilic triblock copolymers with PEGylated hydrocarbon structures as environmentally friendly marine antifouling and fouling-release coatings. *Biofouling* **2014,** *30* (5), 589-604.

105. Calabrese, D. R.; Wenning, B.; Finlay, J. A.; Callow, M. E.; Callow, J. A.; Fischer, D.; Ober, C. K., Amphiphilic oligopeptides grafted to PDMS-based diblock copolymers for use in antifouling and fouling release coatings. *Polymers for Advanced Technologies* **2015,** *26* (7), 829-836.

106. Noguer, A. C.; Olsen, S. M.; Hvilsted, S.; Kiil, S., Diffusion of surface-active amphiphiles in silicone-based fouling-release coatings. *Progress in Organic Coatings* **2017,** *106*, 77-86.

107. Berndt, E.; Behnke, S.; Dannehl, A.; Gajda, A.; Wingender, J.; Ulbricht, M., Functional coatings for anti-biofouling applications by surface segregation of block copolymer additives. *Polymer* **2010,** *51* (25), 5910-5920.

108. Faÿ, F.; Hawkins, M. L.; Réhel, K.; Grunlan, M. A.; Linossier, I., Non-toxic, anti-fouling silicones with variable PEO–silane amphiphile content. *Green Materials* **2016,** *4* (2), 53-62.

109. Rufin, M. A.; Ngo, B. K. D.; Barry, M. E.; Page, V. M.; Hawkins, M. L.; Stafslien, S. J.; Grunlan, M. A., Antifouling silicones based on surface-modifying additive amphiphiles. *Green Materials* **2017**, 1-10.

110. Murthy, R.; Cox, C. D.; Hahn, M. S.; Grunlan, M. A., Protein-resistant silicones: incorporation of poly (ethylene oxide) via siloxane tethers. *Biomacromolecules* **2007,** *8* (10), 3244-3252.

111. Rufin, M. A.; Barry, M. E.; Adair, P. A.; Hawkins, M. L.; Raymond, J. E.; Grunlan, M. A., Protein resistance efficacy of PEO-silane amphiphiles: Dependence on PEO-segment length and concentration. *Acta Biomaterialia* **2016,** *41*, 247-252.

112. Thorlaksen, P. C. W., Novel fouling control coating compositions. US 20140170426 A1, **June 19, 2014**.

113. Williams, D. N.; Stark, D. A.; Lee, A. J.; Davies, C. M., Antifouling coating composition based on curable polyorganosiloxane polyoxyalkylene copolymers. US 8450443 B2, **May 28, 2013**.

114. Bodkhe, R. B.; Stafslien, S. J.; Daniels, J.; Cilz, N.; Muelhberg, A. J.; Thompson, S. E. M.; Callow, M. E.; Callow, J. A.; Webster, D. C., Zwitterionic siloxane-polyurethane fouling-release coatings. *Progress in Organic Coatings* **2015,** *78*, 369-380.

115. Jiang, S.; Cao, Z., Ultralow-fouling, functionalizable, and hydrolyzable zwitterionic materials and their derivatives for biological applications. *Advanced Materials* **2010,** *22* (9), 920-932.

116. Vaisocherova, H.; Yang, W.; Zhang, Z.; Cao, Z.; Cheng, G.; Piliarik, M.; Homola, J.; Jiang, S., Ultralow fouling and functionalizable surface chemistry based on a zwitterionic polymer enabling sensitive and specific protein detection in undiluted blood plasma. *Analytical Chemistry* **2008,** *80* (20), 7894-7901.

117. Chen, S.; Zheng, J.; Li, L.; Jiang, S., Strong resistance of phosphorylcholine self-assembled monolayers to protein adsorption: insights into nonfouling properties of zwitterionic materials. *Journal of the American Chemical Society* **2005,** *127* (41), 14473-14478.

118. He, Y.; Hower, J.; Chen, S.; Bernards, M. T.; Chang, Y.; Jiang, S., Molecular simulation studies of protein interactions with zwitterionic phosphorylcholine self-assembled monolayers in the presence of water. *Langmuir* **2008,** *24* (18), 10358-10364.

119. Aldred, N.; Li, G.; Gao, Y.; Clare, A. S.; Jiang, S., Modulation of barnacle (Balanus amphitrite Darwin) cyprid settlement behavior by sulfobetaine and carboxybetaine methacrylate polymer coatings. *Biofouling* **2010,** *26* (6), 673-683.

120. Cheng, G.; Li, G.; Xue, H.; Chen, S.; Bryers, J. D.; Jiang, S., Zwitterionic carboxybetaine polymer surfaces and their resistance to long-term biofilm formation. *Biomaterials* **2009,** *30* (28), 5234-5240.

121. Bauer, S.; Alles, M.; Finlay, J. A.; Callow, J. A.; Callow, M. E.; Rosenhahn, A., Influence of zwitterionic SAMs on protein adsorption and the attachment of algal cells. *Journal of Biomaterials Science, Polymer Edition* **2014,** *25* (14-15), 1530-1539.

122. Quintana, R.; Gosa, M.; Jańczewski, D.; Kutnyanszky, E.; Vancso, G. J., Enhanced stability of low fouling zwitterionic polymer brushes in seawater with diblock architecture. *Langmuir* **2013,** *29* (34), 10859-10867.

123. Zhang, Z.; Finlay, J. A.; Wang, L.; Gao, Y.; Callow, J. A.; Callow, M. E.; Jiang, S., Polysulfobetaine-grafted surfaces as environmentally benign ultralow fouling marine coatings. *Langmuir* **2009,** *25* (23), 13516-13521.

124. Gao, C.; Li, G.; Xue, H.; Yang, W.; Zhang, F.; Jiang, S., Functionalizable and ultra-low fouling zwitterionic surfaces via adhesive mussel mimetic linkages. *Biomaterials* **2010,** *31* (7), 1486-1492.

125. Li, G.; Cheng, G.; Xue, H.; Chen, S.; Zhang, F.; Jiang, S., Ultra low fouling zwitterionic polymers with a biomimetic adhesive group. *Biomaterials* **2008,** *29* (35), 4592-4597.

126. Kuang, J.; Messersmith, P. B., Universal surface-initiated polymerization of antifouling zwitterionic brushes using a mussel-mimetic peptide initiator. *Langmuir* **2012,** *28* (18), 7258-7266.

127. Li, G.; Xue, H.; Cheng, G.; Chen, S.; Zhang, F.; Jiang, S., Ultralow fouling zwitterionic polymers grafted from surfaces covered with an initiator via an adhesive mussel mimetic linkage. *The Journal of Physical Chemistry B* **2008,** *112* (48), 15269-15274.

128. Donlan, R. M., Biofilm formation: a clinically relevant microbiological process. *Clinical Infectious Diseases* **2001,** *33* (8), 1387-1392.

129. Hasan, J.; Crawford, R. J.; Ivanova, E. P., Antibacterial surfaces: the quest for a new generation of biomaterials. *Trends in Biotechnology* **2013,** *31* (5), 295-304.

130. Knetsch, M. L. W.; Koole, L. H., New strategies in the development of antimicrobial coatings: the example of increasing usage of silver and silver nanoparticles. *Polymers* **2011,** *3* (1), 340-366.

131. Gordon, O.; Slenters, T. V.; Brunetto, P. S.; Villaruz, A. E.; Sturdevant, D. E.; Otto, M.; Landmann, R.; Fromm, K. M., Silver coordination polymers for prevention of implant infection: thiol interaction, impact on respiratory chain enzymes, and hydroxyl radical induction. *Antimicrobial Agents and Chemotherapy* **2010,** *54* (10), 4208-4218.

132. Charnley, M.; Textor, M.; Acikgoz, C., Designed polymer structures with antifouling–antimicrobial properties. *Reactive and Functional Polymers* **2011,** *71* (3), 329-334.

133. Onaizi, S. A.; Leong, S. S. J., Tethering antimicrobial peptides: current status and potential challenges. *Biotechnology Advances* **2011,** *29* (1), 67-74.

134. Glinel, K.; Jonas, A. M.; Jouenne, T.; Leprince, J.; Galas, L.; Huck, W. T. S., Antibacterial and antifouling polymer brushes incorporating antimicrobial peptide. *Bioconjugate Chemistry* **2008,** *20* (1), 71-77.

135. Som, A.; Vemparala, S.; Ivanov, I.; Tew, G. N., Synthetic mimics of antimicrobial peptides. *Peptide Science* **2008,** *90* (2), 83-93.

136. Damodaran, V. B.; Murthy, N. S., Bio-inspired strategies for designing antifouling biomaterials. *Biomaterials Research* **2016,** *20* (1), 18.

137. Statz, A. R.; Meagher, R. J.; Barron, A. E.; Messersmith, P. B., New peptidomimetic polymers for antifouling surfaces. *Journal of the American Chemical Society* **2005,** *127* (22), 7972-7973.

138. Lin, J.; Qiu, S.; Lewis, K.; Klibanov, A. M., Mechanism of bactericidal and fungicidal activities of textiles covalently modified with alkylated polyethylenimine. *Biotechnology and Bioengineering* **2003,** *83* (2), 168-172.

139. Thallinger, B.; Prasetyo, E. N.; Nyanhongo, G. S.; Guebitz, G. M., Antimicrobial enzymes: an emerging strategy to fight microbes and microbial biofilms. *Biotechnology Journal* **2013,** *8* (1), 97-109.

140. Fik, C. P.; Krumm, C.; Muennig, C.; Baur, T. I.; Salz, U.; Bock, T.; Tiller, J. C., Impact of functional satellite groups on the antimicrobial activity and hemocompatibility of telechelic poly (2-methyloxazoline) s. *Biomacromolecules* **2011,** *13* (1), 165-172.

141. Waschinski, C. J.; Barnert, S.; Theobald, A.; Schubert, R.; Kleinschmidt, F.; Hoffmann, A.; Saalwächter, K.; Tiller, J. C., Insights in the antibacterial action of poly (methyloxazoline) s with a biocidal end group and varying satellite groups. *Biomacromolecules* **2008,** *9* (7), 1764-1771.

142. Murata, H.; Koepsel, R. R.; Matyjaszewski, K.; Russell, A. J., Permanent, non-leaching antibacterial surfaces—2: How high density cationic surfaces kill bacterial cells. *Biomaterials* **2007,** *28* (32), 4870-4879.

143. Buffet-Bataillon, S.; Tattevin, P.; Bonnaure-Mallet, M.; Jolivet-Gougeon, A., Emergence of resistance to antibacterial agents: the role of quaternary ammonium compounds—a critical review. *International Journal of Antimicrobial Agents* **2012,** *39* (5), 381-389.

144. Gilbert, P.; Moore, L. E., Cationic antiseptics: diversity of action under a common epithet. *Journal of Applied Microbiology* **2005,** *99* (4), 703-715.

145. Venkataraman, S.; Zhang, Y.; Liu, L.; Yang, Y.-Y., Design, syntheses and evaluation of hemocompatible pegylated-antimicrobial polymers with well-controlled molecular structures. *Biomaterials* **2010,** *31* (7), 1751-1756.

146. Brizzolara, R. A.; Stamper, D. M., The effect of covalent surface immobilization on the bactericidal efficacy of a quaternary ammonium compound. *Surface and Interface Analysis* **2007,** *39* (7), 559-566.

147. Waschinski, C. J.; Zimmermann, J.; Salz, U.; Hutzler, R.; Sadowski, G.; Tiller, J. C., Design of Contact-Active Antimicrobial Acrylate-Based Materials Using Biocidal Macromers. *Advanced Materials* **2008,** *20* (1), 104-108.

148. Broxton, P.; Woodcock, P. M.; Gilbert, P., A study of the antibacterial activity of some polyhexamethylene biguanides towards Escherichia coli ATCC 8739. *Journal of Applied Microbiology* **1983,** *54* (3), 345-353.

149. Ikeda, T.; Yamaguchi, H.; Tazuke, S., New polymeric biocides: synthesis and antibacterial activities of polycations with pendant biguanide groups. *Antimicrobial Agents and Chemotherapy* **1984,** *26* (2), 139-144.

150. Kawabata, N.; Nishiguchi, M., Antibacterial activity of soluble pyridinium-type polymers. *Applied and Environmental Microbiology* **1988,** *54* (10), 2532-2535.

151. Tiller, J. C.; Liao, C.-J.; Lewis, K.; Klibanov, A. M., Designing surfaces that kill bacteria on contact. *Proceedings of the National Academy of Sciences* **2001,** *98* (11), 5981-5985.

152. Fuchs, A. D.; Tiller, J. C., Contact-Active Antimicrobial Coatings Derived from Aqueous Suspensions. *Angewandte Chemie International Edition* **2006,** *45* (40), 6759-6762.

153. Liu, K.; Jiang, L., Bio-inspired design of multiscale structures for function integration. *Nano Today* **2011,** *6* (2), 155-175.

154. Ivanova, E. P.; Hasan, J.; Webb, H. K.; Truong, V. K.; Watson, G. S.; Watson, J. A.; Baulin, V. A.; Pogodin, S.; Wang, J. Y.; Tobin, M. J., Natural bactericidal surfaces: mechanical rupture of Pseudomonas aeruginosa cells by cicada wings. *Small* **2012,** *8* (16), 2489-2494.

155. Pogodin, S.; Hasan, J.; Baulin, V. A.; Webb, H. K.; Truong, V. K.; Nguyen, T. H. P.; Boshkovikj, V.; Fluke, C. J.; Watson, G. S.; Watson, J. A., Biophysical model of bacterial cell interactions with nanopatterned cicada wing surfaces. *Biophysical Journal* **2013,** *104* (4), 835-840.

156. Hasan, J.; Raj, S.; Yadav, L.; Chatterjee, K., Engineering a nanostructured “super surface” with superhydrophobic and superkilling properties. *RSC Advances* **2015,** *5* (56), 44953-44959.

157. Xue, F.; Liu, J.; Guo, L.; Zhang, L.; Li, Q., Theoretical study on the bactericidal nature of nanopatterned surfaces. *Journal of Theoretical Biology* **2015,** *385*, 1-7.

158. Leslie, D. C.; Waterhouse, A.; Berthet, J. B.; Valentin, T. M.; Watters, A. L.; Jain, A.; Kim, P.; Hatton, B. D.; Nedder, A.; Donovan, K., A bioinspired omniphobic surface coating on medical devices prevents thrombosis and biofouling. *Nature Biotechnology* **2014,** *32* (11), 1134-1140.

159. Banerjee, I.; Pangule, R. C.; Kane, R. S., Antifouling coatings: recent developments in the design of surfaces that prevent fouling by proteins, bacteria, and marine organisms. *Advanced Materials* **2011,** *23* (6), 690-718.

160. Dalsin, J. L.; Messersmith, P. B., Bioinspired antifouling polymers. *Materials Today* **2005,** *8* (9), 38-46.

161. Krishnan, S.; Weinman, C. J.; Ober, C. K., Advances in polymers for anti-biofouling surfaces. *Journal of Materials Chemistry* **2008,** *18* (29), 3405-3413.

162. Yoshimoto, K.; Nishio, M.; Sugasawa, H.; Nagasaki, Y., Direct observation of adsorption-induced inactivation of antibody fragments surrounded by mixed-PEG layer on a gold surface. *Journal of the American Chemical Society* **2010,** *132* (23), 7982-7989.

163. Sofia, S. J.; Premnath, V.; Merrill, E. W., Poly (ethylene oxide) grafted to silicon surfaces: grafting density and protein adsorption. *Macromolecules* **1998,** *31* (15), 5059-5070.

164. Harder, P.; Grunze, M.; Dahint, R.; Whitesides, G. M.; Laibinis, P. E., Molecular conformation in oligo (ethylene glycol)-terminated self-assembled monolayers on gold and silver surfaces determines their ability to resist protein adsorption. *The Journal of Physical Chemistry B* **1998,** *102* (2), 426-436.

165. Zheng, J.; Li, L.; Chen, S.; Jiang, S., Molecular simulation study of water interactions with oligo (ethylene glycol)-terminated alkanethiol self-assembled monolayers. *Langmuir* **2004,** *20* (20), 8931-8938.

166. Kingshott, P.; Wei, J.; Bagge-Ravn, D.; Gadegaard, N.; Gram, L., Covalent attachment of poly (ethylene glycol) to surfaces, critical for reducing bacterial adhesion. *Langmuir* **2003,** *19* (17), 6912-6921.

167. Harbers, G. M.; Emoto, K.; Greef, C.; Metzger, S. W.; Woodward, H. N.; Mascali, J. J.; Grainger, D. W.; Lochhead, M. J., Functionalized poly (ethylene glycol)-based bioassay surface chemistry that facilitates bio-immobilization and inhibits nonspecific protein, bacterial, and mammalian cell adhesion. *Chemistry of Materials* **2007,** *19* (18), 4405-4414.

168. Branch, D. W.; Wheeler, B. C.; Brewer, G. J.; Leckband, D. E., Long-term stability of grafted polyethylene glycol surfaces for use with microstamped substrates in neuronal cell culture. *Biomaterials* **2001,** *22* (10), 1035-1047.

169. Victor, R., Poly (2-oxazoline) s as materials for biomedical applications. *Journal of Materials Science: Materials in Medicine* **2014,** *25* (5), 1211-1225.

170. Konradi, R.; Pidhatika, B.; Mühlebach, A.; Textor, M., Poly-2-methyl-2-oxazoline: a peptide-like polymer for protein-repellent surfaces. *Langmuir* **2008,** *24* (3), 613-616.

171. Pidhatika, B.; Möller, J.; Vogel, V.; Konradi, R., Nonfouling surface coatings based on poly (2-methyl-2-oxazoline). *CHIMIA International Journal for Chemistry* **2008,** *62* (4), 264-269.

172. Cho, W. K.; Kong, B.; Choi, I. S., Highly efficient non-biofouling coating of zwitterionic polymers: poly ((3-(methacryloylamino) propyl)-dimethyl (3-sulfopropyl) ammonium hydroxide). *Langmuir* **2007,** *23* (10), 5678-5682.

173. Chang, Y.; Liao, S.-C.; Higuchi, A.; Ruaan, R.-C.; Chu, C.-W.; Chen, W.-Y., A highly stable nonbiofouling surface with well-packed grafted zwitterionic polysulfobetaine for plasma protein repulsion. *Langmuir* **2008,** *24* (10), 5453-5458.

174. Yoshimoto, K.; Hirase, T.; Madsen, J.; Armes, S. P.; Nagasaki, Y., Non-fouling character of poly[2-(methacryloyloxy) ethyl phosphorylcholine]-modified gold surfaces fabricated by the 'grafting to' method: comparison of its protein resistance with poly(ethylene glycol)-modified gold surfaces. *Macromolecular Rapid Communications* **2009,** *30* (24), 2136-2140.

175. Cheng, G.; Zhang, Z.; Chen, S.; Bryers, J. D.; Jiang, S., Inhibition of bacterial adhesion and biofilm formation on zwitterionic surfaces. *Biomaterials* **2007,** *28* (29), 4192-4199.

176. Nath, N.; Hyun, J.; Ma, H.; Chilkoti, A., Surface engineering strategies for control of protein and cell interactions. *Surface Science* **2004,** *570* (1), 98-110.

177. Stadler, V.; Kirmse, R.; Beyer, M.; Breitling, F.; Ludwig, T.; Bischoff, F. R., PEGMA/MMA copolymer graftings: generation, protein resistance, and a hydrophobic domain. *Langmuir* **2008,** *24* (15), 8151-8157.

178. Tugulu, S.; Klok, H.-A., Stability and nonfouling properties of poly (poly (ethylene glycol) methacrylate) brushes under cell culture conditions. *Biomacromolecules* **2008,** *9* (3), 906-912.

179. Yoshikawa, C.; Goto, A.; Tsujii, Y.; Fukuda, T.; Kimura, T.; Yamamoto, K.; Kishida, A., Protein repellency of well-defined, concentrated poly (2-hydroxyethyl methacrylate) brushes by the size-exclusion effect. *Macromolecules* **2006,** *39* (6), 2284-2290.

180. Yoshikawa, C.; Goto, A.; Ishizuka, N.; Nakanishi, K.; Kishida, A.; Tsujii, Y.; Fukuda, T. Size-exclusion effect and protein repellency of concentrated polymer brushes prepared by surface-initiated living radical polymerization. *Macromolecular Symposia* **2007,** *248* (1), 189-198.

181. Yoshikawa, C.; Goto, A.; Tsujii, Y.; Ishizuka, N.; Nakanishi, K.; Fukuda, T., Surface interaction of well-defined, concentrated poly (2-hydroxyethyl methacrylate) brushes with proteins. *Journal of Polymer Science Part A: Polymer Chemistry* **2007,** *45* (21), 4795-4803.

182. Cringus-Fundeanu, I.; Luijten, J.; van der Mei, H. C.; Busscher, H. J.; Schouten, A. J., Synthesis and characterization of surface-grafted polyacrylamide brushes and their inhibition of microbial adhesion. *Langmuir* **2007,** *23* (9), 5120-5126.

183. Cheng, G.; Xue, H.; Zhang, Z.; Chen, S.; Jiang, S., A switchable biocompatible polymer surface with self-sterilizing and nonfouling capabilities. *Angewandte Chemie International Edition* **2008,** *47* (46), 8831-8834.

184. Wach, J. Y.; Bonazzi, S.; Gademann, K., Antimicrobial surfaces through natural product hybrids. *Angewandte Chemie International Edition* **2008,** *47* (37), 7123-7126.

185. Guan, J.; Song, Y.; Lin, Y.; Yin, X.; Zuo, M.; Zhao, Y.; Tao, X.; Zheng, Q., Progress in study of non-isocyanate polyurethane. *Industrial & Engineering Chemistry Research* **2011,** *50* (11), 6517-6527.

186. Baur, X.; Marek, W.; Ammon, J.; Czuppon, A. B.; Marczynski, B.; Raulf-Heimsoth, M.; Roemmelt, H.; Fruhmann, G., Respiratory and other hazards of isocyanates. *International Archives of Occupational and Environmental Health* **1994,** *66* (3), 141-152.

187. Zapp Jr, J. A., Hazards of isocyanates in polyurethane foam plastic production. *Arch. Indust. Health* **1957,** *15* (4), 324-30.

188. O'Brien, I. M.; Harries, M. G.; Burge, P. S.; Pepys, J., Toluene di-isocyanate-induced asthma I. Reactions to TDI, MDI, HDI and histamine. *Clinical & Experimental Allergy* **1979,** *9* (1), 1-6.

189. Tanser, A. R.; Bourke, M. P.; Blandford, A. G., Isocyanate asthma: respiratory symptoms caused by diphenyl-methane di-isocyanate. *Thorax* **1973,** *28* (5), 596-600.

190. Rokicki, G.; Parzuchowski, P. G.; Mazurek, M., Non-isocyanate polyurethanes: synthesis, properties, and applications. *Polymers for Advanced Technologies* **2015,** *26* (7), 707-761.

191. Edwards, P. A.; Striemer, G.; Webster, D. C., Novel polyurethane coating technology through glycidyl carbamate chemistry. *JCT Research* **2005,** *2* (7), 517-527.

192. Edwards, P. A.; Striemer, G.; Webster, D. C., Synthesis, characterization and self-crosslinking of glycidyl carbamate functional resins. *Progress in Organic Coatings* **2006,** *57* (2), 128-139.

193. Chattopadhyay, D. K.; Muehlberg, A. J.; Webster, D. C., Organic–inorganic hybrid coatings prepared from glycidyl carbamate resins and amino-functional silanes. *Progress in Organic Coatings* **2008,** *63* (4), 405-415.

194. Chattopadhyay, D. K.; Zakula, A. D.; Webster, D. C., Organic–inorganic hybrid coatings prepared from glycidyl carbamate resin, 3-aminopropyl trimethoxy silane and tetraethoxyorthosilicate. *Progress in Organic Coatings* **2009,** *64* (2), 128-137.

195. Chattopadhyay, D. K.; Webster, D. C., Hybrid coatings from novel silane-modified glycidyl carbamate resins and amine crosslinkers. *Progress in Organic Coatings* **2009,** *66* (*1*), 73-85.

196. Harkal, U. D.; Muehlberg, A. J.; Li, J.; Garrett, J. T.; Webster, D. C., The influence of structural modification and composition of glycidyl carbamate resins on their viscosity and coating performance. *Journal of Coatings Technology and Research* **2010,** *7* (5), 531-546.

197. Harkal, U. D.; Muehlberg, A. J.; Edwards, P. A.; Webster, D. C., Novel water-dispersible glycidyl carbamate (GC) resins and waterborne amine-cured coatings. *Journal of Coatings Technology and Research* **2011,** *8* (6), 735-747.

198. Harkal, U. D.; Muehlberg, A. J.; Webster, D. C., UV curable glycidyl carbamate based resins. *Progress in Organic Coatings* **2012,** *73* (1), 19-25.

199. Ravindran, N.; Chattopadhyay, D. K.; Zakula, A.; Battocchi, D.; Webster, D. C.; Bierwagen, G. P., Thermal stability of magnesium-rich primers based on glycidyl carbamate resins. *Polymer Degradation and Stability* **2010,** *95* (7), 1160-1166.

200. Harkal, U. D.; Muehlberg, A. J.; Webster, D. C., Linear glycidyl carbamate (GC) resins for highly flexible coatings. *Journal of Coatings Technology and Research* **2013,** *10* (2), 141-151.

CHAPTER 2. EFFECT OF SURFACE ABRASIONS ON FOULING-RELEASE PERFORMANCE OF SELF-STRATIFIED SILOXANE-POLYURETHANE FOULING-RELEASE MARINE COATINGS

Introduction

Marine biofouling is the unwanted accumulation, attachment, and growth of microorganisms, plants, and animals on surfaces submerged in natural bodies of water.[1] In general, there are four stages of biofouling: accumulation of a layer of organic molecules (called conditioning layer) like proteins and polysaccharides,[1] accumulation of microorganisms like diatoms and bacteria, settlement of algal species and finally, attachment of macrofoulants like barnacles and mussels.[2] Biofouling results in approximately 2% reduction in the speed of the ship, up to 45% increase in fuel consumption,[2] and combating biofouling can cost as high as one billion dollars annually.[3] Traditionally, antifouling coatings containing tin, copper or organic biocides have been used to combat biofouling.[2] The biocides from the anti-fouling coatings leach out to prevent the accumulation of the marine organisms on the ship hulls.[4] The potential hazards associated with the toxic leachates have necessitated the need to replace these anti-fouling coatings.[3] Fouling release (FR) coatings have been developed as alternate environment-friendly marine coatings.[4] FR coatings allow weak attachment of the organism on the surface, which can be easily broken by the hydrodynamic forces, experienced during the movement of the ship.[5] Commercial FR coatings are based exclusively on silicone elastomers. Lack of mechanical strength, poor adhesion to metal substrates, and low durability of the commercial coatings make them less viable for marine applications.[4] In one such attempt, the siloxane (Si)-polyurethane (PU) FR coating system has been developed as a potential substitute to the anti-fouling and the commercial FR coatings. The polyurethane matrix provides the necessary adhesion and mechanical strength. The siloxane self-stratifies due to surface energy minimization, forming the outer low surface energy layer of the coating.[4, 6] In general, low surface energy materials have been shown to disallow attachment of organisms to the surface, out of which PDMS is the most preferred material.

Chemical composition of the surface determines the extent of “wetting”. Wettability is also a function of the surface topography, which can be tailored as per requirement.[7] Water contact angle greater than 90° indicates a hydrophobic surface, while values lower than 90° indicate a hydrophilic

surface. Abrading a hydrophobic or hydrophilic surface increases the surface area, thereby enhancing the hydrophobicity or hydrophilicity of the surface.[7] But the different attachment mechanisms of the different marine organisms make it difficult to base the FR properties of the coatings on hydrophobicity or hydrophilicity alone.

Another approach to improve the FR performance of the coatings involves tailoring the surface topography by the formation of nano- and micro-gradients on the surface. Biomimetic approaches have shown potential as novel and futuristic FR systems. One such biomimetic surface, based on the Lotus leaf, exhibits an inherent tendency to repel water because of its waxy nature with nanoscopic surface gradients, rendering the surface superhydrophobic (water contact angle greater than 150°).[7] But the biggest challenge with synthetic Lotus leaf- like surfaces is maintaining the characteristic superhydrophobicity of the surface for longer duration. Similar to the Lotus leaf, another interesting approach is mimicking shark skin on synthetic surfaces. Sharklet AF™ coatings with shark skin topography have shown significant improvement in FR performance of coatings as compared to regular smooth coatings. Further analysis of the biomimetic Sharklet AF™ AF coating indicated the dependence of the FR performance on the size and shape of the surface features. For example, the Sharklet AF™ topography with 3 µm feature height reduced the algal settlement by 63%. Similarly, a feature height of 40 µm showed 97% reduction in barnacle attachment on barnacle specific Sharklet AF™ AF coatings.[8] Marine organisms adhere to ship hulls by secreting proteinaceous adhesives.[9] But, proteins conform irreversibly onto hydrophobic surfaces.[7] Factors such as “wetting” of the surface and interlocking of the organism adhesive play an important role in determining the strength of attachment between the organism and the surface.[10] The surface features provide contact points, which support growth and metamorphosis of the organism, with higher number of contact points resulting in higher attachment of the organism. Marine organisms show less tendency to attach onto surfaces with features less than the size of the organism.[10, 11] To further understand the attachment behavior of the organism, engineering models have been devised to study the surfaces with distinct localized textures that provide insights into techniques to deter the marine foulants.[12] Generation of stresses in the bulk of the organism due to variations in the size and shape of the features renders the surface less conducive to the growth and metamorphosis of the organism.[13] Attachment point theory deals with the creation of such non-equilibrium

in the organism.[13, 14] Later, Engineered Roughness Index (ERI) was developed to understand the effect of the feature size and geometry on the attachment behavior of the organism.[15] ERI is a dimensionless quantity that correlates Wenzel's roughness factor with the degrees of freedom of movement and the amount of depressed surface.[9] According to ERI theory, continuous recessed grooves show greater tendency of settlement than isolated ones, since degree of freedom is comparatively higher in case of a continuous network.[15] ERI theory also predicts critical sizes of the features for optimum performance of the surface to be 2 µm for algal spores and 20 µm for barnacle cyprids. For instance, cyprids did not settle on PDMS with gradient size 256 µm, because the groove hampers metamorphosis and interferes with the growth of the cyprids.[10] Furthermore, the surface energetic attachment (SEA) model, which serves as a combination of both the attachment point theory and the ERI, predicts the settlement of the organisms with respect to the number, the size, and the geometry of the surface topography.[16] In spite of theoretical development of an optimized surface to deter most of the organisms, it is difficult to accurately predict the practical performance of the textured coatings because of the variations in the different attachment behavior of the target organisms.[7, 9, 16]

Although the self-stratified SiPU coatings exhibit FR performance on par with commercial silicone elastomer coatings, one question that remains unanswered is the performance of the coatings upon damage, that can be encountered in use such as damage due to suspended dirt or sand or use of cleaning tools. To understand the effect of surface damage on the FR performance of the SiPU coatings, the coatings were abraded using two different Scotch Brite pads. The number of abrasions were varied. Additional weights were applied depending on the roughness of the Scotch Brite pads. The smooth and the abraded coatings were characterized using contact angle experiment, SEM and XPS to analyze the surface topography and the surface composition of the SiPU coatings. Lastly, FR performance of the coatings with respect to micro- and macrofoulants was evaluated. The results obtained led to the hypothesis that the FR performance of the SiPU coatings is a function of the size of the features formed after abrasions relative to the size of the fouling organism. Detailed analysis of the surface features further supported this hypothesis.

Experimental Section

Materials

Trimer of isophorone diisocyanate (IPDI trimer; Desmodur Z 4470BA) was provided by Covestro (Bayer MaterialScience). Catalyst dibutyltin diacetate (DBTDAc), pot-life extender acetylacetone and solvents, 2-heptanone and toluene, were purchased from Sigma Aldrich.

Hydroxy terminated acrylic polyol was synthesized using butyl acrylate and hydroxyethyl acrylate by free radical polymerization, according to a previously published procedure.[5] Hydroxyethyl acrylate and butyl acrylate were purchased from Sigma Aldrich. Initiator Vazo 67 was provided by The Chemours Company (Dupont). Briefly, a monomer mixture of butyl acrylate, hydroxyethyl acrylate, and initiator Vazo 67 was added dropwise to a round bottom flask that was charged with toluene. Temperature was maintained between 85-95°C. After completion of monomer addition, the reaction was allowed to continue for 2 hours. A chaser solution of Vazo 67 and toluene was then added to the reaction mixture. The reaction is allowed to proceed for another 3 hours. Finally, the mixture was cooled to room temperature. Concentration of the synthesized polyol was determined to be 50% solids in toluene according to ASTM D2369.

Aminopropyl terminated polydimethylsiloxane (APT-PDMS) was synthesized in a fashion similar to the one described in prior publication.[4] Chemicals for the synthesis of APT-PDMS, siloxane monomer (D_4), benzyltrimethylammonium hydroxide and blocker bis(3-aminopropyl)-tetramethyldisiloxane (BAPTDMS) were purchased from Dow Chemical, Sigma Aldrich, and Gelest respectively. D_4, (BAPTDMS), and benzyltrimethylammonium hydroxide solution (40% in methanol) were equilibrated at 80°C for 24 hours in a round bottom flask, equipped with a nitrogen inlet, condenser, heating mantle, and temperature controller. After 24 hours, temperature was increased to 170°C for 2 hours to decompose the catalyst. The product was cooled to room temperature and stored. MW of the synthesized APT-PDMS was between 18-22k g/mol, as determined from GPC.

Coating Formulation and Application

Based on the results obtained from the previous studies, “A4” coating formulation was selected for the abrasion study.[5] 20% by weight APT-PDMS was mixed with the synthesized acrylic polyol and 10% by weight acetylacetone (pot-life extender). The solution was stirred overnight to compatibilize APT-

PDMS with the polyol.[5] The next day, IPDI trimer and 0.05% by weight DBTDAc (1% solution in 2-heptanone) was added to the formulation. The formulation was allowed to stir for another 60 minutes. Prior to application of the formulation, aluminum substrates (4 in. x 8 in. x 0.6 mm, type A, alloy 3003 H14 from Q-Lab) were coated with Intergard 264 epoxy primer. The final formulation was applied using a Mayer wire wound rod (RDS 80) on the primed aluminum panels. The coatings were allowed to cure under ambient conditions overnight. After 24 hours, the coatings were oven-cured at 80°C for 45 min to remove any residual solvent. Same formulation was used to make all samples for the study.

Abrasion Experiment

Two different Scotch Brite pads, the scouring pad (SP) and the general purpose pad (GP), were used to abrade the cured A4 coatings. The roughness of SP is significantly lower than that of GP. Therefore, 5 lb (2.25 kg) and 7 lb (3.15 kg) additional weights were applied while using SP. GP was used without (0 lb) any additional weight and 1 lb (0.45 kg) additional weight. A laboratory experimental set up, comprising of a long plastic plank, with a handle on one end and a sponge attached to the plank on the opposite end, was used to abrade the SiPU coatings (Figure 2.1). Abrasion pads were attached to the sponge with the help of Velcro. The level of the plank was maintained parallel to the ground at all times using an adjustable screw attached below the handle. One at a time, the coating panels were taped to the bottom of a plastic tray using an electrical tape to prevent the panels from slipping. 10-15 mL distilled water was poured onto the panels before abrasions to wet the coatings. Additional weights were applied when required, depending on the roughness of the Scotch Brite pads. The plank was moved back and forth manually, with the abrasion pad in contact with the coating. One forward movement of the plank was counted as one abrasion. Combinations of the different Scotch Brite pads, additional weights, and the number of abrasions are tabulated in Table 2.1. In this study, the coatings labels are of the format: abrasion pad_additional weight applied_number of abrasions. For example, SP_5lb_300 stands for a coating abraded with SP under 5 lb additional weight and 300 abrasions.

Table 2.1. Combinations of abrasion pads, additional weights, and number of abrasions.

Abrasion pad	Additional load (lb.)	Number of abrasions
Scouring pad (SP)	5, 7	0, 20, 60, 100, 150, 200, 250, 300
General purpose pad (GP)	0, 1	0, 20, 40, 60, 80, 100, 120, 140, 160, 180, 200, 220

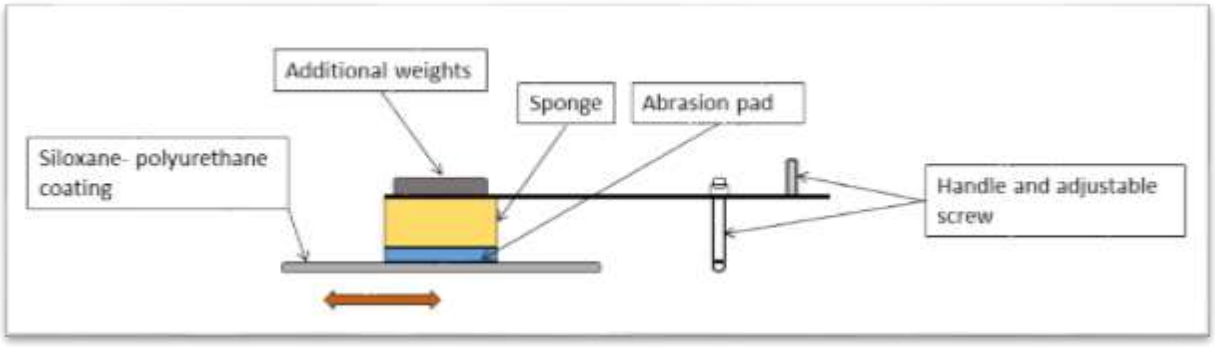

Figure 2.1. Schematic representation of the experimental set up.

Laboratory Biofouling Assays

Preleaching and Leachate Toxicity Analysis

In order to remove toxic leachates, impurities, and catalyst from the smooth and the abraded SiPU coatings, the coatings were placed in a recirculating water tank for four weeks.[5] The coatings were then tested for leachate toxicity by introducing algae in artificial sea water (ASW) with nutrients. The growth of algae on the coatings was observed using fluorescence by obtaining extracts from each coating after 48 hours. The growth of the organisms on the coatings was reported as a fluorescence ratio to a positive growth control. A negative growth control (medium + bacteria + triclosan) was also included in the experiment. The coatings were compared to the negative control to confirm the absence of toxic leachates.[4]

Biofilm Cellulophaga lytica (C.lytica) Adhesion and Removal

Attachment and removal of biofilm *C.lytica* was conducted according to a previous publication.[4, 17-19] Briefly, circular discs were carefully punched from the smooth and the abraded SiPU coating panels. The discs were then glued to 24-well plates using a silicone adhesive from Dow Corning, such that the glue covered the circular basal area of the disc completely. 5% suspension of *C.lytica* in ASW (10^7 cells/mL) with nutrients was prepared. 1 mL suspension was added to each well of the 24-well plates. The well plates were incubated for 24 hours at 28°C to allow colonization of the biofilm on the coating surfaces. The plates were rinsed three times with deionized water to remove any unattached biofilm. Crystal violet was used to stain the samples. Extractions of crystal violet in acetic acid (33%) were observed under 600 nm absorbance to determine the amount of biofilm retained on the coatings. To determine the fouling release performance of the coatings, the plates were subjected to water jets at 10

psi and 20 psi, after 24 hours of the biofilm growth.[20] The first column in each 24-well plates served as bacterial growth before water jetting and was not exposed to the water jet. The second and the third columns were exposed to 10 psi and 20 psi water jet respectively for 5 seconds. The results show the amount of biofilm attached to the coatings before exposure to water jet and percent removal from the coating at 10 psi and 20 psi water jet pressures.

Diatom Navicula incerta (N.incerta) Attachment and Removal

Diatom *N.incerta* adhesion was carried out in a fashion similar to *C.lytica* adhesion explained earlier.[4, 21-24] 24-well plates were prepared by carefully punching out discs from the smooth control and abraded coatings. The plates with the glued discs were treated with 1 mL solution of diatoms in ASW. The plates were incubated for 2 hours to allow diatom adhesion. Fluorescence was used to quantify the algal settlement on the coatings. FR performance of the coatings was determined by exposing the well plates to 10 psi and 20 psi water jet after 2 hours of cell settlement. The first column was used as a reference for the initial cell settlement and was not treated with the water jet. The second and the third columns were exposed to water jet at 10 psi and 20 psi for 10 seconds. This chapter includes results for the amount of diatoms attached to the coatings and percent removal at 20 psi water jet pressure. Removal at 10 psi water jet pressure are not reported since 10 psi pressure could not facilitate sufficient removal of the diatoms from the commercial standards.

Microalgae Ulva linza (U.linza) Removal

Similar to diatoms and biofilm, 24-well assay plates were prepared by carefully punching out discs and gluing the discs from the smooth and select preleached abraded coatings. The coatings chosen for this experiment are the smooth SiPU coating, SP_5lb_300, SP_7lb_300, GP_0lb_220, and GP_1lb_160. The plates were then shipped to Newcastle University (United Kingdom) to determine the FR performance of the coatings against microalgae *U.linza*. Before the bioassay experiment, the assay plates were equilibrated in 0.22 µm ASW for 2 hours. Then, 1 mL *U.linza* sporelings suspension (3.3×10^5 spores/mL) in enriched sea water was dispensed into each of the wells. The spores were grown in an illuminated incubator at 18°C for 6 days. After 6 days, the biomass from a single row of wells (6 wells) was assessed by extracting chlorophyll. Chlorophyll was extracted in 1 mL dimethyl sulfoxide (DMSO). Fluorescence was then determined using excitation of 360 nm and wavelength of 670 nm. To determine

the release performance of the coatings, single rows of wells from each plate was sprayed using a spinjet apparatus at 18, 67 and 111 kPa water pressure. Chlorophyll was again extracted, as explained earlier. Microalgae removal at each pressure was determined by comparing the sprayed and the unsprayed wells. The results were reported as the percent removal of the algal sporelings after exposure to water pressure.

Adult Barnacle Amphibalanus amphitrite (A.amphitrite) Adhesion

Adult barnacle adhesion experiment was conducted to determine the FR performance of the smooth and the abraded coatings against hard foulants.[4, 25, 26] 4 or 5 adult *A.amphitrite* barnacles, with basal diameter of approximately 5 mm, were allowed to grow and attach to the coating panels in ASW for 2 weeks with daily supply of brine shrimp nauplii. After 2 weeks, a hand held digital gauge was used to measure the force required to detach the barnacles from the coatings. Adhesion strength (MPa) of the barnacles was then calculated as the shear force required for barnacle removal to the basal area of the barnacle.

Mussel Geukensia demissa Adhesion

Not just barnacles, the smooth and the abraded coatings were also evaluated for marine mussels *Geukensia demissa* adhesion according to a previously published procedure.[27-29] Marine mussels were received from Duke University Marine Laboratory, North Carolina, USA. Prior to the experiment, each mussel was fitted with an acetal rod (4 cm in length) using a 3M acrylic adhesive. The rods were attached perpendicular to the ventral edge of the mussel. Six mussels were immobilized on the surface of the smooth and abraded SiPU coatings, using a custom designed PVC template. The coatings were placed in ASW and the mussels were fed live marine phytoplankton for 3 days. After 3 days, the number of mussels showing attachment of byssus threads was recorded for each coating. The acetal rods on the mussels were attached to a tensile force gauge, such that all the mussels were pulled from the coating at the same time.

Over the course of the experiment, none of the mussels attached to the smooth or the abraded coatings, irrespective of the abrasion treatment. Therefore, quantitative assessment of mussel adhesion strengths was not possible. Qualitatively, the SiPU coatings successfully deterred attachment of mussels, even after abrasions.

Surface Characterization

A Symyx First Ten Angstrom Coating Surface Energy Measurement System was used to measure water contact angles (WCA) and methylene iodide contact angles (MICA) of the pre-leached smooth and the abraded coatings by the sessile drop method. For each coating, three WCA and MICA were measured at three different spots and analyzed using FTA software. The averages of the three WCA and MICA values were used to calculate the surface energy (SE) values by Owens-Wendt method.[30] WCA and MICA of the coatings were measured once a week for a month for each abraded coating. Statistical analysis was conducted using Minitab 17 software. One-way ANOVA was used to determine statistically significant variations in WCA values with changing surface abrasion treatments. Tukey-Kramer test was used to compare individual values with constant 95% confidence limit. In this study, select coatings, chosen based on FR performance against barnacles, were compared to the smooth SiPU coating. The coatings selected for analysis were the smooth coating, GP_0lb_200, GP_0lb_220, GP_1lb_100, GP_1lb_120, GP_1lb_160, GP_1lb_180, GP_1lb_200, and GP_1lb_220.

A JEOL JSM-6490LV High-Performance Variable Pressure Scanning Electron Microscope (SEM) was used to analyze the surface of the smooth and select abraded coatings. Samples of the smooth SiPU coating, SP_5lb_300, SP_7lb-300, GP_0lb_220, and GP_1lb_160 coatings were coated with a thin layer of gold before imaging. The gold coated samples were then observed under 250, 1000 and 3000 magnifications. The images obtained for the abraded coatings were compared to the images of the smooth SiPU coating.

In order to determine the surface composition of the coatings after abrasions, select coatings were analyzed using a Thermo Scientific KAlpha X-Ray Photoelectron Spectroscopy (XPS) instrument with Al K_α X-ray source (1468.68 eV) and Ar^+ ion source gun (up to 8000 eV) source. Survey spectra and high resolution spectra were taken from surfaces of the smooth SiPU coating, SP_7lb_300, and GP_1lb_160 coatings. High resolution scans were collected at an angle perpendicular to the coating surfaces. The results show a survey scan and atom percent for C1s, O1s, and Si2p elements. The scans were taken at chamber pressure below 1.5×10^{-7} Torr under ambient conditions.

Analysis of Surface Features

In this study, the term “features” represents the valleys or the recessed zones formed on the SiPU surfaces after abrasions. The surfaces of the smooth and select abraded coatings (SP_5lb_300, SP_7lb_300, GP_0lb_220, and GP_1lb_160) were analyzed using a Wyko NT Series Optical Profiler (OP) from Veeco. Magnification was maintained at 10X for all the coatings. Feature depth was considered to be the maximum distance between the highest point and the lowest valley of the feature. Mean roughness depth, R_z, is the average of five deepest features on the area scanned using OP. In this study, the average of five such R_z values for each coating was recorded. Further, Fourier Transform analysis from ImageJ software (Java- based program developed at National Institute of Health) was used to determine the peak to peak distance or width of the features formed on the surface of the select abraded coatings. The results were reported as the average of five feature widths for the select coatings.

Results and Discussion

Self-stratified SiPU FR coatings were synthesized using IPDI trimer, acrylic polyol, and APT-PDMS. Due to the lower surface energy of PDMS and incompatibility between the polar PU and non-polar APT-PDMS phases in the coating system, APT-PDMS stratifies to form the outer layer of the coating.[31] Presence of amine functional groups in APT-PDMS chains keeps the siloxane chains bound to the underlying urethane matrix. The highly crosslinked PU coating matrix provides mechanical strength and high adhesion to the substrate. In the past, extensive research in developing this novel one-pot system showed that the SiPU coatings showed comparable FR performance compared to the commercially available silicone elastomer based FR coatings. In practical applications, ship hulls are cleaned periodically to remove foulants attached to the ship’s surface. The elastomeric commercial coatings are extremely susceptible to damage during such cleaning activities. Although past results showed potentially successful use of the SiPU formulations in practical applications, this study aims at showing effect of abrasions or surface damage on FR performance of SiPU formulations.

After comparing FR performance of previously developed SiPU formulations, formulation with polyisocyanate, acrylic polyol, and 20% APT-PDMS (A4 formulation) was identified as the optimum FR formulation. Therefore, all coatings were made using the A4 formulation. The SiPU coatings were abraded using a laboratory abrasion set up shown in Figure 2.1. Two Scotch Brite pads— scouring pad

(SP) and general purpose pad (GP)— were used to abrade the coatings with varying number of abrasions. Roughness of GP is significantly higher than SP. Therefore, no additional weight (0lb) or 1 lb additional weight was applied during abrasions with GP, but 5 lb and 7 lb additional weight were applied with SP to obtain minimum surface abrasions. The smooth and the abraded SiPU coatings were placed in a pre-leaching water tank to remove catalyst, impurities, and unreacted monomers from the coating films for 28 days. After 28 days, the coatings were analyzed for surface chemistry and topography. Figure 2.2 shows data for WCA and SE for the smooth and the abraded SiPU coatings. WCA for the smooth and the abraded SiPU coatings was greater than 90°. The coatings, thus, retained their hydrophobicity, even after abrasions. Among all the coatings, GP_0lb_80 showed highest WCA of 116° (Figure 2.2(c)). The SE of the coatings ranged from 15 mN/m to 25 mN/m. Statistical analysis was conducted using select WCA values to observe any significant differences in WCA values with changing abrasion treatments over a one month period. For coatings abraded with GP with no additional weight and 200 abrasions (Figure 2.2(c)), WCA values for week 2 to week 4 were significantly different from WCA for week 1; with 220 abrasions, value in week 3 was significantly different from the other three measurements. Similarly, when coatings were abraded using GP under 1 lb additional weight, 3 out of 4 WCA values appeared to show no significant difference. Variations in WCA values of the SiPU coatings (“0” abrasions) can be attributed to rearrangement of PDMS chains on the surface of the smooth and the abraded coatings.[5, 32]

(a)

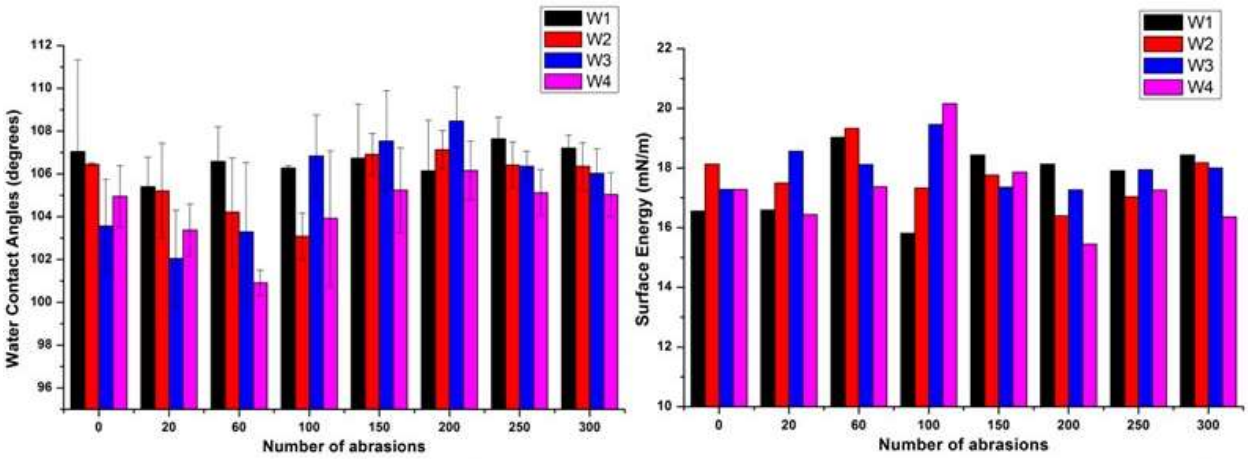

Figure 2.2. WCA and SE values for coatings abraded with SP (a) under 5 lb, and (b) under 7 lb additional loads, and with GP (c) under no additional load, and (d) under 1 lb additional load. Legends W1 to W4 indicate the weeks over which WCA values were measured. Error bars represent standard deviation. Same alphabets on select data points in (c) and (d) indicate values that are not statistically different from one another ($p < 0.001$ for both (c) and (d)).

(b)

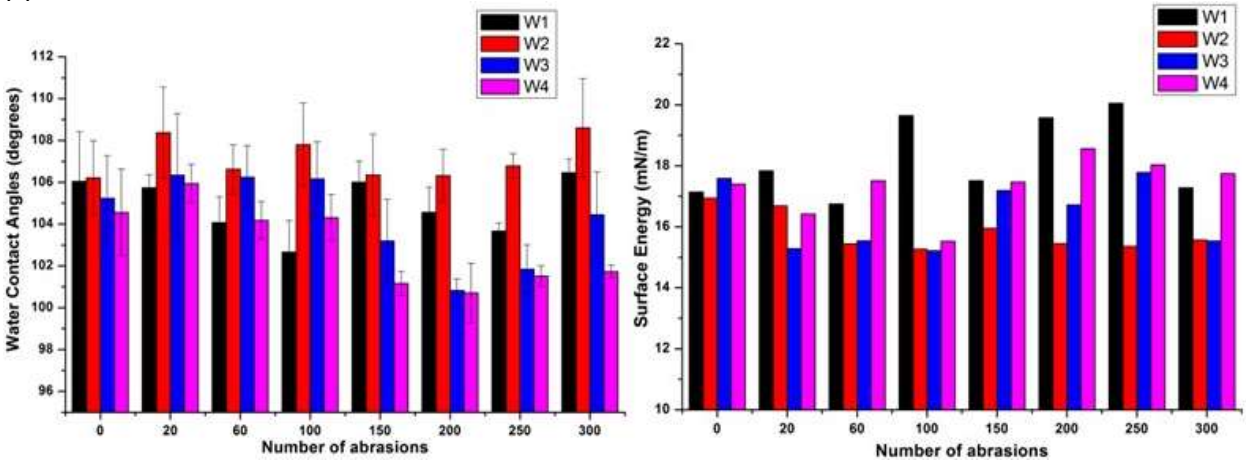

(c)

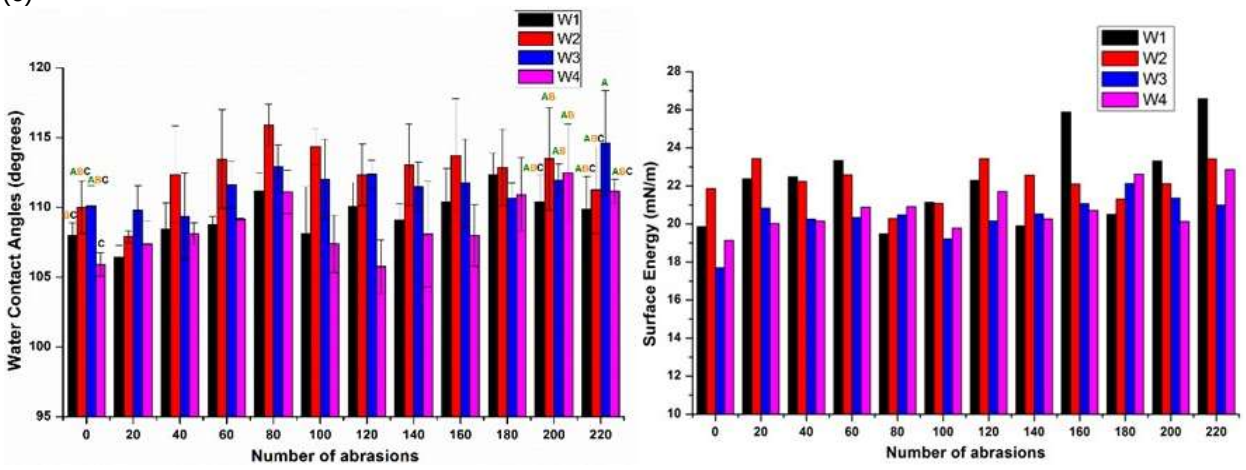

(d)

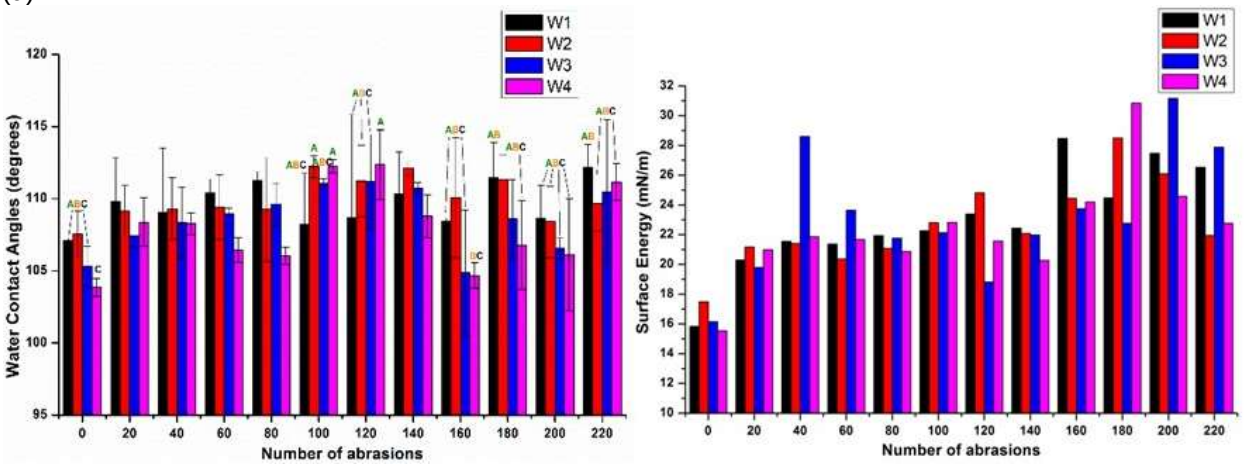

Figure 2.2. WCA and SE values for coatings abraded with SP (a) under 5 lb, and (b) under 7 lb additional loads, and with GP (c) under no additional load, and (d) under 1 lb additional load (continued). Legends W1 to W4 indicate the weeks over which WCA values were measured. Error bars represent standard deviation. Same alphabets on select data points in (c) and (d) indicate values that are not statistically different from one another ($p < 0.001$ for both (c) and (d)).

SEM was used to observe the surface of the smooth and the abraded coatings. Figure 2.3 shows SEM images for the smooth and the abraded SiPU coatings. As expected, the smooth SiPU coating was devoid of any surface abrasions or “features”. Minor defects present on the smooth surface may have been from impurities on the coating substrate. Coatings abraded using SP showed formation of small, randomly distributed “scratches” on the coating surface. More “scratches” were formed from abrading the SiPU coatings with GP, a pad with significantly higher roughness. Roughness of the coatings abraded using GP was significantly higher than the coatings abraded using SP. Since all the coatings were abraded along the length of the coating, the abrasions formed continuous parallel “channels” along the length of the coating.

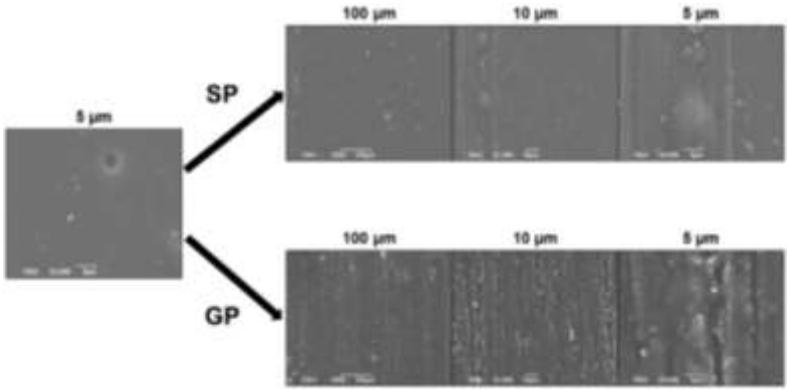

Figure 2.3. Comparison of SEM scans of the smooth and the abraded SiPU coatings. All surfaces abraded with the same abrasion pad (SP or GP), irrespective of the number of abrasions, looked similar.

The pre-leached SiPU coatings were analyzed for their FR behavior against micro- and macrofoulants like biofilm, diatoms, microalgae, barnacles, and mussels. The FR performance of the SiPU coatings were compared to the performance of the commercial FR coatings like Silastic T2, Intersleek 700, Intersleek 900, and a regular polyurethane coating (no siloxane). Figure 2.4 shows attachment and removal of biofilm *C.lytica* from all the SiPU coatings. In general, the amount of biofilm attached to the coating increased with increasing roughness of the coatings. Most of the abraded coatings showed lower biofilm attachment as compared to the commercial standards and regular PU. GP_1lb_160 showed the highest biofilm attachment among all the treatments. Percent biofilm removal from the abraded coatings was similar to or higher than the commercial coatings at 10 psi and 20 psi water jet pressure. 20 psi water jet pressure facilitated higher biofilm removal as compared to 10 psi. Almost 98-100% removal was obtained for some abrasion treatments at 20 psi water jet pressure.

(a)

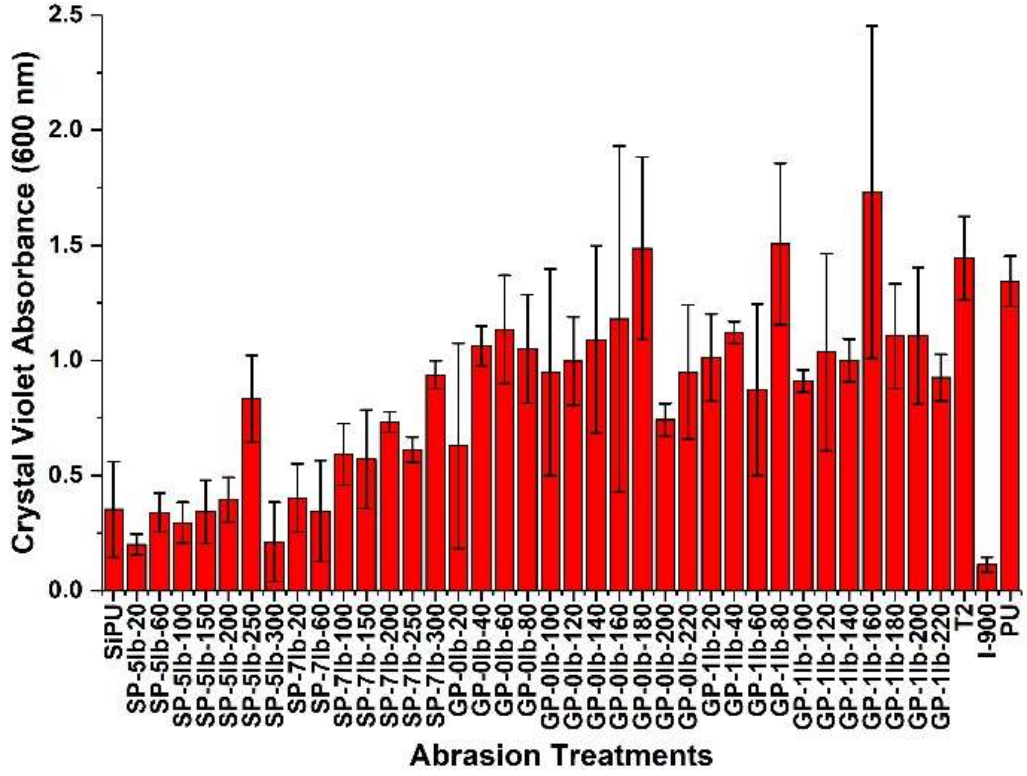

(b)

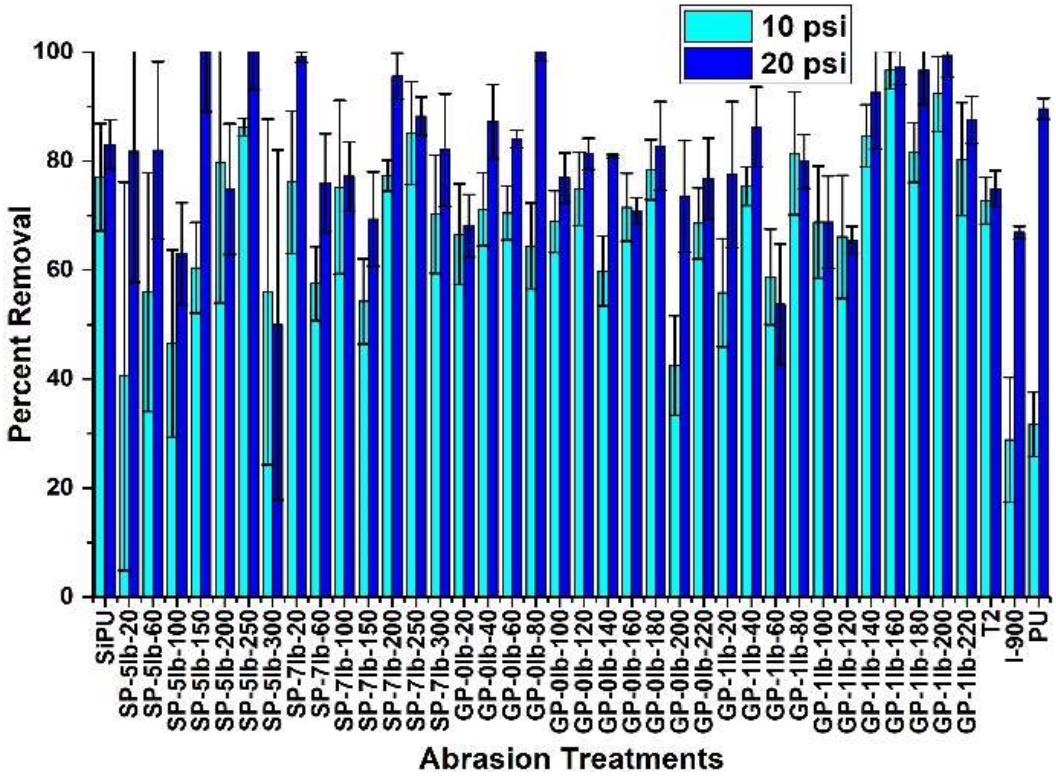

Figure 2.4. Biofilm *C.lytica* (a) attachment and (b) removal at 10 psi and 20 psi water jet pressure for the smooth and the abraded SiPU coatings.

Figure 2.5 shows data for diatom attachment and removal at 20 psi water jet pressure from the smooth and the abraded coatings. The smooth and the abraded coatings showed diatom attachment similar to T2 and regular PU and significantly higher than I-900 coating. At 20 psi, diatom removal from the SiPU coatings (smooth and abraded) was lower than T2, I-900, and PU. Percent removal of diatoms decreased with increasing roughness of the coatings. Lowest removal was obtained with GP_1lb_160 abrasion treatment.

(a)

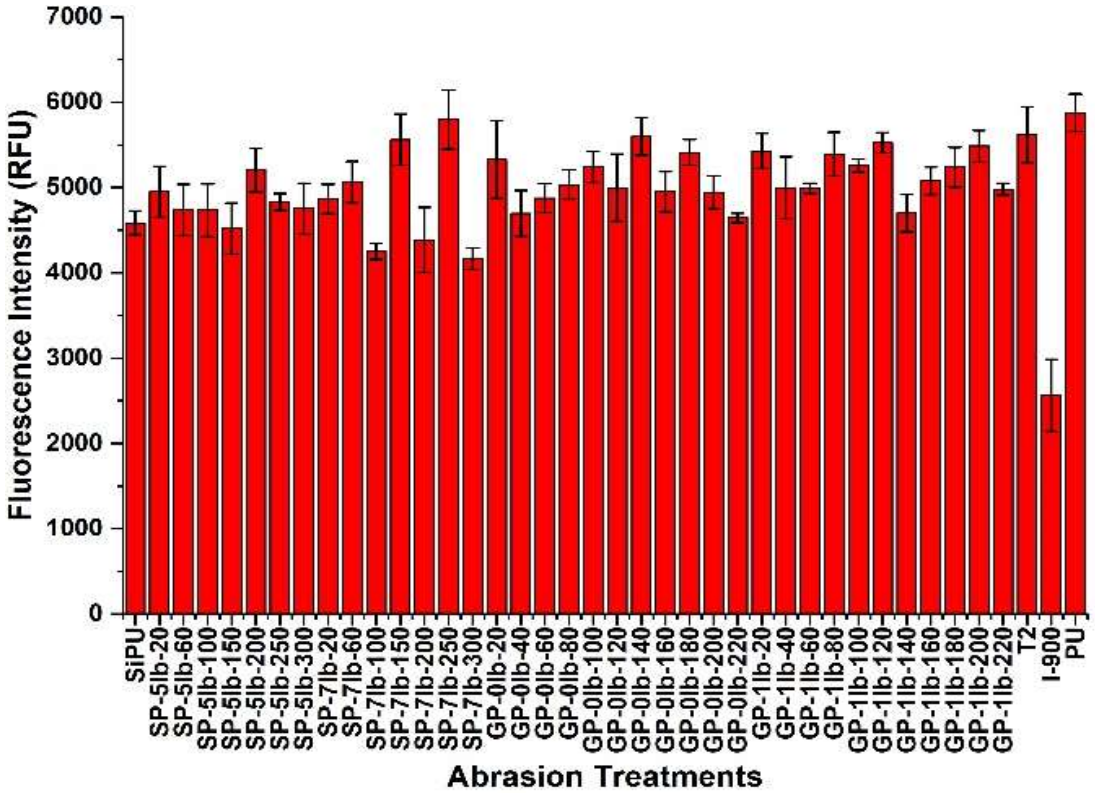

Figure 2.5. Diatom *N.incerta* (a) attachment and (b) removal at 20 psi for all the SiPU treatments.

(b)

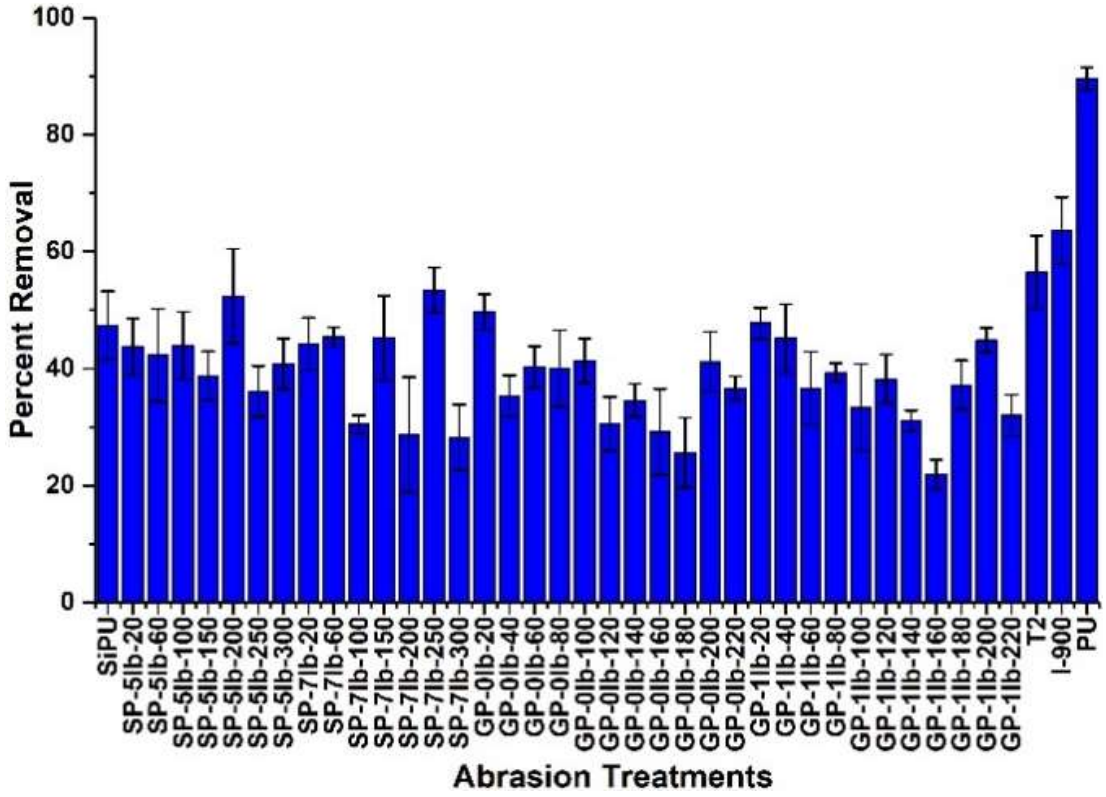

Figure 2.5. Diatom *N.incerta* (a) attachment and (b) removal at 20 psi for all the SiPU treatments (continued).

Figure 2.6 shows barnacle adhesion for the smooth and the abraded SiPU coatings. Ratios above each data point indicate the number of barnacles that attached to the coatings during the experiment to the number of barnacle bases that broke during experimentation. As compared to the commercial standards, significantly higher force of removal was required for the coatings abraded using SP (Figure 2.6). Barnacle removal from the coatings abraded using SP reduced with increasing number of abrasions. Under 7 lb additional weight (Figure 2.6(b)), several barnacle bases broke at 200-300 abrasions, indicating strong attachment of barnacles onto the SP-abraded coatings.

In contrast to the SP-abraded coatings, abrading coatings with GP resulted in a decrease in attachment strength of barnacles onto the abraded surface. The number of barnacles that adhered to the coatings reduced significantly with increase in roughness of the coatings (Figure 2.7). Moreover, adding 1 lb. additional weight and increasing the number of abrasions with GP successfully deterred barnacle attachment onto the abraded coating surfaces. For example, for coating with GP_1lb_160 treatment, 3 out of 4 barnacles did not attach to the coating over the course of the experiment. The force of removal

required to detach the only barnacle that attached to GP_1lb_160 was lower than 0.10 MPa, which is significantly lower than removal force from the commercial standards.

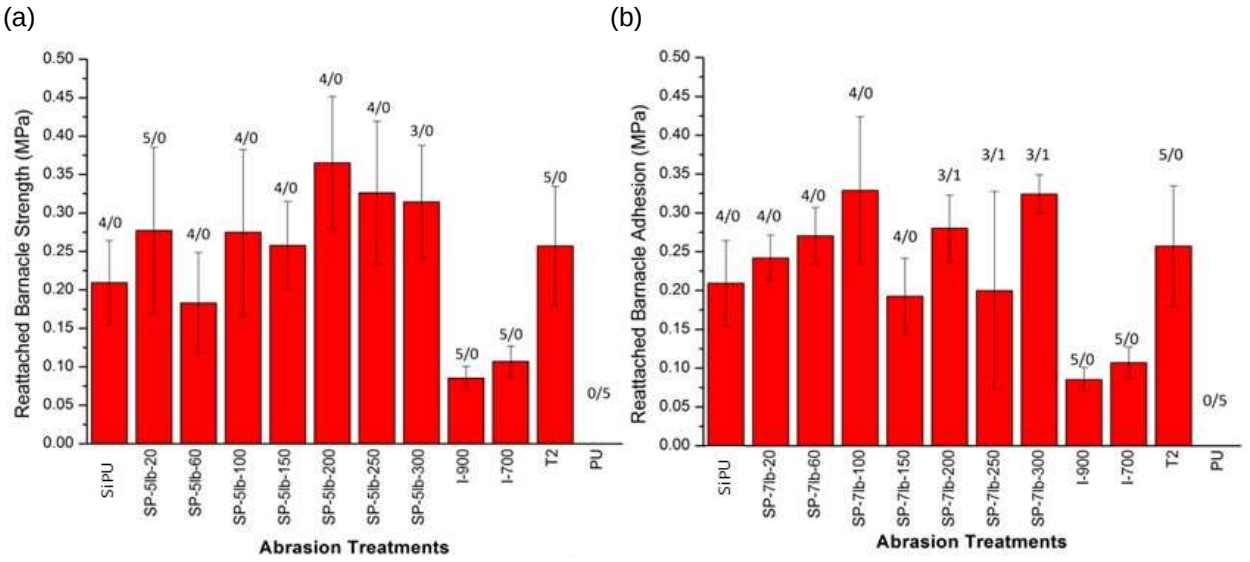

Figure 2.6. Barnacle removal for coatings abraded using SP under (a) 5 lb and (b) 7 lb additional weights. Ratios above individual data points indicate the number of barnacles that were successfully removed from the coating to the number of barnacle bases that broke during the experiment.

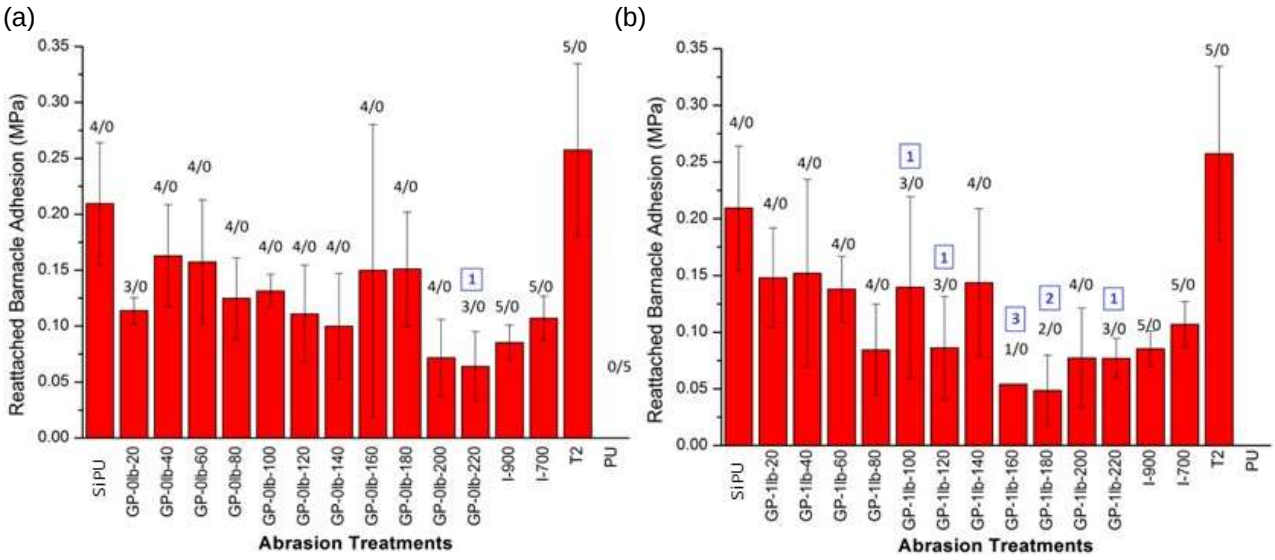

Figure 2.7. Barnacle removal for coatings abraded with GP (a) without additional weight and (b) under 1 lb. additional weights. Ratios above individual data points indicate the number of barnacles that were successfully removed from the coating to the number of barnacle bases that broke during the experiment. The number above select data points indicates the number of barnacles that did not attach to the coatings during experimentation.

Figure 2.8 shows microalgae *U.linza* removal from the smooth and select abraded SiPU after exposure to water jets at 18, 67 and 111 kPa. Selection of the abraded coatings was based on the FR

performance of the coatings against barnacles. Therefore, abraded coatings included in the experiment were the smooth SiPU coating (control) coatings with abrasions treatments SP_5lb_300 and SP_7lb_300 (worst performance) and GP_0lb_220 and GP_1lb_160 (best performance). For this experiment, polystyrene (PS) coating was added as a standard instead of the commercially available coatings. Removal of microalgae decreased as the roughness of the coatings increased. 111 kPa water pressure facilitated maximum removal of the microalgae. Among the SiPU coatings, coating with GP_1lb_160 treatment showed lowest microalgae removal of 40%. PS surface showed lowest removal of the microalgae, due to the absence of a PDMS rich coating on the surface of PS.

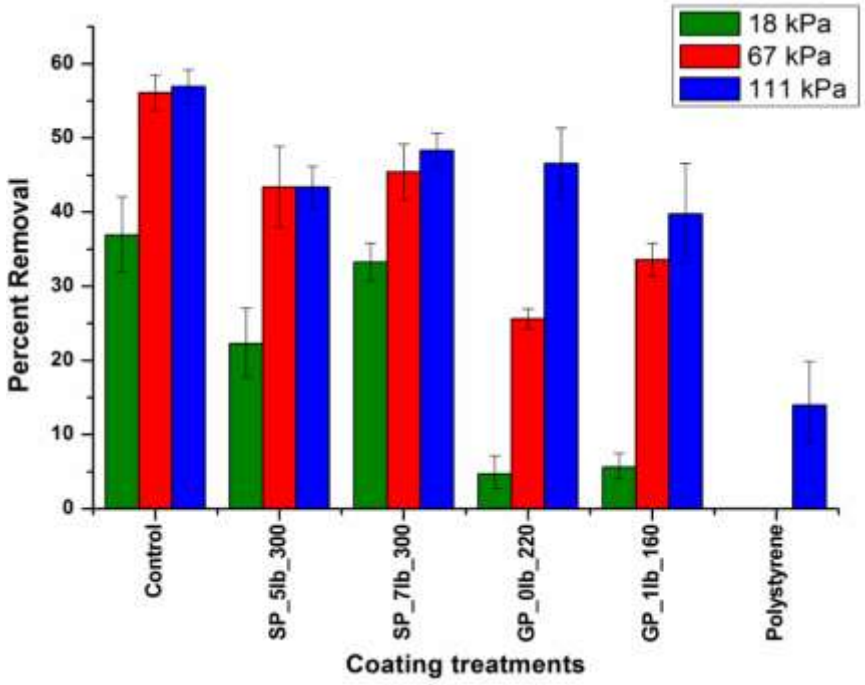

Figure 2.8. Percent removal of microalgae *U.linza* from the smooth and the select abraded coatings after exposure to 18, 67, and 111 kPa water pressure. Control indicates the smooth SiPU coating. Polystyrene was used as the standard for this experiment.

Past research with SiPU coatings has showed that hydrophobic surfaces successfully deter attachment of mussels. In this study, mussel adhesion experiment showed that even after abrasions, the SiPU coatings also did not allow mussels to attach onto the rough coatings, probably due to enhanced hydrophobic character of the coatings upon abrasions. This study also showed that as long as hydrophobic nature of surfaces remained intact, attachment of mussels was potentially independent of surface topography of the coatings.

Select abraded coatings were analyzed using XPS to determine the effect of abrasions on the surface composition of SiPU coatings. Table 2.2 shows the results obtained from XPS for the smooth SiPU coating, coating with SP_7lb_300 treatment (worst barnacle removal) and coating with GP_1lb_160 treatment (best barnacle removal). The results show that concentrations of individual elements Si, C and O detected on the coating surfaces were approximately 25%, 50% and 25% respectively (Si:C:O ratio of 1:2:1). The binding energies from Figure 2.9, combined with the ratio of the individual elements, indicated the presence of PDMS on the surface even after abrasions.

Table 2.2. Elemental composition of the select coatings obtained using XPS.

Abrasion treatments	Atom %		
	Si	C	O
Smooth PU-PDMS coatings	25.19	48.93	25.88
SP_7lb_300	25.00	50.33	24.68
GP_1lb_160	24.59	50.66	24.76

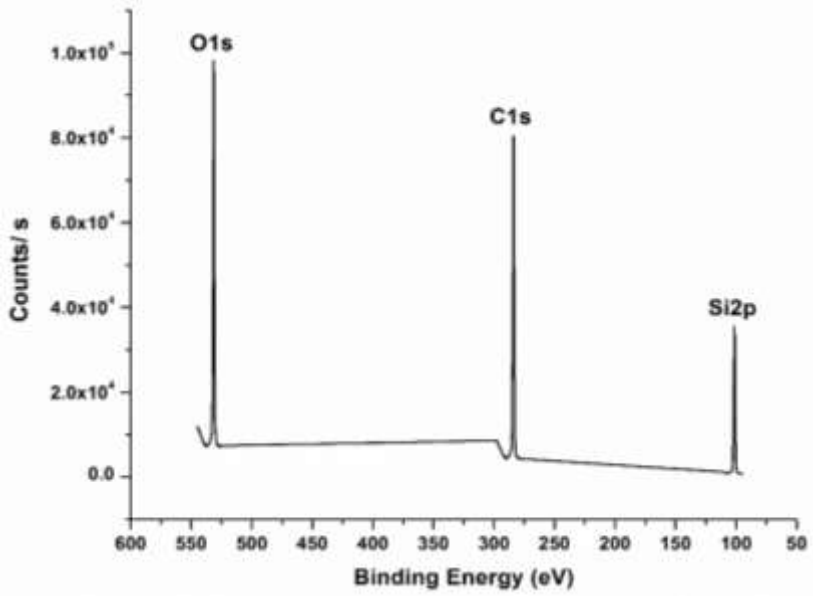

Figure 2.9. Survey scan for the smooth and the select abraded SiPU coatings.

Based on the unusual FR performance of the abraded coatings against barnacles, it was hypothesized that the FR performance of the coatings was dependent on the size of the surface features formed upon abrading the coatings with different abrasion treatments, relative to the size of barnacles. To understand the interesting behavior of the abraded coatings, the smooth and select abraded coatings were analyzed for surface roughness using optical profilometry. Roughness analysis showed that R_z values (average feature depth) of the abraded coatings increased with the number of abrasions,

additional weights, and roughness of the Scotch Brite pad. The smooth SiPU coating and the SP-abraded coatings exhibited similar surface topography as shown in Figure 2.10. Coatings abraded using GP exhibited significantly higher roughness.

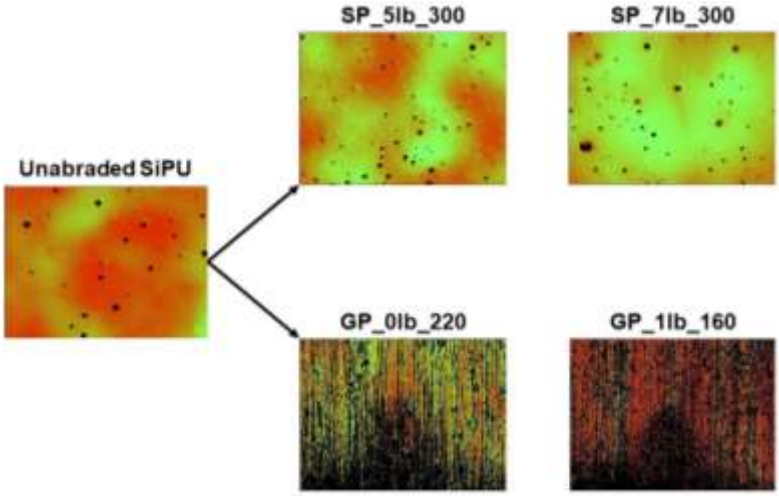

Figure 2.10. Images of the smooth and the abraded SiPU coatings from optical profilometer.

Determination of dimensions of the surface features showed that abrading the coatings with SP resulted in formation of shallower features, with depth ranging from 3.5 µm to 4.5 µm (Table 2.3). The depth of the features increased to 9-12 µm upon abrading the SiPU coatings with GP. Width of the features was determined as the peak to peak distance between the highest surface features (Table 2.3). Abrading the coatings with SP resulted in formation of non-uniform (high standard deviation) wide surface features (40-55 µm). On the other hand, the width of the features significantly reduced upon abrasions with GP (10-12 µm), with low standard deviation values indicating uniformity of the surface features. The data points at 0 abrasions in Figure 2.11 indicate R_z for the smooth SiPU coating. Variations in the R_z values for the smooth coatings may be attributed to movement of PDMS chains on the coating surface or presence of surface defects. Although complexity and non-uniformity of the shape of the protruding peaks made the analysis of the width of the individual peaks extremely difficult, results obtained from analysis of the surface features provides a good estimation of the topography of the abraded coatings.

Table 2.3. Height and distance between the features for different abrasion treatments determined using optical profilometry.

Coating treatments	Depth (avg. R_z) (microns)	Width (microns)
Smooth SiPU	4 ± 2	46.49 ± 8.63
SP_5lb_300	3.5 ± 0.25	40.70 ± 13.38
SP_7lb_300	4.42 ± 0.96	57.02 ± 11.99
GP_0lb_220	9.28 ± 2.32	12.27 ± 1.54
GP_1lb_160	11.21 ± 1.43	10.69 1.00

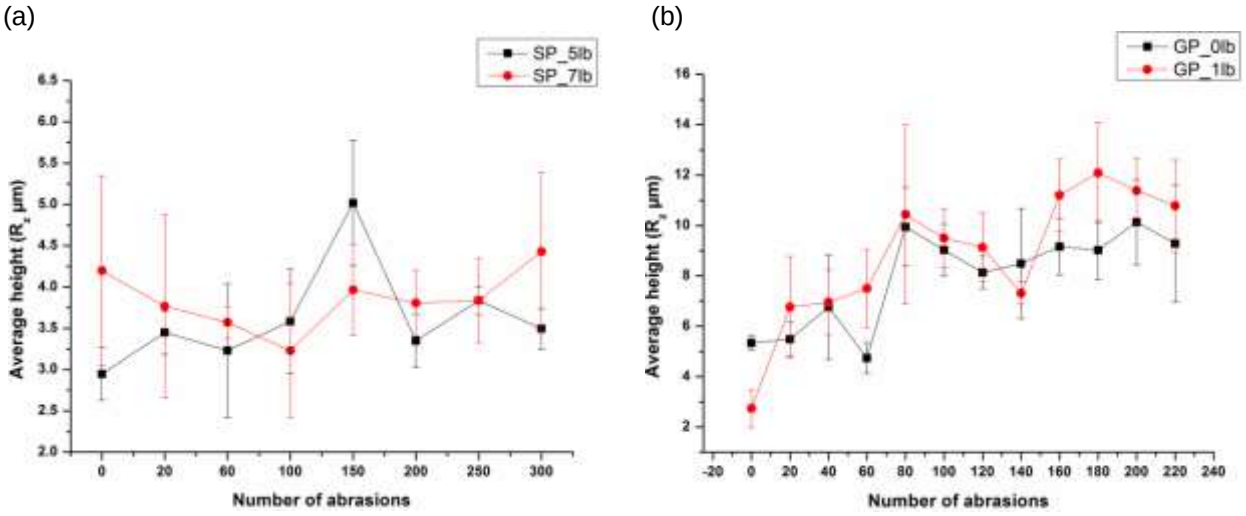

Figure 2.11. Depth of the surface features (R_z) in microns after abrasions with (a) SP and (b) GP. Error bars represent standard deviation.

Past attempts at understanding FR performance of coatings have shown that the FR performance of the coatings is dependent on the size of the organism relative to the dimensions of the surface features. Abrading the coatings caused an increase in the roughness of the SiPU coating surface, which resulted in an increase in surface area and number of contact points between the fouling organism and the abraded surfaces. Diatoms show tendency to attach strongly onto hydrophobic siloxane rich surfaces.[33] Presence of APT-PDMS on the surface even after abrasions combined with an increase in the number of contact points upon abrasions resulted in stronger attachment of the diatoms on the abraded surfaces (Figure 2.5). The diatoms may have been able to occupy the space between the features, shielding the diatoms from the impact of water jet. Microalgae (size— 5 to 7 µm) removal from the GP-abraded coatings decreased with increasing roughness (Figure 2.8). Determination of the size of the surface features formed using GP showed that the features formed were significantly bigger than the size of the microalgae (Table 2.3). Moreover, comparatively deeper “grooves” with GP provided a “cozy”

environment for potential growth of the microalgae, protecting the spores from incoming water. Therefore, even though hydrophobic surfaces generally reduce attachment of algal spores, FR performance against microalgae deteriorated with increasing roughness of the coatings. Availability of extra points of contact between biofilm and the abraded coatings allowed more bacterial biofilm to attach onto the surface of the abraded coatings as compared to the smooth SiPU coatings (Figure 2.4). Due to smaller size (width and depth) of the surface features as compared to the size of the bacterial biofilm, the biofilm may have remained suspended between the features. Exposure to water pressure may have easily removed the suspended biofilm. FR performance against barnacles (cyprids— 200 to 500 µm; adult barnacles in this study— ~5mm) showed that the adult barnacles attached strongly onto the SP-abraded coatings, but the GP-abraded surfaces successfully deterred barnacle attachment (Figures 2.6 and 2.7). The shallower and wider grooves on the SP-abraded coatings may have increased the mechanical interlocking between the barnacle adhesive and the abraded coating by increasing the number of contact points available for attachment. On the other hand, the narrower and deeper features on the GP-abraded coatings appeared to make it difficult for the barnacles to attach to the coatings, requiring the barnacles to "balance" on the protruded peaks on the abraded coatings. Strain developed in the barnacles to maintain their balance made the coatings less conducive for growth.[13] Among all the SiPU coatings (smooth and abraded) and the commercial standards, coating with GP_1lb_160 abrasion treatment showed best FR performance against barnacles and bacterial biofilm (and mussels), but, the abrasion treatment allowed highest diatom and microalgal attachment. Correlation between FR performance of the abraded coatings and dimensions of the surface features supported the initial hypothesis that FR behavior is a function of the feature size relative to size of the foulant.

Conclusions

Self-stratified SiPU FR coatings were successfully made using polyisocyanate, acrylic polyol, and 20% APT-PDMS (20k g/mol). The coatings were abraded using two different Scotch Brite pads. The roughness of the coatings increased with the number of abrasions, additional weight used during the experiment, and the roughness of the Scotch Brite pad. Contact angle experiment showed that the coatings maintained their hydrophobicity even after abrasions. Although *C.lytica* biofilm attachment on the abraded coatings was higher than the commercial I-900, percent removal of the biofilm from the abraded

coatings was greater than the commercial standards, with some abrasions treatments like GP_1lb_160 facilitating 98-100% removal at 20 psi water jet pressure. The abraded coatings showed higher attachment of diatom *N.incerta* and increasing roughness of the coatings could not facilitate removal of the diatoms, with abrasion treatment GP_1lb_160 showing the lowest diatom removal. Similarly, microalgae *U.linza* removal decreased with increasing roughness of the abraded coatings. The smooth and the abraded SiPU coatings successfully deterred attachment of mussels, showing independence of mussel adhesion on coating topographies. The abraded coatings exhibited unusual FR performance against barnacles. The number of barnacles that attached to the abraded coatings reduced significantly with increasing roughness of the coatings. Coating with abrasion treatment GP_1lb_160 showed the best performance against barnacles, with 3 out of 4 barnacles not attaching to the coating at all and 1 barnacle requiring ~0.05 N removal force.

To understand this interesting behavior of the abraded coatings, attempts were made to quantify the dimensions of the surface features, depth (R_z) and width. Results showed that abrasions with SP resulted in formation of shallower and wider features, while abrading the surfaces with GP resulted in the formation of deeper and narrower features. Wide surface features with SP could not shield microorganisms from the impact of water jets. Availability of more points of contact may have allowed interlocking of barnacle adhesive with the SP-abraded surface. Conversely, the coatings abraded using GP may have provided a “secure” environment for the growth of microalgae. Further, trying to balance on top of the narrow and deep features on the GP-abraded coatings caused internal strains in the barnacles, making the GP-abraded coatings less attractive for attachment. Therefore, although suitable to microalgae and diatoms, the surfaces abraded using GP successfully deterred barnacle and biofilm attachment. The above study shows potential to use regular Scotch Brite pads to form “textured” surfaces to deter macrofoulants in practical marine applications.

References

1. Yebra, D. M.; Kiil, S.; Dam-Johansen, K., Antifouling technology—past, present and future steps towards efficient and environmentally friendly antifouling coatings. *Progress in Organic Coatings* **2004,** *50* (2), 75-104.

2. Magin, C. M.; Cooper, S. P.; Brennan, A. B., Non-toxic antifouling strategies. *Materials Today* **2010,** *13* (4), 36-44.

3. Sommer, S.; Ekin, A.; Webster, D. C.; Stafslien, S. J.; Daniels, J.; VanderWal, L. J.; Thompson, S. E. M.; Callow, M. E.; Callow, J. A., A preliminary study on the properties and fouling-release performance of siloxane–polyurethane coatings prepared from poly (dimethylsiloxane)(PDMS) macromers. *Biofouling* **2010,** *26* (8), 961-972.

4. Sommer, S. A.; Byrom, J. R.; Fischer, H. D.; Bodkhe, R. B.; Stafslien, S. J.; Daniels, J.; Yehle, C.; Webster, D. C., Effects of pigmentation on siloxane–polyurethane coatings and their performance as fouling-release marine coatings. *Journal of Coatings Technology and Research* **2011,** *8* (6), 661-670.

5. Bodkhe, R. B.; Stafslien, S. J.; Cilz, N.; Daniels, J.; Thompson, S. E. M.; Callow, M. E.; Callow, J. A.; Webster, D. C., Polyurethanes With Amphiphilic Surfaces Made Using Telechelic Functional PDMS Having Orthogonal Acid Functional Groups. *Progress in Organic Coatings,* **2012,,** *75* (*(1-2),*), 38-48.

6. Bodkhe, R. B.; Thompson, S. E. M.; Yehle, C.; Cilz, N.; Daniels, J.; Stafslien, S. J.; Callow, M. E.; Callow, J. A.; Webster, D. C., The effect of formulation variables on fouling-release performance of stratified siloxane–polyurethane coatings. *Journal of Coatings Technology and Research* **2012,** *9* (3), 235-249.

7. Genzer, J.; Efimenko, K., Recent developments in superhydrophobic surfaces and their relevance to marine fouling: a review. *Biofouling* **2006,** *22* (5), 339-360.

8. Schumacher, J. F.; Aldred, N.; Callow, M. E.; Finlay, J. A.; Callow, J. A.; Clare, A. S.; Brennan, A. B., Species-specific engineered antifouling topographies: correlations between the settlement of algal zoospores and barnacle cyprids. *Biofouling* **2007,** *23* (5), 307-317.

9. Wiegemann, M., Adhesion in blue mussels (Mytilus edulis) and barnacles (genus Balanus): mechanisms and technical applications. *Aquatic Sciences-Research Across Boundaries* **2005,** *67* (2), 166-176.

10. Aldred, N.; Scardino, A.; Cavaco, A.; de Nys, R.; Clare, A. S., Attachment strength is a key factor in the selection of surfaces by barnacle cyprids (Balanus amphitrite) during settlement. *Biofouling* **2010,** *26* (3), 287-299.

11. Vucko, M. J.; Poole, A. J.; Carl, C.; Sexton, B. A.; Glenn, F. L.; Whalan, S.; de Nys, R., Using textured PDMS to prevent settlement and enhance release of marine fouling organisms. *Biofouling* **2014,** *30* (1), 1-16.

12. Long, C. J.; Finlay, J. A.; Callow, M. E.; Callow, J. A.; Brennan, A. B., Engineered antifouling microtopographies: mapping preferential and inhibitory microenvironments for zoospore attachment. *Biofouling* **2010,** *26* (8), 941-952.

13. Schumacher, J. F.; Long, C. J.; Callow, M. E.; Finlay, J. A.; Callow, J. A.; Brennan, A. B., Engineered nanoforce gradients for inhibition of settlement (attachment) of swimming algal spores. *Langmuir* **2008,** *24* (9), 4931-4937.

14. Cooper, S. P.; Finlay, J. A.; Cone, G.; Callow, M. E.; Callow, J. A.; Brennan, A. B., Engineered antifouling microtopographies: kinetic analysis of the attachment of zoospores of the green alga Ulva to silicone elastomers. *Biofouling* **2011,** *27* (8), 881-892.

15. Schumacher, J. F.; Carman, M. L.; Estes, T. G.; Feinberg, A. W.; Wilson, L. H.; Callow, M. E.; Callow, J. A.; Finlay, J. A.; Brennan, A. B., Engineered antifouling microtopographies–effect of feature size, geometry, and roughness on settlement of zoospores of the green alga Ulva. *Biofouling* **2007,** *23* (1), 55-62.

16. Decker, J. T.; Kirschner, C. M.; Long, C. J.; Finlay, J. A.; Callow, M. E.; Callow, J. A.; Brennan, A. B., Engineered antifouling microtopographies: an energetic model that predicts cell attachment. *Langmuir* **2013,** *29* (42), 13023-13030.

17. Majumdar, P.; Lee, E.; Patel, N.; Ward, K.; Stafslien, S. J.; Daniels, J.; Chisholm, B. J.; Boudjouk, P.; Callow, M. E.; Callow, J. A., Combinatorial materials research applied to the development of new surface coatings IX: an investigation of novel antifouling/fouling-release coatings containing quaternary ammonium salt groups. *Biofouling* **2008,** *24* (3), 185-200.

18. Kugel, A. J.; Jarabek, L. E.; Daniels, J. W.; Vander Wal, L. J.; Ebert, S. M.; Jepperson, M. J.; Stafslien, S. J.; Pieper, R. J.; Webster, D. C.; Bahr, J., Combinatorial materials research applied to the development of new surface coatings XII: Novel, environmentally friendly antimicrobial coatings derived from biocide-functional acrylic polyols and isocyanates. *Journal of Coatings Technology and Research* **2009,** *6* (1), 107-121.

19. Stafslien, S. J.; Bahr, J. A.; Feser, J. M.; Weisz, J. C.; Chisholm, B. J.; Ready, T. E.; Boudjouk, P., Combinatorial materials research applied to the development of new surface coatings I: a multiwell plate screening method for the high-throughput assessment of bacterial biofilm retention on surfaces. *Journal of Combinatorial Chemistry* **2006,** *8* (2), 156-162.

20. Stafslien, S. J.; Bahr, J. A.; Daniels, J. W.; Vander Wal, L.; Nevins, J.; Smith, J.; Schiele, K.; Chisholm, B., Combinatorial materials research applied to the development of new surface coatings VI: an automated spinning water jet apparatus for the high-throughput characterization of fouling-release marine coatings. *Review of Scientific Instruments* **2007,** *78* (7), 072204.

21. Ekin, A.; Webster, D. C.; Daniels, J. W.; Stafslien, S. J.; Cassé, F.; Callow, J. A.; Callow, M. E., Synthesis, formulation, and characterization of siloxane–polyurethane coatings for underwater marine applications using combinatorial high-throughput experimentation. *Journal of Coatings Technology and Research* **2007,** *4* (4), 435-451.

22. Cassé, F.; Stafslien, S. J.; Bahr, J. A.; Daniels, J.; Finlay, J. A.; Callow, J. A.; Callow, M. E., Combinatorial materials research applied to the development of new surface coatings V. Application of a spinning water-jet for the semi-high throughput assessment of the attachment strength of marine fouling algae. *Biofouling* **2007,** *23* (2), 121-130.

23. Chen, Z.; Chisholm, B.; Kim, J.; Stafslien, S.; Wagner, R.; Patel, S.; Daniels, J.; Wal, L. V.; Li, J.; Ward, K., UV-curable, oxetane-toughened epoxy-siloxane coatings for marine fouling-release coating applications. *Polymer International* **2008,** *57* (6), 879-886.

24. Kim, J.; Nyren-Erickson, E.; Stafslien, S.; Daniels, J.; Bahr, J.; Chisholm, B. J., Release characteristics of reattached barnacles to non-toxic silicone coatings. *Biofouling* **2008,** *24* (4), 313-319.

25. Majumdar, P.; Stafslien, S.; Daniels, J.; Webster, D. C., High throughput combinatorial characterization of thermosetting siloxane–urethane coatings having spontaneously formed microtopographical surfaces. *Journal of Coatings Technology and Research* **2007,** *4* (2), 131-138.

26. Rittschof, D.; Orihuela, B.; Stafslien, S.; Daniels, J.; Christianson, D.; Chisholm, B.; Holm, E., Barnacle reattachment: a tool for studying barnacle adhesion. *Biofouling* **2008,** *24* (1), 1-9.

27. Bell, E. C.; Gosline, J. M., Strategies for life in flow: tenacity, morphometry, and probability of dislodgment of two Mytilus species. *Marine Ecology Progress Series* **1997,** *159*, 197-208.

28. Burkett, J. R.; Wojtas, J. L.; Cloud, J. L.; Wilker, J. J., A method for measuring the adhesion strength of marine mussels. *The Journal of Adhesion* **2009,** *85* (9), 601-615.

29. Crisp, D. J.; Walker, G.; Young, G. A.; Yule, A. B., Adhesion and substrate choice in mussels and barnacles. *Journal of Colloid and Interface Science* **1985,** *104* (1), 40-50.

30. Owens, D. K.; Wendt, R. C., Estimation of the surface free energy of polymers. *Journal of Applied Polymer Science* **1969,** *13* (8), 1741-1747.

31. Stein, J.; Truby, K.; Wood, C. D.; Takemori, M.; Vallance, M.; Swain, G.; Kavanagh, C.; Kovach, B.; Schultz, M.; Wiebe, D.; Holm, E.; Montemarano, J.; Wendt, D.; Smith, C.; Meyer, A., Structure-property relationships of silicone biofouling-release coatings: effect of silicone network architecture on pseudobarnacle attachment strengths. *Biofouling* **2003,** *19* (2), 87-94.

32. Tezuka, Y.; Kazama, H.; Imai, K., Environmentally induced macromolecular rearrangement on the surface of polyurethane–polysiloxane block copolymers. *Journal of the Chemical Society, Faraday Transactions* **1991,** *87* (1), 147-152.

33. Holland, R.; Dugdale, T. M.; Wetherbee, R.; Brennan, A. B.; Finlay, J. A.; Callow, J. A.; Callow, M. E., Adhesion and motility of fouling diatoms on a silicone elastomer. *Biofouling* **2004,** *20* (6), 323-329.

CHAPTER 3. NOVEL NON-ISOCYANATE SILOXANE MODIFIED GLYCIDYL CARBAMATE COATINGS FOR FOULING-RELEASE MARINE APPLICATIONS

Introduction

Biofouling is the undesirable attachment and colonization of aquatic organisms, like microalgae and barnacles, on submerged surfaces.[1, 2] The process of biofouling can be commonly explained as the initial formation of an organic conditioning layer, followed by accumulation of microorganisms like bacteria and algal species and finally attachment and growth of macrofoulants like barnacles and mussels.[2, 3] Common disadvantages of biofouling include increase in drag and therefore, increase in fuel consumption, reduction in the speed of the vessel, and migration of aquatic species to non-native environments.[1, 4, 5] Furthermore, the economic impact of biofouling also cannot be ignored; combating biofouling can cost as high as one billion dollars annually.[5] Two main technologies have been introduced to combat biofouling. Traditional anti-fouling (AF) coatings contained tin, copper or organic biocides, which would leach out over time and completely prevent the attachment of organisms.[5] Although highly effective, potentially toxic nature of the leachates has led to the replacement of AF coatings with “safer” fouling-release (FR) coatings.[1, 5] FR coatings allow attachment of organisms, but the weak bond can be easily broken by hydrodynamic forces.[6, 7] Commercial FR coatings are typically based on soft silicone elastomers. These commercial FR coatings lack mechanical strength and adhesion, making them less viable in long term applications.[6, 7] As an improvement over the commercial FR coatings, a self-stratified siloxane-polyurethane (SiPU) system was developed in the Webster research group.[6-10] A typical coating formulation with the SiPU system comprises of an isocyanate, a polyol, and difunctional high MW siloxane (APT-PDMS). Upon curing, the siloxane component stratifies to form the outer low surface energy layer, while the PU matrix provides mechanical strength and improved adhesion to the substrate. But, concerns have been raised about using isocyanate hardeners in 2K coating formulations. Factory workers exposed to isocyanates are prone to ailments like asthma, inflammation, and acute bronchitis. Long term hazards of using isocyanates have necessitated further research into finding potentially “safer” alternatives to the PU matrix. In an attempt to find a practical, “safer” alternatives for polyurethanes to make self-stratified FR marine coatings, a novel non-isocyanate coating system based on glycidyl carbamate (GC) technology was explored. GC resins can be easily synthesized by reacting an isocyanate

with glycidol to form carbamate linkages (-CO-NH-).[11-18] The resultant resin combines the strength and abrasion resistance of polyurethanes with convenient epoxy-amine crosslinking chemistry. A typical formulation with GC resin consists of the carbamate resin and a diamine crosslinker. Properties of the thermoset formed after curing can be easily altered depending on the application by changing the type and amount of amine crosslinkers. Although isocyanate is used to synthesize GC resins, absence of free isocyanates in the final coating formulation is expected to greatly reduce hazards associated with spraying unreacted isocyanates.

In this study, "safer" low surface energy, hydrophobic coatings were explored as viable FR surfaces. To this end, a novel self-stratified isocyanate-free siloxane modified GC resin (IGC_PDMS) was synthesized using an isocyanate trimer, glycidol, and dicarbinol terminated PDMS. The resin was characterized using FTIR, ^{13}C-NMR, and GPC. The synthesized resin was crosslinked using PACM, polyamines, Ancamine 2143 and Ancamine 2432, and polyamides, Ancamide 2634 and Ancamide 2767 crosslinkers. Ratios of epoxy: AHEW were also varied as 1:1, 1:2, and 2:1. Additionally, varying amounts of 20k g/mol aminopropyl terminated PDMS (APT-PDMS) were incorporated into the formulations to identify the formulation(s) that show optimum FR performance. Formulations with PACM were cured at 80°C for 45 minutes; the polyamine cured and the polyamide cured formulations were cured at RT for 3 weeks. The cured coatings were analyzed for their mechanical properties such as hardness, flexibility, and impact strength. Thermal analysis experiments were used to determine glass transition temperature, degradation behavior, and crosslink density of the cured coatings. Surface analysis of the coatings was conducted using contact angle measurements, ATR-FTIR, AFM, and XPS. Lastly, select IGC_PDMS coatings were characterized for their FR performance against common fouling organisms: diatoms, biofilm, microalgae, mussels, and barnacles.

Experimental Section

Materials

Trimer of hexamethylene diisocyanate (HDI trimer; Desmodur N 3300A) was provided by Covestro (Bayer MaterialScience). Dicarbinol terminated PDMS (DMS-C21) with molecular weight (MW) 5k g/mol was purchased from Gelest. Glycidol, supplied by Dixie Chemicals, was refrigerated to reduce the formation of impurities.[19] Catalyst dibutyltin diacetate (DBTDAc), ethyl-3-ethoxy propionate (EEP) and

toluene were purchased from Sigma Aldrich. Diamines, PACM (AHEW = 52.5 g/eq.), Ancamine 2143 (AHEW = 115 g/eq.), Ancamine 2432 (AHEW = 88 g/eq.), Ancamide 2634 (AHEW = 90 g/eq.), and Ancamide 2767 (AHEW = 114 g/eq.), were provided by Air Products. Intergard 264 primer and hardener (products of International Paint) were purchased from Interbay Coatings.

Aminopropyl terminated polydimethylsiloxane (APT-PDMS) was synthesized in a fashion similar to the one described in prior publication.[6] Chemicals for the synthesis of APT-PDMS, siloxane monomer (D_4), benzyltrimethylammonium hydroxide, and blocker bis(3-aminopropyl)-tetramethyldisiloxane (BAPTDMS) were purchased from Dow Chemical, Sigma Aldrich, and Gelest respectively. D_4, BAPTDMS, and 40% benzyltrimethylammonium hydroxide solution in methanol were equilibrated at 80°C for 24 hours in a round bottom flask, equipped with a nitrogen inlet, condenser, heating mantle, and temperature controller. After 24 hours, temperature was increased to 170°C for 2 hours to decompose the catalyst. The product was cooled to room temperature and stored. MW of the synthesized APT-PDMS was between 18-20k g/mol, as determined from GPC.

Synthesis of Siloxane Modified Glycidyl Carbamate Resin (IGC_PDMS Resin)

A four-necked round bottom flask was fitted with a condenser, a nitrogen inlet, a thermocouple, and a mechanical stirrer. Equivalents of dicarbinol terminated PDMS modifier were maintained at 5% of equivalents of isocyanurate (HDI trimer). Amounts of solvents, EEP and toluene, were calculated such that the final resin contained target 50% resin solids in 1:1 w/w solvent blend of EEP and toluene. In the first stage of synthesis, the flask was charged with HDI trimer and the required amount of EEP solvent. Once HDI trimer and EEP were homogeneously mixed, PDMS modifier and catalyst DBTDAc (0.020-0.025% by weight of total solids) were added to the flask. Temperature was maintained at 80°C for 1-1.5 hours. In the next step, temperature was reduced to ~40°C before the addition of glycidol. A solution of glycidol in required amount of toluene was then added to the flask at ~40°C. The reaction of glycidol with isocyanate is highly exothermic; glycidol solution in toluene provides better temperature control. The reaction was allowed to proceed at 45-50°C for another 1-1.5 hours. Completion of the reaction was determined from the disappearance of the isocyanate peak at 2272 cm^{-1} as observed using Fourier Transformed Infrared Spectroscopy (FTIR).

Resin Characterization

The synthesized resin was analyzed using FTIR, Nuclear Magnetic Resonance Spectroscopy (^{13}C-NMR), and Gel Permeation Chromatography (GPC). A Thermo Scientific Nicolet 8700 instrument was used to conduct FTIR experiments. A small amount of the IGC_PDMS resin was coated onto a potassium bromide plate and 32 scans were taken for the sample. For ^{13}C-NMR, dilute resin solution in $CDCl_3$ was analyzed using Bruker 400 NMR instrument. Further, the resin was also analyzed using an EcoSEC HLC-8320 GPC system from Tosoh Bioscience, Japan, fitted with a differential refractometer (DRI) detector. Two TSKgel SuperH3000 6.00 mm ID × 15 cm were used as separation columns. The columns and detectors were maintained at 40ºC. A flow rate of 0.35 mL/min was maintained for tetrahydrofuran (THF), which was used as the eluent. Prior to testing the sample, the equipment was calibrated using Agilent EasiVial PS-H 4mL polystyrene standard. A 20 µL dilute solution (1 mg/mL) of the IGC_PDMS resin in THF then analyzed using GPC. A dilute sample of HDI trimer in THF was also separately analyzed. Elution time of 20 min was maintained for the resin and HDI trimer. GPC result for the IGC_PDMS resin was compared to HDI trimer to confirm absence of polymerization reactions during synthesis of the resin.

To determine experimental percent solids, ~1 g resin, measured accurately, was added to aluminum pans. The pans were heated in an oven at 120°C for 1 hour. Three replicates were measured with the IGC_PDMS resin. Weights of the pans with the resin before and after heating were measured. The average of the three replicates was recorded as the experimental value of percent solids. Epoxy equivalent weight (EEW) was determined experimentally according to ASTM D 1652. ~1 g of the resin, accurately measured up to the fourth decimal place, was added to an Erlenmeyer flask. 10-15 mL chloroform was added to the flask to completely dissolve the resin sample. 3-5 drops of crystal violet solution (0.1% solution in glacial acetic acid) were used as the indicator. The resin solution was titrated against standardized 0.1 N HBr solution. Color change from violet to blue-green was considered to be the end point of titration. EEW titrations were conducted three times. The average of the three values was reported as the experimental EEW of the synthesized resin.

Coating Formulations

The IGC_PDMS resin was crosslinked using amine crosslinkers, PACM, polyamines, Ancamine 2143 and Ancamine 2432, and polyamides, Ancamide 2634 and Ancamide 2767. Epoxy: AHEW ratio was varied as 1:1, 1:2 and 2:1. Additionally, varying amounts of high MW APT-PDMS (20k g/mol), as a 33% solution in toluene, were added to make different formulations. The formulations were first stirred using a magnetic stirrer for 20 min and then, sonicated for another 10 min to remove bubbles. Coatings used for mechanical tests and thermal analysis were applied onto degreased (using isopropanol) bare 3" x 6" aluminum (purchased from Q-Lab, specifications— smooth mill finish, type A, alloy 3003 H14), bare 3" x 6" steel (purchased from Q-Lab, specifications— smooth mill finish, type QD, alloy 1008/1010) and glass substrates, using a drawdown bar with 8 mils wet film thickness. Coatings used for FR experiments were applied onto primed (Intergard 264) 4" x 8" aluminum panels (purchased from Q-Lab, specifications— smooth mill finish, type A, alloy 3003 H14), using a Mayer rod (RDS 80). Formulations containing PACM crosslinker were cured at 80°C for 45 min. Formulations containing the polyamines and the polyamides were cured under ambient conditions for 3 weeks. In this study, coatings labels are of the format: amine crosslinker_epoxy: AHEW ratio_F%APT-PDMS.

Mechanical Characterization

Upon curing, all the IGC_PDMS coatings were characterized for their solvent resistance, mechanical properties and impact resistance. Chemical resistance and extent of crosslinking of the coating network was analyzed by methyl ethyl ketone (MEK) double rubs test (ASTM D 5402). A 26-oz hammer with three layers of cheesecloth was soaked in MEK solvent. The cheesecloth was rewet with MEK after every 100 double rubs. The number of double rubs that resulted in surface mar or discoloration of the surface were recorded. Hardness of the coatings was measured using König pendulum hardness (ASTM 4366). The hardness values were reported in seconds (s). Pencil hardness values (ASTM 3363) were determined using pencils of different hardness from 9B (softest) to 9H (hardest). The results were reported as the hardest pencil that does not leave surface mar. Reverse impact strength of the coatings was determined according to ASTM D 2794 using a Gardener impact tester, with maximum drop height of 43 in. and a drop weight of 4 lb. The results were reported as the impact value that causes crazing or loss of adhesion or film failure in inch–pounds (in.-lb), with > 160 in.-lb indicating coatings that showed no

failure during experimentation. Flexibility of coatings was determined conical mandrel bend (ASTM D 522). The results were reported as no failure (NF) or “tear” in the film. Crosshatch adhesion test was conducted on the coatings per ASTM D 3359, using a Gardco crosshatch adhesion instrument and tape. The results were reported as 5B (best) to 0B (worst), depending on the amount of film removed after the tape was ripped off. 60° gloss was measured using a BYK Gardner gloss meter. Three measurements at different spots on each coating with a glass substrate were taken. The average of the three measurements was recorded as the 60° gloss value for the formulation. Instron 5542 was used to test tensile strength of the PACM and Ancamine 2432 cured coatings. Free coating films were prepared according to ASTM 882. Young’s modulus and elongation were measured at room temperature at a rate of 5 mm/min.

Thermal Analysis

Based on the results obtained from the mechanical tests, only PACM_1:1_Fx, 2143_1:1_Fx and 2432_1:1_Fx were analyzed using DSC, DMA, and TGA. A TA Instruments Q1000 Differential Scanning Calorimetry (DSC) instrument was used to determine glass transition temperature of the select IGC_PDMS coatings. 7-8 mg samples were subjected to heat-cool-heat cycle at heating and cooling rates of 10°C/min and 5°C/min respectively. Temperature was between -20°C to 250°C for all the samples. Glass transition temperature (T_g °C) was determined as the temperature at the midpoint of the inflection in the second heating cycle. Degradation behavior of the cured coatings was determined using a TA Instruments Q500 Thermogravimetric Analysis (TGA) instrument. The coatings were heated up to 800°C at a heating rate of 10°C/min. Temperature of onset of degradation ($T_{d\ 5\%}$ °C) was determined for all the coatings. A TA Instruments Q800 Dynamic Mechanical Analysis (DMA) system was used to determine crosslink density (v_e mol/L), tan delta and storage modulus (E' MPa) of the cured coatings. Poisson’s ratio of 0.44 was used for all the coatings. Temperature was between -20 to 200°C, with heating rate of 5°C/min and 1 Hz frequency. v_e was calculated using E' values in the rubbery plateau region, 60°C above the T_g, using the equation, $E' = 3v_eRT$, where, E'= storage modulus (Pa); v_e = crosslink density (mol/L); R= gas constant (8.314 J/K/mol); T= (T_g + 60°C + 273) K.

Laboratory Biofouling Assays

Preleaching and Leachate Toxicity Analysis

Laboratory FR experiments were conducted only on IGC_PDMS formulations cured using PACM, Ancamine 2143, and Ancamine 2432 at 1:1 epoxy: AHEW ratio. Before FR tests, the coatings were placed in a recirculating water tank for six weeks (42 days) to remove toxic leachates, impurities, and catalyst before analysis with biological organisms.[20] After six weeks, algal solution in artificial sea water (ASW) with nutrients was introduced onto the coatings to test leachate toxicity. Fluorescence was used to observe the growth of algae on the coatings after 48 hours. The growth of the organisms on the coatings was reported as a fluorescence ratio to a positive growth control. A negative growth control (medium+ bacteria+ triclosan) was also included in the experiment. The coatings were compared to the negative control to confirm the absence of toxic leachates.[6] Leachate toxicity experiment showed that the Ancamine 2143 cured coatings exhibited severe toxicity against biological organisms. Therefore, FR analysis and surface characterization experiments with the Ancamine 2143 cured coatings were discontinued.

Diatom Navicula incerta (N.incerta) Attachment and Removal

Diatom *N.incerta* adhesion was carried out as explained in earlier publications.[6, 9, 21-23] 24-well plates were prepared by carefully punching out discs from PACM_1:1_Fx and 2432_1:1_Fx coatings. The discs were then glued to the well plates using a silicone adhesive from Dow Corning, such that the glue covered the circular basal area completely. The plates were then treated with 1 mL solution of algae in ASW and incubated for 2 hours to allow diatom adhesion. The settlement of the diatoms on the coatings was quantified using fluorescence. After 2 hours, the well plates were subjected to water jet at 10 psi and 20 psi for 10 seconds to determine release of diatoms from the coatings. The first column in each well plate was used as a reference for the initial cell settlement and was not subjected to water jet. The result obtained from the test was reported as the number of diatoms attached to the coatings and diatom removal at 10 psi and 20 psi water jet pressure.

Biofilm Cellulophaga lytica (C.lytica) Adhesion and Removal

Bacterial biofilm *C.lytica* adhesion test was carried out in a fashion similar to diatom attachment.[6, 24-26] Briefly, circular discs were carefully punched from PACM_1:1_Fx and 2432_1:1_Fx coatings. The

discs were glued to the plates using a silicone adhesive from Dow Corning. 5% suspension of *C.lytica* in ASW (10^7 cells/mL) with nutrients was prepared. 1 mL suspension was dispensed in each well. The plates were incubated for 24 hours at 28°C to allow colonization of the biofilm on the coatings. The plates were rinsed three times with deionized water to remove unattached biofilm. Crystal violet was used to stain the samples. Extractions of crystal violet in acetic acid (33%) were observed under 600 nm absorbance, to determine amount of biofilm retained on the coatings. After 24 hours, the wells were subjected to water jets at 10 psi and 20 psi for 5 seconds.[27] The first column in each 24-well plate served as a reference for bacterial growth before water jetting and was not exposed to water jet. The final result was reported as the amount of biofilm attached to the coatings and the percent removal of the biofilm from the coatings at 10 psi and 20 psi water jet pressures.

Microalgae Ulva linza (U.linza) Attachment and Removal

Similar to diatoms and biofilm, 24-well assay plates were prepared by carefully punching out discs from the preleached IGC_PDMS coatings. The discs were glued to the 24-well plates using a silicone adhesive from Dow Corning. The plates were then shipped to Newcastle University (United Kingdom) to determine the FR performance of the coatings toward microalgae *U.linza*. Before the bioassay experiment, the assay plates were equilibrated in 0.22 µm ASW for 2 hours. Then, 1 mL *U.linza* sporelings suspension (3.3×10^5 spores/mL) in enriched ASW was dispensed into each of the wells. The spores were grown in an illuminated incubator at 18°C for 6 days. After 6 days, the biomass from a single row of wells (6 wells) was assessed by extracting chlorophyll. Chlorophyll was extracted in 1 mL DMSO. Fluorescence was then determined using excitation of 360 nm and wavelength of 670 nm. To determine the release performance of the coatings, single rows of wells from each plate was sprayed using the spinjet apparatus at 18, 67, 110 kPa water pressure. Chlorophyll was again extracted, as explained earlier. The removal at each pressure was determined by comparing the sprayed and the unsprayed wells. The results were reported as the percent removal of the sporelings after exposure to water jet. In this paper, only microalgae removal at 110 kPa is shown. 18 and 67 kPa water pressure resulted less than or equal to 5% removal of the microalgae.

Mussel Geukensia demissa Adhesion

Select PACM_1:1_Fx and 2432_1:1_Fx coatings were evaluated for adhesion of marine mussels *Geukensia demissa*, according to a previously published procedure.[28-30] Before the start of the experiment, individual marine mussels (received from Duke University Marine Laboratory, North Carolina, USA) were fitted with a 4 cm long acetal rod, using a 3M acrylic adhesive. The rods were attached perpendicular to the ventral edge of each mussel. Six mussels were immobilized on the select PACM_1:1_Fx and 2432_1:1_Fx coatings using a custom designed polyvinyl chloride (PVC) template. The select coatings were placed in ASW so that the mussels can be fed live marine phytoplankton for 3 days. After 3 days, the number of mussels showing attachment of byssus threads was recorded for each coating. The acetal rods on the mussels were attached to a tensile force gauge, such that all the mussels were pulled from the coating at the same time. The result was reported as the average force in Newtons required to completely detach all byssus threads of the mussel from the surface.

Adult Barnacle Amphibalanus amphitrite (A.amphitrite) Adhesion

Select PACM_1:1_Fx and 2432_1:1_Fx coatings were also analyzed for barnacle adhesion to determine their FR performance against barnacles.[6, 31, 32] Six adult *A.amphitrite* barnacles, with basal diameter of approximately 5 mm, were allowed to grow and attach to the select coatings for 2 weeks. The barnacles were fed brine shrimp nauplii in ASW for 2 weeks. After 2 weeks, a hand held digital gauge was used to measure the force required to detach the barnacles in shear from the coatings. Adhesion strength (MPa) of the barnacles was then calculated as the shear force required for barnacle removal to the basal area of the barnacle. The result was reported as the adhesion strength of the barnacles.

Surface Characterization

Surface chemistry and topography of the pre-leached PACM_1:1_Fx and 2432_1:1_Fx coatings were studied using characterization techniques such as contact angle, Attenuated Total Reflectance Fourier Transformed Infrared Spectroscopy (ATR-FTIR), Atomic Force Microscopy (AFM), and X-Ray Photoelectron Spectroscopy (XPS). A First Ten Angstroms (FTA 125) system was used to measure water contact angles (WCA) and methylene iodide contact angles (MICA) of PACM_1:1_Fx and 2432_1:1_Fx coatings by the sessile drop method. Three WCA and MICA for each coating were measured at three different spots on the coating panel. The contact angles were analyzed using FTA software. The

averages of the three WCA and MICA values for each formulation were used to calculate the surface energy (SE) of the coatings by Owens-Wendt method.[33]

A Thermo Scientific Nicolet 8700 instrument, with iTR diamond crystal plate attachment, was used to conduct ATR-FTIR on select PACM_1:1_Fx and 2432_1:1_Fx coatings. 32 scans were taken for each coating sample. The spectra shown in this chapter are an average of the 32 scans.

Surface topography of select samples was analyzed using AFM. 20 µm x 20 µm and 100 µm x 100 µm areas of the select pre-leached coatings were scanned using a Dimension 3100 Microscope system with Nanoscope controller. A silicon probe with a spring constant of 0.3-0.8 N/m and resonant frequency of 20-40 kHz was used to scan the surfaces in tapping mode in air under ambient conditions.

A Thermo Scientific K-Alpha XPS system with monochromatic Al K_α X-ray source (1468.68 eV) and Ar^+ ion source gun (up to 8000 eV) was used to conduct XPS analysis for investigation of chemical composition of select IGC_PDMS coatings. Chamber pressure was maintained below 1.5 x 10^{-7} Torr at all times. Prior to analysis of the coatings, the surfaces were cleaned for 60 seconds to remove impurities using an Ar^+ ion MAGCIS cluster gun with 8000 eV power. Survey spectra were collected at a low resolution with constant pass energy of 200 eV. Three scans were collected at energy increment of 1.000 eV/step for 10 microseconds. High resolution scans were collected at an angle perpendicular to the coating surfaces. Pass energy was maintained at 50 eV. Ten scans were collected for each sample with energy increment of 0.100 eV/step for 50 microseconds. Atomic concentrations of individual elements, C1s, O1s, and N1s, were determined by integrating area under the peaks. Both surface etching and high resolution experiments were conducted at ambient temperature.

Results and Discussion

In an attempt to find a “safer” alternative for conventional isocyanate based polyurethane for use in FR marine applications, a novel siloxane modified isocyanate-free glycidyl carbamate (IGC_PDMS) resin was synthesized using HDI trimer, glycidol, and dicarbinol terminated PDMS as modifier (MW = 5k g/mol). The amount of the PDMS modifier was maintained at 5% of equivalents of isocyanurate. High viscosity of GC resins can be attributed to presence of strong intermolecular hydrogen bonds, necessitating incorporation of a modifier to reduce the viscosity. Similar to the previously developed siloxane-polyurethane (SiPU) coatings, it was anticipated that upon curing, self-stratification of the

hydrophobic siloxane chains in the IGC_PDMS formulations will lead to formation of low surface energy coatings. The resultant slippery surface will then reduce attachment strength of fouling organisms. 20k MW APT-PDMS was incorporated into coating formulations with the IGC_PDMS resin to study effect of increasing hydrophobicity on FR performance of the coatings. One of the biggest challenges in the project involved compatibilization of the highly polar GC resin with the non-polar siloxane components to form smooth, glossy, uniform, and preferably transparent coatings. Curing reactions, mechanical properties, appearance, and FR performance are dependent on compatibility between the different components of the coating formulation. Therefore, dicarbinol PDMS was specifically used as the modifier not only to reduce the viscosity of the GC resin, but also as a medium to compatibilize the high MW APT-PDMS with the GC matrix. Not just the PDMS modifier, initial stages of the project involved an extensive study with a number of different solvents and solvent blends to identify the best solvent or solvent combination that formed smooth and uniform modified GC films. A 1:1 w/w solvent blend of EEP and toluene was identified as the best combination. Further, 50% solvent blend in the resin provided sufficient viscosity for completion of synthesis reaction and convenient coating application, without causing thickness variations or surface sag.

Before identifying dicarbinol terminated PDMS as the best potential resin modifier, ethylene glycol butyl ether (EB) and 1-butanol (B) were explored as potential resin modifiers. To make hydrophobic FR coatings, APT-PDMS was incorporated into formulations with the modified GC resins. PACM was used as the crosslinker for all initial formulations. The resultant coatings showed good mechanical properties and uniform, glossy appearance. Preliminary FR performance with the EB modified resin showed potential use of GC resins in FR applications. But, incompatibility of non-polar siloxanes in polar GC resin resulted in formation of hazy, opaque coatings. To increase compatibility of APT-PDMS with the GC matrix, the alcohol modifiers were replaced with monocarbinol terminated PDMS (PDMS-OH; 1k g/mol). PDMS-OH appeared to drastically increase compatibility between APT-PDMS and the PDMS-OH modified GC resin, resulting in formation of clear, uniform, and glossy coatings. But, the monofunctional PDMS severely hampered epoxy-amine curing reactions. Curing behavior of the coatings was similar to lacquers, instead of cured thermoset coatings. Temperatures greater than 120°C, which facilitated self-crosslinking of epoxy rings, were required to obtain sufficient crosslinking in the PDMS-OH modified formulations.

The proposed structure of the synthesized IGC_PDMS resin is shown in Figure 3.1. The reaction of HDI trimer with glycidol and difunctional PDMS resulted in the formation of -CO-NH- linkages. Due to excess of isocyanate groups as compared to hydroxyl groups from the PDMS modifier, probability of reaction between hydroxyl groups and isocyanate groups from two different HDI trimer molecules is higher than formation of PDMS "loops" by reaction with isocyanates from the same trimer molecule. Glycidol provides reactive epoxy functional groups that can be crosslinked using a variety of amine crosslinkers. Absence of the isocyanate peak at 2272 cm^{-1} as observed from FTIR (Figure 3.2(a)) indicated formation of an isocyanate-free resin at the end of the synthesis reaction. Comparison of GPC spectra of unreacted HDI trimer and IGC_PDMS resin (Figure 3.2(b)) showed absence of polymerization reactions during synthesis. Further, analysis using ^{13}C-NMR indicated (Figure 3.3) formation of carbamate linkages with chemical shift at 149 ppm. Similarly, shifts at 1 ppm, 26-29 ppm, 44-49 ppm and 148 ppm represented C atoms from dicarbinol PDMS, alkyl groups from the HDI trimer and epoxy rings in the synthesized resin. The synthesized resin was also characterized for experimental percent solids and EEW. Experimental value of resin solids was calculated to be 48-50% (theoretical target— 50%). EEW values for the resin was found to be 400 ± 20 g/eq.

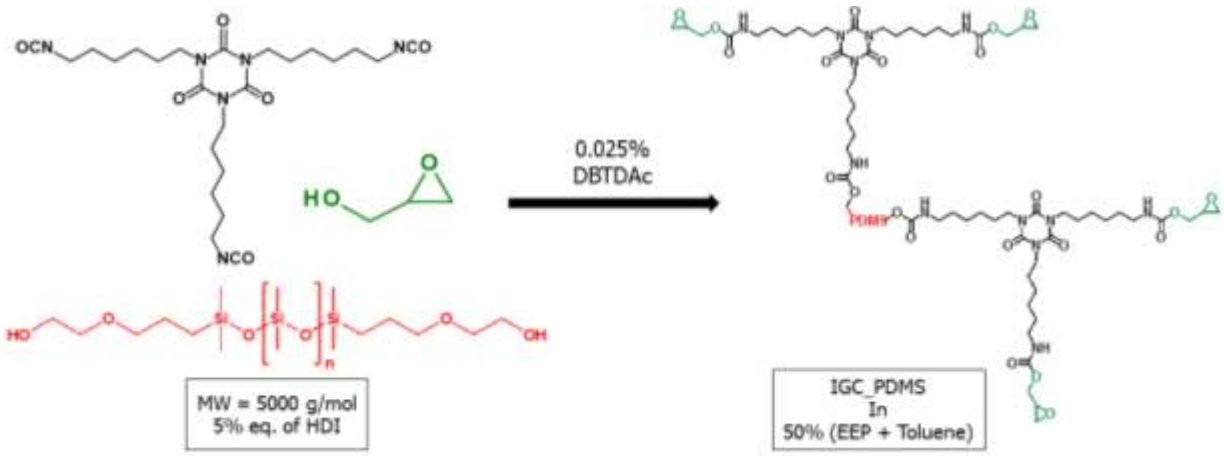

Figure 3.1. Reaction scheme for synthesis of IGC_PDMS resin.

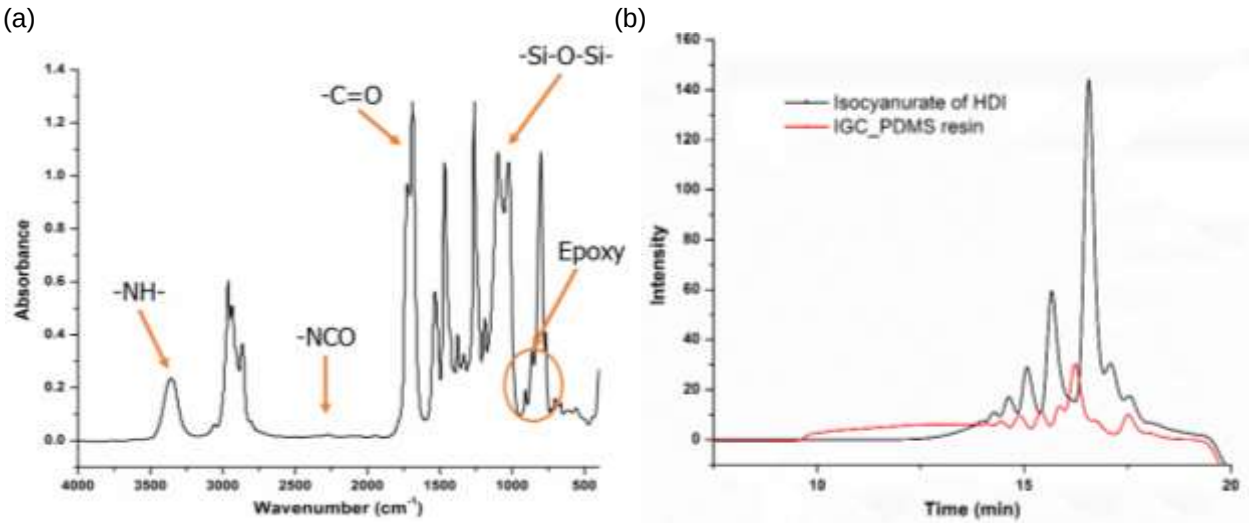

Figure 3.2. (a) FTIR spectrum and (b) GPC chromatogram for the IGC_PDMS resin.

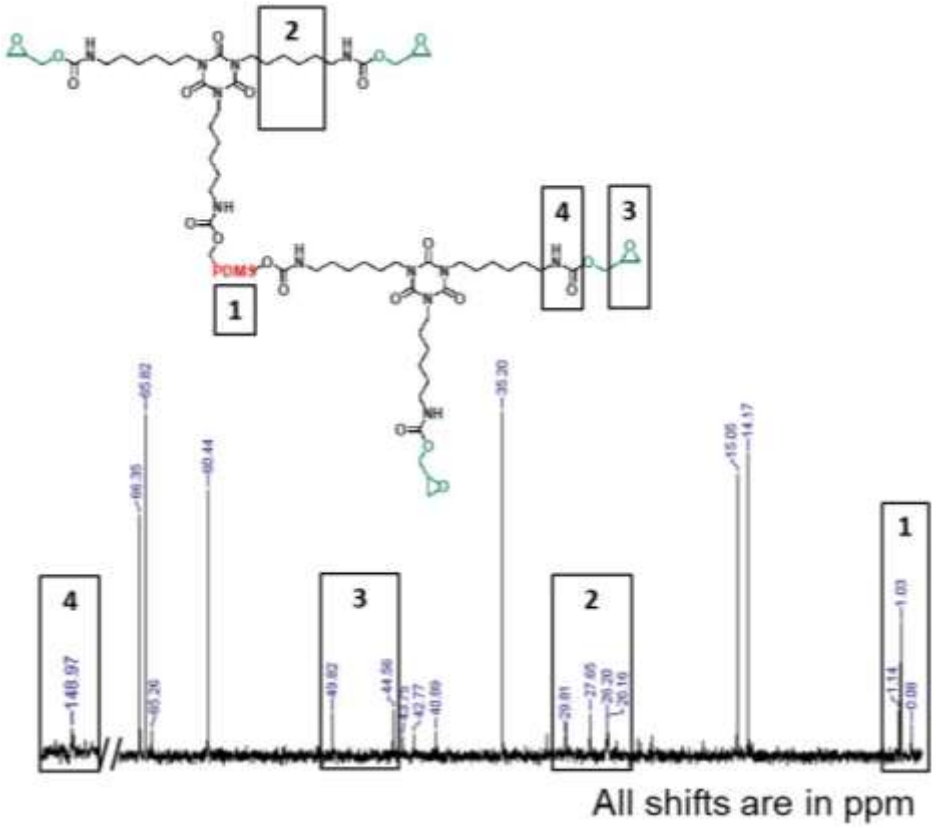

Figure 3.3. ^{13}C-NMR spectrum for the IGC_PDMS resin.

Formulations were made using the synthesized IGC_PDMS resin and amine crosslinkers, PACM, Ancamine 2143, Ancamine 2432, Ancamide 2634, and Ancamide 2767. Epoxy: AHEW ratios were varied as 1:1, 1:2, and 2:1. Different diamines were used as curing agents to study effect of the structure, the functionality, and the amount of the crosslinker on coating properties and FR performance of the coatings.

Varying amounts of APT-PDMS were incorporated into the different formulations to increase hydrophobicity of the coatings. Formulations with PACM were cured at 80°C for 45 minutes, while formulations with the other four diamines were allowed to cure under ambient laboratory conditions. Although very reactive, PACM (AHEW = 52.5 g/eq.) failed to provide sufficient crosslinking of the resin under ambient conditions; severe amine blush caused formation of hazy, non-glossy coatings. On the other hand, force curing the polyamine or the polyamide cured coatings imparted slight discoloration and foul odor to the coatings.

Upon curing, all coatings were characterized for their solvent resistance, hardness, flexibility, and impact strength. Results from mechanical tests showed that coatings with 1:1 epoxy: AHEW ratio exhibited the best overall (properties and appearance) performance. Stoichiometric equivalents of epoxy and amine groups in the formulation allows reaction of primary and secondary amines with oxirane rings. Therefore, theoretically, the coatings with 1:1 ratio are devoid of any unreacted epoxy or amine groups. Changing the stoichiometry results in higher concentration of either one of the unreacted functional groups. The unreacted groups, therefore, affect crosslink density of the coatings, in turn affecting overall properties of the cured coatings. The different curing schedules used are shown in Table 3.1.

Table 3.1. List of formulations made using the IGC_PDMS resin.

Amines	Coating labels[a]	% resin solids APT-PDMS	Curing schedules
PACM	PACM_x: y_Fx	0, 1, 2, 3, 4, 5, 10, 15, 20, 30	80°C, 45 minutes
Ancamine 2143	2143_ x: y_Fx	0, 1, 2, 3, 4	RT, 3 weeks
Ancamine 2432	2432_ x: y_Fx		
Ancamide 2634	2634_x: y_Fx		
Ancamide 2767	2767_x: y_Fx		

[a]All coating labels are of the format amine crosslinker_epoxy: AHEW_F%APT-PDMS.

Overall, PACM_1:1_Fx coatings appeared uniform and glossy and exhibited good hardness, flexibility, and impact strength. On the other hand, the polyamine and the polyamide cured coatings exhibited higher hardness as compared to the PACM cured coatings, but the coatings appeared non-uniform and exhibited lower surface gloss. This difference in appearance of coatings with the different crosslinkers may be attributed to the different curing schedules. Curing at elevated temperature for the PACM cured coatings allowed better compatibilization of the components in the coatings, leading to formation of smooth, glossy coatings. The IGC_PDMS coatings, irrespective of the crosslinker, exhibited excellent adhesion to the substrates (4B-5B) as determined from crosshatch adhesion. Table 3.2 shows

results for hardness, impact strength, solvent resistance, and gloss for the IGC_PDMS coatings with epoxy: AHEW = 1:1. MEK double rubs exceeded 400 for all the PACM_1:1_Fx formulations, indicating high solvent resistance of the coatings. PACM_1:1_F4 coatings showed the highest König pendulum hardness of 95 s and pencil hardness of 6H. Above and below 4% APT-PDMS content, addition of APT-PDMS did not have a significant effect on pendulum hardness or pencil hardness of the PACM cured coatings. Most of the coatings exhibited high reverse impact strength > 160 in.-lb. APT-PDMS content of the PACM cured coatings between 10-20% may have interfered with curing reactions in the coating film, resulting in drop in impact strength values.

Similar to the PACM cured coatings, the polyamine cured coatings exhibited high solvent resistance, with MEK double rubs > 400. Pendulum hardness values were in the range between 64-98 s. 2143_1:1_F4 and 2432_1:1_F4 showed pendulum hardness values of 98 s and 87 s respectively, indicating reinforcement of the coatings with addition of 4% APT-PDMS. 2143_1:1_Fx coatings exhibited the highest pencil hardness values among all the IGC_PDMS coatings. Reverse impact strength values for 2143_1:1_Fx coatings lied in the range between 70-80 in.-lb. Limited chain movement in the hard 2143_1:1_Fx coatings may have increased susceptibility of the coatings to impact. But, addition of 4% APT-PDMS resulted in slight softening of 2432_1:1_F4 coating, causing increase in impact strength. 2143_1:1_F4 showed highest gloss of 95 among all the IGC_PDMS coatings. Addition of APT-PDMS resulted in decrease in surface gloss for the Ancamine 2432 cured coatings. Among all the IGC_PDMS formulations, the polyamide cured formulations showed the worst overall performance. Only 5 out of 10 total formulations with the polyamides showed MEK double rubs > 400. The polyamide cured coatings showed highest hardness among the IGC_PDMS coatings, but poor impact strength. The polyamide formulations also showed lowest surface gloss among all the IGC_PDMS formulations, due to non-uniform separation of PDMS domains on the surfaces. Above 4% APT-PDMS content, the polyamine cured and the polyamide cured coatings could not withstand above 100 MEK double rubs, indicating higher concentration of unreacted functional groups. Upon contact with MEK solvent, the unreacted components may have dissolved, damaging the coating networks. Further, above 4% APT-PDMS content may have increased softness of the coatings by reducing network density in the coatings. Based on the overall performance (mechanical properties and appearance) of the IGC_PDMS coatings, the

formulations cured using PACM and the two polyamines at epoxy: AHEW = 1:1 were used for further experimentation.

Table 3.2. Results from ASTM tests for the IGC_PDMS coatings with epoxy: AHEW = 1:1.

Amine_ratio	F%APT-PDMS	MEK double rubs	König pendulum hardness (s)	Pencil hardness	Reverse impact (in.-lb)	[a]Mandrel bend	60° gloss
PACM_1:1	F0	>400	78	2H	>160	NF	82.37
	F1	>400	74	HB	>160	NF	87.30
	F2	>400	68	B	>160	NF	85.70
	F3	>400	62	2B	>160	NF	85.27
	F4	>400	95	6H	>160	NF	89.86
	F5	>400	79	HB	>160	NF	92.03
	F10	>400	67	B	47	NF	82.87
	F15	>400	74	HB	74	NF	86.20
	F20	>400	77	3B	67	NF	82.90
	F30	>400	73	2B	>160	NF	77.60
2143_1:1	F0	>400	68	6H	78	NF	57.13
	F1	>400	76	7H	70	NF	57.67
	F2	>400	78	5H	70	NF	60.63
	F3	>400	75	6H	70	NF	54.43
	F4	>400	98	4H	>160	NF	95.83
2432_1:1	F0	>400	64	3B	118	NF	85.77
	F1	>400	64	3B	94	NF	75.87
	F2	>400	67	2B	110	NF	71.13
	F3	>400	67	3B	125	NF	67.07
	F4	>400	87	2B	141	NF	67.33
2634_1:1	F0	220	88	B	86	NF	13.67
	F1	>400	83	B	118	NF	17.47
	F2	>400	82	HB	141	NF	45.13
	F3	175	82	HB	[b]-	NF	41.77
	F4	>400	93	B	>160	NF	92.90
2767_1:1	F0	>400	104	6H	39	NF	45.30
	F1	300	99	6H	39	NF	35.70
	F2	200	100	5H	20	Tear	60.53
	F3	75	101	5H	35	Tear	73.13
	F4	>400	100	2B	>160	NF	40.43

[a]NF indicates no failure occurred in the film during experimentation. [b]Non-uniformity of the coatings resulted in large variation in the reverse impact strength values.

Evaluation of tensile tests showed that the coatings cured using PACM showed lower Young's modulus compared to the Ancamine 2432 cured coatings (Figure 3.4). For the PACM cured coatings, modulus dropped from 150 MPa for no additional APT-PDMS (F0) to 50 MPa for F10 and 100 MPa for F30. 2432_1:1_F0 showed highest modulus of 375 MPa. Increasing APT-PDMS content to 4% resulted in

decrease in modulus to 310 MPa. The Ancamine 2432 cured coatings showed lower elongation as compared to the PACM cured coatings, indicating coatings with higher stiffness. Elongation dropped drastically with addition of 10% APT-PDMS, but increased when APT-PDMS content was increased to 30%. With Ancamine 2432, a slight drop in elongation was observed when APT-PDMS content was increased to 4%. Overall, the IGC_PDMS formulations exhibited significantly higher modulus than the commercial silicone elastomer coatings (~5 MPa).

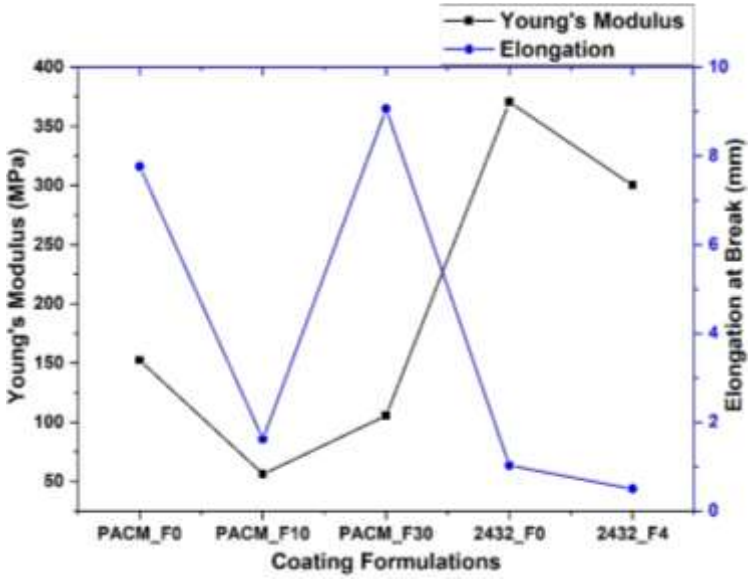

Figure 3.4. Young's modulus and elongation of select IGC_PDMS coatings.

PACM_1:1_Fx, 2143_1:1_Fx, and 2432_1:1_Fx coatings were characterized using DSC, DMA, and TGA to analyze their glass transition temperature (T_g °C), crosslink density, and degradation behavior. Figure 3.5 shows DSC scans for coatings cured using PACM, Ancamine 2143, and Ancamine 2432. T_g values for PACM_1:1_Fx coatings were between 83°C for 30% APT-PDMS to 103°C for 2% APT-PDMS. For the PACM cured coatings, increasing APT-PDMS content resulted in reduction in T_g values (Figures 3.5(a)). Among all the IGC_PDMS formulations analyzed using DSC, 2143_1:1_Fx coatings exhibited highest T_g values, ranging from 100°C to 107°C, while 2432_1:1_Fx coatings exhibited lowest T_g values in the range from 78°C to103°C. For the polyamine cured coatings (Figures 3.5(b)), the T_g values increased until 2% additional APT-PDMS content and then dropped drastically with further increase in APT-PDMS content. Increasing APT-PDMS content to 2% may have reinforced the matrix by

formation of tighter crosslinks, but increasing APT-PDMS content above 2% resulted in plasticization of the networks.

(a)

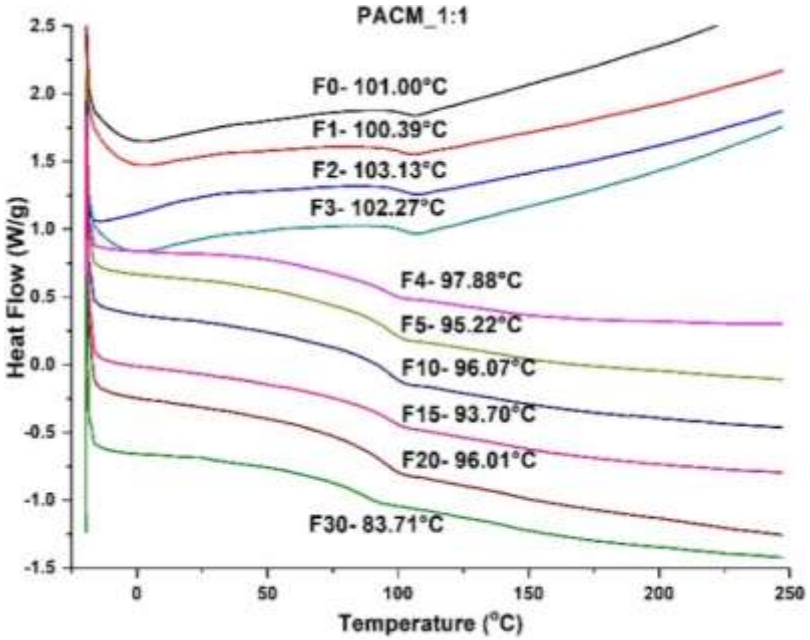

(b)

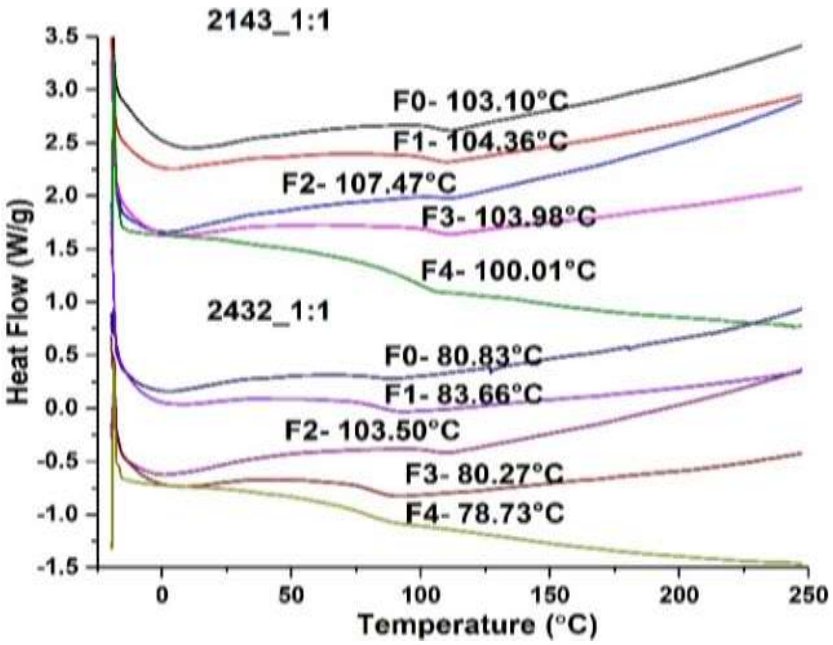

Figure 3.5. DSC scans for (a) PACM_1:1_Fx and (b) 2143_1:1_Fx and 2432_1:1_Fx coatings.

Figure 3.6 shows results for thermal degradation behavior of the IGC_PDMS coatings cured using PACM, Ancamine 2143, and Ancamine 2432. All the coatings showed similar degradation behavior. For all the coatings, 5% weight loss ($T_{d\,5\%}$) occurred at temperatures between 250-265°C. Coatings cured

with PACM showed highest $T_{d\ 5\%}$ of 265°C, while 2432_1:1_Fx coatings showed lowest $T_{d\ 5\%}$ of 252°C. 1-3% initial weight loss for the PACM cured coatings may be attributed to the presence of residual solvent in the coatings after curing. 2143_1:1_Fx and 2432_1:1_Fx coatings showed higher initial weight loss (2-5%). Since the polyamine cured coatings crosslinked at RT, higher amount of residual solvent may have been present in the coating films after curing.

Figure 3.7 shows results for tan delta and storage modulus obtained from DMA for the PACM cured and the polyamine cured coatings. In general, the PACM_1:1_Fx showed higher T_g values compared to the polyamine cured coatings. Tan delta curves for most of the IGC_PDMS coatings appeared narrow and uniform. PACM_1:1_F0 coating exhibited the highest T_g of 120°C among all the IGC_PDMS coatings. Addition of APT-PDMS decreased T_g to 107°C for PACM_1:1_F5. Above 10% APT-PDMS, the coatings failed above T_g due to softening of the coating films. For PACM_1:1_F0, PACM_1:1_F5 and PACM_1:1_F10 coatings, storage modulus values increased in temperature range between 150-200°C. At higher temperatures, the coatings may have undergone residual crosslinking reactions, which in turn caused a spike in tan delta peaks.

(a)

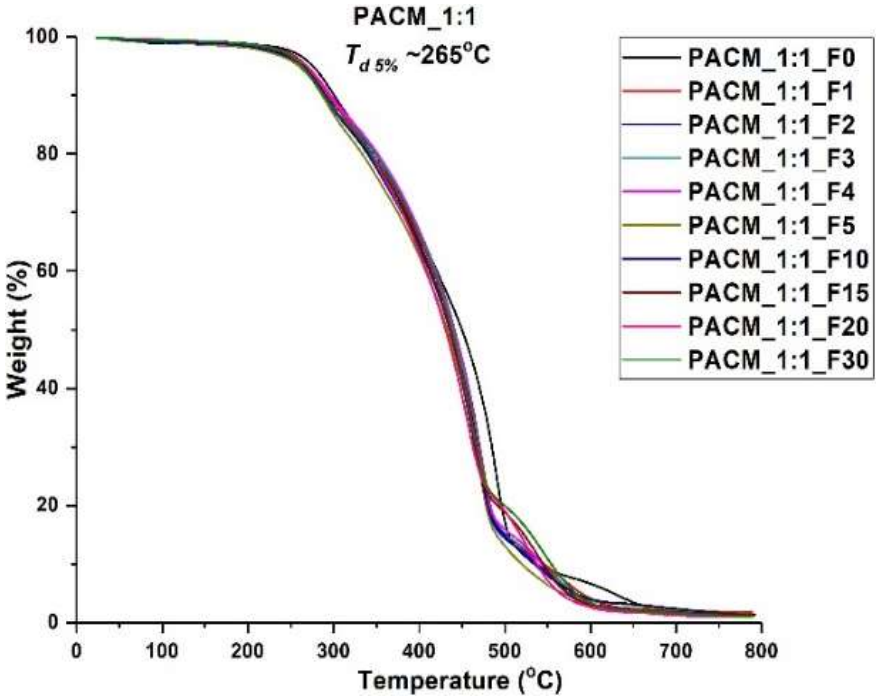

Figure 3.6. Thermal degradation behavior and initial weight loss in percentage for (a) the PACM cured and (b) the polyamine cured coatings.

(b)

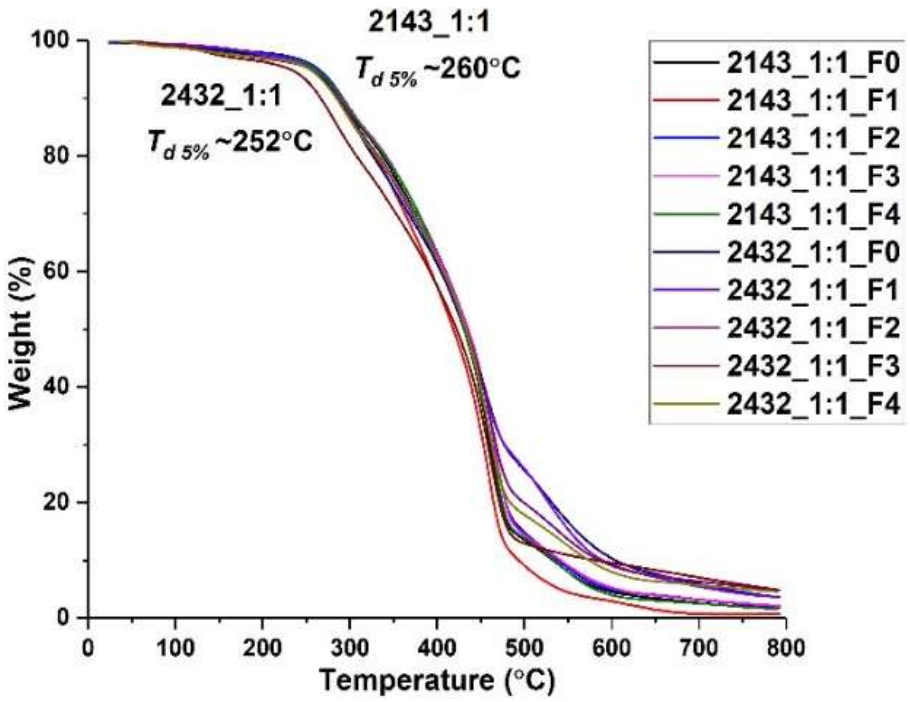

Figure 3.6. Thermal degradation behavior and initial weight loss in percentage for (a) the PACM cured and (b) the polyamine cured coatings (continued).

Formulations with the polyamines showed similar T_g values in the range from 77-82°C, irrespective of the polyamine. For 2143_1:1_Fx and 2432_1:1_Fx formulations, above 4% and 2% APT-PDMS respectively, the films yielded above T_g. In the high temperature region, softening of the coating film with increasing APT-PDMS content may have caused slipping of the film between the equipment clamps, resulting in noise. Similar to the PACM cured coatings, 2432_1:1_F0 coating showed a sudden rise in tan delta peak in the high temperature zone. 2432_1;1_F2 and 2432_1:1_F4 coatings failed above T_g, indicating significant plasticization of the coatings with addition of APT-PDMS. Presence of a possible secondary phase in 2432_1:1_F0 coating was indicated by presence of a minor peak at ~85°C.

Crosslink density (v_e mol/L) of the coatings was calculated using T_g and storage modulus (E' MPa) values in the rubbery plateau region. Table 3.3 shows crosslink density values for the select IGC_PDMS coatings. For the PACM cured coatings, increasing APT-PDMS content increased v_e from 0.29 mol/L for PACM_1:1_F0 to 0.79 mol/L for PACM_1:1_F10. Up to 10% APT-PDMS, E' at 25°C increased drastically from 96 MPa for PACM_1:1_F0 to 825 MPa for PACM_1:1_F10. Conversely, for the polyamine cured coatings, increasing APT-PDMS content to 2% caused decrease in E' at 25°C, but E' at 25°C increased with addition of APT-PDMS above 2%. Addition of APT-PDMS also caused decrease in

v_e values of the polyamine cured coatings. With PACM, a tighter coating network, with higher modulus and v_e, was formed upon curing. But, APT-PDMS provided more freedom of movement to the chains, thereby decreasing T_g of the PACM cured coatings. For the polyamine cured coatings, addition of APT-PDMS may have reinforced the coating network at first, but above 2%, the high MW siloxane chains appeared to "insert" themselves, within the network. Therefore, density of network junctions in the coatings decreased, decreasing the crosslink density of the coatings.

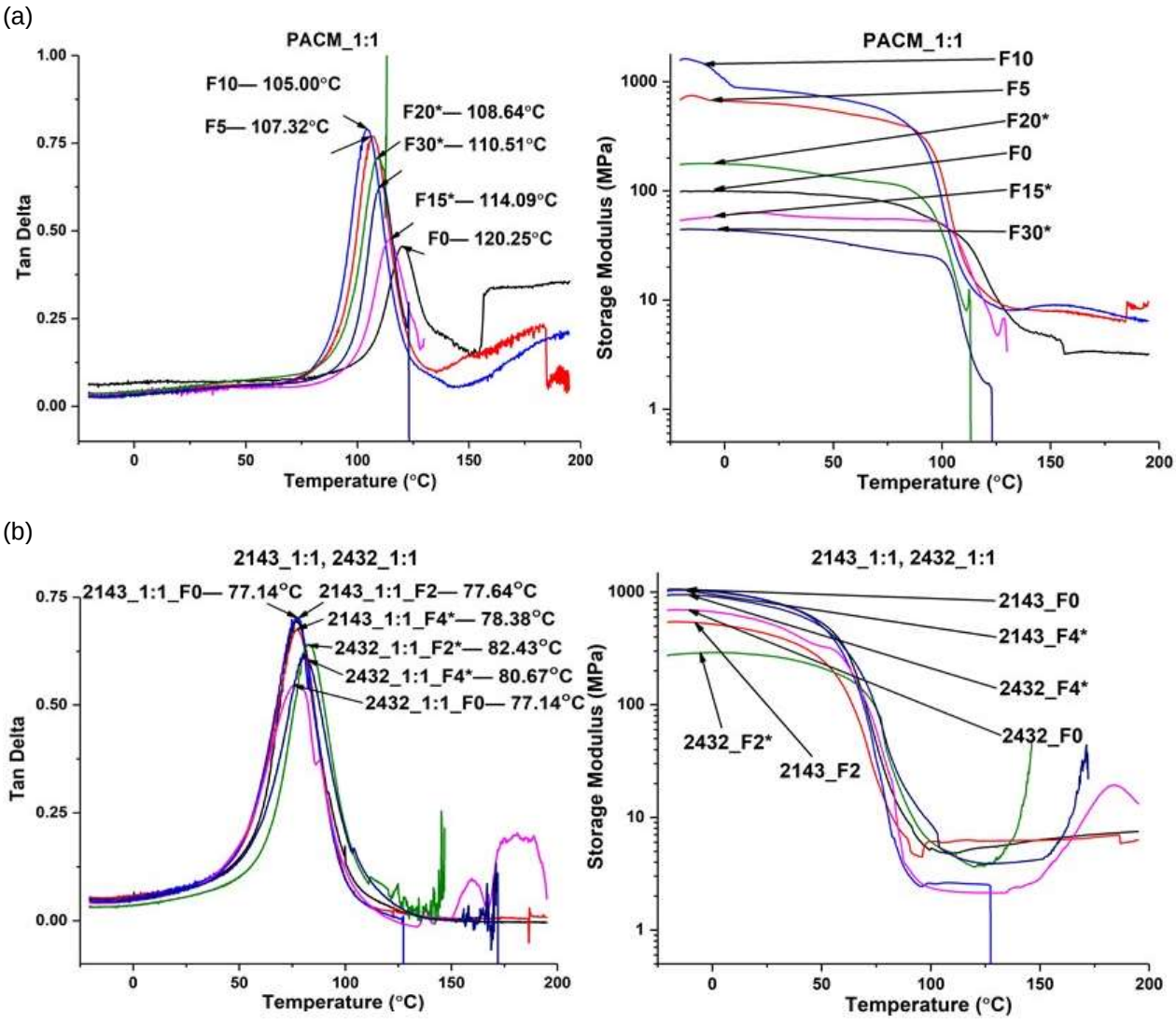

Figure 3.7. Tan delta peaks and storage modulus curves for (a) the PACM cured and (b) the polyamine cured coatings. Asterisk (*) indicates coatings that failed above T_g temperatures.

Table 3.3. Crosslink density and glass transition values for the select IGC_PDMS coatings.

Amines_ E: AHEW	Formulations	*E′* at 25°C (MPa)	T_g (°C)	v_e (mol/L)
PACM_1:1	F0	96.95	120.35	0.29
	F5	623.90	107.32	0.66
	F10	825.40	105.00	0.79
	F15*	60.34	114.09	0.43
	F20*	161.00	108.64	0.77
	F30*	40.00	110.51	0.15
2143_1:1	F0	842.72	77.14	0.57
	F2	426.20	77.64	0.61
	F4*	836.20	78.38	0.29
2432_1:1	F0	532.50	77.14	0.23
	F2*	271.50	82.43	0.41
	F4*	752.50	80.67	0.39
***indicates coatings that failed beyond T_g.**				

Prior to conducting biological tests and surface characterization experiments, PACM_1:1_Fx, 2143_1:1_Fx, and 2432_1:1_Fx coatings were immersed in a circulating water tank to remove catalyst, impurities, and any unreacted monomers for 42 days. After 42 days, leachate toxicity test was conducted on the IGC_PDMS coatings. From the toxicity tests, it was concluded that the Ancamine 2143 cured coatings showed severe toxicity against all fouling organisms even after 42 days of water leaching. Therefore, further FR tests with the 2143_1:1_Fx coatings were discontinued. High toxicity of the Ancamine 2143 cured coatings may be attributed to the glassy nature of the coatings; tightly bound hydrophobic matrix may have disallowed water to penetrate the coating matrices to remove tin catalyst (DBTDAc) used during synthesis of the IGC_PDMS resin. The biological organisms were killed upon contact with the tin moieties in the coatings. Inherent chemical composition of Ancamine 2143 crosslinker may have been another factor responsible for toxicity of the coatings.

PACM_1:1_Fx and 2432_1:1_Fx coatings were analyzed using contact angle experiment to determine formation of hydrophobic coatings. Figure 3.8 shows contact angles and surface energies for PACM_1:1_Fx and 2432_1:1_Fx coatings. For PACM_1:1_Fx and 2432_1:1_Fx coatings, WCA values were greater than 90°, indicating self-stratification of APT-PDMS to form hydrophobic surfaces. Highest WCA value of 118° was obtained for PACM_1:1_F20 and PACM_1:1_F30. SE of PACM_1:1_Fx lied in the range from 10.5-21 mN/m, with PACM_1:1_F30 exhibiting lowest SE of 10.5 mN/m. Among the Ancamine 2432 coatings, 2432_1:1_F4 showed highest WCA of 110° and 2432_1:1_F3 exhibited lowest SE of 16.3 mN/m. Poor compatibility of PDMS with the polar GC matrix and surface energy minimization

are the two main causes of stratification of APT-PDMS. A uniform tightly bound coating network with PACM crosslinker may have forced APT-PDMS chains towards coating-air interface, forming a low surface energy outer layer. On the other hand, a comparatively loose coating network with Ancamine 2432 may have caused APT-PDMS to remain “bound” within the coating network, thereby limiting stratification of the PDMS chains.

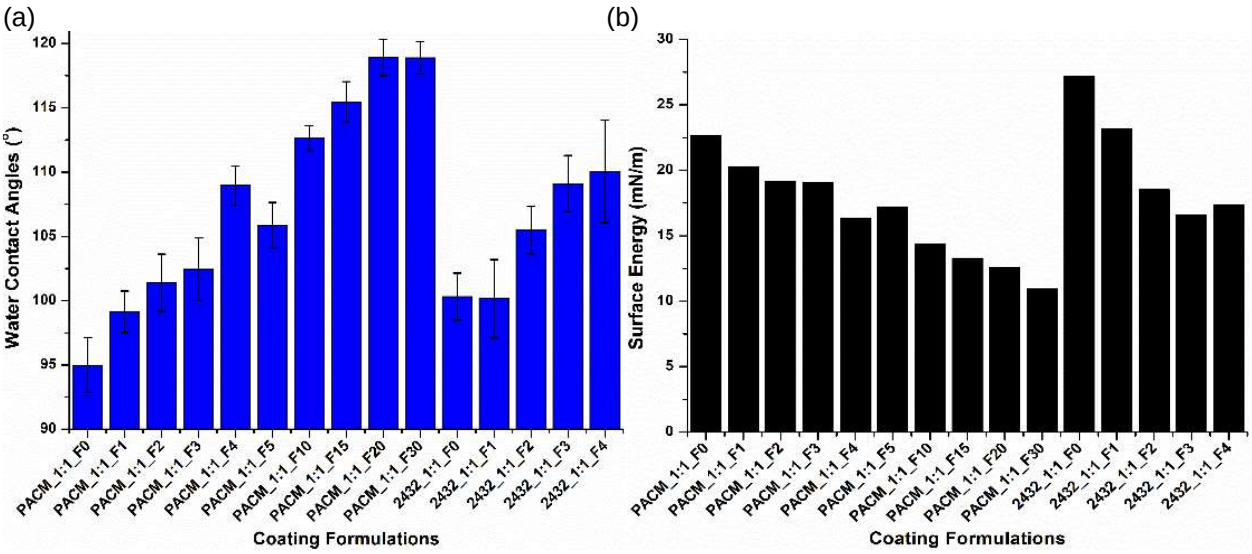

Figure 3.8. (a) Water contact angles and (b) surface energy values for PACM_1:1_Fx and 2432_1:1_Fx coatings. Error bars indicate standard deviation.

To investigate FR performance of PACM_1:1_Fx and 2432_1:1_Fx coatings, biological tests with diatoms *N.incerta,* biofilm *C.lytica,* microalgae *U.linza,* mussels *Geukensia demissa*, and barnacles *A.amphitrite* were conducted on the pre-leached IGC_PDMS coatings. FR performance of the IGC_PDMS coatings was compared to the commercially available standards, Silastic T2 (T2), Intersleek 700 (I-700), Intersleek 900 (I-900) and Intersleek 1100SR (1100SR) and regular polyurethanes (PU; no siloxane) coatings. Figure 3.9 shows results for diatom *N.incerta* attachment and removal for PACM_1:1_Fx and 2432_1:1_Fx coatings. In general, the IGC_PDMS coatings showed significantly higher attachment of *N.incerta* as compared to I-900 and 1100SR coatings, but similar attachment as regular PU, T2, and I-700 coatings. For the PACM cured coatings, diatom *N.incerta* attachment was slightly lower with 10-30% APT-PDMS compared to other formulations. The Ancamine 2432 cured coatings showed slightly higher attachment of the diatoms compared to the PACM cured coatings; for 2432_1:1_Fx coatings, the number of attached diatoms increased slightly with increasing APT-PDMS

content. *N.incerta* removal at 20 psi was significantly higher than 10 psi water jet pressure. The PACM cured coatings with 10-30% APT-PDMS facilitated 70-90% removal of *N.incerta*, similar to regular polyurethane coatings. Conversely, APT-PDMS content between 0-2% for 2432_1:1_Fx coatings was required to facilitate 75-92% removal of the diatoms, with 2432_1:1_F0 showing highest removal of the diatoms among all the formulations. Increasing APT-PDMS content with the Ancamine 2432 cured coatings decreased the diatom release from the coatings. The commercial standards showed only 30-60% removal of *N.incerta* at 20 psi water jet pressure.

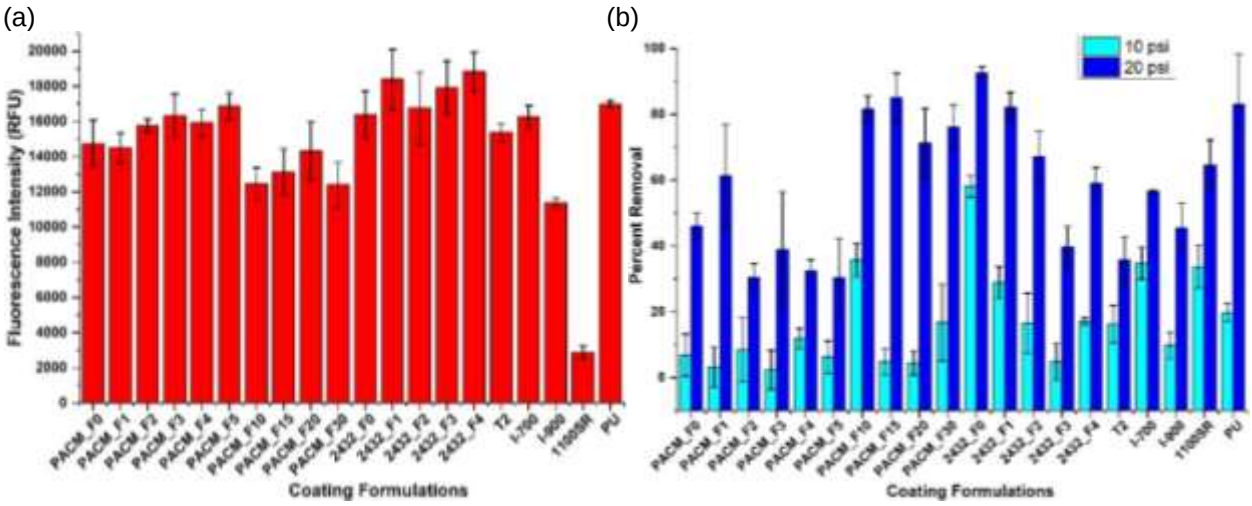

Figure 3.9. Diatom *N.incerta* (a) attachment and (b) removal at 10 psi and 20 psi water jet pressures from the PACM and Ancamine 2432 cured coatings. Error bars indicate standard deviation.

Figure 3.10 shows results for bacterial biofilm *C.lytica* attachment and removal for PACM_1:1_Fx and 2432_1:1_Fx coatings. From Figure 3.10(a), it can be seen that the amount of *C.lytica* attached to the IGC_PDMS coatings was significantly lower than I-700. Further, 2432_1:1_Fx coatings showed lower biofilm attachment compared to PACM_1:1_Fx coatings. Similar to the diatoms, 20 psi water jet pressure facilitated slightly higher removal of *C.lytica* compared to 10 psi water jet. At 20 psi, 65-70% biofilm was removed from the surface of the IGC_PDMS coatings, similar to regular PU coatings. Among the commercial standards, I-900 and 1100SR, facilitated ~98% removal of biofilm from the surface, while I-700 showed only 55% removal.

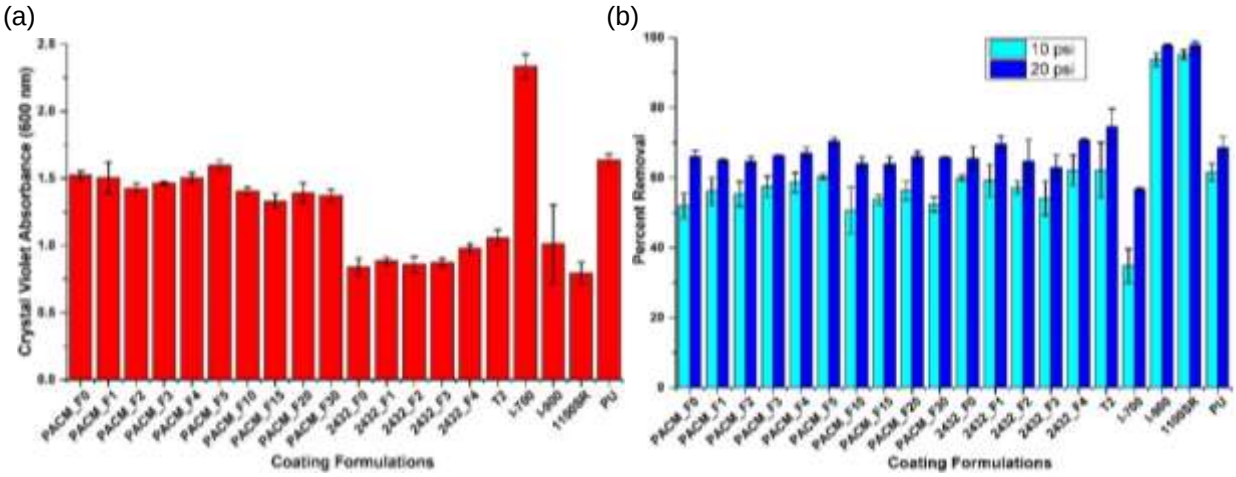

Figure 3.10. Bacterial biofilm *C.lytica* (a) attachment and (b) removal at 10 psi and 20 psi water jet pressures. Error bars indicate standard deviation.

Figure 3.11 shows results for attachment and removal of microalgae *U.linza* at 110 kPa water jet pressure. I-700 and I-900 showed severe toxicity against the microalgae; the two commercial standards were, therefore, excluded from the experiment. Polystyrene (PS) coating was added as a control for this experiment. The IGC_PDMS coatings showed lower attachment of *U.linza* as compared to the commercial standards, PU, and PS. But, while T2 and 1100SR facilitated 75-90% removal of *U.linza*, the IGC_PDMS coatings could not facilitate more than 25% microalgae removal even at 110 kPa. PACM_1:1_Fx coatings showed higher removal of the microalgae compared to 2432_1:1_Fx coatings. PACM_1:1_F10 showed highest percent removal (25%) of *U.linza*, while 2432_1:1_F4 showed the worst FR performance against *U.linza* (~5% removal). At water jet pressures of 18 and 67 kPa, the IGC_PDMS coatings showed negligible (< 5%) microalgae removal.

Figure 3.12 shows mussel adhesion data for PACM_1:1_Fx and 2432_1:1_Fx coatings. For the IGC_PDMS coatings, 1-2 mussels out of 6 did not attach to most of the coatings during experimentation. PACM_1:1_Fx coatings showed lower attachment strength of the mussels as compared to 2432_1:1_Fx coatings. Higher APT-PDMS content in the PACM cured coatings facilitated removal of the mussels, while the force of removal of the mussels increased with increase in APT-PDMS content for the Ancamine 2432 cured coatings. Formulations PACM_1:1_F5, PACM_1:1_F10 and PACM_1:1_F15 showed mussel adhesion strength slightly lower than I-700 and PU. Among all the formulations, PACM_1:1_F10 showed the best FR performance against mussels, with ~10 N force of removal required for 4 out 6 mussels that attached to the coating. No mussels attached to I-900 and 1100SR coatings.

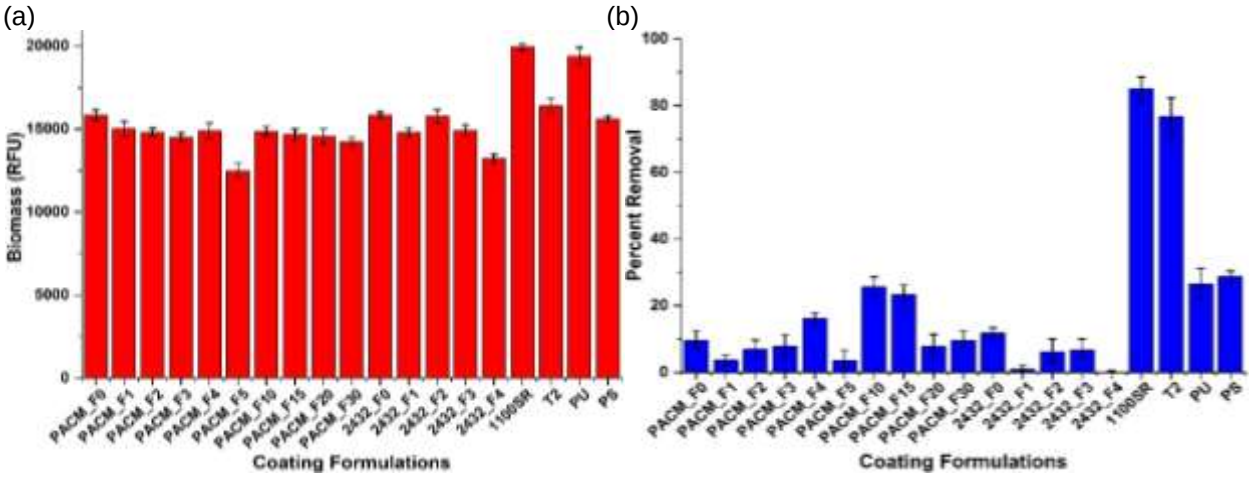

Figure 3.11. Microalgae *U.linza* (a) attachment and (b) removal at 110 kPa water pressure. Error bars indicate standard deviation.

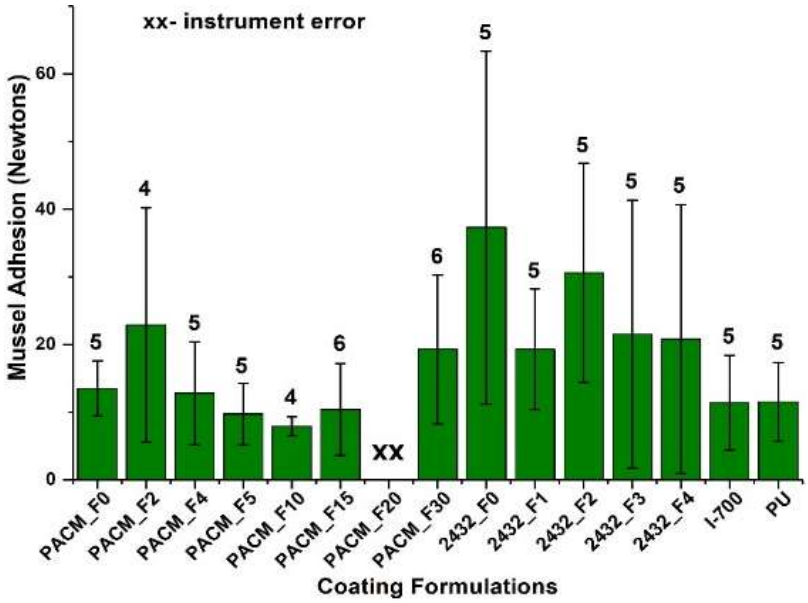

Figure 3.12. Mussel *Geukensia demissa* adhesion for select PACM_1:1_Fx coatings. Numbers above data points indicate the number of mussels out of six that attached to the coatings during experimentation. None of the mussels attached to I-900 or 1100SR coatings. Error bars indicate standard deviation.

Based on the FR results of the IGC_PDMS coatings against microfoulants and mussels, select formulations were chosen for barnacle attachment experiment (Figure 3.13). Ratios above each data point indicate the number of barnacles that attached to the coatings to the number of barnacles that broke during the experiment. In general, the IGC_PDMS coatings showed significantly higher attachment of barnacles as compared to I-900 and 1100SR. 2432_1:1_Fx coatings showed the worst barnacle removal performance among all the coatings. PACM_1:1_Fx coatings required slightly lower removal force as

compared to I-700. Increasing APT-PDMS content in PACM_1:1_Fx coatings resulted in decrease in barnacle attachment strength, while the inverse was true for 2432_1:1_Fx coatings. Among all the select IGC_PDMS formulations, PACM_1:1_F30 required lowest average force of removal of ~0.12 MPa for 5 (out of 6) barnacles that attached to the coating. Conversely, 2432_1:1_F0 exhibited the worst FR performance among all IGC_PDMS formulations; all 6 barnacles attached onto the coating, with 2 barnacles breaking during experimentation.

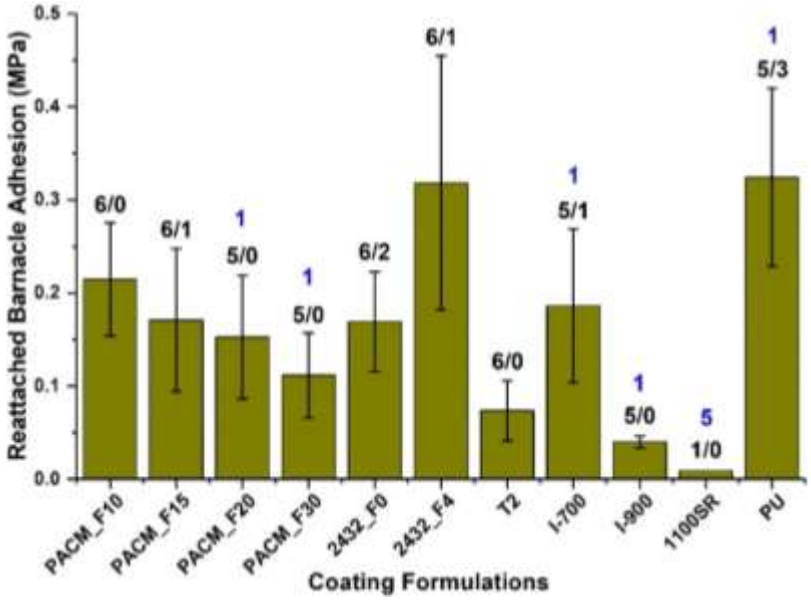

Figure 3.13. Barnacle reattachment data for select IGC_PDMS coatings. Ratios above each data point indicate the number of barnacles attached to the coatings to the number of barnacles that broke during experimentation. Numbers above some data points indicate the number of barnacles that did not attach to the coatings during the experiment. Error bars indicate standard deviation.

Subpar FR performance of the IGC_PDMS coatings, in spite of formation of highly hydrophobic surfaces, necessitated extensive surface characterization of the coatings to better understand their surface chemistry. As observed from the contact angle experiment (Figure 3.8), the IGC_PDMS coatings exhibited high hydrophobicity, with SE decreasing with increasing APT-PDMS content. But, an interesting observation was made for PACM_1:1_F20 and PACM_1:1_F30 coatings, where WCA appeared to change with time, in spite of the purely hydrophobic nature of the coatings. WCA dropped from ~118° for PACM_1:1_F20 and PACM_1:1_F30 to ~80° in 10 minutes. Surfaces of PACM_1:1_F20 and PACM_1:1_F30 coatings were extremely “oily” to touch. The “oil” was believed to be unreacted APT-PDMS from the coatings. To identify its chemical composition, the “oil” was characterized using FTIR. The

oil was transferred onto a KBr plate by carefully rubbing the KBr plate on the surfaces of PACM_1:1_F20 and PACM_1:1_F30 formulations. The spectrum of the “oil” was compared to FTIR spectrum of APT-PDMS (analyzed separately). Comparison of the two spectra (Figure 3.14) showed that the “oil” on the coating films was excess APT-PDMS from the coatings. The PACM cured coating films may have become saturated with APT-PDMS at 15%. Above 15%, APT-PDMS could not remain bound to the underlying coating matrix, in spite of the presence of reactive amine terminated chain ends. The unbound, free APT-PDMS chains accumulated to the surface due to self-stratification of APT-PDMS during crosslinking. Dynamic WCA changes were probably caused by the motion of the free APT-PDMS chains on the coating surface.

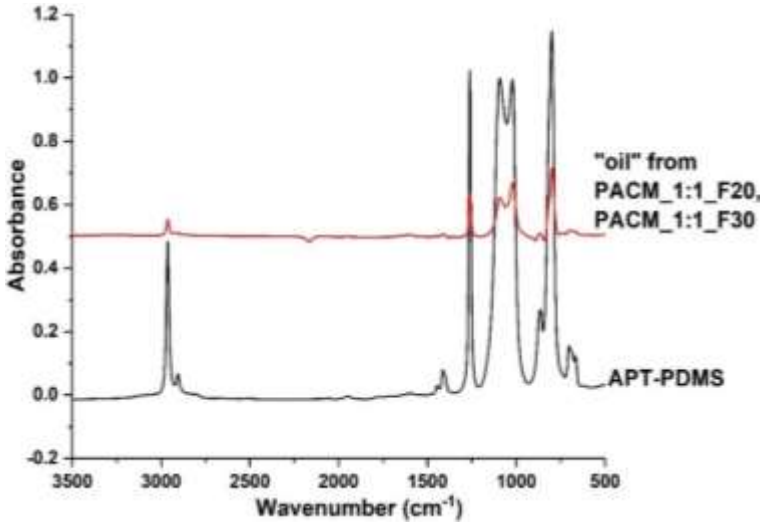

Figure 3.14. Comparison of FTIR spectra of APT-PDMS and “oil” from surfaces of PACM_1:1_F20 and PACM_1:1_F30.

PACM_1:1_Fx and 2432_1:1_Fx coatings were also characterized using ATR-FTIR (Figure 3.15). ATR-FTIR spectra for the coatings showed absence of reactive epoxy groups at ~915 cm^{-1}, indicating potentially complete epoxy-amine crosslinking reactions with PACM and Ancamine 2432 diamines. Further, peaks at 1018-1089 cm^{-1} indicated Si-O-Si linkages on the surface of the coatings, indicating self-stratification of APT-PDMS on the surface. Secondary amine (-NH-) peak and carbonyl (-C=O) peak on the surface indicated that the underlying cured GC matrix was partially present on the coating surface. For PACM_1:1_Fx coatings, with increasing APT-PDMS content, a slight decrease in intensity of the -NH- peak and increase in intensity of Si-O-Si peak may be due to rise in concentration of the coating surfaces with siloxane chains. Among the IGC_PDMS coatings, the intensity of -NH- and -C=O peaks was higher

for coatings with Ancamine 2432 as compared to the PACM cured coatings, due to lower APT-PDMS content of the Ancamine 2432 cured coatings. Moreover, WCA values (Figure 3.8) showed that the Ancamine 2432 cured coatings were not as hydrophobic as PACM_1:1_Fx at similar APT-PDMS loading. Therefore, the surfaces of 2432_1:1_Fx showed comparatively higher carbamate concentration.

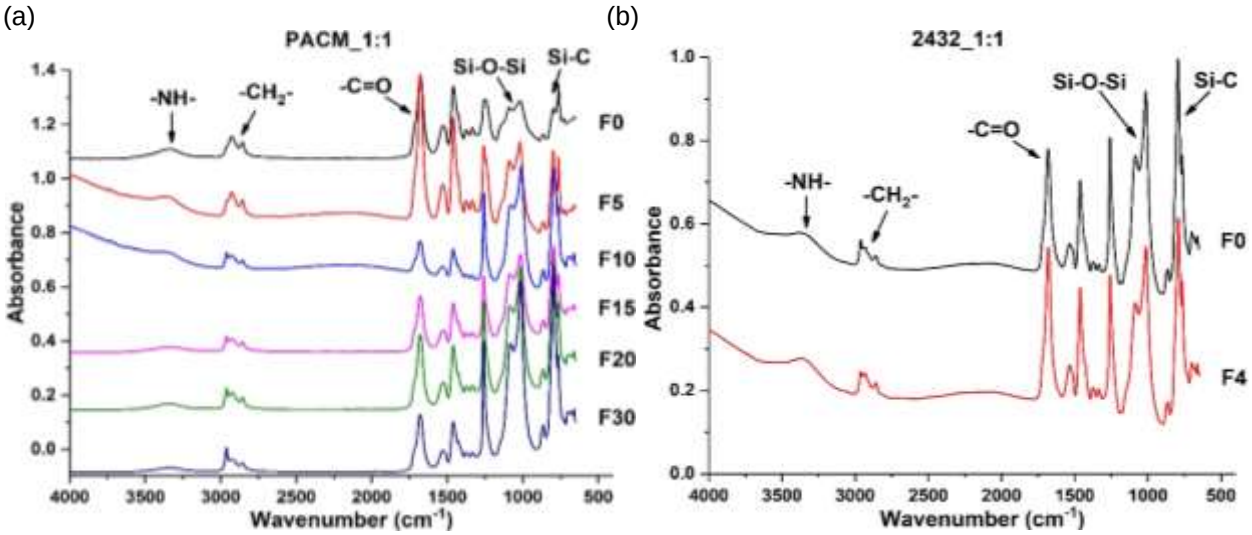

Figure 3.15. ATR-FTIR spectra for IGC_PDMS coatings cured using (a) PACM and (b) Ancamine 2432 diamines.

Visually, the PACM cured coatings appeared smooth and uniform. Conversely, visual analysis of the Ancamine 2432 showed presence of discolored domains on the surface of the coatings, probably due to oxidation of amine rich domains on the coating surfaces. Figure 3.16 shows AFM scans for select IGC_PDMS coatings. With both PACM and Ancamine 2432, coatings with 0% additional APT-PDMS exhibited a rough outer surface. The surfaces appeared to be smoother with the addition of APT-PDMS. But, addition of APT-PDMS also resulted in formation of “pores” on the coating surfaces. Concentration of “pores” increased with increase in APT-PDMS content.

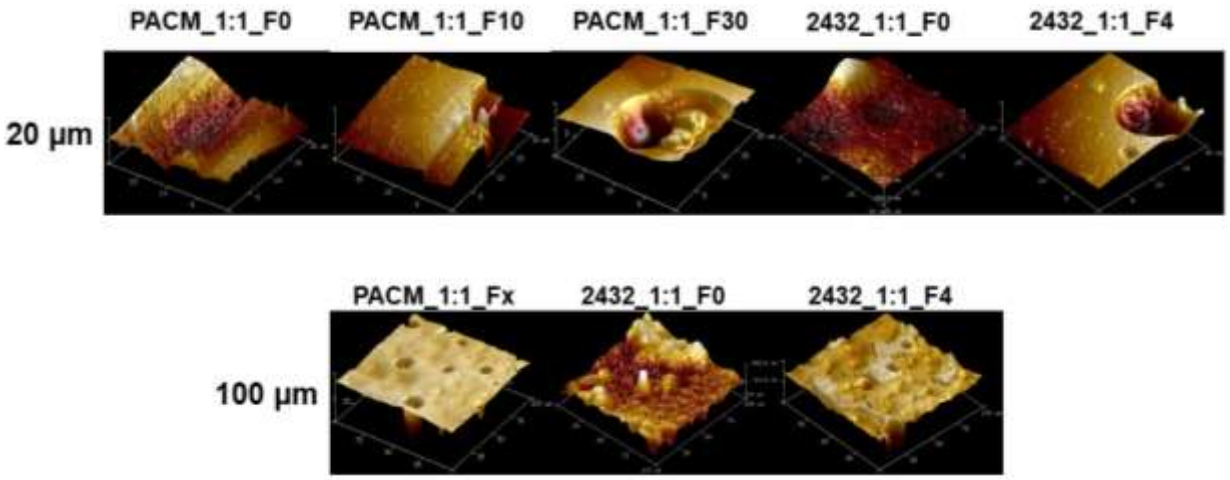

Figure 3.16. AFM scans for 20 µm x 20 µm and 100 µm x 100 µm area of select PACM and Ancamine 2432 cured coatings.

Figure 3.17 shows high resolution XPS spectra for individual O1s, C1s, and N1s elements on the surfaces of PACM_1:1_F30 and 2432_1:1_F4 coatings. Curve fitting was conducted on the individual elements to determine the concentration of PDMS components on the surface of the coatings. Results from XPS were anticipated to provide insights into the surface composition of the hydrophobic GC formulations at the highest permissible loading of APT-PDMS. Both the coatings showed characteristic Si2p peak at 102.25-102.28 eV, indicating presence of siloxane on the coating surfaces. Table 3.4 shows atomic percent of the individual C1s, O1s, and N1s elements as determined from peak fitting. The two formulations also showed presence of N1s peaks, with higher N content on PACM_1:1_F30 (5.57%) as compared to 0.87% on 2432_1:1_F4. Three different chemical states for O1s and C1s were observed for both the coatings. Peaks at ~532, 531.48, and 533.27 eV were indicative of O from siloxane, C-O-C/C-O-H linkages and carbamate (urethane) linkages. Similarly, peaks at ~284.20, 285.90-286.18, and 288.83-289.14 indicated C atoms from the C-C/C-H, C-O/C-N and carbamate/urethane linkages respectively. Presence of higher concentrations of O and C atoms from carbamate linkages and C-O-C/C-O-H bonds on the surface of PACM_1:1_F30 as compared to 2432_1:1_F4 may be attributed to movement of the excess APT-PDMS in the vacuum chamber of the XPS instrument, which may have exposed the carbamate matrix to the incident X-ray beam.

Table 3.4. Chemical composition of the coatings determined after peak fitting.

Formulations	Chemical states		Binding energies (eV)	Atom %
PACM_1:1_F30	O1s	Si-O-Si	532.00	12.57
		C-O	531.48	11.99
		C=O	533.27	3.18
	C1s	C-C/C-H	284.29	49.87
		C-O/C-N	285.90	13.16
		C=O	289.14	3.66
	N1s	Total	399.91	5.57
2432_1:1_F4	O1s	Si-O-Si	531.79	18.81
		C-O	531.48	6.63
		C=O	533.27	2.09
	C1s	C-C/C-H	284.20	65.69
		C-O/C-N	286.16	4.98
		C=O	288.83	0.94
	N1s	Total	399.30	0.87

(a)

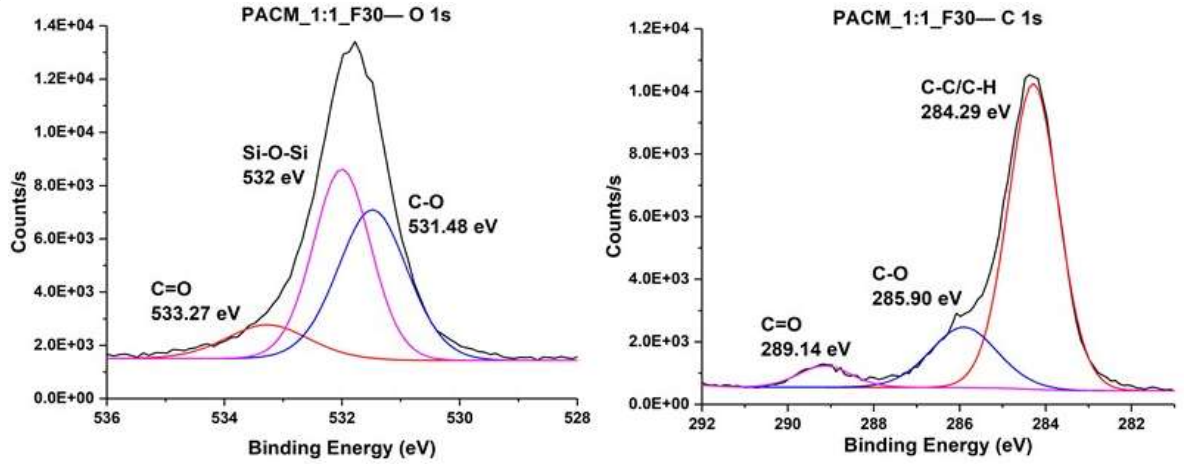

(b)

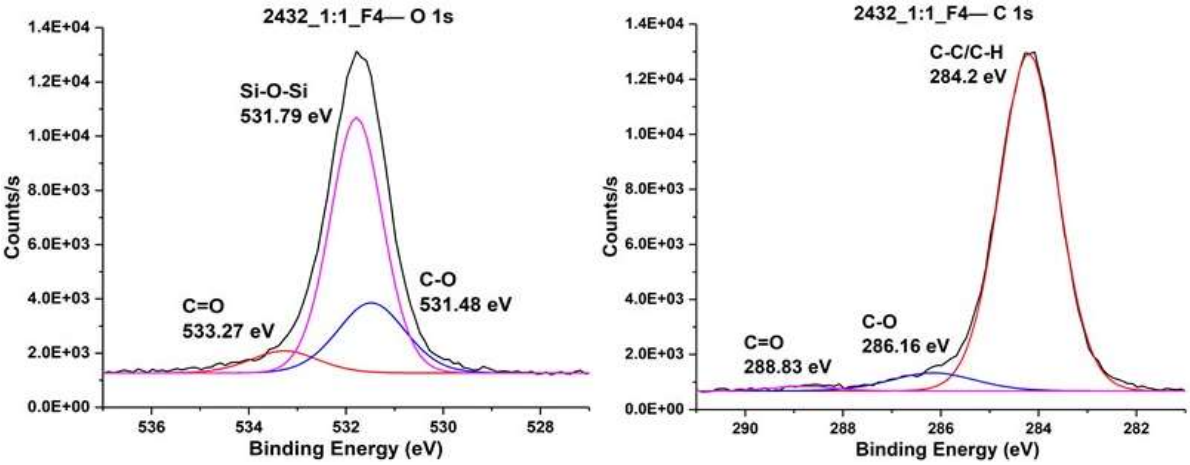

Figure 3.17. High resolution XPS spectra for O1s and C1s with peak fitting for (a) PACM_1:1_F30 and (b) 2432_1:1_F4 coatings.

The above results showed that versatile nature of the IGC_PDMS resin allows formation of hard and flexible coatings using a variety of amine crosslinkers, with different chemical compositions and functionalities. Cycloaliphatic nature of PACM and Ancamine 2143 imparted hardness and rigidity to the coatings, resulting in high T_g values. Conversely, the aliphatic Ancamine 2432 provided a softer core to the coatings, allowing higher chain movement in the coating matrix. Soft nature of the coatings combined with potential hydrophobic chain interactions between APT-PDMS chains and alkyl chains from the GC resin and the amine crosslinker may have hampered self-stratification of APT-PDMS chains, causing comparatively lower hydrophobicity of the Ancamine 2432 cured coatings than the PACM cured coatings. Further evidence of a softer matrix with Ancamine 2432 was observed from the comparatively shorter tan delta peaks for the 2432_1:1_Fx coatings, indicating presence of high concentration of elastomeric components in the matrix. AFM and ATR-FTIR for the Ancamine 2432 cured coatings showed higher intensities of -NH and -C=O as compared to the PACM cured coatings, indicating more carbamate on the surface compared to the PACM cured coatings. Further, siloxane content of 12-18% on PACM_1:1_F30 and 2432_1:1_F4 and presence of significant amount of C-O-C/C-O-H on the two coatings may have reduced FR efficiency of PDMS, thereby hampering FR performance of the coatings. In spite of presence of 30% APT-PDMS on the PACM cured formulation, movement of unreacted PDMS chains resulted in exposure of the underlying GC coating.

Results obtained from FR experiments showed interesting behavior of the coatings. Past research shows that hydrophobic PDMS-rich surfaces tend to allow stronger attachment of diatoms compared to hydrophilic surfaces.[34] Therefore, among the Ancamine 2432 cured formulations, 2432_1:1_F0 showed highest diatom removal and increasing APT-PDMS content in the Ancamine 2432 formulations decreased diatom removal. But, the PACM cured formulations showed the opposite trend, where diatom removal increased with increasing APT-PDMS content. For the PACM cured coatings, the coatings were completely saturated with APT-PDMS by 15%. Above 15%, the coatings showed presence of unreacted APT-PDMS chains on the surfaces. Although no unreacted APT-PDMS was observed on formulations with 10 or 15% APT-PDMS, movement of the long APT-PDMS chains on the formulations with 10-30% APT-PDMS may have exposed the underlying polar GC matrix to the diatoms. The polar carbamate rich coatings may have disallowed the diatoms from attaching strongly onto the surfaces.

When the coatings were exposed to water jet, the loosely attached diatoms were easily removed. Unlike diatoms, microalgae, barnacles and mussels tend to attach weakly to hydrophobic surfaces.[7, 23] Therefore, barnacle attachment strength decreased for the PACM cured coatings with increasing APT-PDMS content. For the Ancamine 2432 coatings, although barnacle attachment strength increased with increasing APT-PDMS content, only 1 barnacle base broke from 2432_1:1_F4 coating as against 2 barnacle bases breaking from 2432_1:1_F0 coating. Higher attachment of the fouling organisms onto the Ancamine 2432 cured coatings may be attributed to limited stratification of APT-PDMS. In spite of the highly hydrophobic nature of the PACM cured coatings, the fouling organisms may have been able to detect the underlying polar GC coatings due to movement of the loosely held PDMS chains, resulting in stronger attachment of microalgae, barnacles and mussels. Furthermore, nanoscale roughness of the IGC_PDMS coatings at 0% APT-PDMS and formation of “pores” with addition of APT-PDMS may be responsible for providing surface “textures” for stronger attachment of the fouling organisms.

Conclusions

A novel isocyanate-free IGC_PDMS resin was synthesized using HDI trimer, glycidol, and dicarbinol terminated PDMS (5k g/mol). EEP and toluene were used as solvents to give ~50% solids resin with 1:1 w/w solvent blend of EEP and toluene. Absence of the isocyanate peak as observed using FTIR showed that isocyanate had completely reacted over the course of the reaction. Diamine crosslinkers, PACM, Ancamine 2143, Ancamine 2432, Ancamide 2634, and Ancamide 2767, were used to cure the synthesized IGC_PDMS resin in 1:1, 1:2, and 2:1 epoxy: AHEW ratios. Additionally, 20k g/mol APT-PDMS (33% in toluene) was added in varying amounts to make different formulations to understand the effect of changing APT-PDMS content on FR performance of the IGC_PDMS coatings. Although all the IGC_PDMS coatings exhibited high hardness, the coatings cured using PACM and the polyamines showed better overall performance (hardness, flexibility, and appearance) as compared to the polyamide cured coatings. Force curing of the PACM cured formulations at 80°C for 45 min resulted in formation of glossy, and uniform coatings, while ambient curing of the polyamine cure coatings caused formation of non-glossy, hazy coatings. WCA > 90° and SE between 10-25 mN/m for all the IGC_PDMS formulations indicated self-stratification of APT-PDMS to form low surface energy, hydrophobic surfaces. PACM_1:1_F30 coating showed highest WCA value of 118° and lowest SE value of 10.5 mN/m among

all the IGC_PDMS coating formulations. With Ancamine 2432, highest WCA of 110° for 2432_1:1_F3 and lowest SE of ~17 mN/m for 2432_1:1_F4 was achieved. Comparatively lower WCA and higher SE with Ancamine 2432 may be attributed to formation of a looser coating network, which disallowed complete stratification of the PDMS chains to the surface of the coatings. Analysis of the coatings with AFM showed formation of rough coatings at 0% APT-PDMS and formation of “pores” with addition of APT-PDMS. ATR-FTIR showed higher concentration of APT-PDMS on surfaces of the PACM cured coatings compared to the Ancamine 2432 cured coatings. But, XPS showed lower percentage of PDMS chains on PACM_1:1_F30 due to possible exposure of GC layer upon movement of the excess siloxane chains on the coating surface.

Laboratory FR experiments with micro- and macrofoulants showed that the IGC_PDMS coatings showed higher attachment of diatom *N.incerta* as compared to the commercial I-900 and 1100SR standards. PACM_1:1_Fx with 10-30% APT-PDMS and 2432_1:1_Fx with 0-2% APT-PDMS facilitated highest diatom removal of 75-90% at 20 psi water jet pressure. 2432_1:1_Fx coatings showed lower attachment of bacterial biofilm *C.lytica* as compared to PACM_1:1_Fx. At 20 psi water jet pressure, only 65-70% *C.lytica* was removed from the surface of the IGC_PDMS coatings, which was significantly lower than ~98% removal from I-900 and 1100SR coatings. Additionally, lower amount of microalgae *U.linza* attached to the IGC_PDMS coatings, but the coatings could not facilitate more than 25% removal of the microalgae. Against the macrofoulants, like barnacles and mussels, all the IGC_PDMS coatings showed subpar FR performance as compared to I-900 and 1100SR. Attachment strength of mussels and barnacles on 2432_1:1_Fx coatings was higher compared to the PACM cured coatings. PACM_1:1_F10 required lowest force of ~10 N for the removal of 4 (out of 6) mussels that attached to the coating. While attachment of barnacles reduced with increasing APT-PDMS content for the PACM cured coatings, the barnacle attachment strength increased with increasing APT-PDMS content for the Ancamine 2432 cured coatings. PACM_1:1_F30 showed lowest barnacle adhesion strength of ~0.11 MPa for 5 out of 6 barnacles that attached to the coating during experimentation. Unusual performance of the hydrophobic PACM cured coatings against diatoms and barnacles may be attributed to presence of nanopores and free mobile PDMS chains on the surfaces of coatings with 20-30% APT-PDMS. Although the performance of the IGC_PDMS coatings was subpar compared to the commercial standards, the results

obtained from this preliminary study show that with proper selection of amine crosslinkers and solvents or solvent blends, isocyanate-free GC based coatings can be successfully used in FR marine applications.

References

1. Callow, J. A.; Callow, M. E., Trends in the development of environmentally friendly fouling-resistant marine coatings. *Nature Communications* **2011,** *2*, 244.

2. Yebra, D. M.; Kiil, S.; Dam-Johansen, K., Antifouling technology—past, present and future steps towards efficient and environmentally friendly antifouling coatings. *Progress in Organic Coatings* **2004,** *50* (2), 75-104.

3. Magin, C. M.; Cooper, S. P.; Brennan, A. B., Non-toxic antifouling strategies. *Materials Today* **2010,** *13* (4), 36-44.

4. Schultz, M. P., Effects of coating roughness and biofouling on ship resistance and powering. *Biofouling* **2007,** *23* (5), 331-341.

5. Sommer, S.; Ekin, A.; Webster, D. C.; Stafslien, S. J.; Daniels, J.; VanderWal, L. J.; Thompson, S. E. M.; Callow, M. E.; Callow, J. A., A preliminary study on the properties and fouling-release performance of siloxane–polyurethane coatings prepared from poly (dimethylsiloxane)(PDMS) macromers. *Biofouling* **2010,** *26* (8), 961-972.

6. Sommer, S. A.; Byrom, J. R.; Fischer, H. D.; Bodkhe, R. B.; Stafslien, S. J.; Daniels, J.; Yehle, C.; Webster, D. C., Effects of pigmentation on siloxane–polyurethane coatings and their performance as fouling-release marine coatings. *Journal of Coatings Technology and Research* **2011,** *8* (6), 661-670.

7. Bodkhe, R. B.; Thompson, S. E. M.; Yehle, C.; Cilz, N.; Daniels, J.; Stafslien, S. J.; Callow, M. E.; Callow, J. A.; Webster, D. C., The effect of formulation variables on fouling-release performance of stratified siloxane–polyurethane coatings. *Journal of Coatings Technology and Research* **2012,** *9* (3), 235-249.

8. Ekin, A.; Webster, D. C., Combinatorial and High-Throughput Screening of the Effect of Siloxane Composition on the Surface Properties of Crosslinked Siloxane− Polyurethane Coatings. *Journal of Combinatorial Chemistry* **2007,** *9* (1), 178-188.

9. Ekin, A.; Webster, D. C.; Daniels, J. W.; Stafslien, S. J.; Cassé, F.; Callow, J. A.; Callow, M. E., Synthesis, formulation, and characterization of siloxane–polyurethane coatings for underwater marine

applications using combinatorial high-throughput experimentation. *Journal of Coatings Technology and Research* **2007,** *4* (4), 435-451.

10. Majumdar, P.; Ekin, A.; Webster, D. C., Thermoset Siloxane—Urethane Fouling Release Coatings. In *Smart Coatings,* ***March 13, 2007****, 61-75*.

11. Edwards, P. A.; Striemer, G.; Webster, D. C., Novel polyurethane coating technology through glycidyl carbamate chemistry. *JCT Research* **2005,** *2* (7), 517-527.

12. Edwards, P. A.; Striemer, G.; Webster, D. C., Synthesis, characterization and self-crosslinking of glycidyl carbamate functional resins. *Progress in Organic Coatings* **2006,** *57* (2), 128-139.

13. Chattopadhyay, D. K.; Muehlberg, A. J.; Webster, D. C., Organic–inorganic hybrid coatings prepared from glycidyl carbamate resins and amino-functional silanes. *Progress in Organic Coatings* **2008,** *63* (4), 405-415.

14. Chattopadhyay, D. K.; Zakula, A. D.; Webster, D. C., Organic–inorganic hybrid coatings prepared from glycidyl carbamate resin, 3-aminopropyl trimethoxy silane and tetraethoxyorthosilicate. *Progress in Organic Coatings* **2009,** *64* (2), 128-137.

15. Harkal, U. D.; Muehlberg, A. J.; Li, J.; Garrett, J. T.; Webster, D. C., The influence of structural modification and composition of glycidyl carbamate resins on their viscosity and coating performance. *Journal of Coatings Technology and Research* **2010,** *7* (5), 531-546.

16. Harkal, U. D.; Muehlberg, A. J.; Webster, D. C., UV curable glycidyl carbamate based resins. *Progress in Organic Coatings* **2012,** *73* (1), 19-25.

17. Chattopadhyay, D. K.; Webster, D. C., Hybrid coatings from novel silane-modified glycidyl carbamate resins and amine crosslinkers. *Progress in Organic Coatings* **2009,** *66* (*1*), 73-85.

18. Harkal, U. D.; Muehlberg, A. J.; Edwards, P. A.; Webster, D. C., Novel water-dispersible glycidyl carbamate (GC) resins and waterborne amine-cured coatings. *Journal of Coatings Technology and Research* **2011,** *8* (6), 735-747.

19. Cardillo, P.; Nebuloni, M., Theoretical and calorimetric evaluation of thermal stability of glycidol. *Journal of Loss Prevention in the Process Industries* **1991,** *4* (4), 242-245.

20. Bodkhe, R. B.; Stafslien, S. J.; Cilz, N.; Daniels, J.; Thompson, S. E. M.; Callow, M. E.; Callow, J. A.; Webster, D. C., Polyurethanes with amphiphilic surfaces made using telechelic functional PDMS having orthogonal acid functional groups. *Progress in Organic Coatings* **2012,** *75* (1), 38-48.

21. Cassé, F.; Stafslien, S. J.; Bahr, J. A.; Daniels, J.; Finlay, J. A.; Callow, J. A.; Callow, M. E., Combinatorial materials research applied to the development of new surface coatings V. Application of a spinning water-jet for the semi-high throughput assessment of the attachment strength of marine fouling algae. *Biofouling* **2007,** *23* (2), 121-130.

22. Chen, Z.; Chisholm, B.; Kim, J.; Stafslien, S.; Wagner, R.; Patel, S.; Daniels, J.; Wal, L. V.; Li, J.; Ward, K., UV-curable, oxetane-toughened epoxy-siloxane coatings for marine fouling-release coating applications. *Polymer International* **2008,** *57* (6), 879-886.

23. Kim, J.; Nyren-Erickson, E.; Stafslien, S.; Daniels, J.; Bahr, J.; Chisholm, B. J., Release characteristics of reattached barnacles to non-toxic silicone coatings. *Biofouling* **2008,** *24* (4), 313-319.

24. Majumdar, P.; Lee, E.; Patel, N.; Ward, K.; Stafslien, S. J.; Daniels, J.; Chisholm, B. J.; Boudjouk, P.; Callow, M. E.; Callow, J. A., Combinatorial materials research applied to the development of new surface coatings IX: an investigation of novel antifouling/fouling-release coatings containing quaternary ammonium salt groups. *Biofouling* **2008,** *24* (3), 185-200.

25. Kugel, A. J.; Jarabek, L. E.; Daniels, J. W.; Vander Wal, L. J.; Ebert, S. M.; Jepperson, M. J.; Stafslien, S. J.; Pieper, R. J.; Webster, D. C.; Bahr, J., Combinatorial materials research applied to the development of new surface coatings XII: Novel, environmentally friendly antimicrobial coatings derived from biocide-functional acrylic polyols and isocyanates. *Journal of Coatings Technology and Research* **2009,** *6* (1), 107-121.

26. Stafslien, S. J.; Bahr, J. A.; Feser, J. M.; Weisz, J. C.; Chisholm, B. J.; Ready, T. E.; Boudjouk, P., Combinatorial materials research applied to the development of new surface coatings I: a multiwell plate screening method for the high-throughput assessment of bacterial biofilm retention on surfaces. *Journal of Combinatorial Chemistry* **2006,** *8* (2), 156-162.

27. Stafslien, S. J.; Bahr, J. A.; Daniels, J. W.; Vander Wal, L.; Nevins, J.; Smith, J.; Schiele, K.; Chisholm, B., Combinatorial materials research applied to the development of new surface coatings VI:

an automated spinning water jet apparatus for the high-throughput characterization of fouling-release marine coatings. *Review of Scientific Instruments* **2007,** *78* (7), 072204.

28. Bell, E. C.; Gosline, J. M., Strategies for life in flow: tenacity, morphometry, and probability of dislodgment of two Mytilus species. *Marine Ecology Progress Series* **1997,** *159*, 197-208.

29. Burkett, J. R.; Wojtas, J. L.; Cloud, J. L.; Wilker, J. J., A method for measuring the adhesion strength of marine mussels. *The Journal of Adhesion* **2009,** *85* (9), 601-615.

30. Crisp, D. J.; Walker, G.; Young, G. A.; Yule, A. B., Adhesion and substrate choice in mussels and barnacles. *Journal of Colloid and Interface Science* **1985,** *104* (1), 40-50.

31. Majumdar, P.; Stafslien, S.; Daniels, J.; Webster, D. C., High throughput combinatorial characterization of thermosetting siloxane–urethane coatings having spontaneously formed microtopographical surfaces. *Journal of Coatings Technology and Research* **2007,** *4* (2), 131-138.

32. Rittschof, D.; Orihuela, B.; Stafslien, S.; Daniels, J.; Christianson, D.; Chisholm, B.; Holm, E., Barnacle reattachment: a tool for studying barnacle adhesion. *Biofouling* **2008,** *24* (1), 1-9.

33. Owens, D. K.; Wendt, R. C., Estimation of the surface free energy of polymers. *Journal of Applied Polymer Science* **1969,** *13* (8), 1741-1747.

34. Holland, R.; Dugdale, T. M.; Wetherbee, R.; Brennan, A. B.; Finlay, J. A.; Callow, J. A.; Callow, M. E., Adhesion and motility of fouling diatoms on a silicone elastomer. *Biofouling* **2004,** *20* (6), 323-329.

CHAPTER 4. FOULING-RELEASE PERFORMANCE OF POLYETHYLENE GLYCOL MODIFIED SILOXANE-GLYCIDYL CARBAMATE MARINE COATINGS

Introduction

The inevitable and undesirable attachment and growth of aquatic organisms, like algae, barnacles, and mussels, on surfaces submerged in natural bodies of water is called marine biofouling or simply biofouling.[1, 2] In spite of its dynamic nature, the mechanism of biofouling can be typically explained in four main stages— formation of a polysaccharides-rich conditioning layer, accumulation of bacteria, settlement of algal spores and diatoms and finally attachment of barnacles and mussels.[1, 3] Biofouling poses many disadvantages, like increase in drag, increase in fuel consumption, reduction in the speed of the vessel, difficulty in maneuvering marine vessels and migration of aquatic species to non-native environments.[1, 2, 4, 5] Combating biofouling costs millions of dollars to the US Navy annually, the costs reaching a billion dollars over 15 years.[2, 5, 6] Historically, lead sheathing was used to combat biofouling, which was later replaced with more sophisticated anti-fouling (AF) coatings.[1] AF coatings contained toxic biocides based on tin or copper, which would prevent the attachment of aquatic organisms by leaching out and killing them.[1, 7] But, the undesired toxic effects of the biocides on organisms like oysters and ducks, led to the proposed replacement of the AF coatings with non-toxic elastomeric fouling-release (FR) coatings.[2, 5] FR coatings allow formation of a weak bond between the organism and the substrate, which can then be easily broken by hydrodynamic forces.[8-10] Hydrophobic siloxane-rich coatings cause slippage of hard foulants on the surface, thereby reducing attachment.[8, 9, 11-13]

Commercially available FR coatings are made using silicone elastomers, which lack mechanical strength and adhesion to substrates, making them less viable in long term marine applications.[8, 9] A novel self-stratified siloxane-polyurethane (SiPU) system was developed previously to overcome the shortcomings of the commercial FR coatings.[8, 9, 14-16] In a typical SiPU formulation, curing reactions of an isocyanate between a polyol and high MW aminopropyl terminated siloxane (APT-PDMS) causes siloxane chains to stratify to form a slippery outer layer, while the underlying PU matrix provides the required mechanical strength and adhesion.[8, 9] Concerns pertaining to exposure of factory workers and personnel to unreacted isocyanates in 2K coating formulations has led to further research into finding “safer” alternatives for polyurethanes.[17, 18] To this end, glycidyl carbamate (GC) technologies are explored

in this study. GC can be easily synthesized using an isocyanate, glycidol, and a modifier to reduce viscosity.[19-24] Reaction of isocyanate with glycidol leads to formation of -CO-NH- carbamate linkages.[19] GC coatings combine properties of polyurethanes with convenient epoxy-amine curing chemistry.[20] A typical coating formulation with GC resin comprises of the modified GC resin and diamine crosslinker. Lack of unreacted isocyanate is expected to reduce hazards associated with using free isocyanate groups.

Till date, over 4000 different marine organisms with different attachment mechanisms have been identified.[2] For example, macrofoulants like barnacles and mussels show affinity toward hydrophilic surfaces, but can be easily removed from silicone rich surfaces.[9, 11, 25] Conversely, diatoms *N.incerta* attach strongly to siloxane rich hydrophobic coatings, but show weak adhesion to hydrophilic coatings.[26-28] Complex nature of adhesion processes of the different marine organisms has led to further research into developing viable “ambiguous” coatings, containing hydrophobic and hydrophilic phases.[2] Aquatic organisms adhere onto substrates by secreting proteinaceous adhesives.[29] One approach to reduce biofouling can be developing coatings that disallow spreading of the protein-rich adhesives. Polyethylene glycols (PEG) have shown great potential to resist protein adsorption.[30] PEG chains form a hydration layer by binding water molecules to the surfaces.[31, 32] Proteins from the adhesives cannot displace the hydration layer to reach the underlying coating. Previous research has shown that PEG-rich surfaces can reduce biofouling by diatoms, although macrofoulants, like barnacles and mussels, attach strongly to hydrophilic surfaces.[25-28] Combination of hydrophobic and hydrophilic moieties in the same coating formulation is expected to reduce fouling by most of the common fouling organisms.[2, 33] Several amphiphilic surfaces have been developed, involving different polymer architectures, surface active block copolymers, amphiphiles with varying PDMS/PEG chain lengths, that show potential for use in practical applications.[27, 34-40] SiPU formulations have also been modified to incorporate hydrophilic moieties, like PEG chains, acid functional groups, and isocyanate based hydrophilic prepolymers, to make amphiphilic coatings.

In this study, novel isocyanate-free glycidyl carbamate based amphiphilic coatings were explored by incorporating two amine terminated PEGs, Jeffamines, as co-crosslinkers in coating formulations with siloxane modified glycidyl carbamate resin (IGC_PDMS resin). Stratification of PEG and PDMS chains is

expected to form separate hydrophobic and hydrophilic domains on the surfaces, forming “ambiguous” coatings. The MW and the amounts of the Jeffamines co-crosslinkers was varied to make different formulations. Diamines, PACM, Ancamine 2143, and Ancamine 2432, were used as primary crosslinkers to cure the formulations. Ratio of epoxy: AHEW was maintained at 1:1 for all the formulations. FTIR and NMR were used characterize the synthesized IGC_PDMS resin. The cured amphiphilic coatings were characterized for their hardness, flexibility, impact strength, tensile strength, and thermal behavior using ASTM standard tests, DSC, DMA, and TGA. Further, FR performance of the Jeffamine coatings against biofilm (*C.lytica*), diatoms (*N.incerta*), mussels (*Geukensia demissa*), and barnacles (*A.amphitrite*) was evaluated. Lastly, the coatings were characterized using contact angle, ATR-FTIR, AFM, and XPS to understand FR behavior of the coatings with changing surface composition and topography.

Experimental Section

Materials

Trimer of hexamethylene diisocyanate (HDI trimer; Desmodur N 3300A) was provided by Covestro (Bayer MaterialScience). Dicarbinol terminated PDMS (DMS-C21; MW = 5k g/mol) was purchased from Gelest. Diamines, PACM (AHEW = 52.5 g/eq.), Ancamine 2143 (AHEW = 115 g/eq.), and Ancamine 2432 (AHEW = 88 g/eq.), were provided by Air Products. Catalyst dibutyltin diacetate (DBTDAc), ethyl-3-ethoxy propionate (EEP), and toluene were purchased from Sigma Aldrich. Glycidol was supplied by Dixie Chemicals. Glycidol was refrigerated immediately to reduce formation of impurities.[41] Jeffamines, with MW 900 g/mol— ED-900 (J900) and 2003 g/mol— ED-2003 (J2003), were provided by Huntsman. Intergard 264 primer and crosslinker, products of International Paint, were purchased from Interbay Coatings.

Aminopropyl terminated polydimethylsiloxane (APT-PDMS; target MW = 20k g/mol) was synthesized according to previously published process.[8] Siloxane monomer (D_4), benzyltrimethylammonium hydroxide, and blocker bis(3-aminopropyl)-tetramethyldisiloxane (BAPTDMS) were purchased from Dow Chemical, Sigma Aldrich, and Gelest respectively. In a round bottom flask, fitted with a nitrogen inlet, a condenser, a heating mantle, and a temperature controller, D_4, BAPTDMS, and benzyltrimethylammonium hydroxide solution (in methanol) were equilibrated at 80°C for 24 hours. After 24 hours, temperature was increased to 170°C for 2 hours to decompose the catalyst. The

synthesized APT-PDMS was cooled to room temperature and stored in a thick-walled glass jar. APT-PDMS was characterized using GPC to confirm MW between 18-20k g/mol.

Synthesis of Siloxane Modified Glycidyl Carbamate Resin (IGC_PDMS Resin)

PDMS modified resin (IGC_PDMS) was synthesized using HDI trimer, glycidol, and dicarbinol terminated PDMS (MW = 5000 g/mol). Amount of PDMS were maintained at 5% of equivalents of isocyanurate. A four-neck round bottom flask was fitted with a mechanical stirrer, a nitrogen inlet, a heating mantle, and a thermocouple. In the first step, the flask was charged with HDI trimer, 25% by weight of resin solids EEP solvent, PDMS, and catalyst DBTDAc (0.020-0.025% resin solids). The charge was allowed to react at 80°C for 1-1.5 hours. After 1.5 hours, temperature was reduced to ~45°C. In the next step, glycidol and 25% by weight of resin solids in toluene was added to the flask at 45-50°C. The reaction was allowed to proceed for another 1-1.5 hours, until the disappearance of the -NCO peak as observed using Fourier Transform Infrared Spectroscopy (FTIR). Amounts of solvents EEP and toluene were determined such that the final resin contained a 1:1 w/w solvent blend of EEP and toluene and target 50% percent solids.

Resin Characterization

The synthesized resin was characterized using FTIR and Nuclear Magnetic Resonance Spectroscopy (^{13}C-NMR). FTIR experiment was conducted using a Thermo Scientific Nicolet 8700 system. A small amount of the IGC_PDMS resin was coated onto a potassium bromide plate and 32 scans were taken for the sample. The FTIR spectrum shown in this chapter is the average of the 32 scans. A dilute solution of the resin in $CDCl_3$ was analyzed using Bruker 400 NMR ^{13}C-NMR instrument. Further, the synthesized resin was characterized for experimental percent solids and epoxy equivalent weight (EEW). Accurately measured ~1 g resin was added to three aluminum pans. The aluminum pans with the resin were heated in an oven at 120°C for 1 hour. Percent solids of the resin was calculated using the weight of the pans before and after heating. The average of the three replicates was recorded as the experimental value of percent solids of the synthesized resin. Epoxy equivalent weight (EEW) of the resin was determined per ASTM D 1652. ~1 g resin, accurately measured up to the fourth decimal place, was added to an Erlenmeyer flask. 10-15 mL chloroform was added to the flask to completely dissolve the resin. 3-5 drops of crystal violet solution (0.1% solution in glacial acetic acid) were added as

the indicator. The resin solution was titrated against standardized 0.1 N HBr solution. Change in color of the solution from violet to blue-green was considered to be the end point of titration. The resin was titrated three times and the average of the three titrations was recorded as the experimental value of EEW of the resin.

Coating Formulations

PACM, Ancamine 2143, and Ancamine 2432, were used as primary crosslinkers to cure the IGC_PDMS resin. Ratio of epoxy: AHEW of the primary amines was maintained at 1:1 for all formulations. Difunctional amine terminated PEGs (Jeffamines)— ED-900 (J900) and ED-2003 (J2003)— were added as co-crosslinkers to impart hydrophilicity to hydrophobic IGC_PDMS coatings. The amounts of the Jeffamine co-crosslinkers were varied as 5, 10, 15, and 20% by weight of resin solids. The Jeffamine co-crosslinkers were added as 33% solution in EEP solvent. Additionally, 2.5% by weight of resin solids APT-PDMS (MW = 20k g/mol; 33% solution in toluene) was incorporated into formulations with 15 and 20% Jeffamines. Table 4.1 shows list of formulations made in this study. Formulation labels are of the format: primary crosslinker_Jeffamine crosslinker_F%Jeffamine crosslinker/%APT-PDMS.

Table 4.1. List of formulations included in the study.

Primary amine crosslinker	Curing schedule	% Jeffamine co-crosslinker	% APT-PDMS
Ancamine 2143	RT, 2 weeks	5, 10, 15, 20% resin solids	2.5% resin solids for Jeffamines >10%
Ancamine 2432			
PACM	80°C, 45 min		

All formulations were stirred for 20 min using magnetic stir bars. The formulations were the sonicated for another 10 min to remove bubbles. Steel (purchased from Q-Lab, specifications— 3” x 6”, smooth mill finish, type QD, alloy 1008/1010), aluminum (purchased from Q-Lab, specifications— 3” x 6”, smooth mill finish, type A, alloy 3003 H14) and glass panels were used as substrates to make coatings for mechanical tests. The substrates were degreased using isopropanol before coating application. Coatings for mechanical and thermal experiments were made using a drawdown bar with 8 mils wet film thickness. Free films for thermal analysis were carefully removed from the glass panels using a blade. Coatings for FR experiments were made by applying formulations on primed (Intergard 264 primer) aluminum panels, using a Mayer rod (RDS 80). Formulations containing Ancamine 2143 and Ancamine 2432 as the primary crosslinkers were cured at RT for 2 weeks; formulations with PACM were cured at

80°C for 45 minutes. Figure 4.1 shows a schematic representation of the different formulations made during the study.

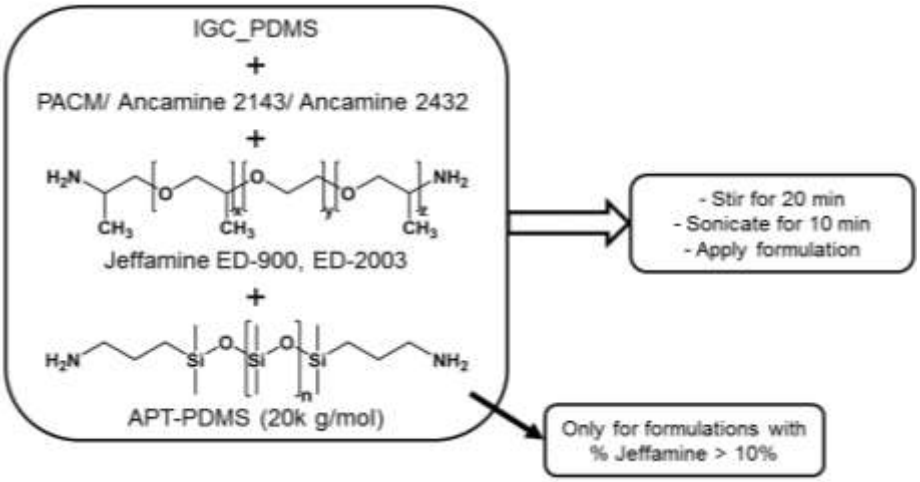

Figure 4.1. Schematic representation of coating formulations made using IGC_PDMS resin and Jeffamine co-crosslinkers.

Coating Characterization

The cured coatings were characterized for their solvent resistance, hardness, flexibility, and impact strength. Methyl ethyl ketone (MEK) double rubs test was conducted per ASTM D 5402 to assess the chemical resistance and extent of crosslinking in the coatings. A 26-oz hammer with cheesecloth was soaked in MEK solvent. Coatings were rubbed using the soaked cheesecloth, until mar or changes in appearance of the coatings were observed. The number of double rubs that caused surface mar or loss of surface gloss or delamination were noted. König pendulum hardness (ASTM 4366) was measured and reported in seconds. Pencils, with softest 9B to hardest 9H hardness values, were used to determine pencil hardness of the coatings (ASTM D3363). The results from the pencil hardness test were reported as the hardest pencil that does not leave a scratch the coating surface. A Gardener impact tester was used to determine reverse impact strength of the coatings (ASTM D 2794). The maximum drop height was 43 in. and drop weight was 4 lb. The results were reported as crazing or loss of adhesion or film failure in inch-pounds (in.-lb). Coatings that did not show any failure were reported as having impact strength > 160 in.-lb. Flexibility of coatings was determined conical mandrel bend according to ASTM D 522. The results were reported as ‘no failure’ or ‘tear’ caused during experimentation. Crosshatch adhesion test was conducted on the coatings according to ASTM D 3359, using a Gardco crosshatch

adhesion instrument and tape. The results were reported as 5B (best) to 0B (worst), depending on the amount of film removed after the tape was ripped off. For select coatings, Young's modulus and elongation at break at ambient temperature was determined using Instron tensile testing equipment, at a rate of 5 mm/min. The samples were prepared according to ASTM D 882.

A TA Instruments Q1000 Differential Scanning Calorimeter (DSC) system was used to determine glass transition temperature (T_g °C) of the cured Jeffamine coatings. 5-10 mg samples of each formulation were subjected to heat-cool-heat cycle for temperature range between -20°C to 250°C. Heating and cooling rates were maintained at 10°C/min and 5°C/min respectively. T_g was determined as the temperature of the inflection at the mid-point of the transition in the second heating cycle. Thermal degradation temperature of the coatings was determined using a TA Instruments Q500 Thermogravimetric Analysis (TGA) instrument. Samples were heated up to 800°C at a heating rate of 10°C/min. Onset of degradation of the coatings ($T_{d\ 5\%}$ °C) was reported. A TA Instruments Q800 Dynamic Mechanical Analysis (DMA) instrument was used to determine crosslink density (v_e mol/L), tan delta, and storage modulus (E' MPa) at 25°C of the cured coatings. Poisson's ratio value of 0.44 was used for all the coatings. Temperature was between -20°C to 200°C, with heating rate of 5°C/min and 1 Hz frequency. v_e was calculated using E' values in the rubbery plateau region 60°C above T_g °C, using the equation, $E' = 3v_eRT$, where, E'= storage modulus (Pa); v_e = crosslink density (mol/L); R= gas constant (8.314 J/K/mol); T= (T_g + 60°C + 273) K.

Laboratory Biofouling Assays

Preleaching and Leachate Toxicity Analysis

The Jeffamine coatings were placed in a recirculating water tank for six weeks to remove toxic leachates, impurities, and catalyst before analysis with biological organisms.[42] After six weeks, algal solution in artificial sea water (ASW) with nutrients was introduced onto the coatings to test leachate toxicity. Fluorescence was used to observe the growth of algae on the coatings after 48 hours. The growth of the organisms on the coatings was reported as a fluorescence ratio to a positive growth control. A negative growth control (medium+ bacteria+ triclosan) was also included in the experiment. The coatings were compared to the negative control to confirm the absence of toxic leachates.[8] Due to severe

toxicity of the Ancamine 2143 cured coatings against most fouling organisms, except biofilm *C.lytica*, FR experiments with the Ancamine 2143 coatings were not conducted with other organisms.

Diatom Navicula incerta (N.incerta) Attachment and Removal

Diatom *N.incerta* adhesion was carried as explained in earlier publications.[8, 15, 43-45] Circular discs were carefully punched out from Jeffamine coatings cured using PACM and Ancamine 2432. The discs were then glued to 24-well plates using a silicone adhesive from Dow Corning, such that the glue covered the circular basal area completely. The plates were then treated with 1 mL solution of algae in ASW and incubated for 2 hours to allow diatom adhesion. Fluorescence was used to quantify the number of attached diatoms on the coatings. After 2 hours, the well plates were subjected to water jet at 10 psi and 20 psi for 10 seconds to determine release of the diatoms from the coatings. The first column in each well plate was used as a reference for the initial cell settlement and was not subjected to water jet. This study shows diatom attachment and removal at 20 psi water jet pressure only. 10 psi water pressure did not facilitate sufficient diatom removal from the commercial standards.

Biofilm Cellulophaga lytica (C.lytica) Adhesion and Removal

Bacterial biofilm *C.lytica* adhesion test was carried out in a fashion similar to diatom attachment.[8, 46-48] Briefly, circular discs, punched out of the PACM cured and the Ancamine 2432 cured coatings, were glued to 24-well plates using a Dow Corning silicone adhesive. 5% suspension of *C.lytica* in ASW (10^7 cells/mL) with nutrients was prepared. 1 mL suspension was dispensed in each well. The plates were incubated for 24 hours at 28°C to allow colonization of the biofilm on the coatings. The plates were rinsed three times with deionized water to remove unattached biofilm. Crystal violet was used to stain the samples. Extractions of crystal violet in acetic acid (33%) were observed under 600 nm absorbance, to determine amount of biofilm retained on the coatings. After 24 hours, the wells were subjected to water jets at 10 psi and 20 psi for 5 seconds.[49] The first column in each 24-well plate served as a reference for bacterial growth before water jetting and was not exposed to water jet. The final results were reported as the amount of biofilm attached to the coatings and the percent removal of the biofilm from the coating surface at 10 psi and 20 psi water jet pressures.

Microalgae Ulva linza (U.linza) Attachment and Removal

Similar to diatoms and biofilm, 24-well assay plates were prepared by carefully punching out and gluing discs (using Dow Corning silicone adhesive) from select PACM cured and select Ancamine 2432 cured preleached coatings. The plates were then shipped to Newcastle University to determine the FR performance of the coatings toward microalgae *U.linza*. Before the bioassay experiment, the assay plates were equilibrated in 0.22 µm filtered ASW for 2 hours. Then, 1 mL *U.linza* sporelings suspension (3.3 x 10^5 spores/mL) in enriched sea water was dispensed into each of the wells. The spores were grown in an illuminated incubator at 18°C for 6 days. After 6 days, the biomass from a single row of wells (6 wells) was assessed by extracting chlorophyll. Chlorophyll was extracted in 1 mL DMSO. Fluorescence was then determined using excitation of 360 nm and wavelength of 670 nm. To determine the release performance of the coatings, single rows of wells from each plate was sprayed using the spinjet apparatus at 18, 67, 110 kPa water pressure. Chlorophyll was again extracted, as explained earlier. The removal at each pressure was determined by comparing the sprayed and the unsprayed wells. The results were reported as the percent removal of the sporelings after exposure to water jet. In this chapter, only microalgae removal at 110 kPa is shown. 18 and 67 kPa water pressures could not facilitate greater than 5% removal of the microalgae.

Mussel Geukensia demissa Adhesion

Select Jeffamine coatings were evaluated for adhesion of marine mussels *Geukensia demissa*, according to a previously published procedure.[11, 50, 51] Before the experiment, each marine mussel (received from Duke University Marine Laboratory, North Carolina, USA) was fitted with a 4 cm long acetal rod, using a 3M acrylic adhesive. The rods were attached perpendicular to the ventral edge of the mussel. Six mussels (five for PACM_J900_F10/0 and PACM_J900_F20/2.5 coatings) were immobilized on the select coatings, using a custom designed PVC template. The select coatings were placed in ASW so that the mussels can be fed live marine phytoplankton for 3 days. After 3 days, the number of mussels showing attachment of byssus threads was recorded for each coating. The acetal rods on the mussels were attached to a tensile force gauge, such that all the mussels were pulled from the coating at the same time. The results were reported as the average force in Newtons required to completely detach all byssus threads of the mussel from the coating surfaces.

Adult Barnacle Amphibalanus amphitrite (A.amphitrite) Adhesion

Select Jeffamine coatings were also analyzed for barnacle adhesion to determine their FR performance against barnacles.[8, 52, 53] Six adult *A.amphitrite* barnacles, with basal diameter of approximately 5 mm, were allowed to grow and attach onto the select coatings for 2 weeks. The barnacles were fed brine shrimp nauplii in ASW for 2 weeks. After 2 weeks, a hand held digital gauge was used to measure the force required to detach the barnacles in shear from the coatings. Adhesion strength (MPa) of the barnacles was then calculated as the shear force required for barnacle removal to the basal area of the barnacle.

Surface Analysis

Surface chemistry and topography of the water leached coatings was studied using characterization techniques such as contact angle, Attenuated Total Reflectance Fourier Transformed Infrared Spectroscopy (ATR-FTIR), Atomic Force Microscopy (AFM), and X-Ray Photoelectron Spectroscopy (XPS). A First Ten Angstroms (FTA 125) system was used to measure dynamic changes in water contact angles (WCA) by the sessile drop method. A single droplet was carefully dispensed onto each coating panel. WCA was measured immediately after the droplet was dispensed and at 10-min intervals for 30 min. The contact angles were analyzed using FTA software. A Thermo Scientific Nicolet 8700 system, with iTR diamond crystal plate attachment, was used to conduct ATR-FTIR. 32 scans were taken for each Jeffamine coating. The spectra shown in this chapter are the average of the 32 scans. Surface topography of select samples was analyzed using a Dimension 3100 Microscope AFM system with Nanoscope controller. 20 µm x 20 µm area of the select pre-leached coatings were scanned using a silicon probe (spring constant = 0.3-0.8 N/m, resonant frequency = 20-40 kHz) in tapping mode in air under ambient laboratory conditions. Lastly, a Thermo Scientific K-Alpha XPS instrument with monochromatic 1468.68 eV Al K_α X-ray source and Ar^+ ion source gun (up to 8000 eV) was used to conduct XPS experiments to investigate chemical composition of select Jeffamine coatings. Prior to analyzing the coatings, Ar^+ ion MAGCIS cluster gun (8000 eV power) was used to clean coating surfaces for 60 seconds to remove impurities. Three survey spectra were collected at a low resolution with constant pass energy of 200 eV at energy increment of 1.000 eV/step for 10 microseconds. High resolution scans were collected at 90° (perpendicular) to the coating surfaces. Ten scans were collected

for each sample with energy increment of 0.100 eV/step for 50 microseconds and pass energy of 50 eV. Atomic concentrations of individual elements, C1s, O1s, and N1s were determined by integrating area under the peaks. Both surface etching and high resolution experiments were conducted at ambient laboratory temperature. Chamber pressure was maintained below 1.5 x 10^{-7} Torr at all times.

Results and Discussion

In this study, a different approach was explored to develop amphiphilic coatings using hydrophobic isocyanate-free siloxane-glycidyl carbamate (IGC_PDMS) resin and amine terminated PEG with varying MWs. The IGC_PDMS resin was synthesized using HDI trimer, glycidol, and dicarbinol terminated PDMS (MW = 5000 g/mol) as shown in Figure 4.2. The amount of PDMS was maintained at 5% equivalents of isocyanurate. The synthesized resin was analyzed using FTIR and ^{13}C-NMR. FTIR spectrum of the synthesized resin showed absence of the -NCO peak at 2272 cm^{-1}, indicating formation of isocyanate-free resin (Figure 4.3). Peaks at 860-910 cm^{-1}, 1050-1150 cm^{-1}, and 3300 cm^{-1} indicated presence of epoxy rings, Si-O-Si chains, and -NH peak in the synthesized resin. Furthermore, ^{13}C-NMR spectrum for the IGC_PDMS resin showed chemical shifts at 148 ppm, 1 ppm, 26-29 ppm, and 44-49 ppm, indicative of C atoms from carbamate linkages, dicarbinol PDMS modifier, HDI trimer, and epoxy rings respectively (Figure 4.4). Experimental percent solids and EEW values of the resin were determined to lie between 48-50% (target— 50%) and 400 ± 20 g/eq. respectively.

Presence of the PDMS modifier in the resin allowed formation of hydrophobic coatings. Upon curing, self-stratification of the siloxane chains results in the formation of a low surface energy coating. To increase “ambiguity” of the coating surface, amine terminated PEGs, Jeffamine ED-900 (J900) and Jeffamine ED-2003 (J2003), were added to coating formulations as co-reactants. The amounts of the two Jeffamine co-reactants was varied as 5, 10, 15, and 20% by weight of resin solids. Amine functional groups from the co-reactants react with the epoxy rings in the IGC_PDMS resin. The hydrophilic PEG chains, therefore, remain tethered to the IGC_PDMS coating. Upon exposure to an aqueous environment, the PEG chains are anticipated to saturate the coating surface, increasing hydrophilicity of the coatings. Since PDMS and PEG chains were incorporated as separate components, the amphiphilic surfaces are expected to show presence of the PDMS and PEG rich surface domains. Hydration of the PEG domains would deter attachment of diatoms and camouflage the underlying surface to reduce

attachment of hard foulants like barnacles, while the PDMS domains would provide slippery character to the coating.

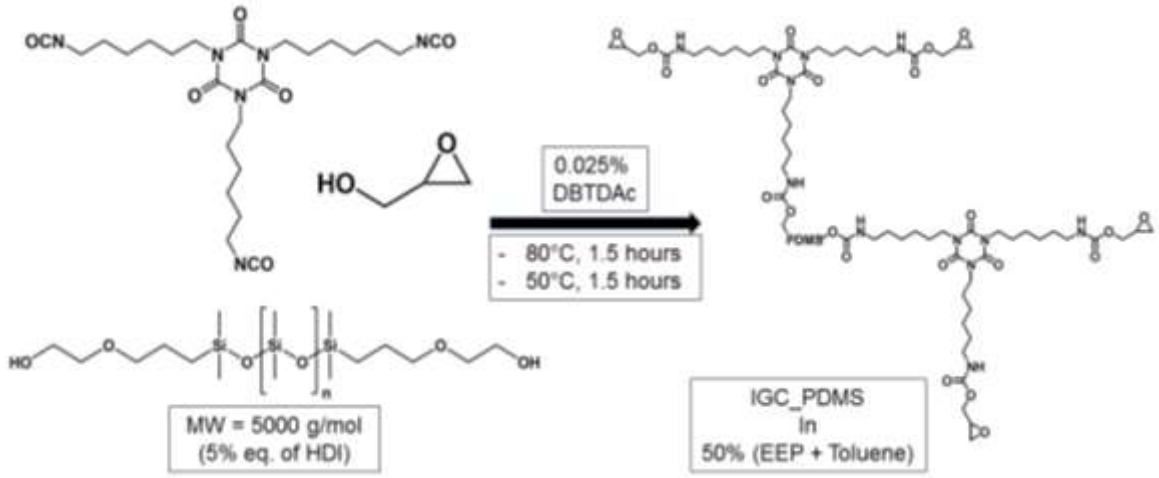

Figure 4.2. Reaction scheme for synthesis of IGC_PDMS resin.

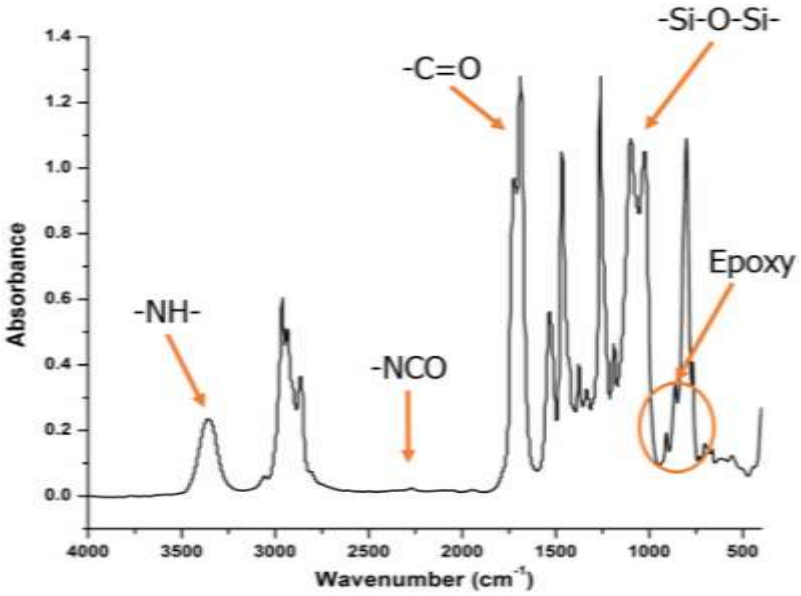

Figure 4.3. FTIR spectrum of the synthesized IGC_PDMS resin.

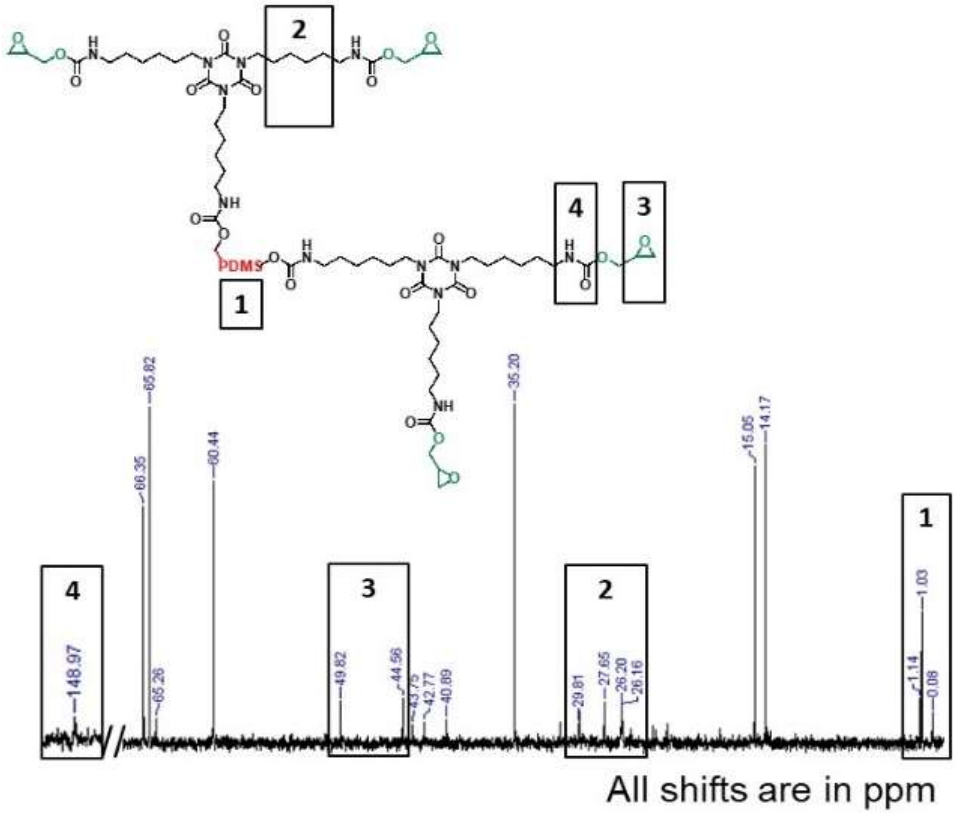

Figure 4.4. ^{13}C-NMR spectrum for the synthesized IGC_PDMS resin.

Diamines, PACM, Ancamine 2143, and Ancamine 2432, were used as primary crosslinkers to cure coating formulations with the IGC_PDMS resin and the Jeffamine co-reactants. The ratio of epoxy: AHEW of the primary crosslinker was maintained at 1:1. In general, GC resins are extremely hydrophilic (surface energy ~43 mN/m). Addition of PEG will further increase hydrophilicity of the coatings. Hard foulants like barnacles attach strongly to high surface energy coatings. Therefore, to increase effectiveness of the Jeffamine coatings against hard foulants, 2.5% by weight of resin solids 20k g/mol MW APT-PDMS was incorporated into formulations with 15% and 20% Jeffamine crosslinkers. Additional APT-PDMS was added to the formulations with higher Jeffamine content in an attempt to balance concentrations of the two phases to make coatings slippery enough for the hard foulants, while maintaining hydrophilicity to deter diatoms. To increase compatibility between the polar PEG and the non-polar PDMS components in the coatings, the Jeffamine co-crosslinkers and APT-PDMS were added as 33% solutions in EEP and toluene respectively (Figure 4.1). PACM cured formulations were cured at 80°C for 45 minutes; formulations with the two polyamines were cured at room temperature for 2 weeks.

After completion of curing, the coatings were analyzed for their mechanical properties, impact strength, tensile strength, and thermal properties. In general, all the coatings appeared smooth and uniform and exhibited good hardness, flexibility, and gloss values. Crosshatch adhesion results of 4B-5B (best) for all the coatings indicated that the coatings exhibited excellent adhesion to the substrates. Mandrel bend test showed that none of the coatings failed during experimentation, except 2143_J900_F5/0 which showed a ~1 cm tear in the coating film. Table 4.2 shows results obtained from mechanical tests for the Jeffamine coatings. Most of the PACM cured formulations showed higher resistance to MEK solvent as compared to the polyamine cured formulations, with MEK double rub values > 400. Increasing the Jeffamine content resulted in a drastic drop (~50% reduction) in pendulum hardness values of the PACM cured coatings. Coatings with 5% and 10% J900 and J2003 exhibited König pendulum hardness values of > 110 seconds, but lower impact strength. Conversely, the pendulum hardness dropped to 40-65 seconds for coatings with 15% and 20% Jeffamines, while the reverse impact strength of the PACM cured coatings improved with 15% and 20% J900 and J2003. For formulations with 15% and 20% Jeffamines co-crosslinkers, addition of 2.5% APT-PDMS may have caused softening of the coatings, resulting in drop in hardness of the coatings. But, plasticization of the coatings due to addition of APT-PDMS allowed higher mobility of the chains, thereby increasing ability of the coatings to withstand impact. Pencil hardness values for the PACM cured coatings lied in the range between 2B and HB.

Compared to the PACM cured coatings, coatings cured using Ancamine 2143 and Ancamine 2432 showed lower solvent resistance, with only 5 out of 16 total formulations exhibiting MEK double rubs > 400. Similar to the PACM cured coatings, pendulum hardness of the polyamine cured coatings dropped with increasing Jeffamine content. Compared to the PACM cured coatings, the polyamine cured coatings exhibited higher pencil hardness values in the range from H-4H. The Ancamine 2143 cured coatings exhibited poorest reverse impact strength as compared to other primary crosslinkers, with 2143_J900_Fa/b coatings showing lowest impact strength = 47 in.-lb. Reverse impact strength of the Ancamine 2143 cured coatings increased at 5-10% J2003 and then reduced again at 15-20% J2003. Among all formulations, Ancamine 2432 resulted in coatings with lowest König pendulum hardness values between 40-70 s, but all the Ancamine 2432 cured coatings showed high impact strength in the range from 145 in.-lb to > 160 in.-lb.

Figure 4.5 shows tensile test results for select Jeffamine coatings. For the PACM cured coatings, increase in J900 content decreased modulus, while increase J2003 content increased the modulus. Among the select formulations, PACM_J900_F5/0 showed the highest modulus value of 678 MPa, while PACM_J2003_F5/0 showed lowest modulus of < 10 MPa. Conversely, increasing J900 content to 20% drastically reduced modulus to < 50 MPa, while increasing J2003 content to 20% increased the modulus of the coating to 150 MPa. For the Ancamine 2432 cured coatings, modulus of coatings with 5% Jeffamines was higher than coatings with 20% Jeffamines. 2432_J2003_F5/0 exhibited highest stiffness with modulus of 470 MPa; 2432_J900_F20/2.5 showed lowest modulus of ~50 MPa. The Jeffamine coatings, except PACM_J900_F20/2.5 and PACM_J2003_F5/0 coatings, exhibited significantly higher modulus than the commercial silicone elastomer coatings (~5 MPa).

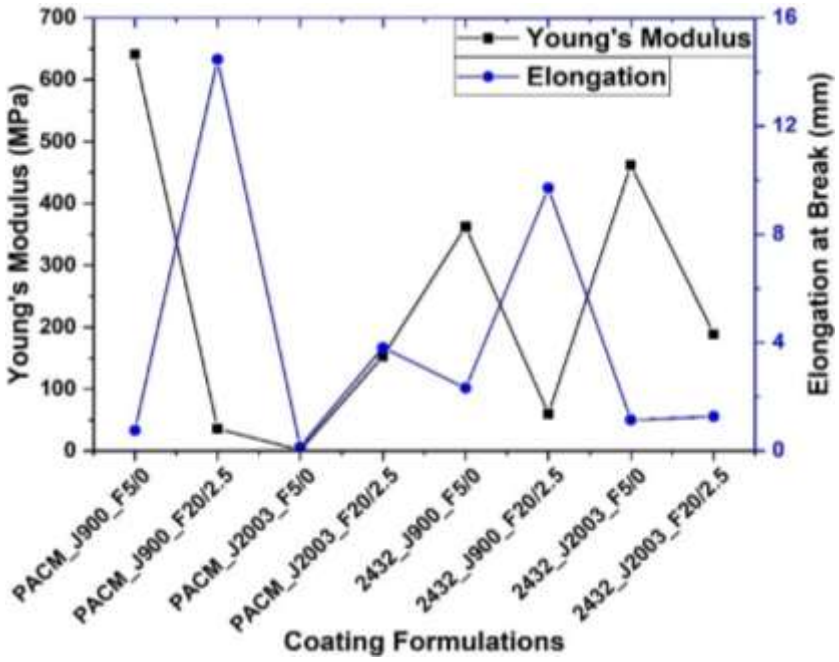

Figure 4.5. Young's modulus and elongation at break for select Jeffamine coatings.

Table 4.2. Mechanical test results for the Jeffamine coatings with epoxy: AHEW = 1:1.

Primary amines	Co-amines	% Co-amines	% APT-PDMS	MEK double rubs	KPH (s)	Pencil hardness	Reverse impact strength (in.-lb)	60° Gloss
PACM	J900	5	-	250	110	2B	71	73.10
		10	-	> 400	117	B	78	94.50
		15	2.5	> 400	63	2B	> 160	80.60
		20	2.5	> 400	41	2B	> 160	78.30
	J2003	5	-	> 400	139	HB	71	75.87
		10	-	> 400	130	HB	125	93.87
		15	2.5	350	46	B	133	80.20
		20	2.5	300	59	2B	> 160	78.13
Anc. 2143	J900	5	-	> 400	98	H	47	79.44
		10	-	380	86	2H	47	72.93
		15	2.5	> 400	76	3H	47	74.20
		20	2.5	340	83	H	47	65.13
	J2003	5	-	300	105	3H	133	41.40
		10	-	250	93	H	149	61.36
		15	2.5	380	73	H	94	72.10
		20	2.5	220	65	H	78	64.10
Anc. 2432	J900	5	-	> 400	70	3H	149	79.53
		10	-	> 400	71	4H	> 160	68.43
		15	2.5	350	51	2H	153	63.47
		20	2.5	280	41	H	> 160	69.96
	J2003	5	-	150	74	H	133	35.87
		10	-	270	56	2H	> 160	39.43
		15	2.5	> 400	43	H	> 160	48.87
		20	2.5	240	49	F	> 160	65.00

[a]KPH indicates König pendulum hardness.

Figure 4.6 shows DSC scans for all the Jeffamine coatings. Among all formulations, Ancamine 2143 resulted in coatings with the highest T_g between 50-92°C, while coatings with Ancamine 2432 exhibited lowest T_g values between 40-75°C. A broad range of T_g values between 36-80°C was observed for formulations cured using PACM. Formulations containing J2003 exhibited higher T_g as compared to J900, with 2143_J2003_F20/2.5 exhibiting highest T_g of 91.74°C. T_g values decreased with increasing Jeffamine co-crosslinker, probably due to presence of APT-PDMS chains.

(a)

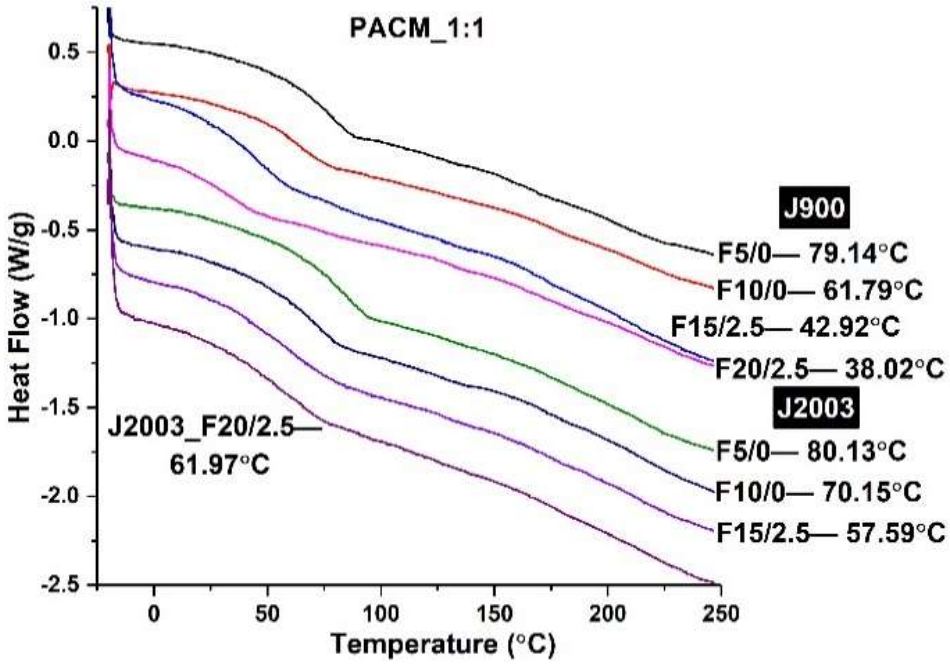

(b)

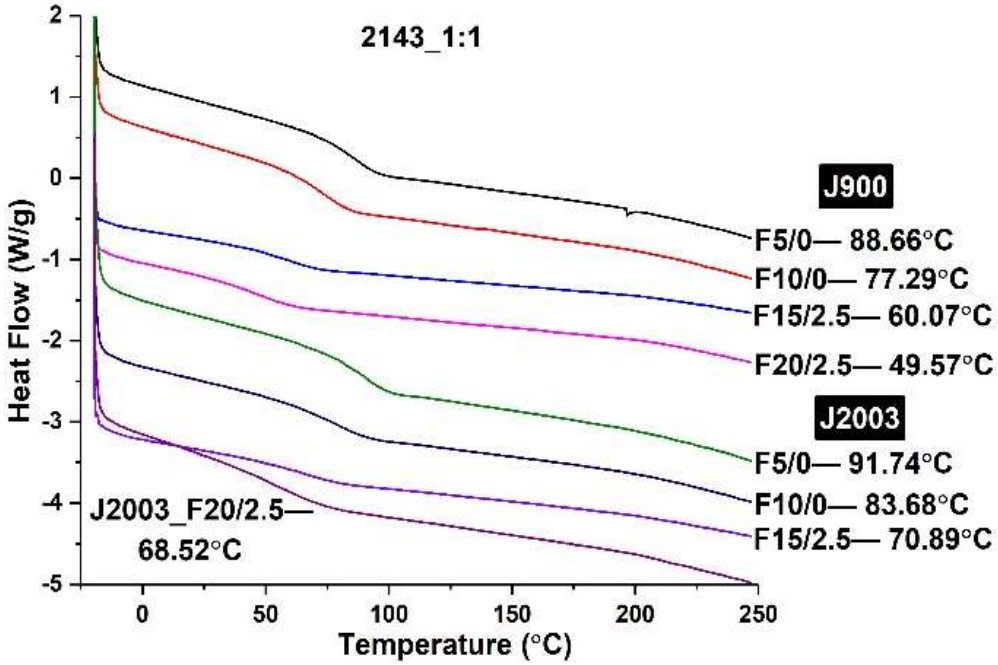

Figure 4.6. DSC scans of the coatings cured using (a) PACM, (b) Ancamine 2143, and (c) Ancamine 2432.

(c)

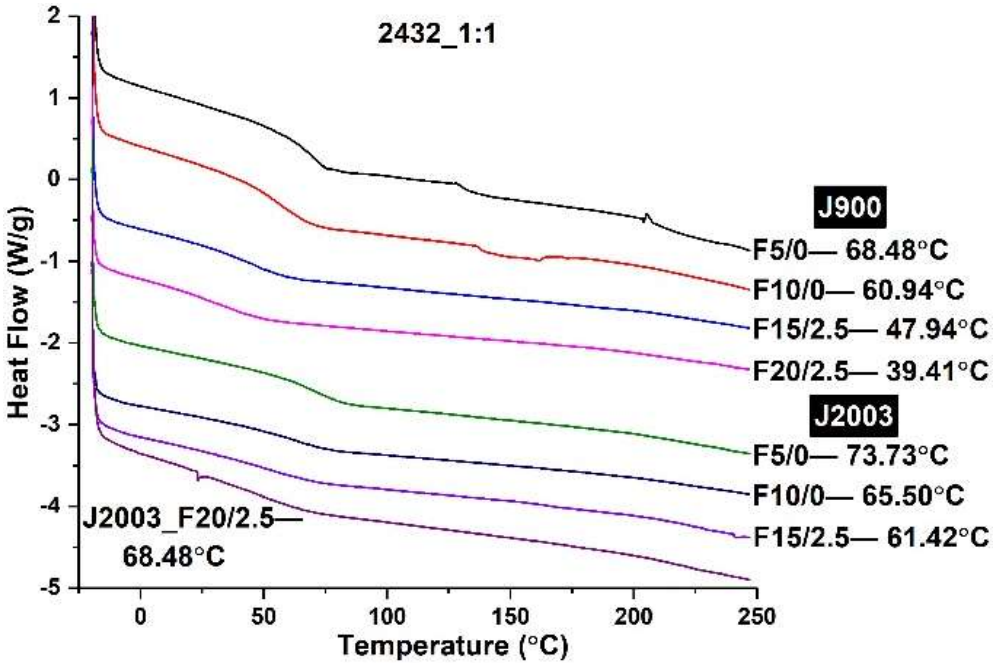

Figure 4.6. DSC scans of the coatings cured using (a) PACM, (b) Ancamine 2143, and (c) Ancamine 2432 (continued).

Figure 4.7 shows degradation behavior of the Jeffamine coatings. All the formulations cured using PACM showed similar degradation behavior, with 5% weight loss ($T_{d\,5\%}$) occurring at ~265°C. For the formulations cured using the polyamines, 5-10% of J900 and J2003 co-crosslinkers in the formulations resulted in $T_{d\,5\%}$ = 135-140°C. As the Jeffamine content was increased to 15-20%, $T_{d\,5\%}$ increased to 250-252°C. Formulations with 5-10% Jeffamines also showed higher initial weight loss and weight loss reduced with increasing amount of Jeffamine crosslinkers in the formulations.

(a)

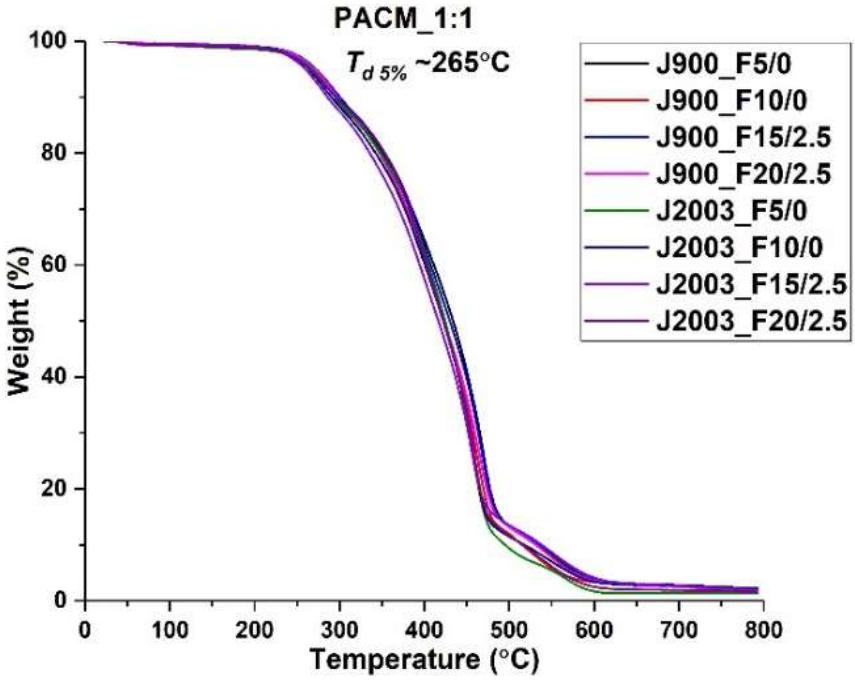

(b)

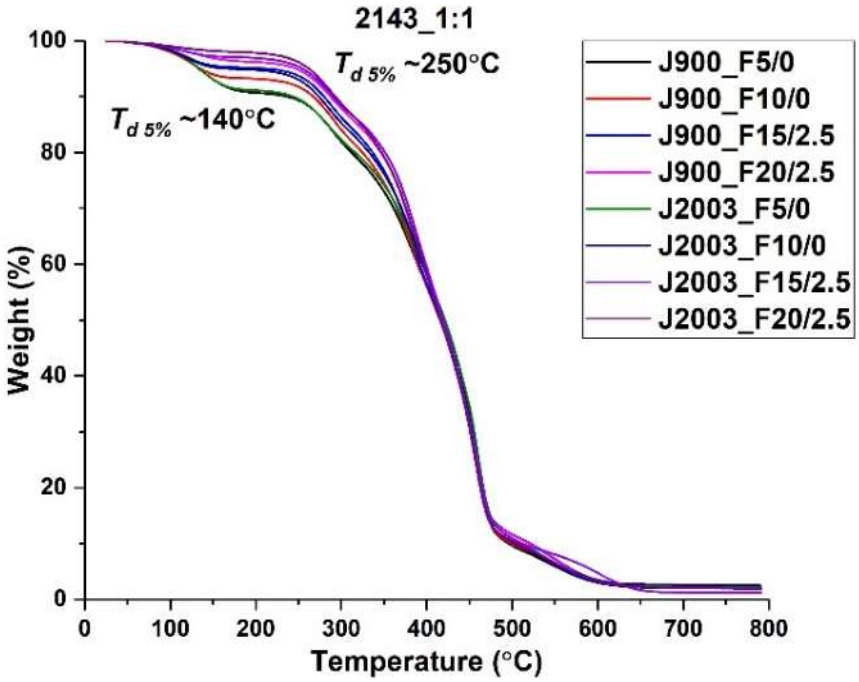

Figure 4.7. TGA thermograms of the coatings cured using (a) PACM, (b) Ancamine 2143, and (c) Ancamine 2432.

(c)

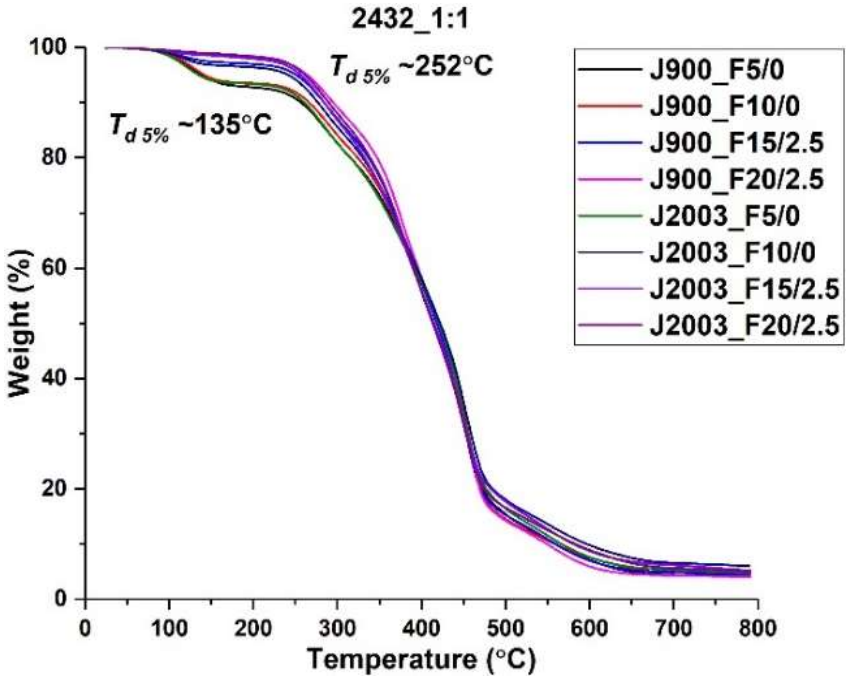

Figure 4.7. TGA thermograms of the coatings cured using (a) PACM, (b) Ancamine 2143, and (c) Ancamine 2432 (continued).

Figure 4.8 shows tan delta peaks and storage modulus for the amphiphilic coatings. Tan delta peaks for the PACM cured formulations appeared narrow and uniform as compared to peaks for the polyamine cured coatings. With PACM, T_g values of the coatings decreased with increasing amount of either Jeffamine co-crosslinker. For the polyamine cured coatings, T_g values decreased for coatings with J900 and increased for coatings with J2003. Coatings with J2003 exhibited higher T_g as compared to coatings with J900. PACM_J2003_Fa/b coatings showed highest T_g in the range from 82-102°C. Secondary peaks in higher temperature zones were visible for PACM_J2003_Fa/b coatings, indicating presence of a second harder phase in the coatings. For the polyamine coatings, the peaks appeared broader for coatings with J2003. Coatings cured using Ancamine 2432 showed lowest T_g values, in the range from 67-76°C for J900 and 80-90°C for J2003. Step change in tan delta peaks was observed for a few formulations cured using PACM and Ancamine 2432 between 110-160°C. At high temperatures, melting of the coatings may have provided mobility to the chains, leading to sharp increase in tan delta and drop in storage modulus. Any unreacted functional groups in the films could have reacted at higher temperatures. Eventual drop in tan delta and therefore, storage modulus may be due to melting of the film as temperature increased. 2143_J2003_F5/0 coating failed at ~160°C.

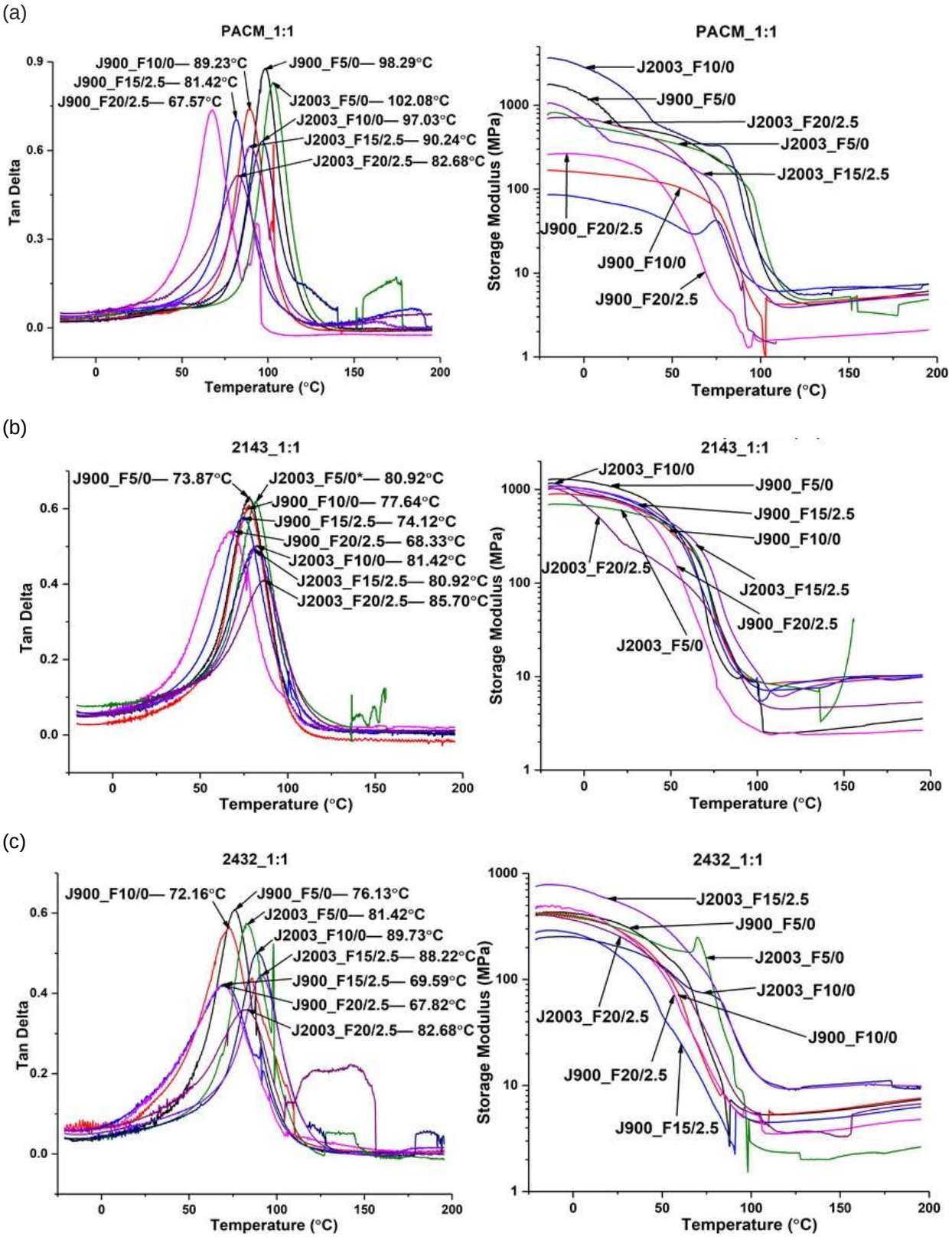

Figure 4.8. Tan delta plots and storage modulus curves for the coatings cured using (a) PACM, (b) Ancamine 2143, and (c) Ancamine 2432. 2143_J2003_F5/0 failed at 162°C.

Table 4.3 shows crosslink density (v_e) and storage modulus at 25°C ($E'_{25°C}$) for the Jeffamine coatings. A range of $E'_{25°C}$ values was obtained for coatings cured using PACM. PACM_J2003_F10/0 exhibited highest $E'_{25°C}$ value of 13 x 10^2 MPa; PACM_J900_F15/2.5 coatings showed lowest modulus value of 0.61 x 10^2 MPa. Most of the Ancamine 2143 cured coatings showed $E'_{25°C}$ in the range between 5-10 x 10^2 MPa, while Ancamine 2432 resulted in coatings with $E'_{25°C}$ = 1-5 x 10^2 MPa. v_e values were calculated using E' values in the rubbery plateau region (60°C above T_g) and T_g values of the coatings. Coatings cured using the polyamines showed higher v_e values compared to PACM cured coatings, indicating the formation of a tighter network in the films. For all coatings, except 2432_J900_Fa/b, v_e increased from 5% to 15% of the co-crosslinker and then dropped drastically when Jeffamine content was increased to 20%. For 2432_J900_Fa/b, v_e decreased with increasing Jeffamine content. Formulations with Ancamine 2143 showed highest change in v_e values; v_e increased from 0.26-0.39 mol/L for 5% Jeffamines to 0.96 mol/L-0.81 mol/L for 15% Jeffamines respectively. Above 15% Jeffamines, v_e values showed significant drop to 0.24 mol/L-0.45 mol/L. For all the coatings, except 2432_J900_Fa/b, Jeffamine content up to 15% allowed formation of tighter crosslinked networks. But, above 15%, formation of crosslinks may have been hampered due to incompatibility of the longer PEG and APT-PDMS chains in the coatings.

Overall, smooth, uniform, and glossy amphiphilic coatings were made using hydrophobic IGC_PDMS resin and Jeffamine crosslinkers. Lower MEK resistance of the polyamine cured coatings may indicate presence of unreacted functional groups in the coatings. Drastic drop in pendulum hardness values with of coatings with15-20% Jeffamines may be attributed due to the addition of 2.5% APT-PDMS. Although hardness of the coatings decreased with addition of APT-PDMS, plasticization of the coatings resulted in increase in their resistance to impact. Softening of the coatings was also evident from decreasing T_g values with increasing Jeffamine content as observed from DSC and DMA. For formulations with PACM and Ancamine 2143, coating networks appeared to tighten with increasing Jeffamine content from 5% to 15%. But, at 20% Jeffamines, v_e decreased drastically probably due to interference in curing reactions by long chain APT-PDMS and PEG chains. But, formulations with Ancamine 2432 showed hampered network formation with increasing Jeffamine content, indicating inefficiency of Ancamine 2432 diamine in presence of PEG and PDMS reactants.

Table 4.3. Crosslink density and modulus of the Jeffamine coatings.

Primary amine	Co-crosslinker	% Jeffamine	% APT-PDMS	$E'_{25°C}$ (MPa)	T_g (°C)	v_e (mol/L)
PACM	J900	5	-	5.38×10^2	98.29°C	0.45
		10	-	1.37×10^2	89.23°C	0.46
		15	2.5	0.61×10^2	81.42°C	0.65
		20	2.5	2.02×10^2	67.57°C	0.17
	J2003	5	-	4.63×10^2	102.08°C	0.31
		10	-	13.55×10^2	97.03°C	0.62
		15	2.5	4.48×10^2	90.24°C	0.80
		20	2.5	4.76×10^2	82.68°C	0.66
Anc. 2143	J900	5	-	9.50×10^2	73.87°C	0.26
		10	-	6.67×10^2	77.64°C	0.88
		15	2.5	7.63×10^2	74.12°C	0.96
		20	2.5	6.77×10^2	68.33°C	0.24
	J2003	5	-	5.76×10^2	80.92°C	0.39
		10	-	6.93×10^2	81.42°C	0.78
		15	2.5	7.86×10^2	80.92°C	0.81
		20	2.5	2.54×10^2	85.70°C	0.45
Anc. 2432	J900	5	-	3.41×10^2	76.13°C	0.55
		10	-	2.97×10^2	72.16°C	0.56
		15	2.5	1.65×10^2	69.59°C	0.47
		20	2.5	2.86×10^2	67.82°C	0.37
	J2003	5	-	2.53×10^2	81.42°C	0.34
		10	-	5.32×10^2	89.73°C	0.94
		15	2.5	2.03×10^2	88.22°C	0.98
		20	2.5	3.03×10^2	82.86°C	0.19

After 42 days of water leaching, the Jeffamine coatings were analyzed using contact angle experiment. Figure 4.9 shows water contact angles (WCA) data for the Jeffamine formulations. Most of the coatings, except PACM_J900_F5/0, 2143_J2003_F5/0, and 2432_J2003_F5/0, showed WCA > 90° when water droplet was first dispensed on the surface of the coatings, indicating formation of a hydrophobic surface. Over time, WCA values dropped below 90°, showing rearrangement of chains to form hydrophilic PEG rich surfaces. Coatings containing J900 co-crosslinker showed slower change in WCA values; after 40 minutes, the contact angle had dropped from ~97° to 54°. On the other hand, coatings containing J2003 co-crosslinker showed faster rearrangement; WCA changes from ~100° or higher to ~35° after 40 minutes. Initial WCA of 95-100° was observed for all the PACM cured coatings. For the polyamine cured coatings, initial WCA lied between 105-122°, with 2432_J2003_F10/0 showing the highest initial WCA of 122° among all the Jeffamine formulations.

(a)

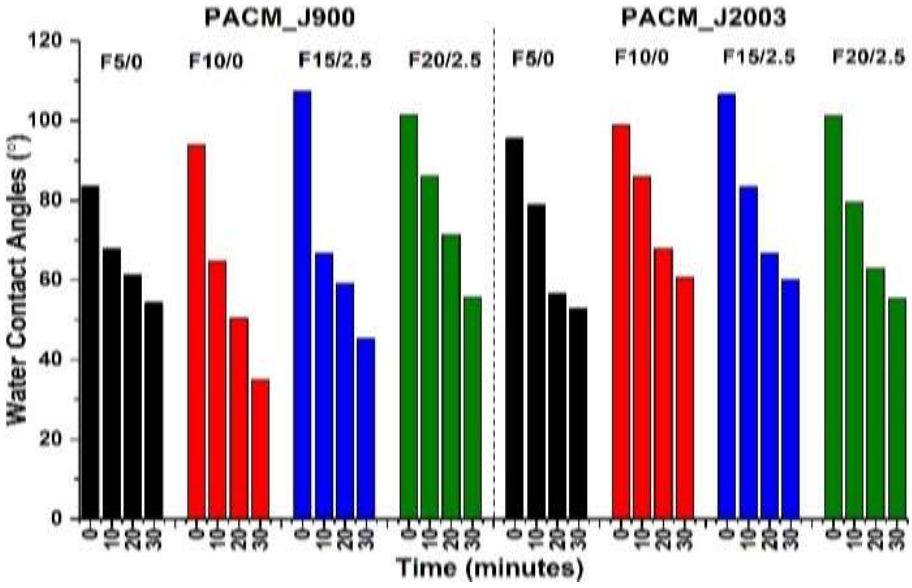

(b)

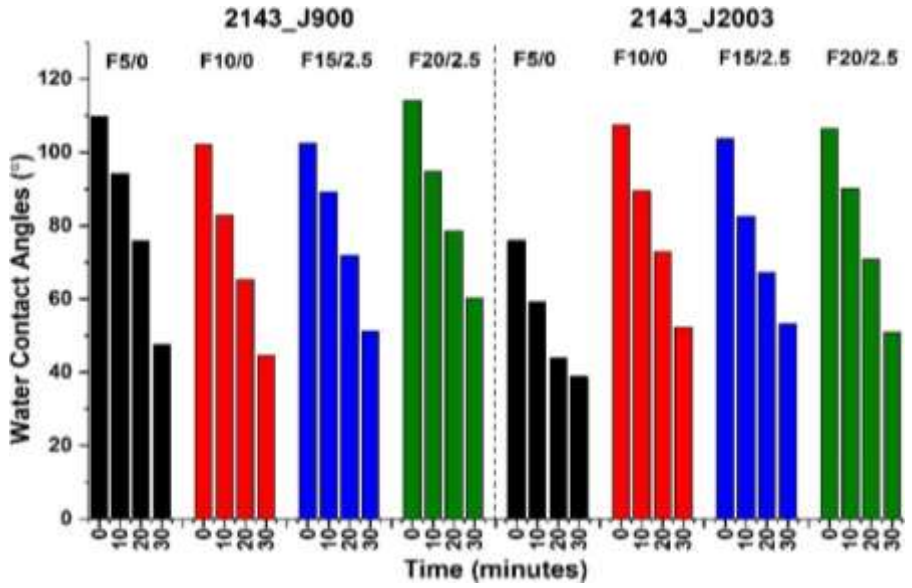

Figure 4.9. WCA changes for Jeffamine coatings cured using (a) PACM, (b) Ancamine 2143, and (c) Ancamine 2432 crosslinkers.

(c)

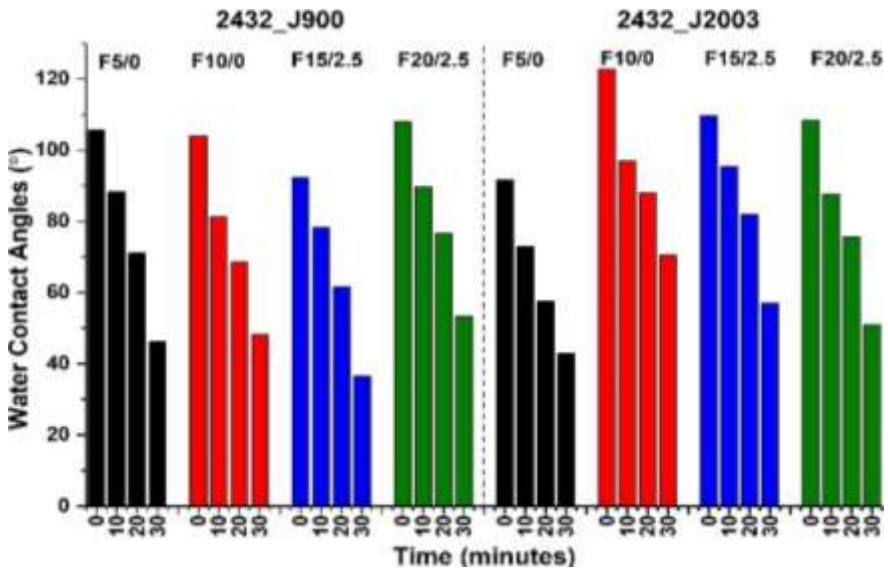

Figure 4.9. WCA changes for Jeffamine coatings cured using (a) PACM, (b) Ancamine 2143, and (c) Ancamine 2432 crosslinkers (continued).

FR performance of the Jeffamine coatings against common foulants: diatoms, biofilm, and hard foulants, barnacles and mussels, was evaluated. The FR performance of the amphiphilic coatings was compared to the commercial standards, Silastic T2 (T2), Intersleek 700 (I-700), Intersleek 900 (I-900), Intersleek 1100SR (1100SR) and regular polyurethanes (PU; no siloxanes). Figure 4.10 shows attachment and removal of diatom *N.incerta* at 20 psi water pressure from coatings cured using PACM and Ancamine 2432. Leachate toxicity tests with the Jeffamine coatings showed that formulations with Ancamine 2143 exhibited severe toxicity against diatoms. Therefore, the Ancamine 2143 cured formulations were excluded from the FR experiment. Significantly higher attachment of diatoms was observed on the formulations cured using PACM and Ancamine 2432 as compared to the commercial standards, I-900 and 1100SR (Figure 4.10(a)). Coatings with J900 and J2003 did not show any difference in diatom attachment. The amphiphilic coatings showed between 40-90% removal of *N.incerta* at 20 psi pressure, as opposed to ~90% removal from I-900 and 1100SR. Coatings containing J2003 co-crosslinker facilitated higher removal of the diatoms compared to J900. Ancamine 2432 cured coatings showed higher removal as compared to the PACM cured coatings. Among the Jeffamine formulations, PACM_J2003_F5/0, PACM_J2003_F10/0, 2432_J2003_F5/0, and 2432_J2003_F10/0 coatings showed the highest removal between 80-90%. 10 psi water jet pressure could not facilitate sufficient removal of diatoms from the commercial standards.

(a)

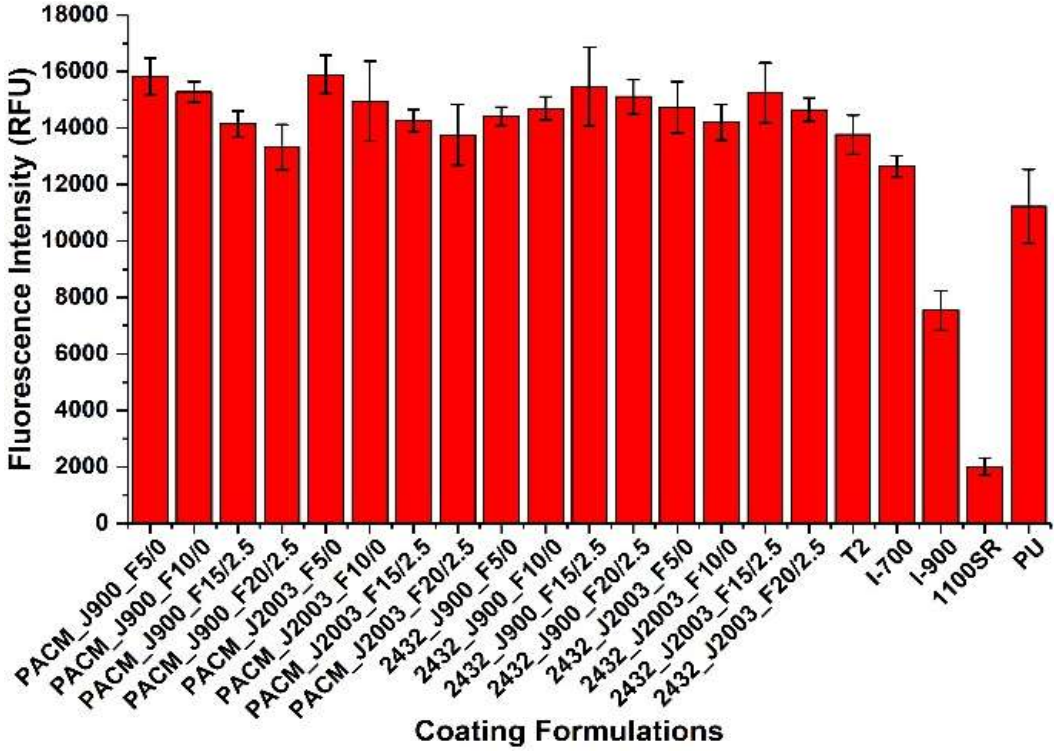

(b)

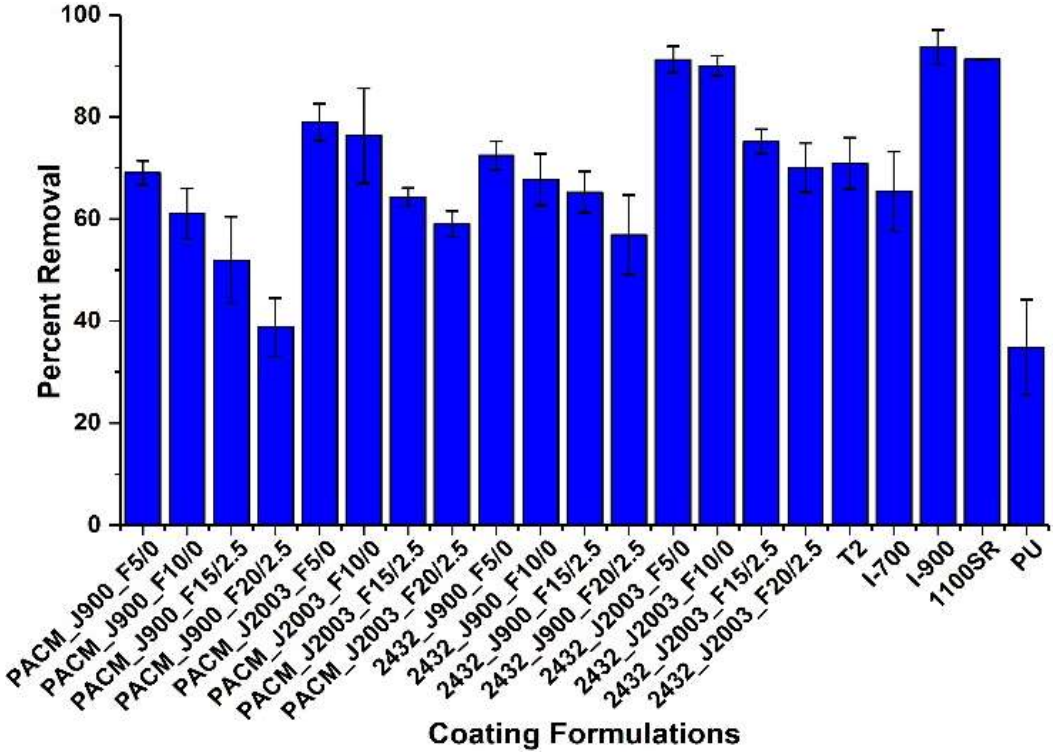

Figure 4.10. Diatom *N.incerta* (a) attachment and (b) removal at 20 psi waterjet pressure.

Figure 4.11 shows biofilm *C.lytica* attachment and removal at 10 psi and 20 psi water jet pressure. Unlike diatoms, the Ancamine 2143 cured coatings did not show toxicity against biofilm *C.lytica.* From Figure 4.11(a), it can be seen that the Jeffamine coatings showed significantly lower attachment of the biofilm as compared to I-700, I-900, and 1100SR. Among the Jeffamine formulations, coatings with Ancamine 2432 showed slightly higher *C.lytica* attachment. But, the amphiphilic Jeffamine coatings showed lower removal of the biofilm, even at 20 psi pressure, as compared to I-900 and 1100SR (~90% removal). 2143_J2003_F5/0 coatings showed highest removal of ~80% at 20 psi, while PACM_J2003_F20/2.5 showed the lowest biofilm removal of ~5% at 20 psi. For coatings with Ancamine 2432 as the primary crosslinkers, *C.lytica* removal increased slightly with increasing J900 and J2003 content.

(a)

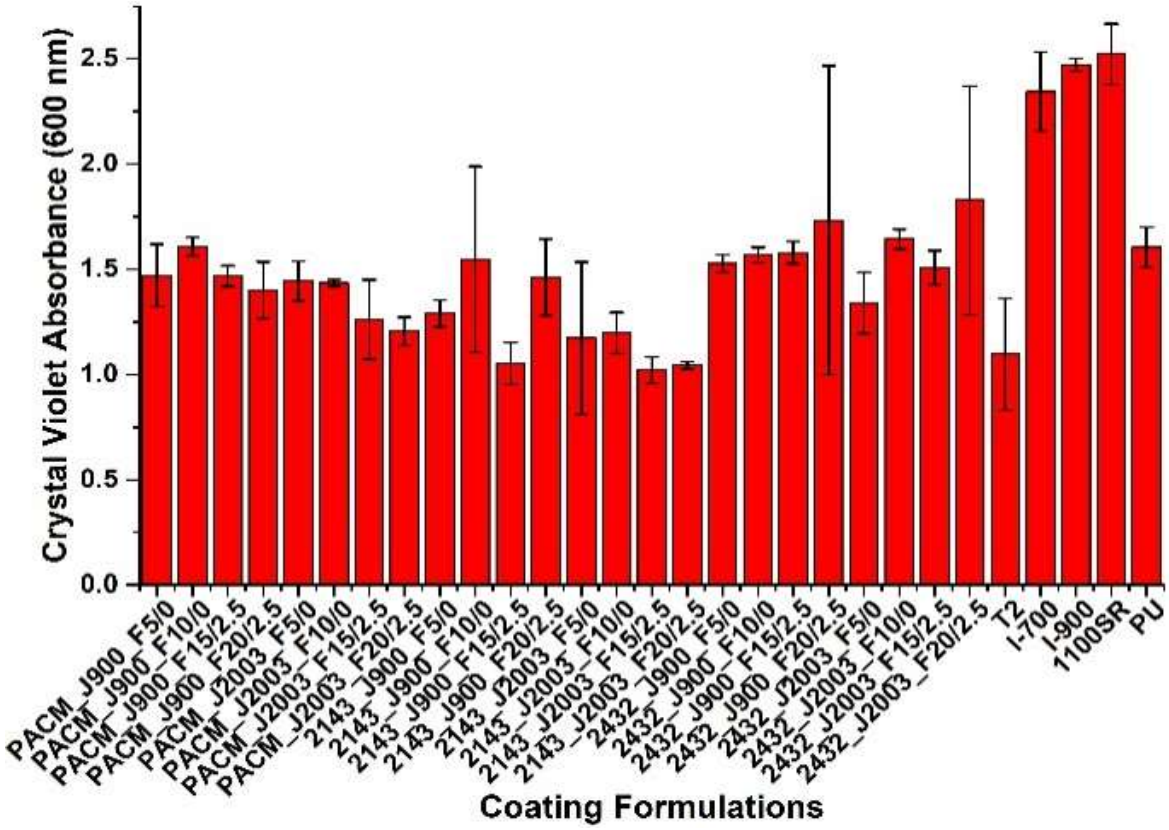

Figure 4.11. Biofilm *C.lytica* (a) attachment and (b) removal at 10 psi and 20 psi waterjet pressure.

(b)

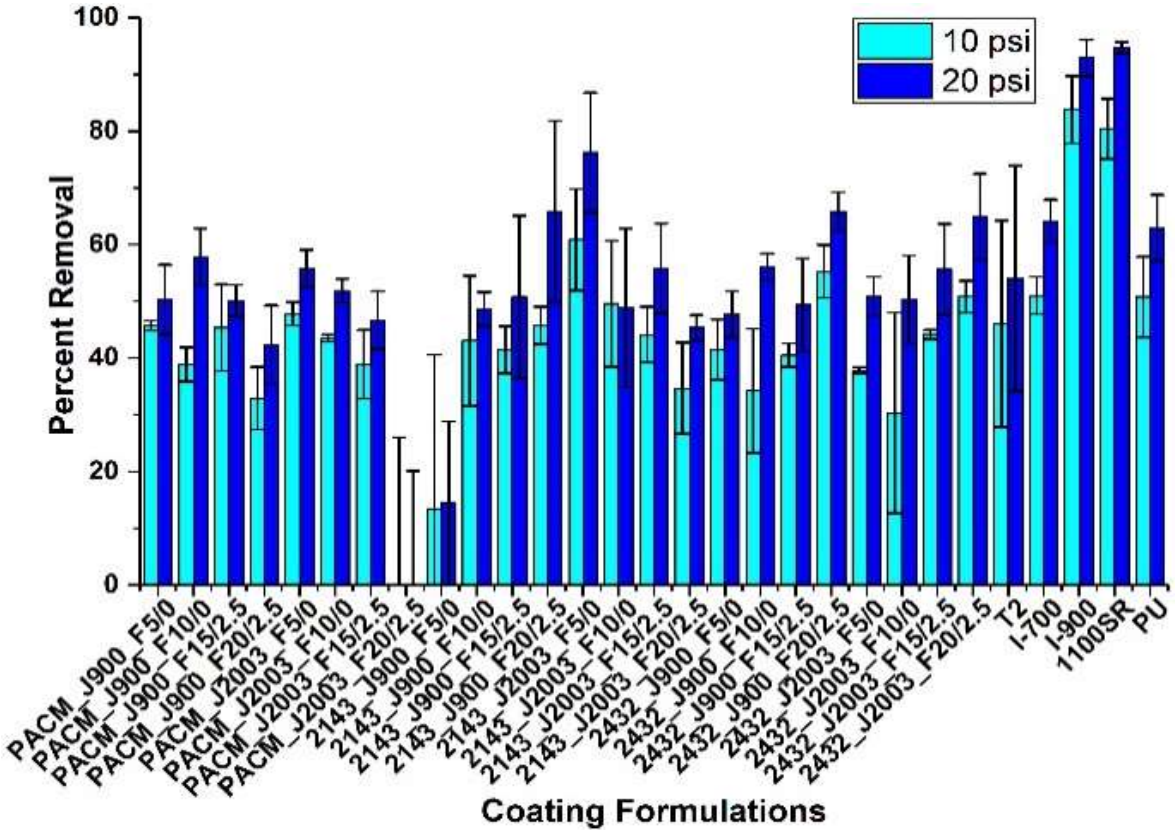

Figure 4.11. Biofilm *C.lytica* (a) attachment and (b) removal at 10 psi and 20 psi waterjet pressure (continued).

Select coatings were chosen for evaluation of FR performance against microalgae *U.linza* and mussels. Selection of coatings was based on prior research that showed lower attachment of microalgae and mussels onto hydrophobic surfaces. Therefore, coatings included in the two experiments were PACM_J900_F10/0, PACM_J900_F20/2.5, PACM_J2003_F5/0, PACM_J2003_F15/2.5, 2432_J900_F10/0, 2432_J900_F20/2.5, 2432_J2003_F5/0, and 2432_J2003_F15/2.5. 10% or 20% J900 (low MW) and 5% or 15% J2003 (high MW) were anticipated to provide a good balance between the hydrophobic and hydrophilic moieties on the coating surfaces. Figure 4.12 shows results for attachment and removal of microalgae *U.linza* from the Jeffamine coatings. Overall, the Jeffamine formulations showed extremely poor FR performance against microalgae. All the select Jeffamine coatings, except PACM_J900_10/0, showed higher attachment of the microalgae as compared to T2, 1100SR, PU, and PS coatings. But, none of the Jeffamine coatings could facilitate more than 25% removal of the microalgae, even at 111 kPa water pressure; on the other hand, T2 and 1100SR showed 85-90%

microalgae removal. PACM_J900_F10/0 showed highest microalgae removal of 25% among all the Jeffamine formulations. Among the Ancamine 2432 cured formulations, 2432_J2003_F5/0 facilitated highest removal of 15%.

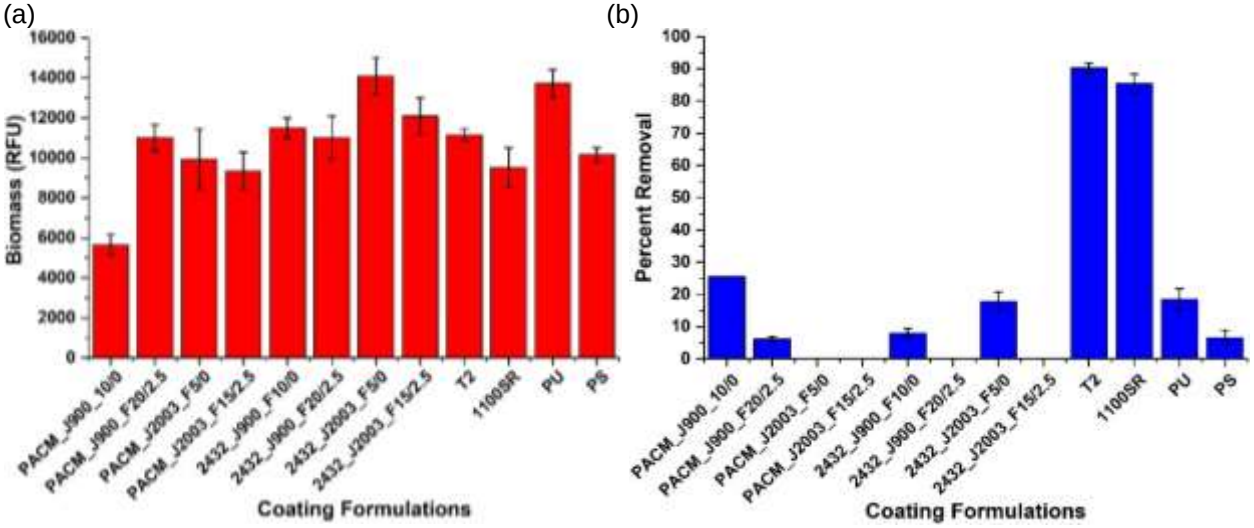

Figure 4.12. Microalgae *Ulva linza* (a) attachment and (b) removal at 111 kPa water pressure.

Figure 4.13 shows mussel adhesion on the select Jeffamine coatings. The Jeffamine coatings allowed stronger attachment of mussels as compared to I-700, I-900, and 1100SR (none of the mussels attached onto I-900 and 1100SR coatings). Coatings cured using Ancamine 2432 showed lower adhesion force as compared to the PACM cured coatings. Among the Jeffamine coatings, PACM_J2003_F5/0 and 2432_J2003_F15/2.5 showed lowest adhesion strength of ~20 N for 5 out 6 mussels attached onto the coatings.

Based on the slightly better FR performance of the Ancamine 2432 cured coatings against most of the common foulants as compared to PACM, four formulations were selected for reattached barnacle adhesion experiment. Figure 4.14 shows results from barnacle adhesion test on the select Ancamine 2432 cured coatings. The Jeffamine coatings showed significantly higher barnacle adhesion as compared to I-700, I-900, and 1100SR. Among the Jeffamine coatings, 2432_J900_F5/0 showed highest adhesion strength of 0.31 MPa for 5 out of 6 barnacles that attached to the coatings. 1 barnacle base broke from 2432_J900_F5/0 formulation during experimentation. 2432_J900_F15/2.5 showed the poorest FR performance against barnacles, with adhesion force of 0.22 MPa required for removal of 6 barnacles, out of which 5 barnacles broke, indicating very strong adhesion of the barnacles. Although lower force of

removal was required for coatings with J2003, 2-3 barnacles bases still broke during experimentation. Conversely, 1100SR and I-700 required only 0.02-0.06 MPa for removal of 3 out of 6 barnacles; I-900 required removal force of 0.06 MPa for 6 attached barnacles.

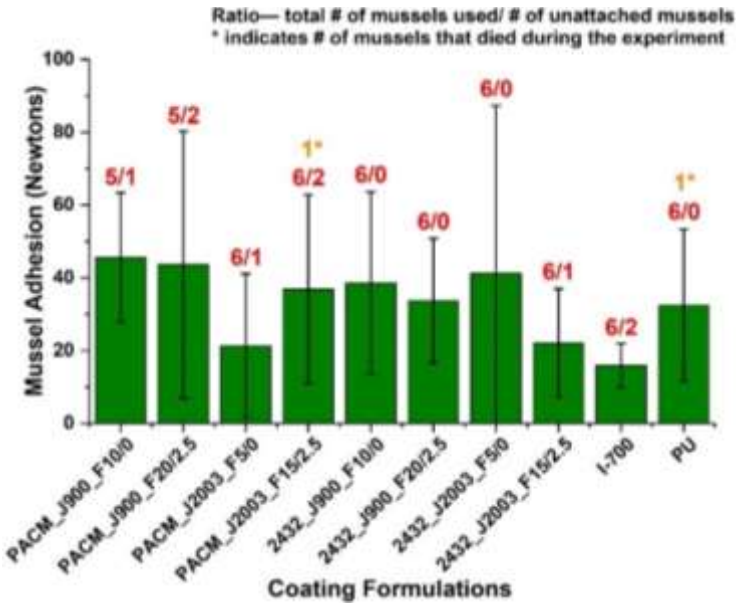

Figure 4.13. Mussel adhesion on select Jeffamine coatings. Ratios above the data points indicate the number of mussels that were immobilized on the coatings during the experiment/ the number of mussels that did not attach to the coatings. Numbers with asterisk (*) above select data points indicate the number of mussels that died during experimentation. None of the mussels attached to I-900 and 1100SR coatings.

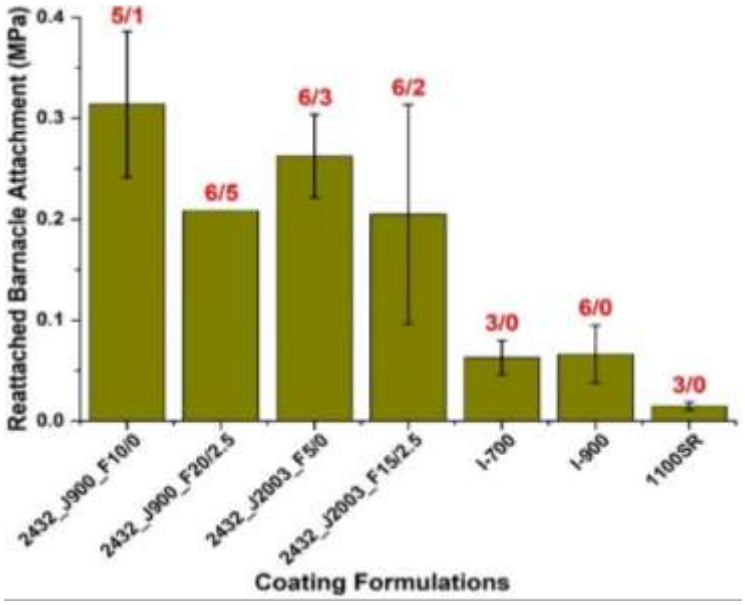

Figure 4.14. Barnacle adhesion on select Jeffamine coatings. Ratios above the data points indicate the number of barnacles out of 6 that attached to the coatings during the experiment/the number of barnacles that broke during experimentation.

To investigate effect of surface chemistry and topography of the Jeffamine coatings on their FR performance, coatings cured using PACM and Ancamine 2432 were analyzed using surface analysis techniques, ATR-FTIR, AFM, and XPS. Due to toxicity of the Ancamine 2143 coatings against most common foulants, further experimentation with these coatings was discontinued. Figure 4.15 shows ATR-FTIR spectra for select Jeffamine coatings. Peaks at ~1330 cm^{-1} and 1050 cm^{-1} indicated presence of PEG and PDMS moieties respectively on the surface of the Jeffamine coatings. Potential minor peak at ~1350 cm^{-1} indicated presence of unreacted amine groups in the Ancamine 2432 cured coatings. Some unreacted epoxy groups may be present in some Jeffamine formulations as observed from visibility of minor peaks at ~913 cm^{-1}.

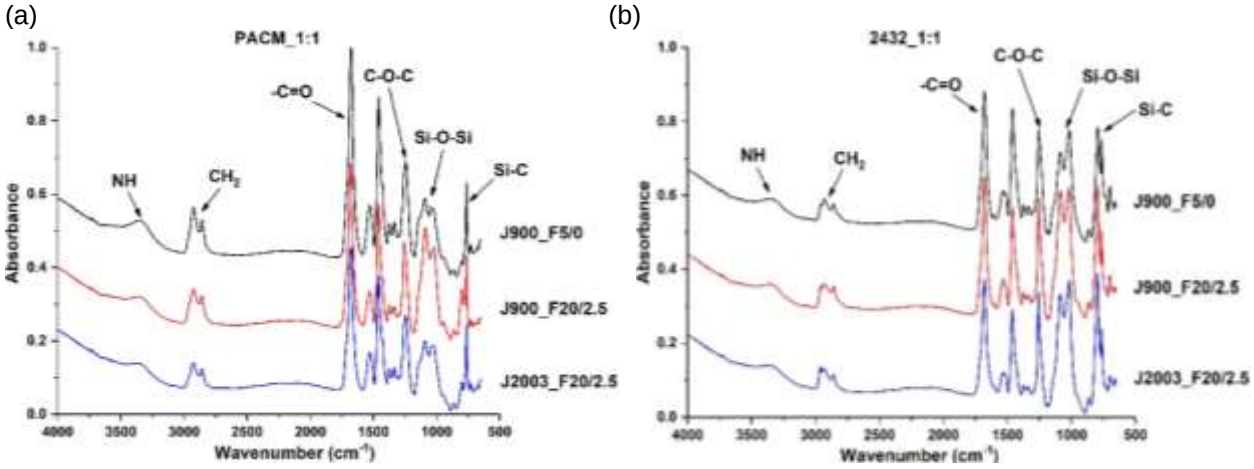

Figure 4.15. ATR-FTIR spectra of Jeffamine coatings cured using (a) PACM and (b) Ancamine 2432 primary amine crosslinkers.

The cured coatings were characterized using AFM to understand effect of MW and loading of the Jeffamine co-reactants on surface topography. Figure 4.16 shows AFM scans obtained for the select coatings. Coatings with 5-10% Jeffamines showed similar surface topographies; coatings with similar topographies were formed with 15-20% Jeffamines. As observed from AFM, the PACM cured formulations appeared smooth with domains scattered across the coating surfaces. At 15-20% Jeffamine content, the domains formed deep valleys or “cracks” on the coating surfaces. Roughness of the Ancamine cured coatings was higher than the PACM cured coatings. Rough “craters” were observed on the surfaces of most of the Ancamine 2432 cured formulations. In the absence of craters, the coatings showed formation of roughness gradients.

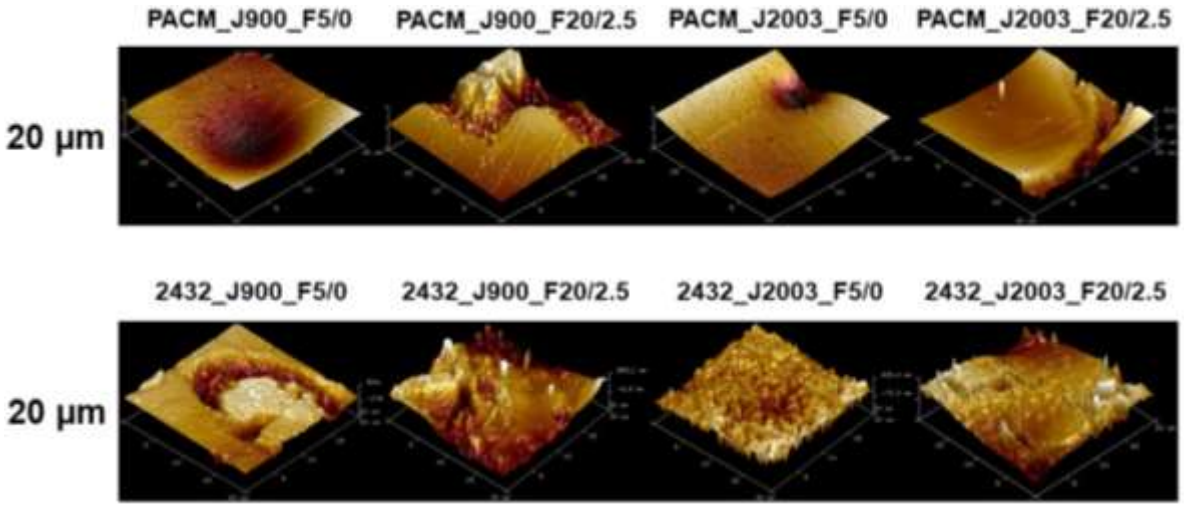

Figure 4.16. AFM scans for the PACM cured and the Ancamine 2432 cured Jeffamine coatings.

XPS was used to determine chemical composition of select Jeffamine coatings with varying Jeffamines content and effect of addition of APT-PDMS on surface chemistry. Figure 4.17 shows high resolution XPS spectra for individual O1s and C1s elements on the surfaces of the Jeffamine coatings. Curve fitting was conducted on O, C, and N elements to determine the concentration of PDMS and PEG components on the coating surfaces. All the Jeffamine coatings showed Si2p peak at 102.08-102.34 eV, indicating presence of PDMS on the coating surfaces. Table 4.4 shows atom percent of O1s, C1s, and N1s elements as determined from peak fitting. N1s peak at ~399 eV was observed on all the coatings. The PACM cured coatings showed higher N content on the surfaces than the Ancamine 2432 cured coatings. N content also appeared to decrease from 9.31% to 8.15% and 8.69% to 3.94% for the coatings cured using PACM and Ancamine 2432 respectively with addition of 2.5% APT-PDMS. Peak fitting for O and C showed presence of three different chemical states for O and C. O1s peaks at ~532, 531.48, and 533.27 eV indicated of O from Si-O-Si, C-O-C, and -NH-C=O (carbamate/urethane) linkages respectively. Similarly, C1s peaks at ~284.20, 285.90-286.18, and 288.83-289.14 indicated C-C/C-H, C-O-C/C-N, and the carbamate linkages respectively. For the PACM cured coatings, amount of PEG moieties (C-O-C = 19-23%) was significantly higher than PDMS component (Si-O-Si = 11-16%). Concentration of PDMS increased from 11% to 16% with the addition of APT-PDMS, which resulted in slight drop in PEG concentration from 23% to 19%. Conversely, with Ancamine 2432, PDMS content (~19.20%) was higher

than PEG (10-13%). Although addition of APT-PDMS did not affect concentration of PDMS on the coatings, concentration of PEG on the surfaces decreased from 13% to 10%.

Table 4.4. Surface composition of the Jeffamine coatings determined from XPS.

Formulations	Chemical states		Binding energies (eV)	Atom %
PACM_J900_F5/0	O1s	Si-O-Si	532.00	11.71
		C-O	531.23	5.97
		C=O	533.27	3.59
	C1s	C-C/C-H	284.49	37.48
		C-O/C-N	285.94	23.21
		C=O	289.11	6.99
	N1s	Total	400.01	9.31
PACM_J2003_F20/2.5	O1s	Si-O-Si	531.89	16.45
		C-O	531.23	5.35
		C=O	533.27	3.72
	C1s	C-C/C-H	284.36	40.54
		C-O/C-N	286.00	19.57
		C=O	289.11	5.81
	N1s	Total	399.95	8.15
2432_J900_F5/0	O1s	Si-O-Si	531.90	19.12
		C-O	531.23	4.51
		C=O	533.27	3.24
	C1s	C-C/C-H	284.33	47.58
		C-O/C-N	286.02	13.08
		C=O	288.97	3.79
	N1s	Total	399.96	8.69
2432_J2003_F20/2.5	O1s	Si-O-Si	531.90	19.33
		C-O	531.23	5.62
		C=O	533.27	2.23
	C1s	C-C/C-H	284.31	53.30
		C-O/C-N	286.23	10.48
		C=O	288.83	2.66
	N1s	Total	399.55	3.94

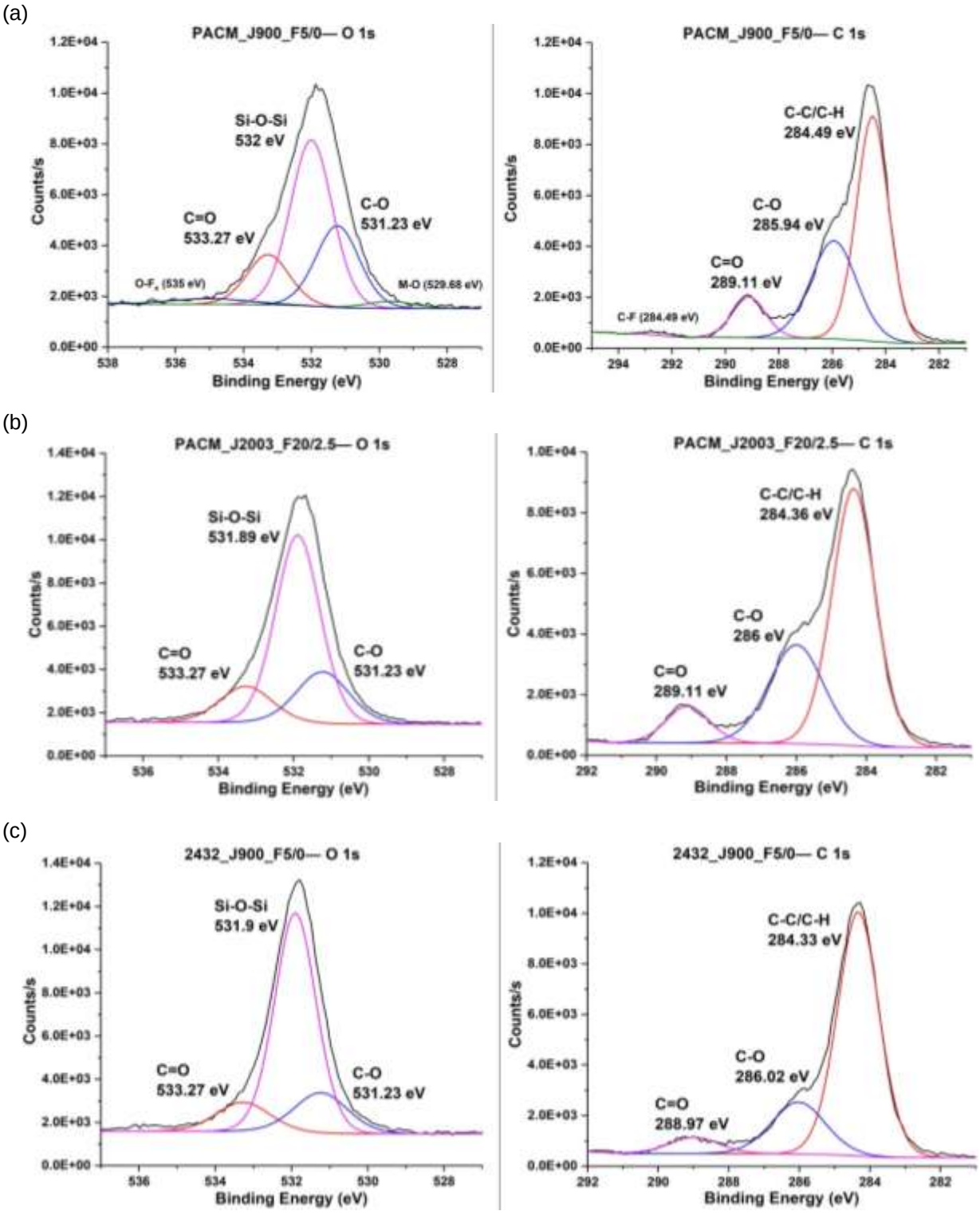

Figure 4.17. High resolution XPS spectra with peak fitting for O1s and C1s peaks for (a) PACM_J900_F5/0, (b) PACM_J2003_F20/2.5, (c) 2432_J900_F5/0, and (d) 2432_J2003_F20/2.5 coatings.

(d)

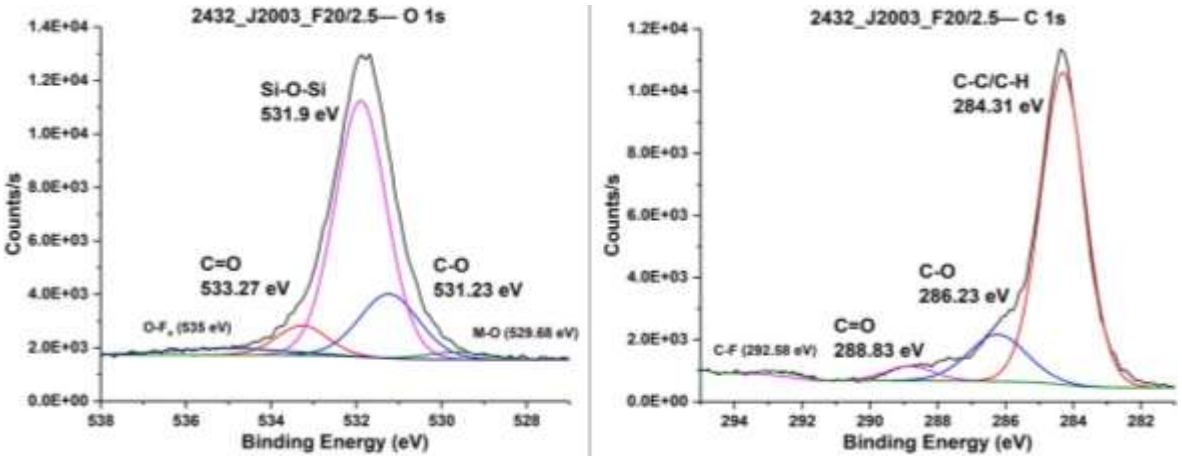

Figure 4.17. High resolution XPS spectra with peak fitting for O1s and C1s peaks for (a) PACM_J900_F5/0, (b) PACM_J2003_F20/2.5, (c) 2432_J900_F5/0, and (d) 2432_J2003_F20/2.5 coatings (continued).

Amphiphilic nature of the Jeffamine coatings was observed from dynamic change in WCA values, indicating alteration of surface chemistries with changing environment (air to water). Slightly higher WCA values for formulations with J2003 as compared to J900 may be due to higher incompatibility between non-polar PDMS chains and polar GC matrix and PEG chains, causing potentially higher self-stratification of PDMS chains onto the coating surfaces. Another reason for the higher WCA with J2003 may have been due to delay in separation of longer PEG chains from the coating matrix. ATR-FTIR and XPS also showed presence of both PDMS and PEG on the coating surfaces. XPS analysis showed that the PACM higher concentration of PEG was observed on the PACM cured coatings as compared to the Ancamine 2432 cured coatings. This behavior may be attributed to the nature of coating network formed during crosslinking. Curing formulations comprising of Jeffamine co-reactants, PDMS, and PACM at elevated temperature may not have allowed sufficient time for self-stratification of the PDMS chains. On the other hand, curing under ambient conditions with Ancamine 2432 caused the PDMS chains to exude to the surface, increasing concentration of PDMS on the coatings. Comparatively higher hydrophilicity of coatings with 5-10% J2003 was beneficial for removal of diatoms. The hydrophilicity of the coatings decreased at 15-20% Jeffamines due to presence of 2.5% 20k APT-PDMS, thereby reducing diatom removal. But, presence of PEG rich domains allowed strong attachment of microalgae, mussels, and barnacles. In spite of addition of high MW APT-PDMS, the coating surfaces did not exhibit adequate balance between PDMS and PEG components.

Conclusions

Amphiphilic coatings were made by incorporating amine terminated PEGs, with varying MW, into formulations with isocyanate-free hydrophobic siloxane modified GC (IGC_PDMS) resin. 5, 10, 15, and 20% by weight resin solids Jeffamine ED-900 (J900) and Jeffamine ED-2003 (J2003) were added as co-crosslinkers to impart hydrophilicity to the IGC_PDMS coatings. PACM, Ancamine 2143, and Ancamine 2432, at epoxy: AHEW = 1:1, were used as primary crosslinkers. Additional 2.5% by weight resin solids APT-PDMS (20k g/mol) was added to the formulations with Jeffamine content = 15% and 20% to balance potentially high hydrophilicity of the coatings. The cured coatings appeared smooth, uniform, and glossy. The coatings exhibited good hardness, flexibility, and impact strength. Most of the coatings with PACM showed MEK double rub values > 400. The PACM cured coatings showed higher König pendulum hardness values, while the polyamine cured coatings showed better pencil hardness. Impact resistance of the coatings improved with addition of J2003 into the formulations. Thermal analysis using DSC and DMA showed that coatings with J2003 co-crosslinker exhibited higher T_g than coatings with J900. Further, increasing Jeffamine content = 15-20% in the coatings resulted in decrease in T_g of the coatings due to presence of APT-PDMS in the formulations. TGA showed that degradation temperatures of most of the coatings lied between 250-265°C. Tighter networks appeared to have formed in coatings with 5-15% Jeffamines with PACM and Ancamine 2143, while the networks loosened with 20% Jeffamines and Ancamine 2432. The cured coatings showed dynamic changes in WCA. Coatings with J2003 showed faster rate of change of WCA. Amphiphilic nature of the coatings was also evident from presence of PEG and PDMS on the surface of the cured coatings as observed using ATR-FTIR and XPS. Concentration of PEG was higher on coatings cured using PACM, while inverse was true for the Ancamine 2432 cured formulations. AFM showed formation of domains on the Jeffamine coatings. Coatings cured using Ancamine 2432 exhibited higher surface roughness as compared to the PACM cured formulations. Evaluation of FR performance against diatoms showed that the Jeffamine coatings facilitated 40-90% diatom *N.incerta* removal at 20 psi water jet pressure. Diatom removal was higher at 5-10% Jeffamine co-crosslinkers as compared to 15-20% Jeffamine due to presence of APT-PDMS in the latter formulations. As compared to the commercial standards, the Jeffamine coatings showed lower biofilm *C.lytica* attachment but lower biofilm removal even at 20 psi water pressure. Although microalgae attachment on

the Jeffamine coatings was similar to the commercial standards, the Jeffamine coatings could not facilitate more than 25% removal of the microalgae (~90% removal from 1100SR and T2). Mussel and barnacle adhesion on the amphiphilic coatings was significantly higher than I-700, I-900, and 1100SR. Mussel adhesion strength was higher for most of the PACM cured coatings as compared to the Ancamine 2432 cured formulations. The Jeffamine coatings allowed stronger attachment of barnacles as compared to the commercial standards, with 20-80% barnacle bases breaking during experimentation. Poor FR performance of the Jeffamine coatings against most of the foulants can be attributed to the presence of 10-23% PEG as against 11-19% PDMS components on coating surfaces as determined from XPS. Further tuning of surface chemistry is required for use of the Jeffamine coatings as successful amphiphilic coatings in practical applications.

References

1. Yebra, D. M.; Kiil, S.; Dam-Johansen, K., Antifouling technology—past, present and future steps towards efficient and environmentally friendly antifouling coatings. *Progress in Organic Coatings* **2004,** *50* (2), 75-104.

2. Callow, J. A.; Callow, M. E., Trends in the development of environmentally friendly fouling-resistant marine coatings. *Nature Communications* **2011,** *2*, 244.

3. Magin, C. M.; Cooper, S. P.; Brennan, A. B., Non-toxic antifouling strategies. *Materials Today* **2010,** *13* (4), 36-44.

4. Schultz, M. P., Effects of coating roughness and biofouling on ship resistance and powering. *Biofouling* **2007,** *23* (5), 331-341.

5. Sommer, S.; Ekin, A.; Webster, D. C.; Stafslien, S. J.; Daniels, J.; VanderWal, L. J.; Thompson, S. E. M.; Callow, M. E.; Callow, J. A., A preliminary study on the properties and fouling-release performance of siloxane–polyurethane coatings prepared from poly (dimethylsiloxane)(PDMS) macromers. *Biofouling* **2010,** *26* (8), 961-972.

6. Schultz, M. P.; Bendick, J. A.; Holm, E. R.; Hertel, W. M., Economic impact of biofouling on a naval surface ship. *Biofouling* **2011,** *27* (1), 87-98.

7. Lejars, M. n.; Margaillan, A.; Bressy, C., Fouling release coatings: a nontoxic alternative to biocidal antifouling coatings. *Chemical Reviews* **2012,** *112* (8), 4347-4390.

8. Sommer, S. A.; Byrom, J. R.; Fischer, H. D.; Bodkhe, R. B.; Stafslien, S. J.; Daniels, J.; Yehle, C.; Webster, D. C., Effects of pigmentation on siloxane–polyurethane coatings and their performance as fouling-release marine coatings. *Journal of Coatings Technology and Research* **2011,** *8* (6), 661-670.

9. Bodkhe, R. B.; Thompson, S. E. M.; Yehle, C.; Cilz, N.; Daniels, J.; Stafslien, S. J.; Callow, M. E.; Callow, J. A.; Webster, D. C., The effect of formulation variables on fouling-release performance of stratified siloxane–polyurethane coatings. *Journal of Coatings Technology and Research* **2012,** *9* (3), 235-249.

10. Brady Jr, R. F.; Singer, I. L., Mechanical factors favoring release from fouling release coatings. *Biofouling* **2000,** *15* (1-3), 73-81.

11. Crisp, D. J.; Walker, G.; Young, G. A.; Yule, A. B., Adhesion and substrate choice in mussels and barnacles. *Journal of Colloid and Interface Science* **1985,** *104* (1), 40-50.

12. Brady, R. F., Properties which influence marine fouling resistance in polymers containing silicon and fluorine. *Progress in Organic Coatings* **1999,** *35* (1), 31-35.

13. Brady, R. F., A fracture mechanical analysis of fouling release from nontoxic antifouling coatings. *Progress in Organic Coatings* **2001,** *43* (1), 188-192.

14. Ekin, A.; Webster, D. C., Combinatorial and High-Throughput Screening of the Effect of Siloxane Composition on the Surface Properties of Crosslinked Siloxane− Polyurethane Coatings. *Journal of Combinatorial Chemistry* **2007,** *9* (1), 178-188.

15. Ekin, A.; Webster, D. C.; Daniels, J. W.; Stafslien, S. J.; Cassé, F.; Callow, J. A.; Callow, M. E., Synthesis, formulation, and characterization of siloxane–polyurethane coatings for underwater marine applications using combinatorial high-throughput experimentation. *Journal of Coatings Technology and Research* **2007,** *4* (4), 435-451.

16. Majumdar, P.; Ekin, A.; Webster, D. C., Thermoset Siloxane—Urethane Fouling Release Coatings. In *Smart Coatings*, **March 13, 2007**.

17. Baur, X.; Marek, W.; Ammon, J.; Czuppon, A. B.; Marczynski, B.; Raulf-Heimsoth, M.; Roemmelt, H.; Fruhmann, G., Respiratory and other hazards of isocyanates. *International Archives of Occupational and Environmental Health* **1994,** *66* (3), 141-152.

18. Musk, A. W.; Peters, J. M.; Wegman, D. H., Isocyanates and respiratory disease: current status. *American Journal of Industrial Medicine* **1988,** *13* (3), 331-349.

19. Edwards, P. A.; Striemer, G.; Webster, D. C., Novel polyurethane coating technology through glycidyl carbamate chemistry. *JCT Research* **2005,** *2* (7), 517-527.

20. Harkal, U. D.; Muehlberg, A. J.; Webster, D. C., Linear glycidyl carbamate (GC) resins for highly flexible coatings. *Journal of Coatings Technology and Research* **2013,** *10* (2), 141-151.

21. Harkal, U. D.; Muehlberg, A. J.; Li, J.; Garrett, J. T.; Webster, D. C., The influence of structural modification and composition of glycidyl carbamate resins on their viscosity and coating performance. *Journal of Coatings Technology and Research* **2010,** *7* (5), 531-546.

22. Chattopadhyay, D. K.; Webster, D. C., Hybrid coatings from novel silane-modified glycidyl carbamate resins and amine crosslinkers. *Progress in Organic Coatings* **2009,** *66* (*1*), 73-85.

23. Harkal, U. D.; Muehlberg, A. J.; Webster, D. C., UV curable glycidyl carbamate based resins. *Progress in Organic Coatings* **2012,** *73* (1), 19-25.

24. Harkal, U. D.; Muehlberg, A. J.; Edwards, P. A.; Webster, D. C., Novel water-dispersible glycidyl carbamate (GC) resins and waterborne amine-cured coatings. *Journal of Coatings Technology and Research* **2011,** *8* (6), 735-747.

25. Finlay, J. A.; Bennett, S. M.; Brewer, L. H.; Sokolova, A.; Clay, G.; Gunari, N.; Meyer, A. E.; Walker, G. C.; Wendt, D. E.; Callow, M. E., Barnacle settlement and the adhesion of protein and diatom microfouling to xerogel films with varying surface energy and water wettability. *Biofouling* **2010,** *26* (6), 657-666.

26. Holland, R.; Dugdale, T. M.; Wetherbee, R.; Brennan, A. B.; Finlay, J. A.; Callow, J. A.; Callow, M. E., Adhesion and motility of fouling diatoms on a silicone elastomer. *Biofouling* **2004,** *20* (6), 323-329.

27. Gudipati, C. S.; Finlay, J. A.; Callow, J. A.; Callow, M. E.; Wooley, K. L., The antifouling and fouling-release perfomance of hyperbranched fluoropolymer (HBFP)-poly (ethylene glycol)(PEG) composite coatings evaluated by adsorption of biomacromolecules and the green fouling alga ulva. *Langmuir* **2005,** *21* (7), 3044-3053.

28. Krishnan, S.; Wang, N.; Ober, C. K.; Finlay, J. A.; Callow, M. E.; Callow, J. A.; Hexemer, A.; Sohn, K. E.; Kramer, E. J.; Fischer, D. A., Comparison of the fouling release properties of hydrophobic fluorinated

and hydrophilic PEGylated block copolymer surfaces: attachment strength of the diatom Navicula and the green alga Ulva. *Biomacromolecules* **2006,** *7* (5), 1449-1462.

29. Galhenage, T. P.; Webster, D. C.; Moreira, A. M. S.; Burgett, R. J.; Stafslien, S. J.; Vanderwal, L.; Finlay, J. A.; Franco, S. C.; Clare, A. S., Poly (ethylene) glycol-modified, amphiphilic, siloxane–polyurethane coatings and their performance as fouling-release surfaces. *Journal of Coatings Technology and Research* **2016,** *2* (14), 307-322.

30. Chen, H.; Yuan, L.; Song, W.; Wu, Z.; Li, D., Biocompatible polymer materials: role of protein–surface interactions. *Progress in Polymer Science* **2008,** *33* (11), 1059-1087.

31. Harder, P.; Grunze, M.; Dahint, R.; Whitesides, G. M.; Laibinis, P. E., Molecular conformation in oligo (ethylene glycol)-terminated self-assembled monolayers on gold and silver surfaces determines their ability to resist protein adsorption. *The Journal of Physical Chemistry B* **1998,** *102* (2), 426-436.

32. Zheng, J.; Li, L.; Chen, S.; Jiang, S., Molecular simulation study of water interactions with oligo (ethylene glycol)-terminated alkanethiol self-assembled monolayers. *Langmuir* **2004,** *20* (20), 8931-8938.

33. Gudipati, C. S.; Greenlief, C. M.; Johnson, J. A.; Prayongpan, P.; Wooley, K. L., Hyperbranched fluoropolymer and linear poly (ethylene glycol) based amphiphilic crosslinked networks as efficient antifouling coatings: an insight into the surface compositions, topographies, and morphologies. *Journal of Polymer Science Part A: Polymer Chemistry* **2004,** *42* (24), 6193-6208.

34. Murthy, R.; Cox, C. D.; Hahn, M. S.; Grunlan, M. A., Protein-resistant silicones: incorporation of poly (ethylene oxide) via siloxane tethers. *Biomacromolecules* **2007,** *8* (10), 3244-3252.

35. Murthy, R.; Bailey, B. M.; Valentin-Rodriguez, C.; Ivanisevic, A.; Grunlan, M. A., Amphiphilic silicones prepared from branched PEO-silanes with siloxane tethers. *Journal of Polymer Science Part A: Polymer Chemistry* **2010,** *48* (18), 4108-4119.

36. Faÿ, F.; Hawkins, M. L.; Réhel, K.; Grunlan, M. A.; Linossier, I., Non-toxic, anti-fouling silicones with variable PEO–silane amphiphile content. *Green Materials* **2016,** *4* (2), 53-62.

37. Rufin, M. A.; Ngo, B. K. D.; Barry, M. E.; Page, V. M.; Hawkins, M. L.; Stafslien, S. J.; Grunlan, M. A., Antifouling silicones based on surface-modifying additive amphiphiles. *Green Materials* **2017**, 1-10.

38. Weinman, C. J.; Finlay, J. A.; Park, D.; Paik, M. Y.; Krishnan, S.; Sundaram, H. S.; Dimitriou, M.; Sohn, K. E.; Callow, M. E.; Callow, J. A., ABC triblock surface active block copolymer with grafted

ethoxylated fluoroalkyl amphiphilic side chains for marine antifouling/fouling-release applications. *Langmuir* **2009,** *25* (20), 12266-12274.

39. Martinelli, E.; Menghetti, S.; Galli, G.; Glisenti, A.; Krishnan, S.; Paik, M. Y.; Ober, C. K.; Smilgies, D. M.; Fischer, D. A., Surface engineering of styrene/PEGylated-fluoroalkyl styrene block copolymer thin films. *Journal of Polymer Science Part A: Polymer Chemistry* **2009,** *47* (1), 267-284.

40. Krishnan, S.; Ayothi, R.; Hexemer, A.; Finlay, J. A.; Sohn, K. E.; Perry, R.; Ober, C. K.; Kramer, E. J.; Callow, M. E.; Callow, J. A., Anti-biofouling properties of comblike block copolymers with amphiphilic side chains. *Langmuir* **2006,** *22* (11), 5075-5086.

41. Cardillo, P.; Nebuloni, M., Theoretical and calorimetric evaluation of thermal stability of glycidol. *Journal of Loss Prevention in the Process Industries* **1991,** *4* (4), 242-245.

42. Bodkhe, R. B.; Stafslien, S. J.; Cilz, N.; Daniels, J.; Thompson, S. E. M.; Callow, M. E.; Callow, J. A.; Webster, D. C., Polyurethanes with amphiphilic surfaces made using telechelic functional PDMS having orthogonal acid functional groups. *Progress in Organic Coatings* **2012,** *75* (1), 38-48.

43. Cassé, F.; Stafslien, S. J.; Bahr, J. A.; Daniels, J.; Finlay, J. A.; Callow, J. A.; Callow, M. E., Combinatorial materials research applied to the development of new surface coatings V. Application of a spinning water-jet for the semi-high throughput assessment of the attachment strength of marine fouling algae. *Biofouling* **2007,** *23* (2), 121-130.

44. Chen, Z.; Chisholm, B.; Kim, J.; Stafslien, S.; Wagner, R.; Patel, S.; Daniels, J.; Wal, L. V.; Li, J.; Ward, K., UV-curable, oxetane-toughened epoxy-siloxane coatings for marine fouling-release coating applications. *Polymer International* **2008,** *57* (6), 879-886.

45. Kim, J.; Nyren-Erickson, E.; Stafslien, S.; Daniels, J.; Bahr, J.; Chisholm, B. J., Release characteristics of reattached barnacles to non-toxic silicone coatings. *Biofouling* **2008,** *24* (4), 313-319.

46. Majumdar, P.; Lee, E.; Patel, N.; Ward, K.; Stafslien, S. J.; Daniels, J.; Chisholm, B. J.; Boudjouk, P.; Callow, M. E.; Callow, J. A., Combinatorial materials research applied to the development of new surface coatings IX: an investigation of novel antifouling/fouling-release coatings containing quaternary ammonium salt groups. *Biofouling* **2008,** *24* (3), 185-200.

47. Kugel, A. J.; Jarabek, L. E.; Daniels, J. W.; Vander Wal, L. J.; Ebert, S. M.; Jepperson, M. J.; Stafslien, S. J.; Pieper, R. J.; Webster, D. C.; Bahr, J., Combinatorial materials research applied to the

development of new surface coatings XII: Novel, environmentally friendly antimicrobial coatings derived from biocide-functional acrylic polyols and isocyanates. *Journal of Coatings Technology and Research* **2009,** *6* (1), 107-121.

48. Stafslien, S. J.; Bahr, J. A.; Feser, J. M.; Weisz, J. C.; Chisholm, B. J.; Ready, T. E.; Boudjouk, P., Combinatorial materials research applied to the development of new surface coatings I: a multiwell plate screening method for the high-throughput assessment of bacterial biofilm retention on surfaces. *Journal of Combinatorial Chemistry* **2006,** *8* (2), 156-162.

49. Stafslien, S. J.; Bahr, J. A.; Daniels, J. W.; Vander Wal, L.; Nevins, J.; Smith, J.; Schiele, K.; Chisholm, B., Combinatorial materials research applied to the development of new surface coatings VI: an automated spinning water jet apparatus for the high-throughput characterization of fouling-release marine coatings. *Review of Scientific Instruments* **2007,** *78* (7), 072204.

50. Bell, E. C.; Gosline, J. M., Strategies for life in flow: tenacity, morphometry, and probability of dislodgment of two Mytilus species. *Marine Ecology Progress Series* **1997,** *159*, 197-208.

51. Burkett, J. R.; Wojtas, J. L.; Cloud, J. L.; Wilker, J. J., A method for measuring the adhesion strength of marine mussels. *The Journal of Adhesion* **2009,** *85* (9), 601-615.

52. Majumdar, P.; Stafslien, S.; Daniels, J.; Webster, D. C., High throughput combinatorial characterization of thermosetting siloxane–urethane coatings having spontaneously formed microtopographical surfaces. *Journal of Coatings Technology and Research* **2007,** *4* (2), 131-138.

53. Rittschof, D.; Orihuela, B.; Stafslien, S.; Daniels, J.; Christianson, D.; Chisholm, B.; Holm, E., Barnacle reattachment: a tool for studying barnacle adhesion. *Biofouling* **2008,** *24* (1), 1-9.

CHAPTER 5. POLYETHYLENE GLYCOL AND SILOXANE MODIFIED GLYCIDYL CARBAMATE RESINS AND THEIR PERFROMANCE AS FOULING-RELEASE MARINE COATINGS

Introduction

Marine biofouling is the undesirable settlement, attachment, and metamorphosis of aquatic species, like algae, barnacles, and mussels, on surfaces submerged in water.[1, 2] Biofouling is a time dependent process; hard foulants like barnacles and mussels will attach to the surfaces over time, irrespective of the availability of nutrients necessary for growth.[3] But, the process of biofouling can be typically explained in four main stages— 1. Formation of a conditioning layer of polysaccharides, 2. Accumulation of unicellular bacteria, 3. Settlement of algal spores and diatoms and 4. eventual attachment and growth of barnacles and mussels.[1, 4] For ships, biofouling poses many disadvantages, like an increase in drag and therefore, an increase in fuel consumption, reduction in the speed of the vessel, difficulty in maneuvering marine vessels, migration of aquatic species to non-native environments and corrosion of substrates.[1, 2, 5, 6] Not just environmental problems, combating biofouling is also an expensive affair that costs millions of dollars annually.[2, 6, 7] Historically, lead sheathing was used protect ship hulls from biofouling.[1] The lead sheathing was then replaced with anti-fouling (AF) coatings, containing tin, copper or organic biocides.[1, 8] The biocides would leach out and completely prevent the attachment of aquatic organism by killing them.[6] AF coatings were highly effective in preventing biofouling. But, toxic nature of the biocides on organisms like oysters, led to the replacement of the AF coatings with “safer” non-toxic fouling-release (FR) coatings.[2, 6] FR coatings allow formation of a weak bond between the organism and the substrate, which can then be easily broken by hydrodynamic forces.[9, 10] Commercially available FR coatings are typically made using slippery, low modulus silicone elastomers. Low mechanical strength and poor adhesion of the FR coatings make them less viable in long term marine applications.[9, 10] To address the shortcomings of the commercial FR coatings, a self-stratified siloxane-polyurethane (SiPU) system was developed in the Webster research group.[9-13] A typical coating formulation with SiPU system comprises of an isocyanate, a polyol and high MW aminopropyl terminated siloxane (APT-PDMS).[9, 10] Upon curing, the siloxane chains stratify to form the outer slippery layer, while the PU matrix provides the required mechanical strength and adhesion to the underlying substrates.[10]

Over 4000 different marine organisms have been identified, all showing different attachment mechanisms.[2] Generally, aquatic organisms secrete proteinaceous adhesives on favorable surfaces.[3] Therefore, developing surfaces that can reduce spreading of protein-rich adhesives may be beneficial to combat biofouling. Surfaces rich in polyethylene glycol have shown tendency to repel proteins.[14] PEG chains bind water molecules to the surfaces, forming a hydration layer.[15, 16] The incoming proteins cannot displace the water molecules, thereby reducing adhesion to the substrates. Hydrophilic PEG surfaces can successfully deter fouling by diatoms, unlike macrofoulants that tend to attach strongly to the hydrophilic surfaces.[17-20] Hydrophobic nature of the SiPU coatings causes slipping of the organisms from the surface of the coatings, thereby reducing the attachment of hard foulants like mussels and barnacles.[10] But, diatoms attach strongly onto hydrophobic siloxane rich surfaces.[17] Therefore, a combination of appropriate concentrations of hydrophobic and hydrophilic components is required to reduce fouling by most of the common aquatic species.

As a replacement for conventional polyurethanes, novel isocyanate-free amphiphilic glycidyl carbamate (GC) technologies are explored for potential use in marine applications. Isocyanate-free systems are aimed at reducing concerns associated with the use of isocyanates to make polyurethanes.[21, 22] GC resins can be easily synthesized using isocyanates and glycidol.[23-30] GC resins, therefore, combine mechanical strength and adhesion of polyurethanes with convenient epoxy-amine crosslinking chemistry.[23] The functional epoxy groups in GC resins can be easily crosslinked using a variety of diamine crosslinkers to form coatings with desired properties.[31] A typical formulation with GC resin consists of the carbamate resin and a diamine crosslinker. Therefore, absence of free isocyanate groups in GC coating formulations is expected to reduce hazards associated with spraying unreacted isocyanates.

In this study, attempts were made to develop amphiphilic coatings with hydrophobic or hydrophilic network chains with comb-like dangling chains of opposite polarity to the hydrophobic or hydrophilic network chains. Presence of modifiers with opposite polarities is expected to from amphiphilic surfaces that can deter most of the common fouling organisms. Over the course of this study, a number of GC resins were synthesized using isocyanate, glycidol, and mono- and difunctional PDMS and PEG modifiers. Amounts and MWs of the PDMS and the PEG modifiers were varied to alter amphiphilic nature

of the resins. Polyamine crosslinkers, Ancamine 2143 and Ancamine 2432, and polyamide crosslinkers, Ancamide 2634 and Ancamide 2767, were used to crosslink the synthesized amphiphilic resins under ambient laboratory conditions. Ratios of epoxy: AHEW (amine hydrogen equivalent weight) of the diamines was varied as 1:1 and 1:2. The resins were characterized using FTIR and NMR to confirm formation of isocyanate-free nature of the resins and determine structures of the synthesized resins. Cured amphiphilic coatings were characterized for mechanical properties, hardness, flexibility, impact strength and tensile strength. Thermal behavior of the coatings was analyzed using DSC, TGA, and DMA. Further, FR performance of the coatings against common foulants, biofilm (*C.lytica*), diatoms (*N.incerta*), microalgae (*U.linza*), mussels (*Geukensia demissa*), and barnacles (*A.amphitrite*), was evaluated. Lastly, the coatings were analyzed using contact angle experiments, ATR-FTIR, AFM, and XPS to understand topography and surface chemistries of the cured coatings.

Experimental Section

Materials

Isocyanurate of hexamethylene diisocyanate (HDI trimer), Desmodur 3300A, was provided by Covestro (Bayer MaterialScience). Both mono- and difunctional PDMS (MCR-C12-1k, DMS-C15-1k, DBE-C25-4k, DMS-C21-5k, DMS-C23-10k g/mol) and PEG (MW = 550, 600, 750, 1k, 2k g/mol) were purchased from Gelest and Sigma Aldrich respectively. Glycidol was provided by Dixie Chemicals, which was immediately refrigerated to avoid formation of impurities.[32] Catalyst dibutyltin diacetate (DBTDAc) was purchased from Sigma Aldrich. Solvents ethyl 3-ethoxypropionate (EEP), toluene, and acetone were purchased from Sigma Aldrich and VWR International. All chemicals were used as is, unless specified.

Synthesis of Amphiphilic Resins (AMP_GC Resins)

A variety of amphiphilic resins (AMP_GC) were synthesized using HDI trimer, glycidol, PDMS, and PEG. The amounts, functionality, and MWs of the PDMS and PEG components were varied as shown in Table 5.1. The amounts of PDMS and PEG were calculated based on equivalents of isocyanurate. Amounts of solvents EEP and acetone (or toluene, in the case of PDMS = 5k, 10k g/mol) were calculated such that the final resin contained a 1:1 solvent blend of EEP and acetone (toluene) and 50% theoretical solids resin. The reaction was carried out in a four-necked round bottom flask, attached with a stirrer, a condenser, a thermocouple, a nitrogen inlet, and a heating mantle. HDI trimer and

required amount of EEP solvent were first charged into the reaction flask. The difunctional component (PDMS or PEG) was then added to the flask and allowed to react with HDI trimer at 80°C for ~1 hour. After 1 hour, the monofunctional PEG or PDMS component was added to the reaction mixture with 0.020-0.025% resin solids of DBTDAc as the catalyst. The reaction was continued for another hour at 80°C. Then, temperature was reduced to 45-50°C before addition of glycidol. Lastly, glycidol solution in acetone (toluene) was added to the flask. The reaction was allowed to proceed for another 1-1.5 hours until the disappearance of NCO peak as observed using Fourier Transform Infrared Spectroscopy (FTIR). A schematic of the synthesis reaction is shown in Figure 5.1.

Table 5.1. List of the synthesized AMP_GC resins.

Resins	PDMS (g/mol)	PEG (g/mol)	% PDMS and % PEG	Comments
R1	1000 (d)	550 (m)	5, 10, 15	> 10%— resin did not crosslink
R2	1000 (m)	600 (d)	5, 10, 15	
R3	5000 (m)	1000 (d)	5	Resin did not crosslink
R4	1000 (d)	750 (m)	5, 10	
R5	4000 (d)	750 (m)	5	Resin may or may not have crosslinked
R6	1000 (d)	2000 (m)	5, 10	
R7	1000 (m)	1000 (d)	5	Resin did not crosslink
R8	5000 (d)	550 (m)	2.5, 5	> 2.5%— resin did not crosslink
R9		750 (m)	2.5	
R10		2000 (m)	2.5	
R11	10,000 (d)	550 (m)	2.5	
R12	10,000 (d)	750 (m)	2.5	Resin did not crosslink

(m), (d)— indicate monofunctional and difunctional PDMS and PEG components in the resins respectively.

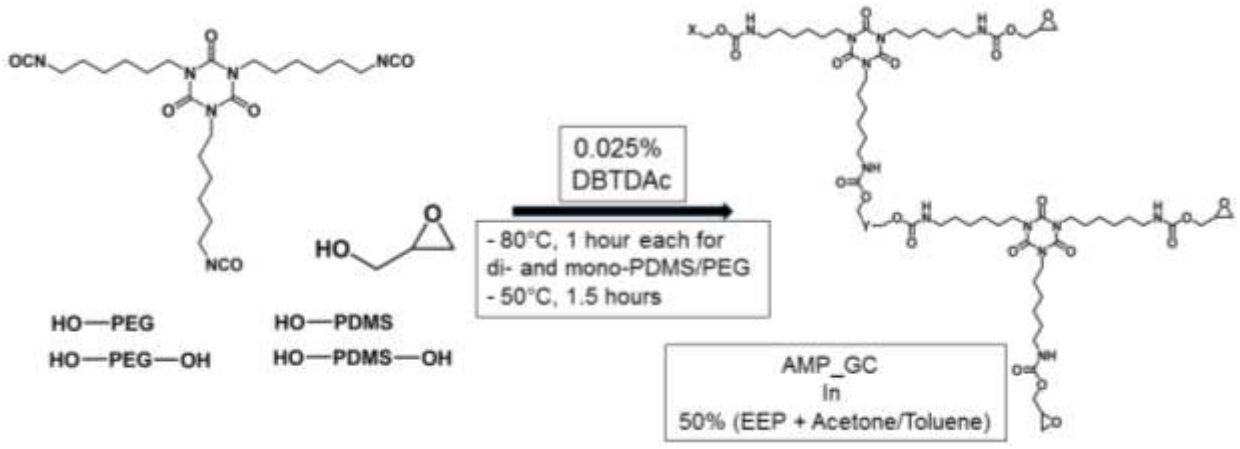

Figure 5.1. Scheme for synthesis of AMP_GC resins. X and Y in the resin structure can be PDMS or PEG depending on the functionality of the two components.

Resin Characterization

The synthesized resins were characterized using FTIR and Nuclear Magnetic Resonance spectroscopy (^{13}C-NMR). FTIR experiments were conducted using a Thermo Scientific Nicolet 8700 instrument. Small amounts of the resins were coated onto a potassium bromide (KBr) plate. 32 scans were taken for each resin sample. The result reported in this chapter is the average of 32 scans of each sample and represents FTIR spectra of all the resins. For ^{13}C-NMR, dilute sample solutions in $CDCl_3$ were analyzed using Bruker 400 NMR. Similar to FTIR, the single NMR spectrum shown in this chapter represents all the synthesized resins. To determine experimental percent solids, ~1 g of resin samples, measured accurately, was added to aluminum pans, which were heated in an oven at 120°C for 1 hour. Weights of the resins before and after heating were used to calculate experimental percent solids. An average of three replicates of each resin sample was considered to be the experimental percent solids of the respective resin. Epoxy equivalent weight (EEW) was determined experimentally according to ASTM D 1652. Accurately measured ~1 g of resin samples was added to an Erlenmeyer flask. The samples were dissolved completely in 10-15 ml chloroform. 3-4 drops of 0.1% crystal violet solution in glacial acetic acid were added as the indicator. All the resin samples were titrated against standardized 0.1 N HBr solution. Color change from violet to blue-green was considered to be the end point of titration for all samples. Average value of three titrations for each resin was considered to be experimental EEW value for the respective resin.

Coating Formulations

The AMP_GC resins were crosslinked using diamine crosslinkers, polyamines (Ancamine 2143 and Ancamine 2432) and polyamides (Ancamide 2634 and Ancamide 2767). Epoxy: AHEW ratios were varied as 1:1 and 1:2 with all the resins. All formulations were stirred using magnetic stirrers for 20 minutes, followed by sonication for 10 minutes to remove bubbles. Coatings for mechanical and thermal experiments were made using a drawdown bar with 8 mils wet film thickness. Degreased (using isopropanol) steel (purchased from Q-Lab, specifications— 3” x 6”, smooth mill finish, type QD, alloy 1008/1010), aluminum (purchased from Q-Lab, specifications— 3” x 6”, smooth mill finish, type A, alloy 3003 H14) and glass panels were used as substrates to make coatings for mechanical tests and thermal analysis experiments. Coatings for FR experiments were made by applying formulations on primed

(Intergard 264 primer) aluminum panels (purchased from Q-Lab, specifications— 4” x 8”, smooth mill finish, type A, alloy 3003 H14), using a Mayer rod (RDS 80). All the AMP_GC formulations were cured under ambient conditions for 2 weeks. Table 5.2 shows a list of formulations made using the different AMP_GC resins.

Table 5.2. List of AMP_GC resins, diamines, and curing schedules included in the study.

Resins	Amine Crosslinkers	Formulations	Curing Schedule
R1 (5,10%), R2 (5, 10%), R4, R6, R8, R9, R10, R11	Ancamine 2143	F1	RT, 2 weeks
	Ancamine 2432	F2	
	Ancamide 2634	F3	
	Ancamide 2767	F4	

Coating Characterization

Upon curing, all coatings (epoxy: AHEW = 1:1, 1:2) were characterized for their solvent resistance, hardness, flexibility, impact strength, and tensile properties. Methyl ethyl ketone (MEK) double rubs test (ASTM D 5402) was conducted to assess the chemical resistance and extent of crosslinking in the coatings. A 26-oz hammer with cheesecloth was soaked in MEK solvent. The number of double rubs that caused surface mar or loss of surface gloss or delamination were noted. König pendulum hardness (ASTM 4366) was measured and reported in seconds. Pencils with different hardness values, ranging from softest 9B to hardest 9H, were used to determine pencil hardness value of the coatings, according to ASTM D3363. The results from the test were reported as the hardest pencil that does not leave any scratch on the surface. A Gardener impact tester was used to determine reverse impact strength of the coatings (ASTM D 2794) with maximum drop height of 43 in. and a drop weight of 4 lb. The results were reported as crazing or loss of adhesion or film failure in inch–pounds (in.-lb). Coatings that did not show any failure were reported as having impact strength > 160 in.-lb. Flexibility of coatings was determined using conical mandrel bend (ASTM D 522). The results were reported as ‘no failure’ or ‘tear’ caused during experimentation. Crosshatch adhesion test (ASTM D 3359) was conducted on the coatings using a Gardco crosshatch adhesion instrument and tape. The results were reported as 5B (best) to 0B (worst), depending on the amount of film removed after the tape was ripped off. Coatings with epoxy: AHEW = 1:1 were analyzed using Instron 5542 tensile test instrument. Samples were prepared according to ASTM D 882 and rate was maintained at 5 mm/min at room temperature. Young’s Modulus and elongation at break for the coatings were recorded.

For thermal analysis experiments, free coating films were carefully peeled from glass substrates. Due to their superior overall performance (mechanical properties and appearance), only formulations with epoxy: AHEW = 1:1 were analyzed using thermal analysis experiments. A TA Instruments Q1000 Differential Scanning Calorimeter (DSC) system was used to determine glass transition temperature (T_g°C) of all the AMP_GC coatings. 5-8 mg samples were subjected to heat-cool-heat cycle at heating and cooling rates of 10°C/min and 5°C/min respectively. Temperature was maintained in the range between -20°C to 250°C for all the samples. The temperature of the inflection at the mid-point for each sample in the second heating cycle was recorded as T_g. Thermal degradation behavior of the cured coatings was determined using a TA Instruments Q500 Thermogravimetric Analysis (TGA) system. Samples were heated up to 800°C at a heating rate of 10°C/min. Onset of thermal degradation for each coating was recorded as the temperature at 5% weight loss ($T_{d\,5\%}$°C). A TA Instruments Q800 Dynamic Mechanical Analysis (DMA) instrument was used to determine crosslink density (v_e mol/L), tan delta, and storage modulus (E' MPa) of the cured coatings. Poisson's ratio was maintained at 0.44 for all the coatings. The experiment was conducted in the temperature range from -20°C to 200°C, with heating rate of 5°C/min and 1 Hz frequency. v_e was calculated using E' values in the rubbery plateau region, 60°C above the glass transition temperature (T_g), using the equation, $E' = 3v_eRT$, where, E'= storage modulus (Pa); v_e = crosslink density (mol/L); R= gas constant (8.314 J/K/mol); T= (T_g + 60°C + 273) K.

Laboratory Biofouling Assays

Preleaching and Leachate Toxicity Analysis

FR experiments were conducted on AMP_GC coatings with epoxy: AHEW = 1:1. Prior to the laboratory FR tests, all the coatings were placed in a recirculating water tank for six weeks to remove toxic leachates, impurities, unreacted monomers, and tin catalyst.[33] After six weeks, algal solution in artificial sea water (ASW) with nutrients was introduced onto the coatings to test leachate toxicity. Fluorescence was used to observe the growth of algae on the coatings after 48 hours. The growth of the organisms on the coatings was reported as a fluorescence ratio to a positive growth control. A negative growth control (medium+ bacteria+ triclosan) was also included in the experiment. The algal growth on the AMP_GC coatings was compared to the negative control to confirm non-toxicity of the coatings.[9] For all FR tests, except microalgae *U.linza*, FR performance of the AMP_GC coatings was compared to

commercial standards, Intersleek 700 (I-700), Intersleek 900 (I-900), Intersleek 1100SR (1100SR), Silastic T2 (T2), and a regular polyurethane (PU— no siloxane) coating. For FR test against microalgae, T2 and polystyrene coatings were used as standards and control.

Diatom Navicula incerta (N.incerta) Attachment and Removal

Diatom *N.incerta* adhesion was carried as explained in earlier publications.[9, 12, 34-36] 24-well plates were prepared by carefully punching out discs from all the coatings. The discs were then glued to the well plates using a silicone adhesive from Dow Corning, such that the glue covered the circular basal area completely. The plates were then treated with 1 ml solution of algae in ASW and incubated for 2 hours to allow diatom adhesion. The settlement of diatoms on the coatings was quantified using fluorescence. After 2 hours, the well plates were subjected to water jet at 10 psi and 20 psi for 10 seconds to determine release of diatoms from the coatings. The first column in each well plate was used as a reference for the initial cell settlement and was not subjected to water jet. In this study, the diatom attachment on the AMP_GC formulations and the percent removal at 20 psi are reported. Equipment anomaly at 10 psi water jet pressure resulted in insufficient removal of diatoms.

Biofilm Cellulophaga lytica (C.lytica) Adhesion and Removal

Bacterial biofilm *C.lytica* adhesion test was carried out in a fashion similar to diatom attachment.[9, 37-39] Briefly, crystal violet colorimetry was used to determine *C.lytica* retention on the cured coatings. Circular discs were carefully punched from all the amphiphilic coatings. The discs were glued to the plates using a silicone adhesive from Dow Corning. 5% suspension of *C.lytica* in ASW (10^7 cells/ml) with nutrients was prepared. 1 ml suspension was dispensed in each well. The plates were incubated for 24 hours at 28°C to allow colonization of the biofilm on the coatings. The plates were rinsed three times with deionized water to remove unattached biofilm. Crystal violet was used to stain the samples. Extractions of crystal violet in acetic acid (33%) were observed under 600 nm absorbance to determine amount of biofilm retained on the coatings. After 24 hours, the wells were subjected to water jets at 10 psi and 20 psi for 5 seconds.[40] The first column in each 24-well plate served as a reference for bacterial growth before water jetting and was not exposed to water jet. The final results were reported as amount of the biofilm adhesion on the coatings and the percent removal of the biofilm from the coating surface at 10 psi and 20 psi water jet pressures.

Microalgae Ulva linza (U.linza) Attachment and Removal

Similar to diatoms and biofilm, select AMP_GC coatings were analyzed for FR performance against microalgae. Circular discs were punched from the select coatings and glued to 24-well plates using a silicone adhesive from Dow Corning. The plates were then shipped to Newcastle University for laboratory microalgae *U.linza* attachment and release experiment. Prior to the experiment, the assay plates were equilibrated in 0.22 µm seawater for 2 hours. Then, 1 ml *U.linza* sporelings suspension (3.3 x 10^5 spores/ml) in enriched sea water was dispensed into each of the wells. The spores were grown in an illuminated incubator at 18°C for 6 days. After 6 days, the biomass from a single row of wells (6 wells) was assessed by extracting chlorophyll. Chlorophyll was extracted in 1 ml DMSO. Fluorescence was then determined using excitation of 360 nm and wavelength of 670 nm. To determine the release performance of the coatings, individual row of wells from each plate was sprayed using a spinjet apparatus at 18, 67, 110 kPa water pressure. Chlorophyll was again extracted, as explained earlier. The removal at each pressure was determined by comparing the sprayed and the unsprayed wells. The results were reported as the percent removal of the sporelings after exposure to water jet. In this paper, only microalgae removal at 110 kPa is shown. 18 and 67 kPa water pressure resulted in less than 5% removal of the microalgae.

Mussel Geukensia demissa Adhesion

Select amphiphilic coatings were evaluated for adhesion of marine mussels *Geukensia demissa*, according to a previously published procedure.[41-43] Before the experiment, each marine mussel (received from Duke University Marine Laboratory, North Carolina, USA) was fitted with a 4 cm long acetal rod, using a 3M acrylic adhesive. The rods were attached perpendicular to the ventral edge of the mussel. Six mussels were immobilized on the coatings, using a custom designed PVC template. The select coatings were placed in ASW so that the mussels can be fed live marine phytoplankton for 3 days. After 3 days, the number of mussels showing attachment of byssus threads was recorded for each coating. The acetal rods on the mussels were attached to a tensile force gauge, such that all the mussels were pulled from the coating at the same time. The results were reported as the average force (Newtons) required to completely detach all byssus threads of the mussels from the surface.

Adult Barnacle Amphibalanus amphitrite (A.amphitrite) Adhesion

Select amphiphilic coatings were also analyzed for barnacle adhesion to determine their FR performance against barnacles.[9, 44, 45] Six adult *A.amphitrite* barnacles, with basal diameter of approximately 5 mm, were allowed to grow and attach to the select coatings for 2 weeks. The barnacles were fed brine shrimp nauplii in ASW for 2 weeks. After 2 weeks, a hand held digital gauge was used to measure the force required to detach the barnacles in shear from the coatings. Adhesion strength (MPa) of the barnacles was then calculated as the shear force required for barnacle removal to the basal area of the barnacle.

Surface Characterization

Select pre-leached AMP_GC coatings were characterized using contact angle, Attenuated Total Reflectance Fourier Transform Infrared Spectroscopy (ATR-FTIR), Atomic Force Microscopy (AFM), and X-Ray Photoelectron Spectroscopy (XPS) to study surface chemistry and topography of the coatings and understand their effect on FR performance. A First Ten Angstroms (FTA 125) system was used to measure dynamic changes in water contact angles (WCA) by sessile drop method. A single droplet was carefully dispensed onto each coating. WCA measured immediately after the droplet was dispensed was recorded as WCA at 0 minutes. Thereafter, WCAs for each coating were measured every 10 minutes for 30 minutes. The contact angles were analyzed using FTA software.

A Thermo Scientific Nicolet 8700 instrument, with iTR diamond crystal plate attachment, was used to conduct ATR-FTIR on the AMP_GC coatings. 32 scans were taken for each coating sample. The spectra shown in this chapter are the average of the 32 scans.

Surface topography of select coatings was analyzed using AFM. 20 µm x 20 µm areas of the select coating surfaces were scanned using a Dimension 3100 Microscope system with Nanoscope controller and a silicon probe (spring constant = 0.3-0.8 N/m, resonant frequency = 20-40 kHz) in tapping mode in air under ambient laboratory conditions.

Lastly, chemical composition of the select AMP_GC coatings were determined using a Thermo Scientific K-Alpha XPS with monochromatic Al K_α X-ray source (1468.68 eV) and 8000 eV Ar^+ ion source gun. Prior to analysis, the coatings were exposed to 8000 eV MAGCIS Ar^+ ion cluster gun for 60 seconds to remove impurities. Three survey spectra were collected at a low resolution with constant pass energy

of 200 eV at energy increment of 1.000 eV/step for 10 microseconds. Further, ten high resolution scans were collected per sample with energy increment of 0.100 eV/step for 50 microseconds and pass energy of 50 eV, such that the laser was perpendicular to the coating surfaces. Atomic concentrations of individual elements, C1s, O1s, and N1s were determined by integrating area under the peaks. Both surface etching and high resolution experiments were conducted at ambient laboratory temperature. Chamber pressure was maintained below 1.5 x 10^{-7} Torr at all times.

Results and Discussion

In an attempt to deter biofouling by common aquatic organisms, novel isocyanate-free amphiphilic resins (AMP_GC resins), synthesized using isocyanurate of HDI, glycidol, and hydrophobic PDMS and hydrophilic PEG modifiers, were explored to make viable FR surfaces. The amounts, MW, and functionality of PDMS and PEG were varied to make AMP_GC resins with varying amphiphilic character. During the first stage of synthesis, the difunctional component (PDMS or PEG) reacts with isocyanate groups from HDI trimer molecules. Since equivalents of isocyanurate are 10 to 20 times higher than equivalents of hydroxyl groups from PDMS or PEG components, the probability of reaction between hydroxyl groups from the same chain and isocyanate groups from the same isocyanurate molecule is low. Therefore, statistically, the synthesized resins contain higher concentration of PDMS or PEG “bridges” formed due to reaction between the difunctional components with isocyanate groups from two different HDI trimer molecules, rather than “loops”. Properties of the modified GC coatings will be affected by amount and MW of the difunctional components since the bridges form a part of the coating matrix. Self-stratification of the difunctional component is expected to form polar or non-polar domains on the surface of the coatings, depending on the polarity of the bridges. Monofunctional PEG or PDMS components provide a comb-like architecture to the coatings. Since the monofunctional components are bound to the coating matrix on one end only, freedom of movement of the “combs” is higher than that of the bridges. Movement of the “combs” is expected to disallow organisms from bonding strongly with the coating surfaces. Combination of polar and non-polar components in the same resin necessitated incorporation of solvent blends of EEP and acetone or toluene to compatibilize all the components of the resin. Initial experiments to determine minimum amount of the solvent blend showed that 50% total solvent content provided the best viscosity for successful completion of synthesis and application of coating formulations.

All the resins were synthesized such that the final resins contained 1:1 w/w EEP: acetone (toluene) and experimental values of percent solids was found to lie in the range between 48-50%. The synthesized resins were characterized using FTIR to determine completion of the synthesis reaction. FTIR spectra of all the resins showed disappearance of the isocyanate peak at 2272 cm^{-1}, confirming formation of isocyanate-free resins (Figure 5.2). Moreover, peaks at 910 cm^{-1},1050 cm-1, and 1280 cm^{-1} wavenumbers were indicative of epoxy rings, PDMS and PEG chains within the resins. Wavenumbers at 1680 cm^{-1} and 1750 cm^{-1} indicated carbonyl bonds from the carbamate linkages (-C=O*) and isocyanurate of HDI (-C=O**) respectively. All the synthesized resins were also characterized using ^{13}C-NMR (Figure 5.3). Peak at 149 ppm was indicative of the formation of -NH-CO- linkages. Chemical shifts for C atoms at 1 ppm, 44 and 49 ppm, and 60 ppm and 70 ppm indicated C atoms from PDMS modifier, epoxy rings, and PEG chains in the resins respectively. Table 5.3 shows the experimental values for EEW for all the synthesized AMP_GC resins. EEW of the AMP_GC resins lied in the range between 400 ± 100 g/eq. EEW values increased with increasing amounts and MW of PDMS and PEG components. Increasing PDMS and PEG content in the resins decreased the number of epoxy groups available for crosslinking.

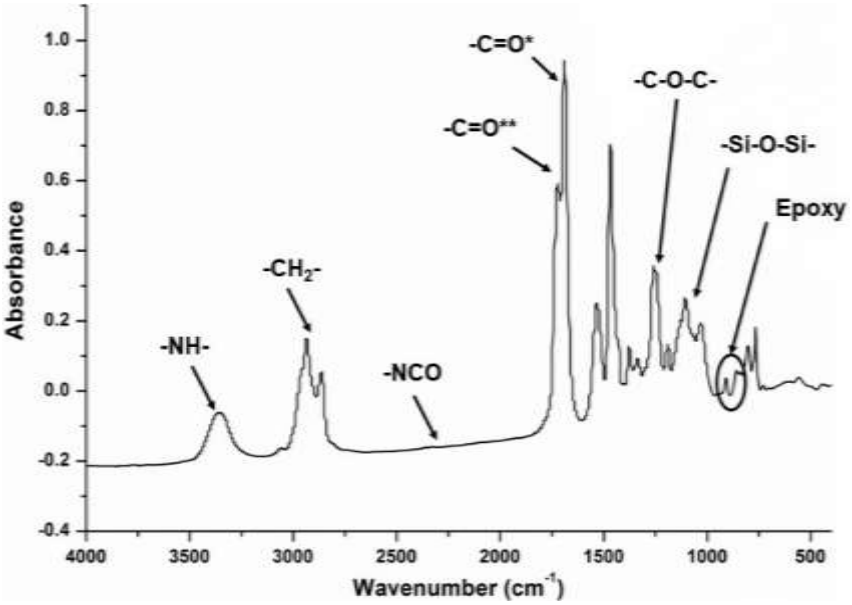

Figure 5.2. Representative FTIR spectrum for the AMP_GC resins.

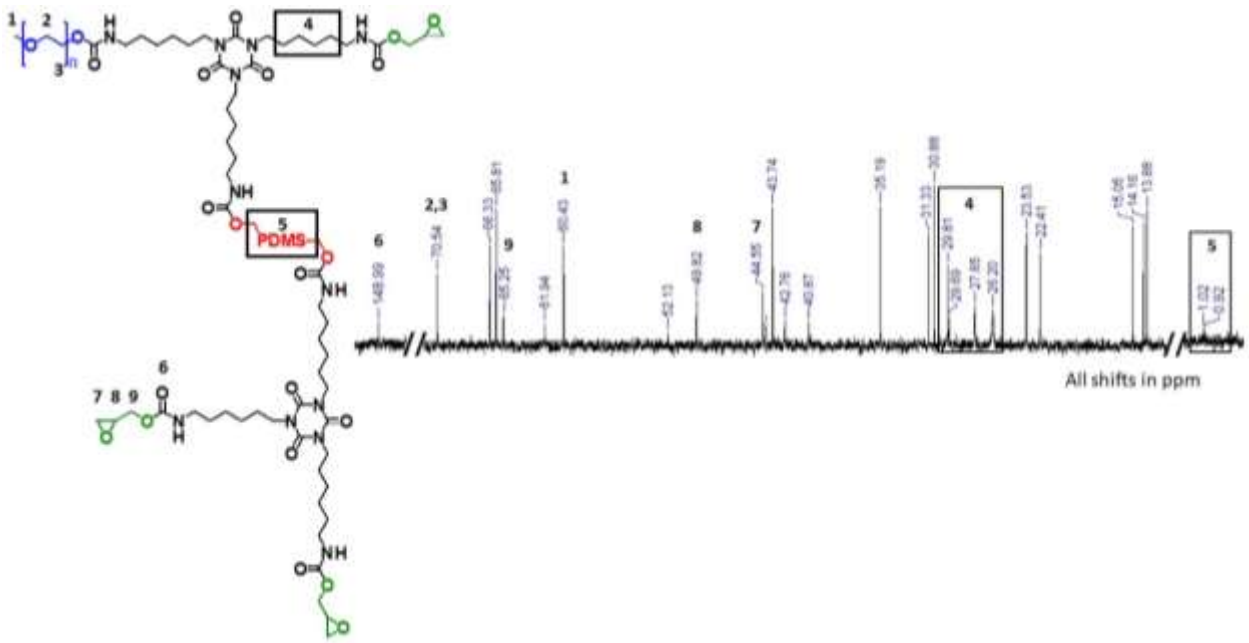

Figure 5.3. Representative ^{13}C-NMR spectrum for the AMP_GC resins.

Table 5.3. Experimental EEW values for the different amphiphilic GC resins.

Resins	% PDMS and % PEG	EEW (g/eq.)
R1	5	356.49
	10	460.65
R2	5	370.86
	10	471.63
R4	5	365.98
R6	5	435.70
R8	2.5	335.74
R9	2.5	354.00
R10	2.5	401.35
R11	2.5	425.92

Four diamines— Ancamine 2143 and Ancamine 2432 (polyamines) and Ancamide 2634 and Ancamide 2767 (polyamides) were used to crosslink the synthesized AMP_GC resins. (Table 5.2). Formulations were made by changing epoxy: AHEW ratios as 1:1 and 1:2. All the formulations were cured under ambient conditions for 2 weeks. Formulations with R2_5% and R2_10% resins were extremely difficult to crosslink. Upon addition of the amine crosslinkers, formation of white agglomerates was observed in the formulation vials with the two R2 resins. But, continuously stirring the formulations resulted in breakdown of the agglomerates, eventually forming clear and translucent solutions in the formulation vials. Labels for the coatings are of the format: resin label from Table 5.1_formulation from Table 5.2.

Upon curing, the AMP_GC coatings (epoxy: AHEW = 1:1, 1:2) were characterized for their solvent resistance, hardness, flexibility, impact strength, and tensile strength. Dry film thicknesses of all the coatings lied in the range between 55 ± 15 µm. Crosshatch adhesion value of 4B-5B (best) for all the coatings showed that the AMP_GC coatings exhibited excellent adhesion to bare substrates. Table 5.4 shows results obtained from mechanical characterization of the coatings. MEK double rubs > 400 were achieved for most of the coatings with R1, R2, R4, and R6 resins, indicating coatings with excellent solvent resistance. But, MEK double rub values dropped slightly for coatings with higher MW (5k-10k) PDMS modifier. For resins R8-R11 (PDMS = 5k-10k), coatings with Ancamine 2432 and Ancamide 2767 showed MEK double rub between 300 to > 400. Among all the coatings, coatings with R10 resin showed the lowest average MEK double rub. Drop in solvent resistance of the coatings may be attributed to presence of comparatively higher unreacted groups within the coating matrix. Most of the cured exhibited good hardness, good flexibility, and impact resistance. Formulations cured using Ancamine 2143 and Ancamide 2634, irrespective of the resins, showed the highest König pendulum hardness, except R2 resin. Cycloaliphatic nature of Ancamine 2143 and Ancamide 2767 provided rigidity to the formulations, imparting higher surface hardness (König pendulum). On the other hand, aliphatic chains of Ancamine 2432 and Ancamide 2767 increased softness of the matrices in formulations cured using the aliphatic diamines. For R2_5% and R2_10% resins, Ancamide 2767 resulted in coatings with highest hardness. Coatings with resin R11 showed the highest average hardness of ~120 seconds, while coatings with R2 showed lowest average hardness of ~65 seconds. R1_5%, R1_10%, and R4 coatings exhibited highest pencil hardness values between 6H-9H. With increasing MW of PDMS, the pencil hardness values dropped to 8B-4H. R2_10% showed lowest pencil hardness values of 8B with the polyamines to 4B with the polyamides. Unrestricted movement of monofunctional PDMS in the coating matrices may have allowed higher chain movement, thereby causing softening of the coatings. Elastomeric nature of the soft films made the films susceptible to damage by softer pencils. For coatings with R6 resin, formation of separate surface domains with high MW PEG-2k and PDMS-1k may be responsible for lower pencil hardness of the resultant coatings. Although the R6 coatings showed MEK double rubs > 400, separation of PEG and PDMS phases within the matrices may have made the R6 coatings susceptible to impact. Visually, all the coatings appeared smooth and glossy, except coatings with R6 coatings. Similarly, higher

EEW of R10 and R11 resins (lower reactive epoxy groups), lower MEK double rub values (more unreacted groups), but high König pendulum hardness depending on the amine crosslinker resulted in poor flexibility and poor impact strength of the cured coatings.

Young's modulus of coatings cured using Ancamine 2432 and Ancamide 2767 with 1:1 epoxy: AHEW was determined using Instron testing instrument (Figure 5.4). For resins R1_5% and R11, Ancamide 2767 resulted in coatings with higher modulus as compared to Ancamine 2432; for resins R4, R8, and R9, Ancamine 2432 coatings exhibited higher modulus compared to Ancamide 2767. R4_F2 exhibited highest modulus of 678 MPa, while R2_10%_F2 appeared to show lowest stiffness. Stiffer coatings (higher modulus) showed lower elongation at break, with R11_F2 showing lowest elongation of 0.12 mm. For coatings R1_10%_F4, R2_F2, R2_10%_F4, R6 coatings, and R10_F4, defect-free films of sufficient length could not be prepared. The AMP_GC formulations showed significantly higher modulus as compared to the commercially available silicone elastomer based FR coatings (~5 MPa).

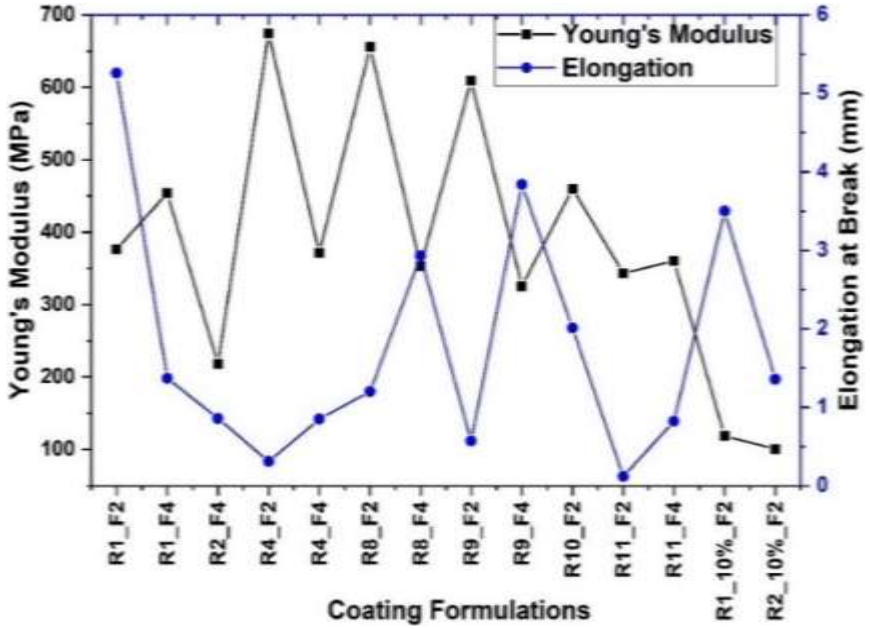

Figure 5.4. Young's modulus and elongation at break of the AMP_GC coatings cured using Ancamine 2432 and Ancamide 2767.

Table 5.4. Mechanical test results for AMP_GC coatings with epoxy: AHEW = 1:1.

Resins	Amines	Labels	MEK Double Rubs	König Pendulum Hardness (s)	Pencil Hardness	Impact Strength (in.-lb)	Mandrel Bend*	60° Gloss
R1_5%	Anc.2143	F1	>400	115	9H	>160	NF	126.33
	Anc.2432	F2	>400	84	8H	>160	NF	114.00
	And.2634	F3	162	119	7H	149	NF	125.00
	And.2767	F4	>400	80	8H	>160	NF	76.63
R1_10%	Anc.2143	F1	>400	118	6H	>160	NF	134.33
	Anc.2432	F2	>400	104	8H	>160	NF	159.00
	And.2634	F3	>400	82	7H	>160	NF	149.33
	And.2767	F4	>400	109	7H	>160	NF	137.33
R2_5%	Anc.2143	F1	>400	64	4H	31	Tear	142.00
	Anc.2432	F2	>400	103	3H	>160	NF	134.67
	And.2634	F3	>400	93	2H	>160	NF	131.33
	And.2767	F4	>400	101	2H	>160	NF	107.03
R2_10%	Anc.2143	F1	60	45	8B	39	Tear	88.03
	Anc.2432	F2	48	39	8B	63	Tear	141.87
	And.2634	F3	>400	76	4B	>160	NF	135.00
	And.2767	F4	>400	103	4B	>160	NF	100.63
R4_5%	Anc.2143	F1	>400	118	9H	129	NF	108.33
	Anc.2432	F2	>400	84	8H	>160	NF	99.90
	And.2634	F3	16	98	8H	>160	NF	106.00
	And.2767	F4	>400	80	8H	>160	NF	62.87
R6_5%	Anc.2143	F1	>400	91	B	70	NF	17.47
	Anc.2432	F2	>400	69	F	86	NF	25.60
	And.2634	F3	>400	74	B	12	NF	33.07
	And.2767	F4	>400	72	B	>160	NF	15.63
R8_2.5%	Anc.2143	F1	300	106	F	157	NF	60.20
	Anc.2432	F2	>400	87	5H	157	NF	89.00
	And.2634	F3	300	131	4H	>160	NF	93.50
	And.2767	F4	>400	91	5H	>160	NF	93.60
R9_2.5%	Anc.2143	F1	>400	104	3H	>160	NF	76.00
	Anc.2432	F2	>400	97	4H	149	NF	92.50
	And.2634	F3	350	115	4H	>160	NF	95.50
	And.2767	F4	>400	86	4H	>160	NF	90.70
R10_2.5%	Anc.2143	F1	200	95	4H	4	NF	66.50
	Anc.2432	F2	300	112	6H	98	NF	83.60
	And.2634	F3	50	97	2B	16	NF	35.70
	And.2767	F4	200	90	2B	4	NF	38.70
R11_2.5%	Anc.2143	F1	200	115	HB	12	Tear	82.50
	Anc.2432	F2	>400	110	F	31	NF	80.40
	And.2634	F3	300	133	HB	39	NF	82.70
	And.2767	F4	>400	127	B	39	NF	88.40

*NF indicates no failure in the coating film.

Figure 5.5 shows DSC scans for the AMP_GC coatings with epoxy: AHEW = 1:1. T_g values for all the coatings was between 40-85°C. Average T_g of coatings cured using the polyamines was higher than the polyamide cured coatings. Among the polyamines, Ancamine 2143 resulted in coatings with higher T_g than Ancamine 2432; among the polyamides, Ancamide 2634 resulted in coatings with higher T_g than Ancamide 2767. For R1 and R2 resins, T_g values dropped by 15-20°C with increasing the amount of PDMS and PEG from 5% to 10%. Increasing the amount of the PDMS or PEG modifier may have allowed higher movement of chains within the matrix due to presence of higher concentration of soft network chains and dangling chain ends. 8-12°C increase in T_g for R2_5% compared to R1_5% coatings may be due to presence of monofunctional PDMS chains present in R2_5% coatings. DSC scans for coatings with resins R6 and R10, which contain difunctional PDMS = 1k and 5k respectively and monofunctional PEG = 2k, showed formation of crystalline phases in the bulk of the films. Melting peaks at ~50°C for all the coatings with R6 and R10 indicated formation of PEG rich crystalline zones after crosslinking. Crystallinity of the coatings was responsible for high hardness yet poor impact resistance and low gloss of the R6 and R10 coatings as seen from Table 5.4. Additionally, secondary transitions between 60-85°C were observed for R10 coatings, indicating a second transition or T_g of the R10 coatings.

(a)

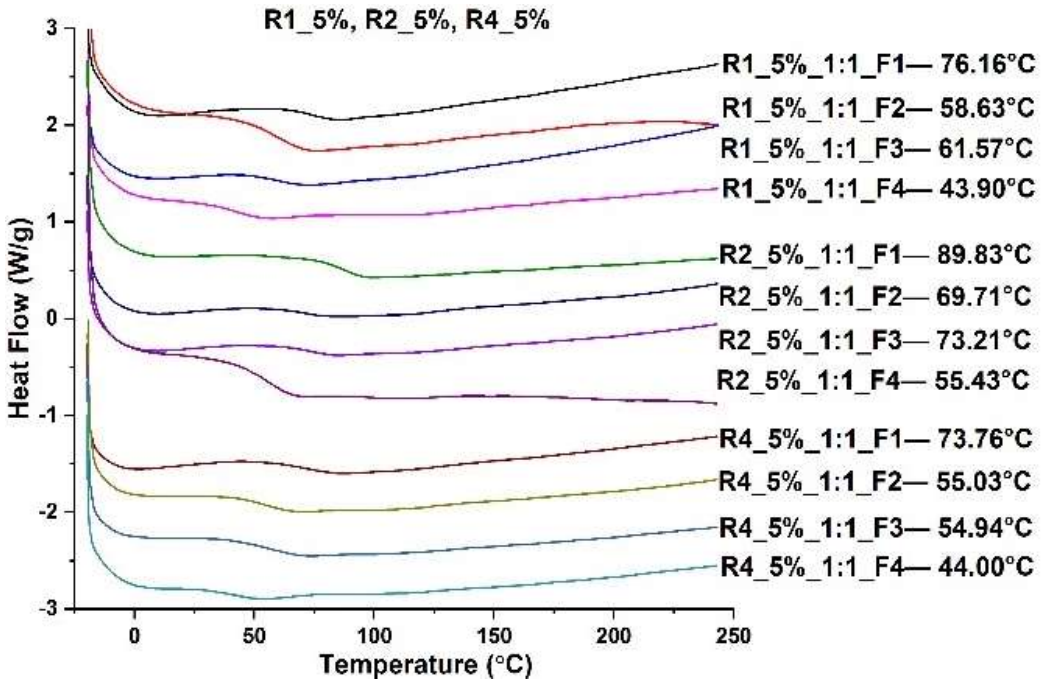

Figure 5.5. Glass transition values from DSC for coatings with (a) R1_5%, R2_5%, and R4, (b) R1_10%, and R2_10%, (c) R8, R9, and R11, and (d) R6, and R10 resins with epoxy: AHEW = 1:1.

(b)

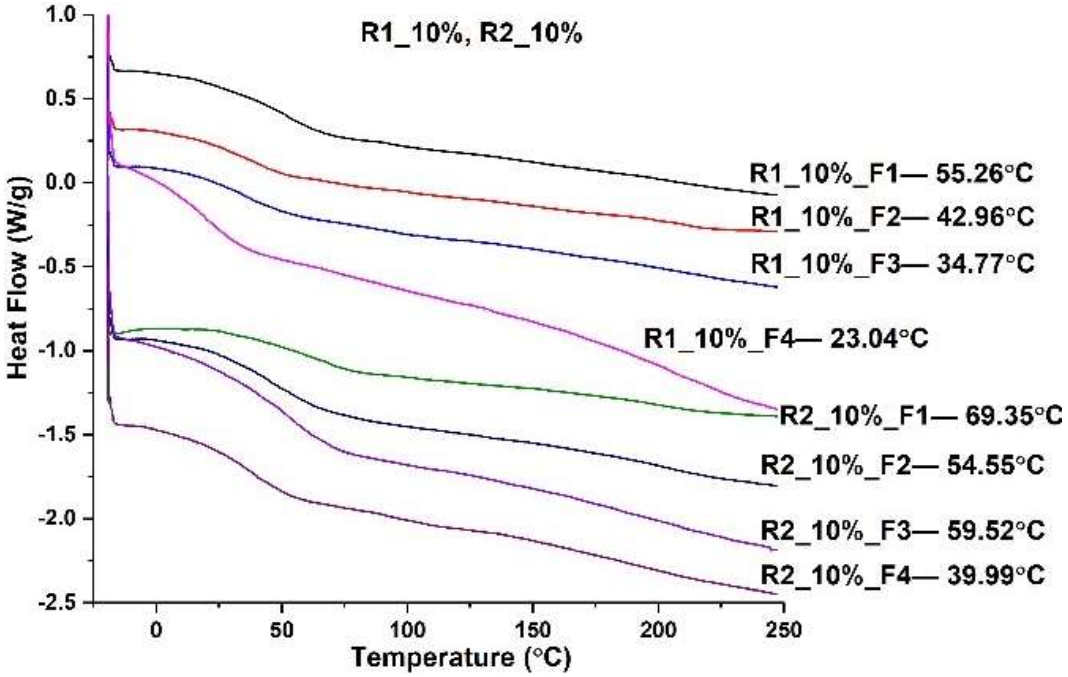

(c)

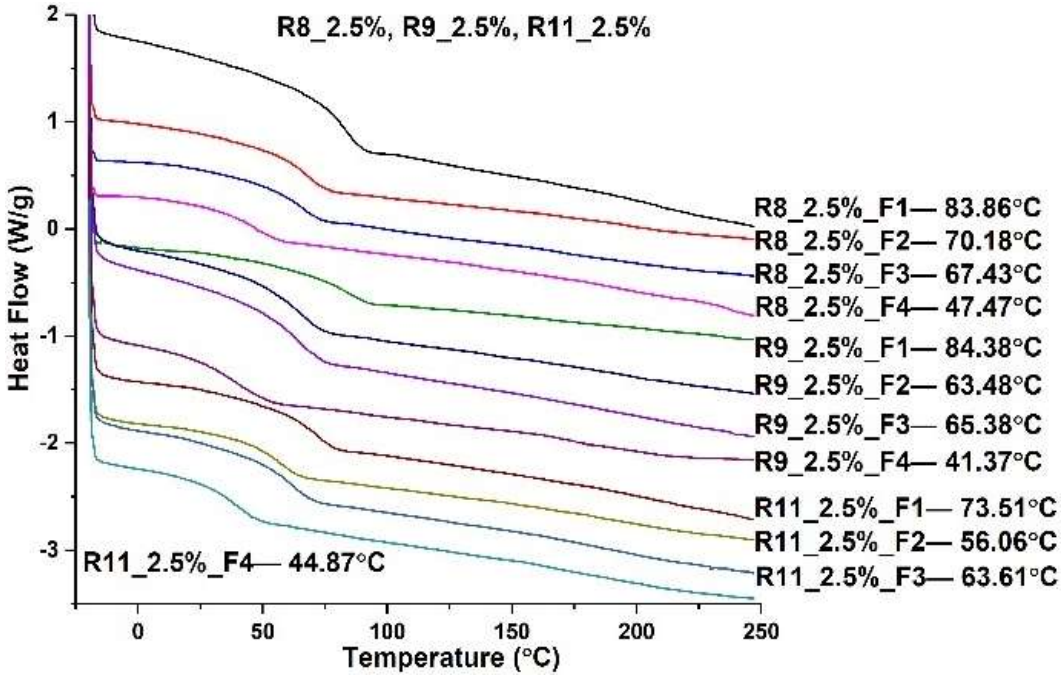

Figure 5.5. Glass transition values from DSC for coatings with (a) R1_5%, R2_5%, and R4, (b) R1_10%, and R2_10%, (c) R8, R9, and R11, and (d) R6, and R10 resins with epoxy: AHEW = 1:1 (continued).

(d)

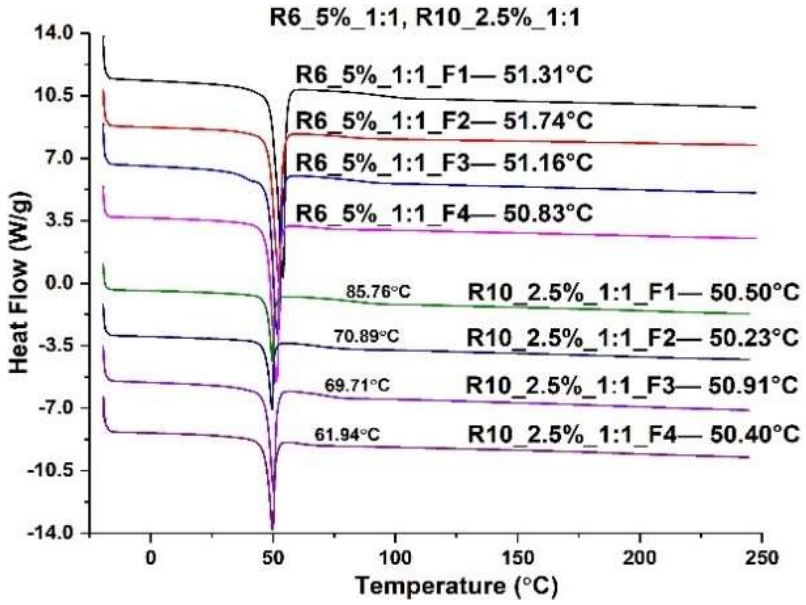

Figure 5.5. Glass transition values from DSC for coatings with (a) R1_5%, R2_5%, and R4, (b) R1_10%, and R2_10%, (c) R8, R9, and R11, and (d) R6, and R10 resins with epoxy: AHEW = 1:1 (continued).

Figure 5.6 shows thermal degradation behavior of the AMP_GC coatings with epoxy: AHEW = 1:1. For coatings with R1-R6 resins, onset of degradation ($T_{d\,5\%}$°C) lied between 225-240°C. Increasing the amount of PDMS and PEG from 5% to 10% for R1 and R2 resins increased $T_{d\,5\%}$ slightly to 250°C (Figure 5.5(b)). But, increasing the MW of the PDMS modifier from 1k to 5k-10k resulted in drastic decrease in $T_{d\,5\%}$ (120-150°C) (Figure 5.5(c)). Coatings with R8, R9, and R11 also showed the highest initial weight loss among all the coatings, which may be attributed to presence of residual solvents in the coatings. A linear drop in weight with temperature between 400-475°C was observed for the R1-R6 coatings.

(a)

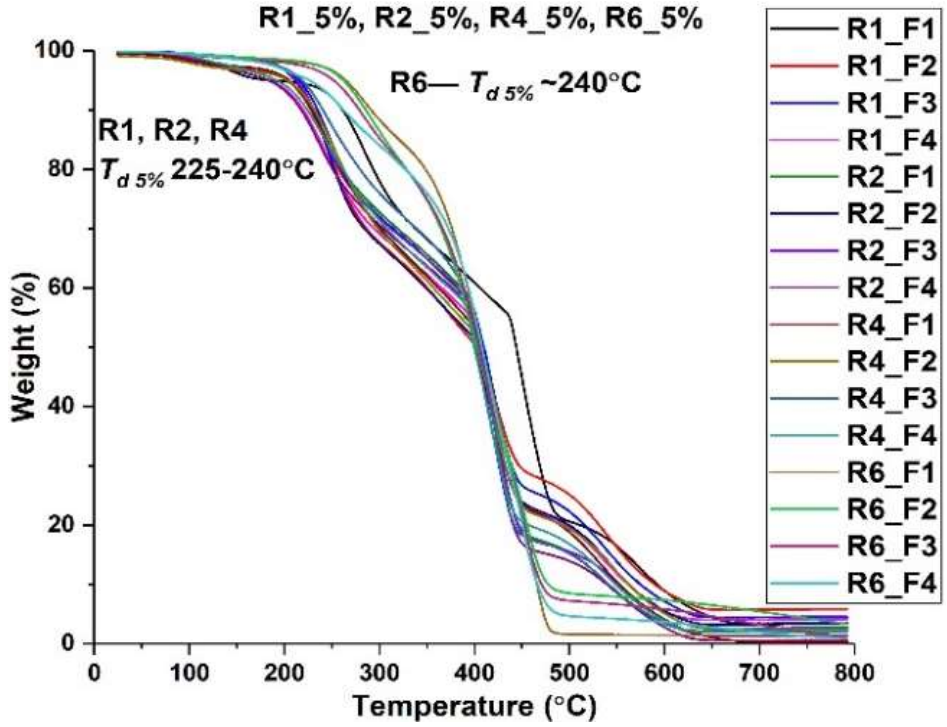

(b)

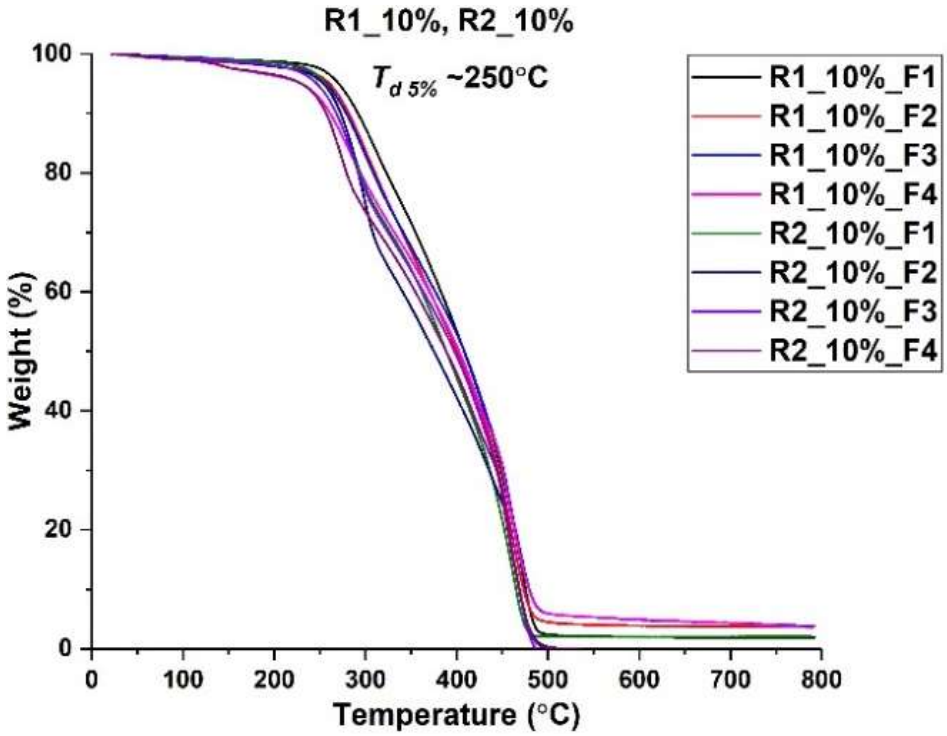

Figure 5.6. TGA plots for coatings with (a) R1-R6, (b) R1_10%, and R2_10%, and (c) R8-R11 resins with epoxy: AHEW = 1:1.

(c)

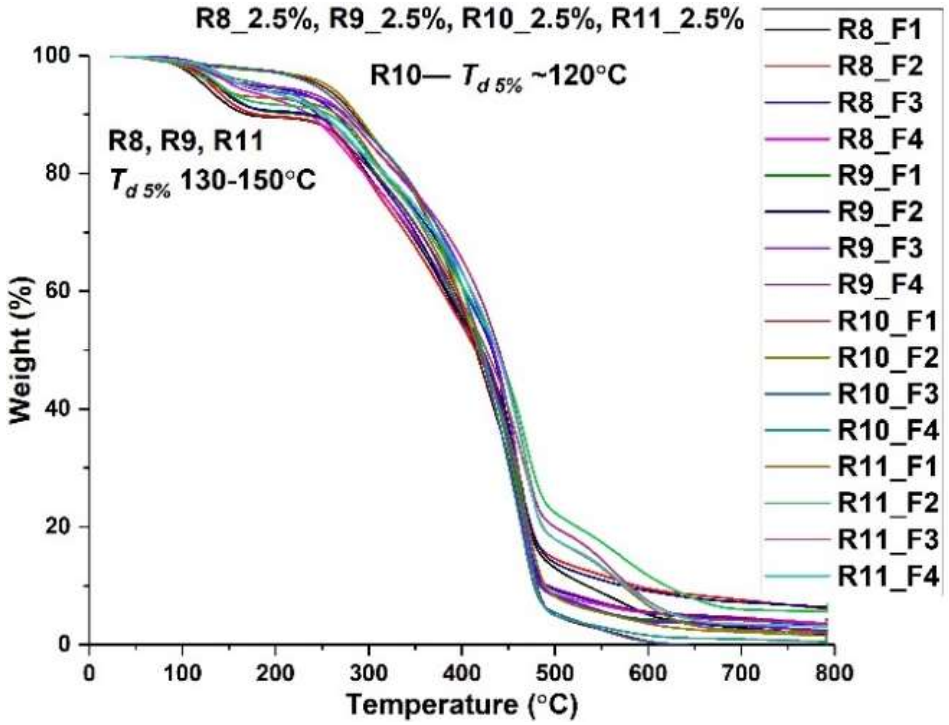

Figure 5.6. TGA plots for coatings with (a) R1-R6, (b) R1_10%, and R2_10%, and (c) R8-R11 resins with epoxy: AHEW = 1:1 (continued).

Figure 5.7 shows tan delta curves for AMP_GC coatings with epoxy: AHEW = 1:1. Narrower tan delta peaks for most of the coatings, except R1_10% and R2_10%, indicated homogeneous nature of the crosslinked coatings. Minor broad peaks in the low or high temperature zones indicated presence of secondary softer PDMS/PEG rich phases or harder GC phases in the coatings respectively. Unlike DSC, for most of the resins, the polyamides resulted in coatings with slightly higher T_g values compared to the polyamines. T_g of the AMP_GC coatings lied in the range between 70-100°C, with coatings with R2_5% exhibiting highest average T_g of ~95°C, probably due to presence of PEG "bridges" in the coating networks. Table 5.5 shows storage modulus (E' GPa) at 25°C and crosslink density (v_e mol/L) for the AMP_GC coatings. Most of the coatings exhibited high E' at 25°C and v_e, except R2_10% coatings which showed average E' = 0.10 GPa and average v_e = ~0.47 mol/L. Monofunctional PDMS in R2 resin may have increased free volume in the coating networks, decreasing the density of network junctions within the matrix. Similarly, increase in MW of PDMS and PEG increased distance between network junctions, thereby increasing free volume of the crosslinked coatings and decreasing v_e. Coatings with epoxy: AHEW = 1:2 were also analyzed using DMA (not shown here). The results showed that T_g values for

coatings with 1:2 ratio were 20-30°C lower than 1:1 ratio. Moreover, v_e also dropped significantly with increasing amount of the amine crosslinkers, due to incomplete formation of coating networks.

(a)

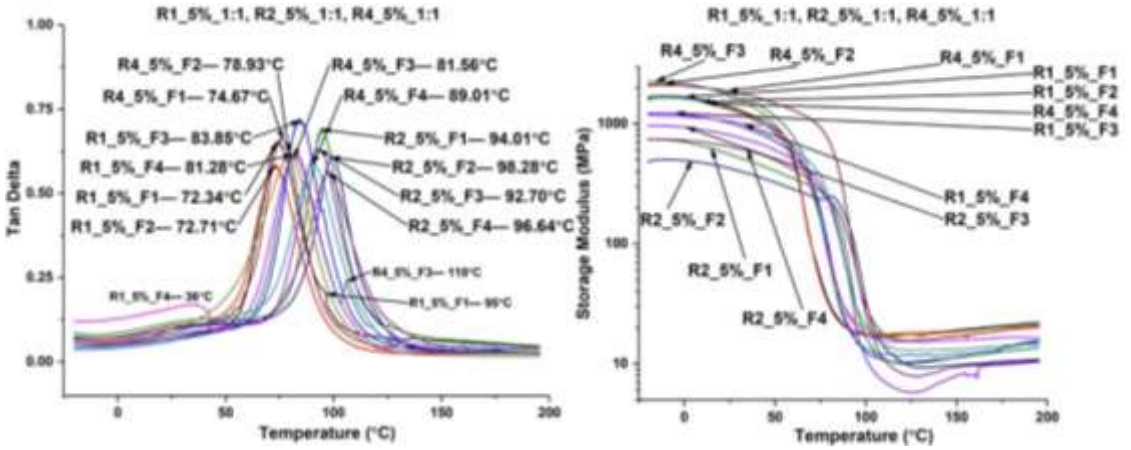

(b)

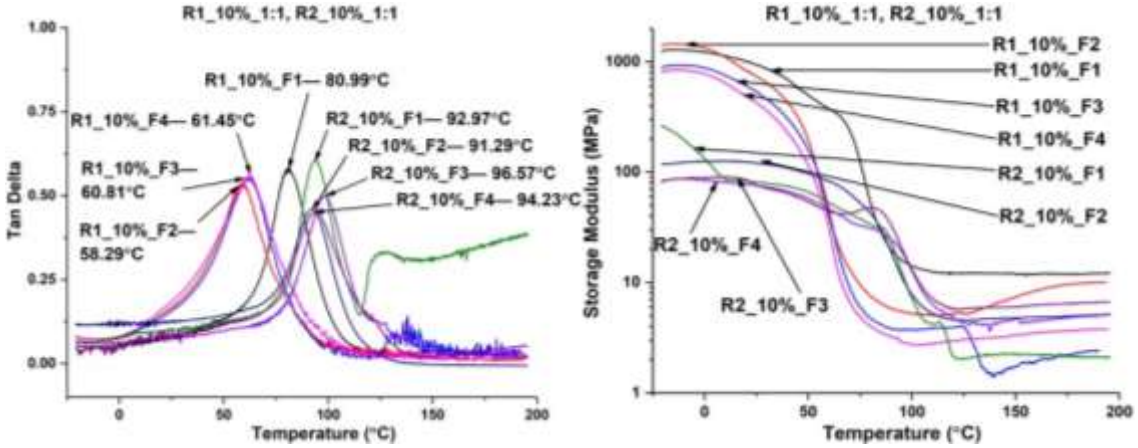

(c)

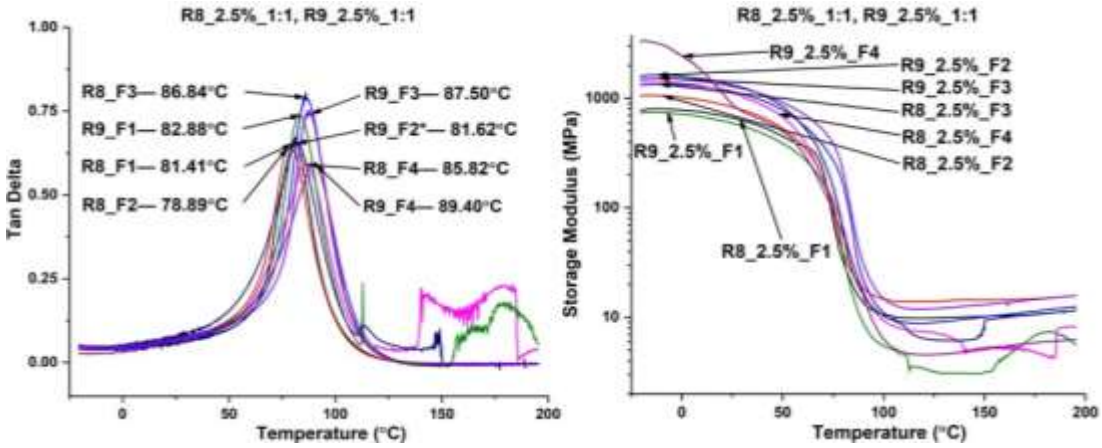

Figure 5.7. Tan delta peaks and storage modulus curves for coatings with (a) R1-R4, (b) R1_10%, and R2_10%, (c) R8, and R9, and (d) R10, and R11 resins with epoxy: AHEW = 1:1.

(d)

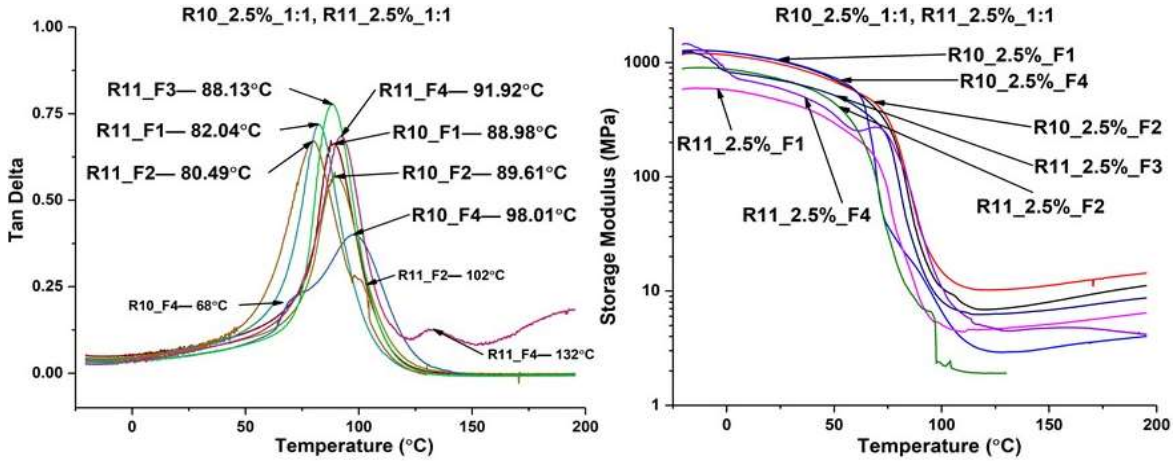

Figure 5.7. Tan delta peaks and storage modulus curves for coatings with (a) R1-R4, (b) R1_10%, and R2_10%, (c) R8, and R9, and (d) R10, and R11 resins with epoxy: AHEW = 1:1 (continued).

Not just coatings with 1:1 ratio, coatings with 1:2 epoxy: AHEW ratio were also analyzed for mechanical properties and thermal behavior over the course of the study. The coatings with 1:2 ratio exhibited good hardness and flexibility. Theoretically, formulations with 1:2 epoxy: AHEW contain higher number of unreacted amines in the matrix due to presence of higher amine concentration. Significantly low gloss of the coatings with 1:2 ratio may be attributed to due to amine blush from unreacted amines. Analysis with DSC and DMA showed significant decrease (~15°C) in T_g values with increasing amine content for the coatings with 1:2 ratio. Theoretically, coatings with epoxy: AHEW = 1:1 are devoid of unreacted epoxy or amine functional groups. At 1:1 ratio, the coatings form a tightly crosslinked network of chains, which results in lowering of movement of the network chains. Therefore, higher temperature is required for movement of chains in 1:1 coatings as compared to coatings with 1:2. Due to superior overall performance (mechanical properties, thermal behavior, and appearance) of AMP_GC coatings with epoxy: AHEW = 1:1 as compared to 1:2, all further experiments were conducted on AMP_GC coatings with 1:1 ratio.

Table 5.5. T_g and crosslink density of AMP_GC coatings with epoxy: AHEW = 1:1 from DMA.

Resins	Amines	Formulations	E' at 25°C (GPa)	T_g (°C)	v_e (mol/L)
R1_5%	Anc.2143	F1	1.38	74.34	1.73
	Anc.2432	F2	1.34	72.71	1.81
	And.2634	F3	1.01	83.85	1.05
	And.2767	F4	1.04	81.28	1.50
R1_10%	Anc.2143	F1	0.94	81.17	1.17
	Anc.2432	F2	0.70	58.25	0.54
	And.2634	F3	0.51	61.28	0.41
	And.2767	F4	0.41	62.03	0.31
R2_5%	Anc.2143	F1	0.55	94.01	1.08
	Anc.2432	F2	0.42	98.28	0.93
	And.2634	F3	0.80	92.70	0.77
	And.2767	F4	0.64	96.64	0.90
R2_10%	Anc.2143	F1	0.08	92.97	0.21
	Anc.2432	F2	0.12	91.29	0.45
	And.2634	F3	0.07	96.28	0.41
	And.2767	F4	0.08	94.01	0.57
R4_5%	Anc.2143	F1	1.07	74.67	1.37
	Anc.2432	F2	1.68	78.93	1.74
	And.2634	F3	1.76	81.56	1.13
	And.2767	F4	1.26	89.01	1.26
R8_2.5%	Anc.2143	F1	0.66	81.67	0.98
	Anc.2432	F2	0.83	78.90	1.40
	And.2634	F3	1.14	86.46	0.94
	And.2767	F4	1.10	86.21	0.50
R9_2.5%	Anc.2143	F1	0.59	82.68	0.30
	Anc.2432	F2*	1.33	81.67	0.60
	And.2634	F3	1.28	87.97	1.23
	And.2767	F4	0.86	89.23	0.48
R10_2.5%	Anc.2143	F1	1.30	88.98	0.75
	Anc.2432	F2	0.96	89.98	1.07
	And.2634	F3**	-	-	-
	And.2767	F4	1.04	98.04	0.31
R11_2.5%	Anc.2143	F1	0.46	82.18	0.48
	Anc.2432	F2	0.71	80.37	0.19
	And.2634	F3	0.69	88.22	0.65
	And.2767	F4	0.59	92.25	0.45

*R9_2.5%_F2 failed above T_g. **R10_2.5%_F3 and all formulations using R6 could not be analyzed using DMA due to crystalline nature of the coatings.

Prior to biological FR tests and surface analysis experiments, the AMP_GC coatings were placed in circulating water tank for 42 days to remove impurities, catalyst, and unreacted monomers. After 42 days, the AMP_GC coatings were analyzed using contact angle experiment. Figure 5.8 shows dynamic changes in WCA values for water leached AMP_GC coatings. Dynamic changes in WCA values were indicative of rearrangement of PEG chains on the surfaces upon contact with water. Coatings cured using

Ancamine 2143 and Ancamide 2634 (potentially similar cycloaliphatic structure) generally showed higher initial WCA values as compared to Ancamine 2432 and Ancamide 2767 (potentially similar aliphatic structure) coatings respectively, indicating dependence of WCA of the coatings on the structure of the amine crosslinker for the same amphiphilic resin. Although WCA > 90° at 0 minutes for most of the formulations, some formulations like R6_5%_F2 showed WCA < 90° at 0 minutes, indicating hydrophilic nature of the coatings even before contact with water. Formulations with R6, R8, and R9 showed fastest change in WCA, with 15-20° drop in values every 10 minutes. Among all the formulations, R10_F2 and R10_F3 showed highest initial WCA of 120°, while lowest initial WCA of 60° was observed for R6_F3 coating. Absorption of water droplet was observed on R6 coatings due to presence of PEG-2k chains. Slow rearrangement of water on R11_F4 coatings resulted in evaporation of water, resulting in decrease in size of the droplet. WCA value for such formulations with absorption and evaporation were not measured.

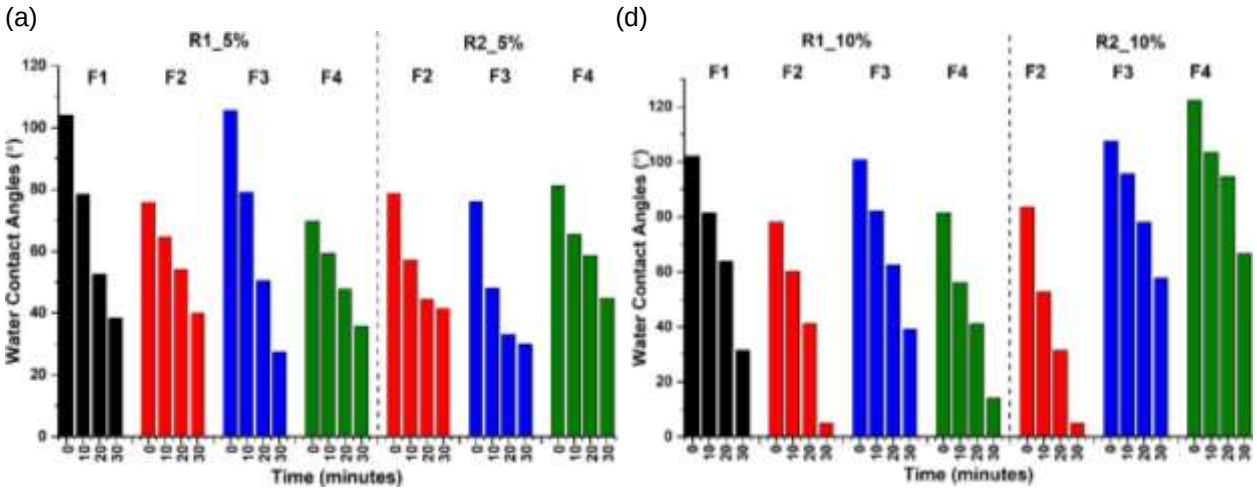

Figure 5.8. Dynamic changes in WCA for coatings with (a) R1_5% and R2_5%, (b) R4 and R6, (c) R10 and R11, (d) R1_10% and R2_10%, and (e) R8 and R9 resins. “x” indicates measurement of WCA was excluded due to significant change in droplet size (evaporation or absorption into the coatings). WCA measurements were not conducted on R2_5%_F1 and R2_10%_F1 coatings due to delamination and severe surface defects after water leaching.

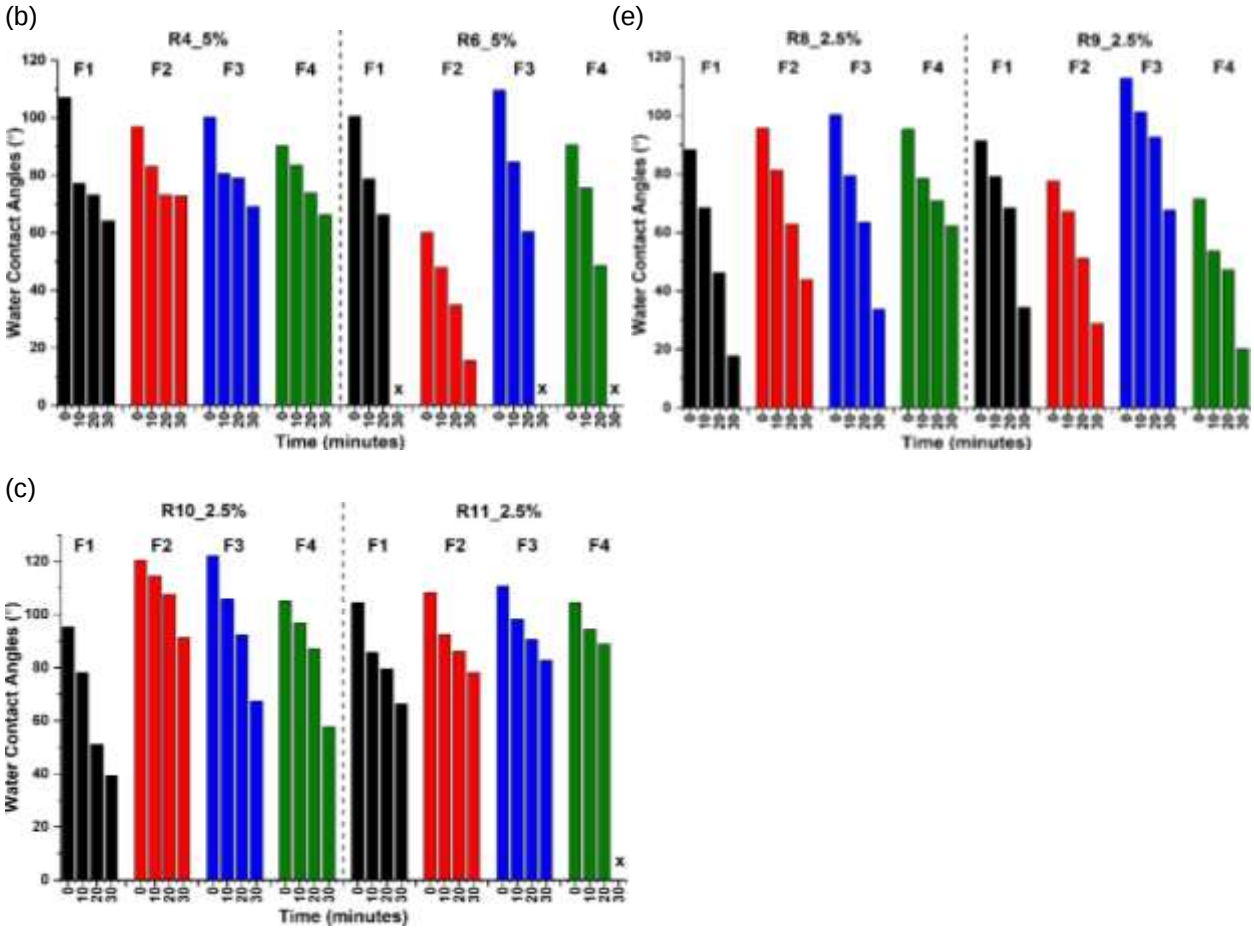

Figure 5.8. Dynamic changes in WCA for coatings with (a) R1_5% and R2_5%, (b) R4 and R6, (c) R10 and R11, (d) R1_10% and R2_10%, and (e) R8 and R9 resins (continued). "x" indicates measurement of WCA was excluded due to significant change in droplet size (evaporation or absorption into the coatings). WCA measurements were not conducted on R2_5%_F1 and R2_10%_F1 coatings due to delamination and severe surface defects after water leaching.

The pre-leached AMP_GC coatings were characterized for their FR performance against diatoms, biofilm, microalgae, mussels, and barnacles. FR performance of the AMP_GC coatings was compared to the commercial standards, I-700, I-900, 1100SR, T2, and PU (no siloxane). Figure 5.9 shows biofilm *C.lytica* attachment and removal from the AMP_GC coatings. In general, attachment of biofilm *C.lytica* on the AMP_GC coatings, T2, and PU was lower than I-700, I-900, and 1100SR (Figure 5.9(a)). Among the AMP_GC coatings, coatings with R8-R11 resins (PDMS= 5k-10k) showed ~40% lower attachment of *C.lytica* as compared to R1-R4 (PDMS-1k) coatings. Changing functionality of PDMS and PEG chains (R1 and R2 resins) did not show any significant change in biofilm attachment. Water pressure of 20 psi facilitated higher removal of the biofilm as compared to 10 psi (Figure 5.9(b)). Only 60-

65% biofilm was removed from the surfaces of most of the AMP_GC coatings and the commercial standards, except 1100SR which showed ~98% removal at 20 psi. Coatings R1_5%_F4, R10_F4, and all coatings with resin R1_10% showed lowest removal of the biofilm of ~40%. Coatings R1_5%_F2 and R4_5%_F2 were severely cracked during the course of the experiment, while R6_5% coatings could not be analyzed due to severe cracking of the coatings and absorption of the crystal violet into the coatings.

(a)

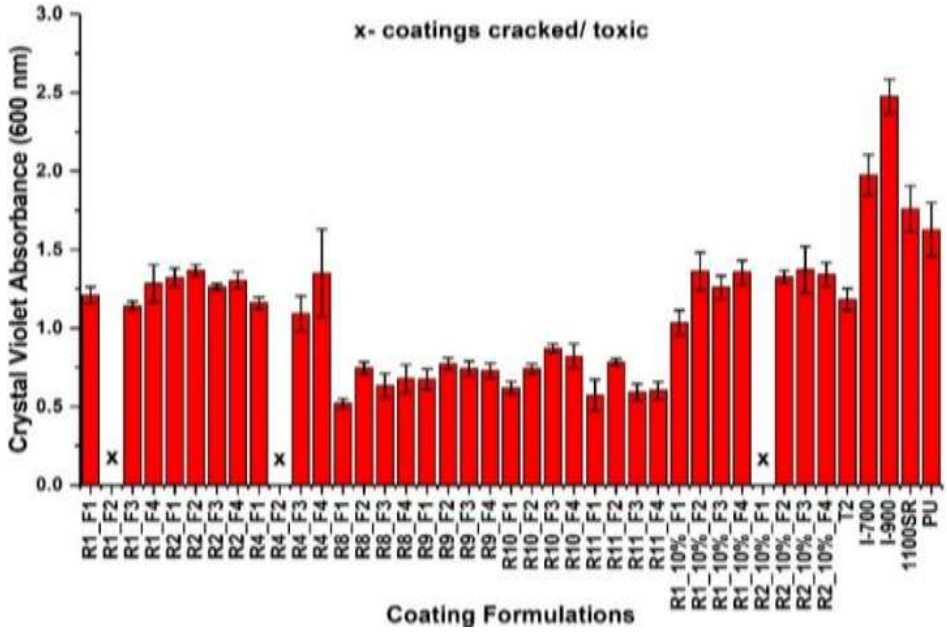

(b)

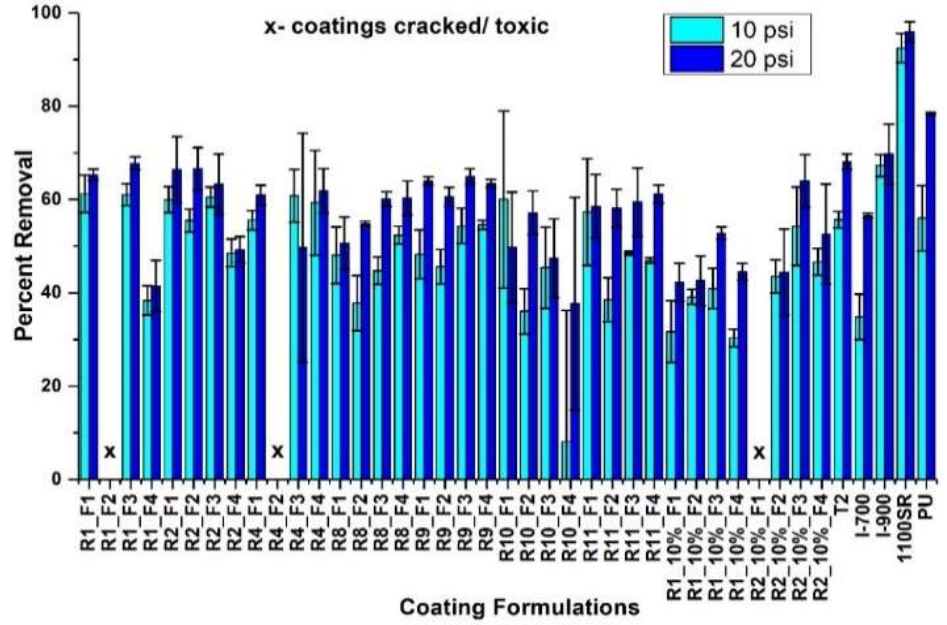

Figure 5.9. Bacterial biofilm *C.lytica* (a) attachment and (b) removal at 10 psi and 20 psi water jet pressures.

Figure 5.10 shows results for attachment and removal of diatom *N.incerta* from the AMP_GC coatings and the commercial standards at 20 psi waterjet pressure respectively. 10 psi water pressure could not facilitate sufficient removal of the diatoms from the commercial coatings. Diatom *N.incerta* attachment onto the AMP_GC coatings and most of the commercial coatings was significantly higher than 1100SR coating. In increasing order of diatom attachment: 1100SR < R1_10%, R2_10% < R6-R11 < R1_5%, R2_5%, R4, I-700, I-900, T2, and PU. Increasing amounts of PDMS and PEG from 5% to 10% appeared to provide a good balance between hydrophobicity and hydrophilicity, thereby decreasing *N.incerta* attachment. Among all the AMP_GC formulations, R6_F4 coatings showed lowest attachment of the diatoms. Most of the AMP_GC coatings facilitated higher removal of *N.incerta* as compared to the commercial standards (Figure 5.9(b)). Most of the coatings, except formulations with R1_5% and R2_5% resins (55-98% removal), showed diatom removal between 85-~100%. Coatings with R11 showed comparatively lower removal probably due to presence of higher MW PDMS chains (10k). The commercial coatings facilitated between 45-85% removal of the diatoms, with I-900 showing highest removal of ~85%.

(a)

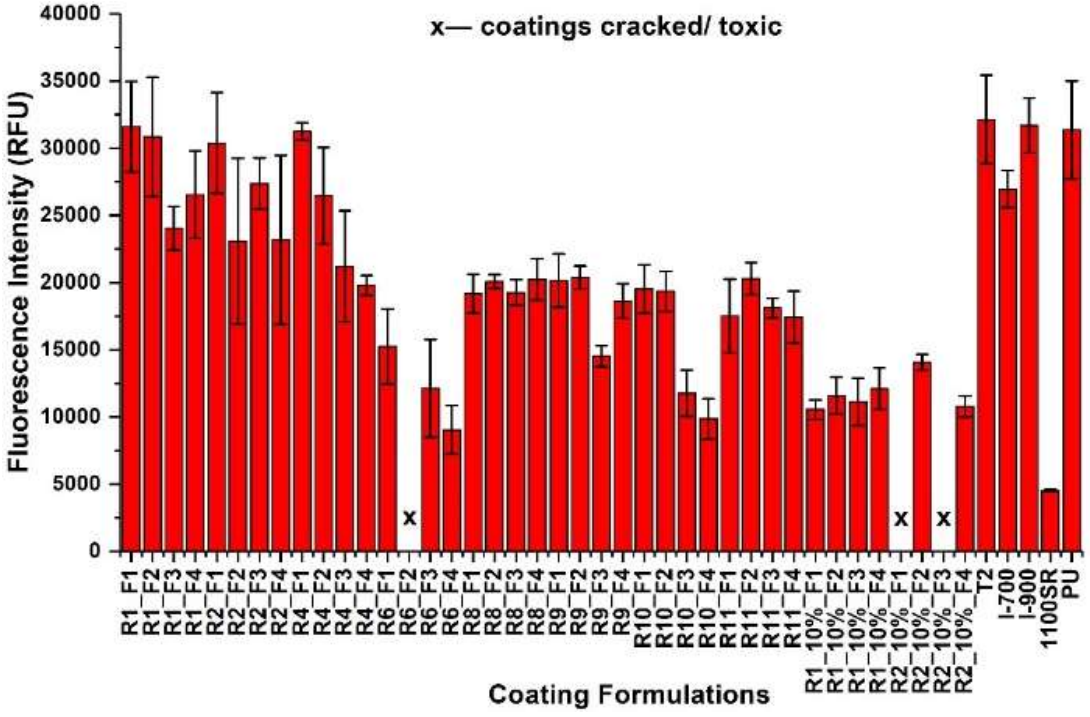

Figure 5.10. Diatom *N.incerta* (a) attachment and (b) removal at 20 psi water jet pressure.

(b)

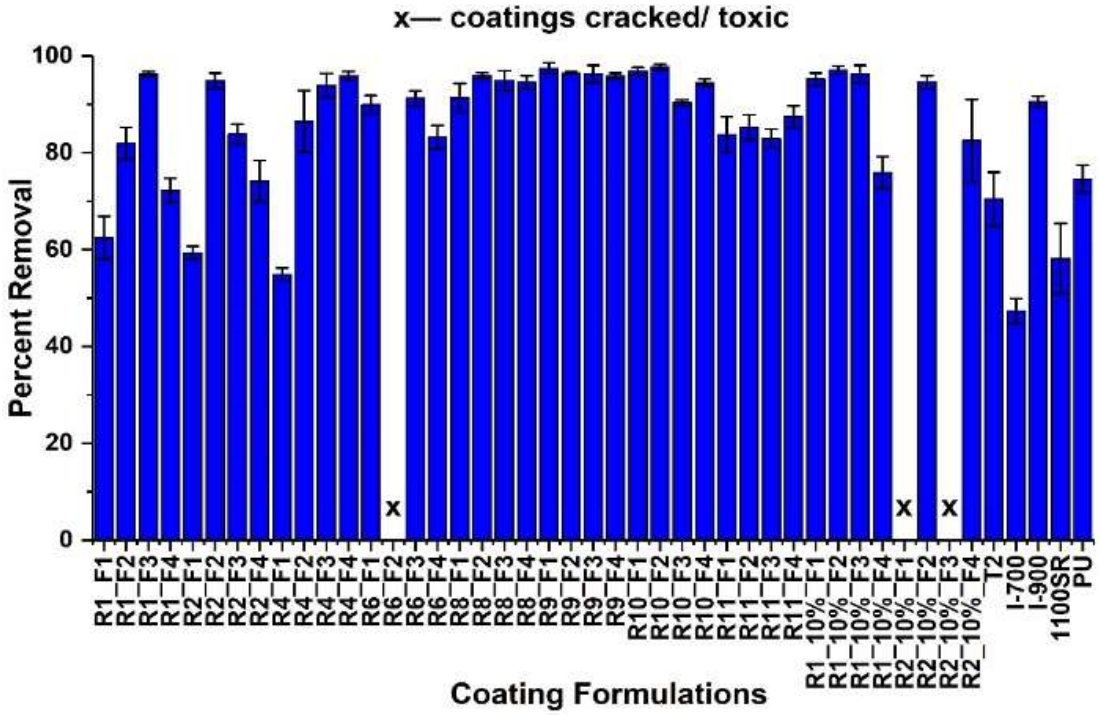

Figure 5.10. Diatom *N.incerta* (a) attachment and (b) removal at 20 psi water jet pressure (continued).

For FR tests with microalgae, mussels and barnacles, select AMP_GC formulations were chosen based on their performance against biofilm and diatoms, relative toxicity, and appearance. Figure 5.11 shows microalgae *U.linza* attachment and removal from the select AMP_GC coatings. In this experiment, only T2 and polystyrene (PS) were used as standards. Although most of the AMP_GC formulations showed microalgae attachment similar to T2 and PS, formulations R4_F4, R6_F4, and R1_10%_F4 showed 40-50% lower microalgae attachment, while attachment on R11_F2 coating was slightly higher than T2. Water pressure of 110 kPa facilitated highest microalgae removal for all the samples. But, the AMP_GC formulations could not facilitate more than 50% microalgae removal. Among the AMP_GC formulations, R6_F4 coating showed best FR performance against microalgae— lower attachment among all the samples and highest removal among AMP_GC formulations (~50%), while other formulations showed between 15-40% microalgae removal even at 110 kPa. PS showed ~30% removal, while the commercial T2 showed highest removal of 80% among all the coatings.

(a)

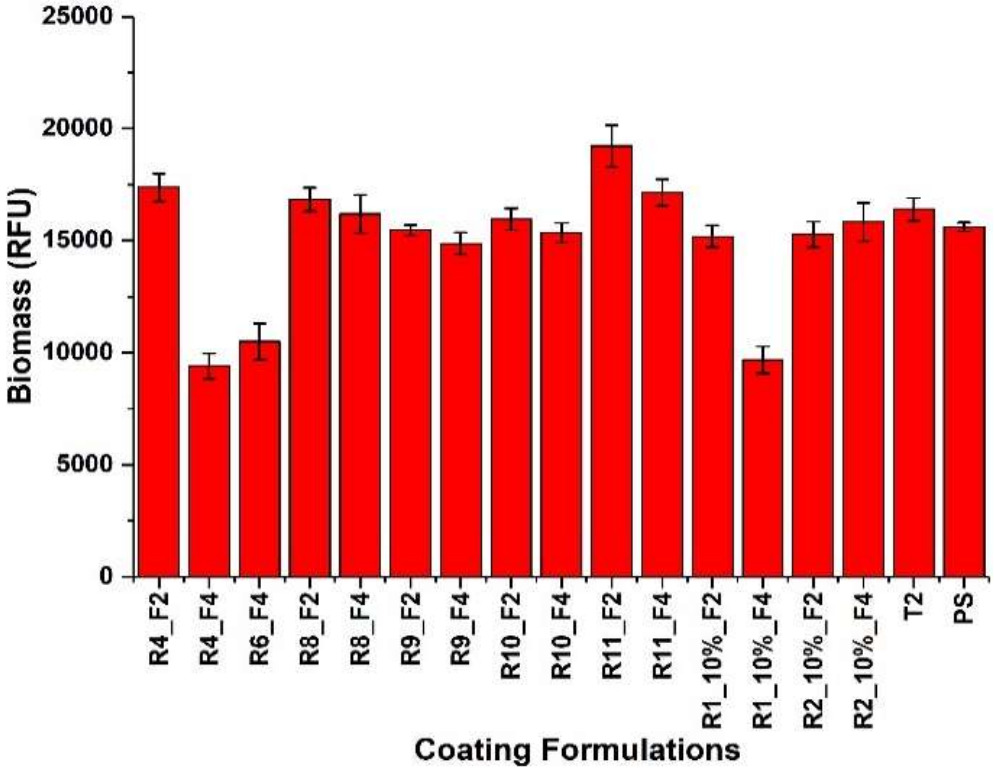

(b)

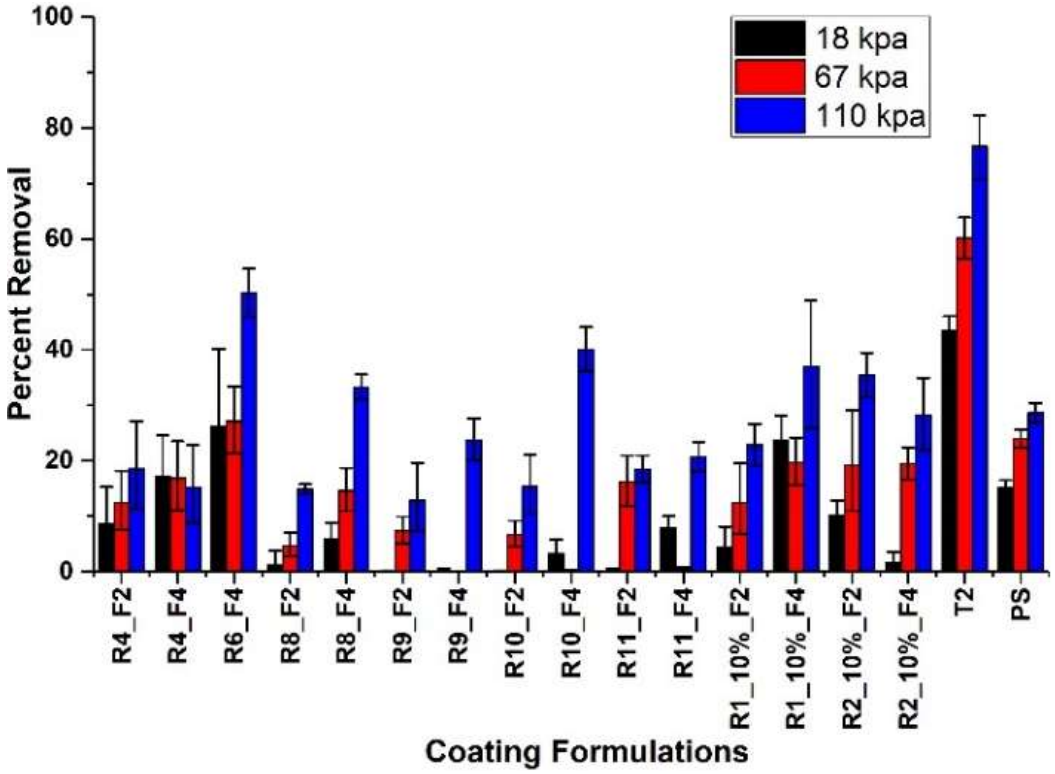

Figure 5.11. Microalgae *U.linza* (a) attachment and (b) removal at 18, 67, and 110 kPa water pressures.

Figure 5.12 shows mussel adhesion on select AMP_GC coatings and the commercial coatings. Mussel adhesion on the AMP_GC coatings varied from 15 N to 45 N. Among all the AMP_GC coatings, R1_10%_F2 showed the best performance, with average adhesion force of 15 N for 5 out of 6 mussels that attached to the coating during experimentation. The results also showed that mussel attachment strengths increased with increasing MW of PDMS from 1k for R1_F2 formulation to 5k for R10_F2 formulation. Further increasing the MW of PDMS to 10k (R11_F2) resulted in a drop in adhesion strength. Increasing the amounts of PDMS and PEG from 5% to 10% for R1 and R2 resins resulted in decrease in mussel adhesion. I-700 and PU showed attachment strength in the range from 20-25 N. I-900 and 1100SR coatings successfully deterred attachment of all mussels.

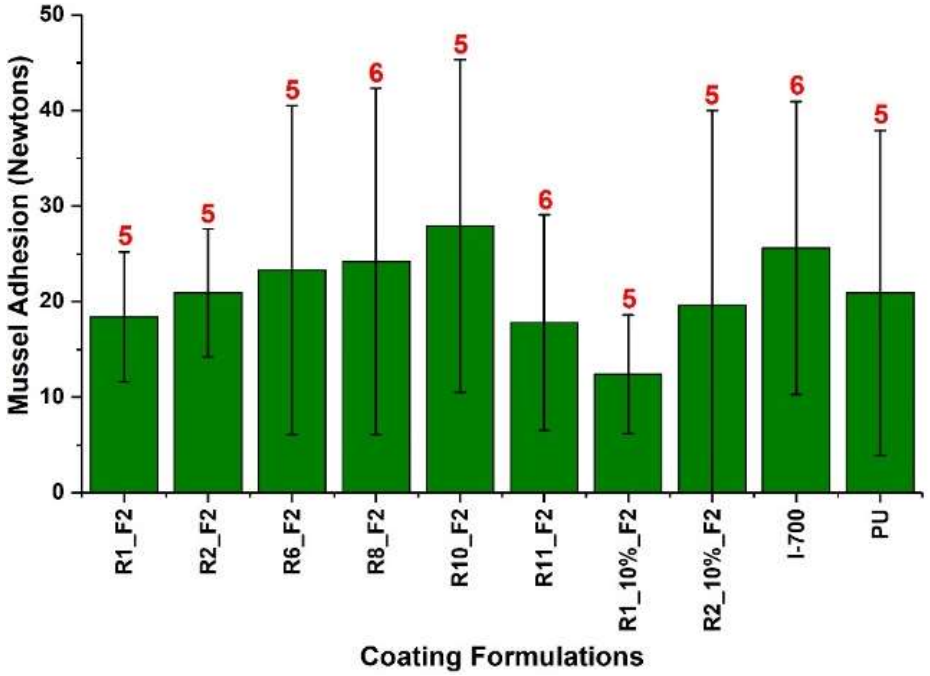

Figure 5.12. Mussel *Geukensia demissa* attachment on the select AMP_GC coatings. Numbers above data points indicate the number of mussels out of 6 that attached to the coatings during the experiment. None of the mussels attached to I-900 and 1100SR standards.

Figure 5.13 shows results for barnacle adhesion on select AMP_GC coatings as compared to the commercial standards. Overall, barnacles *A.amphitrite* attached strongly onto the select AMP_GC coatings as compared to the commercial standards. All 6 barnacles immobilized onto each coating during experimentation attached onto the select AMP_GC coatings. For the AMP_GC coatings, barnacle adhesion strength was in the range from 0.18-0.45 MPa, which was significantly higher than the commercial coatings (0.10-0.25 MPa). For R8_F2 formulation, adhesion force of the barnacles was the

lowest at 0.18 MPa, but 2 barnacle bases broke during experimentation. Coating R4_F2 showed the poorest barnacle release, with 5 out of 6 barnacles breaking during the experiment. Conversely, only 4-5 barnacles attached onto the Intersleek coating samples and a low force of removal was required for removal of the attached barnacles. Increasing the MW of PDMS chains from 1k (R1-R6 resins) to 5k (R8 resin) reduced the adhesion. But, attempts to increase the MW of PDMS to 10k (R11_F2) or increase PDMS and PEG content (R1_10% and R2_10%) further facilitated adhesion of the barnacles.

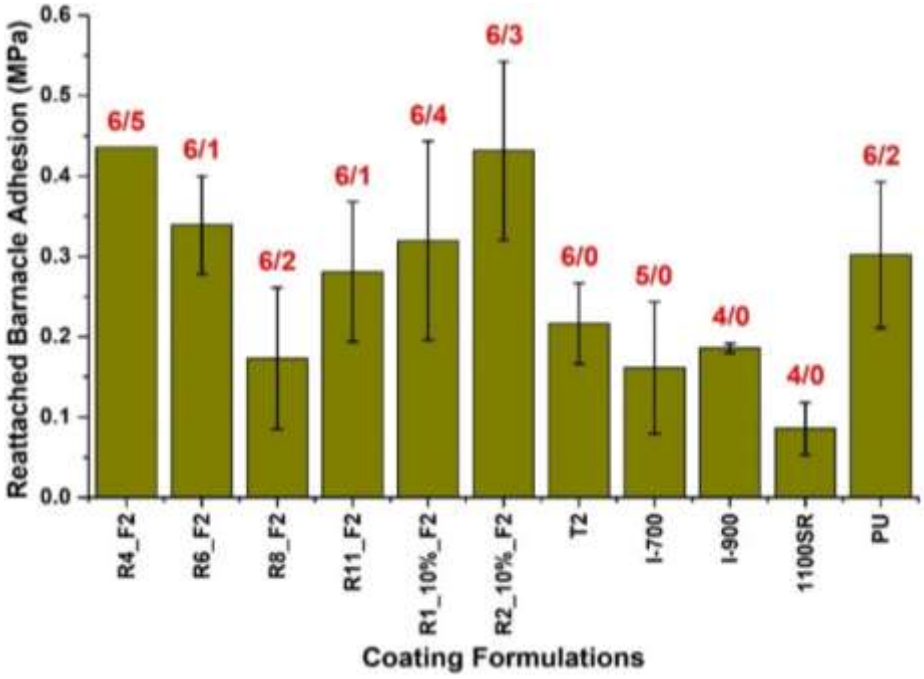

Figure 5.13. Adult barnacle *A.amphitrite* adhesion on the select AMP_GC coatings. Ratios above each data point are of the format the number of barnacles that attached to the coatings to the number of barnacles that broke during experimentation.

Surface analysis techniques— ATR-FTIR, AFM, and XPS— were used to correlate surface chemistry and FR behavior of the AMP_GC coatings. Figure 5.14 shows comparison between ATR-FTIR spectra of select AMP_GC coatings. The AMP_GC surfaces showed similar spectra, comprising of PDMS and PEG components. Minor peak at ~915 cm^{-1} indicated presence of some unreacted epoxy groups for coatings with R1_5%, R1_10%, R6_5%, and R10_2.5% resins. Further, intensity of -NH- peak at 3300 cm^{-1} and -C=O peak at 1658 cm^{-1} was slightly higher for coatings with R2_5% and R2_10% resins as compared to the other formulations, indicating slightly higher concentration of carbamate groups on the coating surfaces.

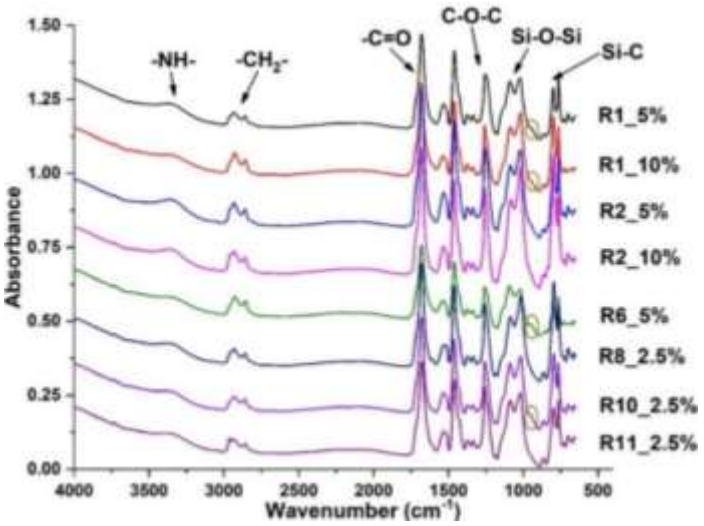

Figure 5.14. ATR-FTIR spectra for the AMP_GC coatings.

Figure 5.15 shows AFM scans for select AMP_GC coatings. Visually, the AMP_GC coatings appeared smooth and uniform, except formulations with R6 resin. But, analyzing the coatings using AFM showed different topographies present on the coating surfaces. R1 and R2 resins with 10% PDMS-1k and PEG components showed surfaces with roughness gradients. Increasing the MW of PDMS to 5k resulted in formation of “pores” for R8-R10 resins, which disappeared when MW of PDMS was increased to 10k (R11 resin). Coatings with R6 resin exhibited extremely high roughness, similar to surface of an unpolished quartz crystal, presumably due to presence of crystalline phases in the R6 coatings. High surface gradients combined with sticky PDMS components on the R6 coating surfaces complicated surface scans in tapping AFM mode.

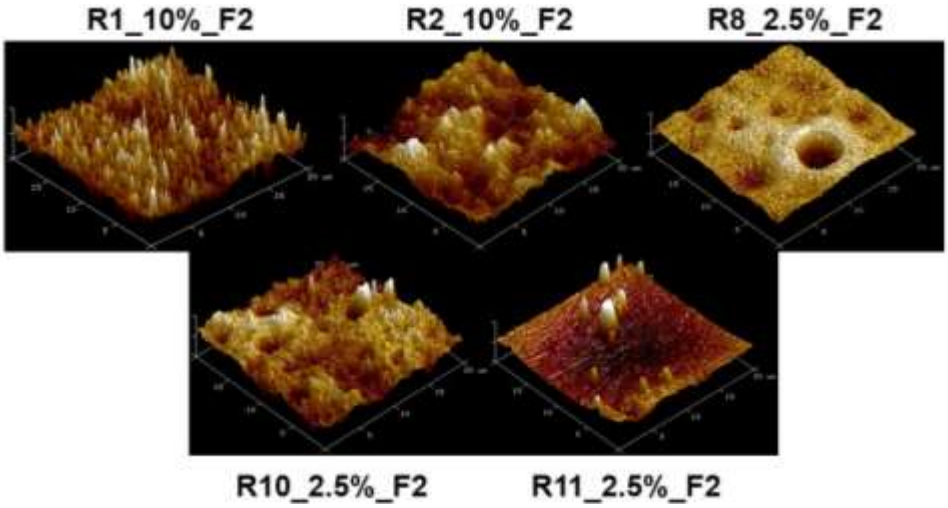

Figure 5.15. 20 µm x 20 µm AFM scans for select AMP_GC coatings.

Table 5.6 and Figure 5.16 shows atom composition and individual peaks for O1s and C1s with curve fitting for select AMP_GC coating surfaces as determined using XPS. The results from XPS showed that the coating surfaces comprised of both PEG and PDMS components. 4-10% N1s peaks were also observed on the surfaces, with R6_F2 showing highest %N of 9.71%. Peaks at ~532, 531.48, and 533.27 eV were indicative of three different states of O1s— siloxane, C-O-C/C-O-H linkages, and carbamate (urethane) linkages respectively. Similarly, peaks at ~284.20, 285.90-286.18, and 288.83-289.14 eV indicated three chemical states of C1s— C-C/C-H, C-O/C-N, and carbamate/urethane linkages respectively. Formulations R1_10%_F2 and R6_F2 showed ~24% PEG as observed from atom % of C-O-C state, while concentration of PDMS on the two formulations lied between 13-15%. On the other hand, R2_10%_F2 comprised of higher PDMS content (14.57%) as compared to PEG (11.40%). This difference in surface chemistries was also observed from the difference in peaks of the individual elements as seen in Figure 5.15. Higher C-O peaks from C1s spectra for R1_10%_F2 and R6_F2 indicated higher concentration of PEG on the coating surfaces. Even after surface cleaning, ~1% impurities were observed on the on the coating surfaces.

Table 5.6. Chemical composition of the select AMP_GC coatings.

Formulations	Chemical states		Binding energies (eV)	Atom %
R1_10%_F2	O1s	Si-O-Si	532.00	15.92
		C-O	531.23	8.07
		C=O	533.27	1.9
	C1s	C-C/C-H	284.22	36.41
		C-O/C-N	285.92	24.96
		C=O	288.83	2.62
	N1s	Total	399.20	5.68
R2_10%_F2	O1s	Si-O-Si	532.00	14.57
		C-O	531.48	10.03
		C=O	533.27	2.70
	C1s	C-C/C-H	284.29	51.18
		C-O/C-N	286.24	11.40
		C=O	288.83	1.93
	N1s	Total	399.18	4.28
R6_F2	O1s	Si-O-Si	532.00	13.84
		C-O	531.23	5.59
		C=O	533.27	3.55
	C1s	C-C/C-H	284.45	35.94
		C-O/C-N	285.99	24.78
		C=O	289.08	6.59
	N1s	Total	399.98	9.71

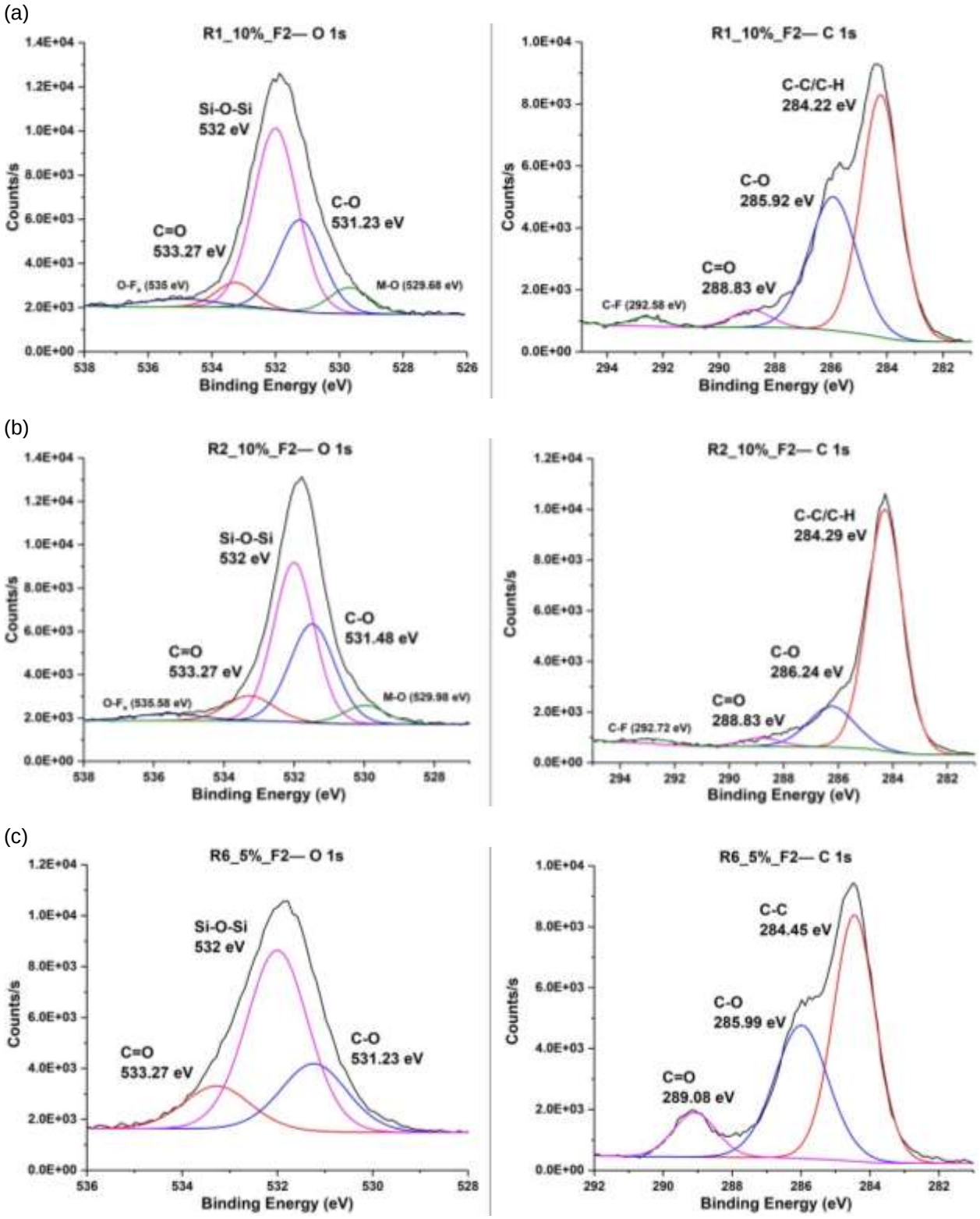

Figure 5.16. High resolution with peak fitting from XPS for (a) R1_10%_F2, (b) R2_10%_F2, and (c) R6_5%_F2 coatings. O-F_x, M-O, and C-F indicate surface impurities.

In this study, amphiphilic surfaces showing a combination of different polymer architectures were explored as potential FR coatings. Presence of PDMS and PEG chains in the coatings was expected to create “ambiguous” surfaces, disallowing fouling organisms from attaching onto the coatings. Analysis of AMP_GC coatings using contact angle experiment showed dynamic changes in WCA, indicating rearrangement of PEG chains on the surface of the coatings. Results from XPS showed that freedom of movement of “combs”, irrespective of polarity, allowed them to saturate the coating surfaces, while minimal separation of “bridges” was possible due to restricted chain movements within the coating matrices. FR results showed that diatom attachment varied with change in both MW and amounts of PDMS or PEG components, but, generally PEG rich surfaces could easily facilitate removal of diatoms. For mussels, strength of mussel adhesion appeared to be a function of PDMS and PEG content rather than the MW, although the difference wasn’t significant. Against microalgae and barnacles, extent of hydrophobic character of the coatings determined their FR behavior. Therefore, R11_F2 coating with 10k MW PDMS showed best barnacle removal performance among all the AMP_GC coatings, with only 1 barnacle base breaking during experimentation. But, presence of PEG chains allowed stronger binding of adhesives secreted by the foulants, increasing adhesion with the underlying substrates. In spite of that, interesting FR results against microalgae and barnacles for R6 and R10 formulations may be attributed to presence of crystalline zones present in the coatings. Reduction in entropy during crosslinking, long chain length of PEG-2k, inter- and intrachain interactions of PEG combs and hydrogen bonding are responsible for formation of PEG crystals in R6 and R10 coatings. PEG content on R6 coating surface was higher than PDMS concentration as observed using XPS. Adhesion of fouling organisms is believed to initiate with secretion of complex proteinaceous adhesives.[2] In this case, PEG rich crystals may have stopped the adhesives from the microalgae and the barnacles from completely penetrating into the PEG rich zones. Moreover, crystallization may have slightly enhanced protein resistance of the surfaces, thereby decreasing stronger surface-organism interactions. Therefore, PEG crystals combined with 1k-5k MW PDMS may have been responsible for highest microalgae removal (40-50%) from R6 and R10 coatings among all the AMP_GC formulations and breaking of only 1 barnacle base from the R6 coating in spite of presence of high MW PEG. Dominant hydrophilic character of the AMP_GC coatings combined with

presence of nano roughness and nanopores on the coating surfaces (from AFM) resulted in subpar performance of the coatings as compared to the commercial standards.

Conclusions

Novel isocyanate-free amphiphilic glycidyl carbamate (AMP_GC) coatings were explored as viable FR surfaces for marine applications. A variety of AMP_GC resins were synthesized using isocyanurate of HDI, glycidol, PDMS, and PEG. The functionality, MW, and amounts of PDMS and PEG components were varied to make the different AMP_GC resins. Polyamines, Ancamine 2143 and Ancamine 2432, and polyamides, Ancamide 2634 and Ancamide 2767, were used to cure the resins at RT with epoxy: AHEW ratios of 1:1 and 1:2. In spite of the presence of polar (GC, PEG) and non-polar (PDMS) components within the resins, visually, most of the cured coatings, except coatings with R6 resin, appeared smooth, uniform, and glossy. Mechanical tests showed that most of the AMP_GC coatings exhibited good hardness, flexibility, impact strength, and solvent resistance. Analysis of the coatings with DSC showed that the AMP_GC coatings exhibited high T_g values— R2_5% coatings showing the highest average T_g value, while the R2_10% coatings exhibiting lowest average T_g values. Melting peaks in DSC scans for coatings with R6 and R10 resins indicated formation of PEG rich crystalline domains, due to thermodynamically and kinetically favorable crystallization conditions present during curing of the two resins. With DSC, the polyamines resulted in coatings with higher T_g as compared to coatings with the polyamides; coatings with Ancamine 2143 and Ancamide 2634 resulted in higher T_g than Ancamine 2432 and Ancamide 2767 respectively. Conversely, DMA showed that T_g of the polyamide cured coatings (T_g with Ancamide 2767 > Ancamide 2634) was higher than the polyamine cured coatings (T_g with Ancamine 2432 > Ancamine 2143). Average values of crosslink density decreased with increase in the MW and the amounts of PDMS and PEG modifiers, with coatings with R2_10% exhibiting lowest crosslink density. $T_{d\ 5\%}$ for all coatings with resins R1-R6, as observed from TGA, lied in the range from 225-250°C. But, further increasing the MW of PDMS to 5k-10k (resins R8-R11) resulted in drastic drop in $T_{d\ 5\%}$ (130-150°C). Characterization of the AMP_GC coatings using ATR-FTIR showed presence of PDMS and PEG on the surface of the coatings. Slightly higher intensities of -NH- and -C=O peaks for R2_5% and R2_10% coatings indicated possibly higher concentration of GC matrix on the surface of the coatings with R2 resin. Dynamic changes in WCA were observed indicating rearrangement of the surfaces with

changing environment. AFM showed formation of coatings with roughness gradients and nanopores. XPS analysis showed that the coating surfaces comprised of higher concentration of “combs” than “bridges”, irrespective of polarity, due to higher freedom of movement of the comb-like chains.

Evaluation of FR performance showed that the AMP_GC coatings showed lower attachment of biofilm as compared to the commercial FR coatings. But, the AMP_GC coatings facilitated only 60-65% removal of the biofilm at 20 psi as opposed to ~98% removal from 1100SR coating. Diatom attachment on the AMP_GC coatings was higher than 1100SR coatings. Most of the AMP_GC coatings showed higher removal of diatoms (~98%) compared to the commercial standards. Against microalgae, coatings with R6 and R10 resins showed best FR performance— lower attachment than T2 and PS and 40-50% removal (highest among AMP_GC formulations). The AMP_GC coatings exhibited poor FR performance against barnacles and mussels as compared to the commercial standards. Mussel adhesion strength lied between 10-25 N for the AMP_GC coatings. R1_10%_F2 showed lowest average adhesion strength of ~15 N for 5 out of 6 attached mussels. Against barnacles, force of barnacle removal was in the range from 0.25-0.65 MPa; R11_F2 showed the best barnacle removal among all the AMP_GC coatings, with removal force of 0.31 MPa and only 1 barnacle breaking during the experiment. In spite of presence of high MW PEG chains in the coatings with R6 and R10, comparatively decent FR performance of the coatings against microalgae and barnacles may be attributed to presence of crystalline zones in the coatings. The PEG crystals may have reduced penetration of adhesives into the coating surfaces, reducing adhesion strength of the fouling organism. The above study provided insights into correlation between biofouling and functionality/MW/amounts of PDMS and PEG components— biofilm attachment reduced with increasing MW of PDMS; diatom attachment reduced with increasing MW and amount of both PDMS and PEG chains; barnacle adhesion was higher for surfaces with monofunctional PDMS than difunctional PDMS.

References

1. Yebra, D. M.; Kiil, S.; Dam-Johansen, K., Antifouling technology—past, present and future steps towards efficient and environmentally friendly antifouling coatings. *Progress in Organic Coatings* **2004,** *50* (2), 75-104.

2. Callow, J. A.; Callow, M. E., Trends in the development of environmentally friendly fouling-resistant marine coatings. *Nature Communications* **2011,** *2*, 244.

3. Galhenage, T. P.; Webster, D. C.; Moreira, A. M. S.; Burgett, R. J.; Stafslien, S. J.; Vanderwal, L.; Finlay, J. A.; Franco, S. C.; Clare, A. S., Poly (ethylene) glycol-modified, amphiphilic, siloxane–polyurethane coatings and their performance as fouling-release surfaces. *Journal of Coatings Technology and Research* **2016,** *2* (14), 307-322.

4. Magin, C. M.; Cooper, S. P.; Brennan, A. B., Non-toxic antifouling strategies. *Materials Today* **2010,** *13* (4), 36-44.

5. Schultz, M. P., Effects of coating roughness and biofouling on ship resistance and powering. *Biofouling* **2007,** *23* (5), 331-341.

6. Sommer, S.; Ekin, A.; Webster, D. C.; Stafslien, S. J.; Daniels, J.; VanderWal, L. J.; Thompson, S. E. M.; Callow, M. E.; Callow, J. A., A preliminary study on the properties and fouling-release performance of siloxane–polyurethane coatings prepared from poly (dimethylsiloxane)(PDMS) macromers. *Biofouling* **2010,** *26* (8), 961-972.

7. Schultz, M. P.; Bendick, J. A.; Holm, E. R.; Hertel, W. M., Economic impact of biofouling on a naval surface ship. *Biofouling* **2011,** *27* (1), 87-98.

8. Lejars, M. n.; Margaillan, A.; Bressy, C., Fouling release coatings: a nontoxic alternative to biocidal antifouling coatings. *Chemical Reviews* **2012,** *112* (8), 4347-4390.

9. Sommer, S. A.; Byrom, J. R.; Fischer, H. D.; Bodkhe, R. B.; Stafslien, S. J.; Daniels, J.; Yehle, C.; Webster, D. C., Effects of pigmentation on siloxane–polyurethane coatings and their performance as fouling-release marine coatings. *Journal of Coatings Technology and Research* **2011,** *8* (6), 661-670.

10. Bodkhe, R. B.; Thompson, S. E. M.; Yehle, C.; Cilz, N.; Daniels, J.; Stafslien, S. J.; Callow, M. E.; Callow, J. A.; Webster, D. C., The effect of formulation variables on fouling-release performance of stratified siloxane–polyurethane coatings. *Journal of Coatings Technology and Research* **2012,** *9* (3), 235-249.

11. Ekin, A.; Webster, D. C., Combinatorial and High-Throughput Screening of the Effect of Siloxane Composition on the Surface Properties of Crosslinked Siloxane− Polyurethane Coatings. *Journal of Combinatorial Chemistry* **2007,** *9* (1), 178-188.

12. Ekin, A.; Webster, D. C.; Daniels, J. W.; Stafslien, S. J.; Cassé, F.; Callow, J. A.; Callow, M. E., Synthesis, formulation, and characterization of siloxane–polyurethane coatings for underwater marine applications using combinatorial high-throughput experimentation. *Journal of Coatings Technology and Research* **2007,** *4* (4), 435-451.

13. Majumdar, P.; Ekin, A.; Webster, D. C., Thermoset Siloxane—Urethane Fouling Release Coatings. In *Smart Coatings;* ***March 13, 2007****, 61-75*.

14. Chen, H.; Yuan, L.; Song, W.; Wu, Z.; Li, D., Biocompatible polymer materials: role of protein–surface interactions. *Progress in Polymer Science* **2008,** *33* (11), 1059-1087.

15. Zheng, J.; Li, L.; Chen, S.; Jiang, S., Molecular simulation study of water interactions with oligo (ethylene glycol)-terminated alkanethiol self-assembled monolayers. *Langmuir* **2004,** *20* (20), 8931-8938.

16. Chen, S.; Li, L.; Zhao, C.; Zheng, J., Surface hydration: principles and applications toward low-fouling/nonfouling biomaterials. *Polymer* **2010,** *51* (23), 5283-5293.

17. Holland, R.; Dugdale, T. M.; Wetherbee, R.; Brennan, A. B.; Finlay, J. A.; Callow, J. A.; Callow, M. E., Adhesion and motility of fouling diatoms on a silicone elastomer. *Biofouling* **2004,** *20* (6), 323-329.

18. Gudipati, C. S.; Finlay, J. A.; Callow, J. A.; Callow, M. E.; Wooley, K. L., The antifouling and fouling-release perfomance of hyperbranched fluoropolymer (HBFP)-poly (ethylene glycol)(PEG) composite coatings evaluated by adsorption of biomacromolecules and the green fouling alga ulva. *Langmuir* **2005,** *21* (7), 3044-3053.

19. Finlay, J. A.; Bennett, S. M.; Brewer, L. H.; Sokolova, A.; Clay, G.; Gunari, N.; Meyer, A. E.; Walker, G. C.; Wendt, D. E.; Callow, M. E., Barnacle settlement and the adhesion of protein and diatom microfouling to xerogel films with varying surface energy and water wettability. *Biofouling* **2010,** *26* (6), 657-666.

20. Krishnan, S.; Wang, N.; Ober, C. K.; Finlay, J. A.; Callow, M. E.; Callow, J. A.; Hexemer, A.; Sohn, K. E.; Kramer, E. J.; Fischer, D. A., Comparison of the fouling release properties of hydrophobic fluorinated and hydrophilic PEGylated block copolymer surfaces: attachment strength of the diatom Navicula and the green alga Ulva. *Biomacromolecules* **2006,** *7* (5), 1449-1462.

21. Baur, X.; Marek, W.; Ammon, J.; Czuppon, A. B.; Marczynski, B.; Raulf-Heimsoth, M.; Roemmelt, H.; Fruhmann, G., Respiratory and other hazards of isocyanates. *International Archives of Occupational and Environmental Health* **1994,** *66* (3), 141-152.

22. Musk, A. W.; Peters, J. M.; Wegman, D. H., Isocyanates and respiratory disease: current status. *American Journal of Industrial Medicine* **1988,** *13* (3), 331-349.

23. Edwards, P. A.; Striemer, G.; Webster, D. C., Novel polyurethane coating technology through glycidyl carbamate chemistry. *JCT Research* **2005,** *2* (7), 517-527.

24. Edwards, P. A.; Striemer, G.; Webster, D. C., Synthesis, characterization and self-crosslinking of glycidyl carbamate functional resins. *Progress in Organic Coatings* **2006,** *57* (2), 128-139.

25. Chattopadhyay, D. K.; Muehlberg, A. J.; Webster, D. C., Organic–inorganic hybrid coatings prepared from glycidyl carbamate resins and amino-functional silanes. *Progress in Organic Coatings* **2008,** *63* (4), 405-415.

26. Chattopadhyay, D. K.; Zakula, A. D.; Webster, D. C., Organic–inorganic hybrid coatings prepared from glycidyl carbamate resin, 3-aminopropyl trimethoxy silane and tetraethoxyorthosilicate. *Progress in Organic Coatings* **2009,** *64* (2), 128-137.

27. Harkal, U. D.; Muehlberg, A. J.; Li, J.; Garrett, J. T.; Webster, D. C., The influence of structural modification and composition of glycidyl carbamate resins on their viscosity and coating performance. *Journal of Coatings Technology and Research* **2010,** *7* (5), 531-546.

28. Harkal, U. D.; Muehlberg, A. J.; Webster, D. C., UV curable glycidyl carbamate based resins. *Progress in Organic Coatings* **2012,** *73* (1), 19-25.

29. Chattopadhyay, D. K.; Webster, D. C., Hybrid coatings from novel silane-modified glycidyl carbamate resins and amine crosslinkers. *Progress in Organic Coatings* **2009,** *66* (*1*), 73-85.

30. Harkal, U. D.; Muehlberg, A. J.; Edwards, P. A.; Webster, D. C., Novel water-dispersible glycidyl carbamate (GC) resins and waterborne amine-cured coatings. *Journal of Coatings Technology and Research* **2011,** *8* (6), 735-747.

31. Harkal, U. D.; Muehlberg, A. J.; Webster, D. C., Linear glycidyl carbamate (GC) resins for highly flexible coatings. *Journal of Coatings Technology and Research* **2013,** *10* (2), 141-151.

32. Cardillo, P.; Nebuloni, M., Theoretical and calorimetric evaluation of thermal stability of glycidol. *Journal of Loss Prevention in the Process Industries* **1991,** *4* (4), 242-245.

33. Bodkhe, R. B.; Stafslien, S. J.; Cilz, N.; Daniels, J.; Thompson, S. E. M.; Callow, M. E.; Callow, J. A.; Webster, D. C., Polyurethanes with amphiphilic surfaces made using telechelic functional PDMS having orthogonal acid functional groups. *Progress in Organic Coatings* **2012,** *75* (1), 38-48.

34. Cassé, F.; Stafslien, S. J.; Bahr, J. A.; Daniels, J.; Finlay, J. A.; Callow, J. A.; Callow, M. E., Combinatorial materials research applied to the development of new surface coatings V. Application of a spinning water-jet for the semi-high throughput assessment of the attachment strength of marine fouling algae. *Biofouling* **2007,** *23* (2), 121-130.

35. Chen, Z.; Chisholm, B.; Kim, J.; Stafslien, S.; Wagner, R.; Patel, S.; Daniels, J.; Wal, L. V.; Li, J.; Ward, K., UV-curable, oxetane-toughened epoxy-siloxane coatings for marine fouling-release coating applications. *Polymer International* **2008,** *57* (6), 879-886.

36. Kim, J.; Nyren-Erickson, E.; Stafslien, S.; Daniels, J.; Bahr, J.; Chisholm, B. J., Release characteristics of reattached barnacles to non-toxic silicone coatings. *Biofouling* **2008,** *24* (4), 313-319.

37. Majumdar, P.; Lee, E.; Patel, N.; Ward, K.; Stafslien, S. J.; Daniels, J.; Chisholm, B. J.; Boudjouk, P.; Callow, M. E.; Callow, J. A., Combinatorial materials research applied to the development of new surface coatings IX: an investigation of novel antifouling/fouling-release coatings containing quaternary ammonium salt groups. *Biofouling* **2008,** *24* (3), 185-200.

38. Kugel, A. J.; Jarabek, L. E.; Daniels, J. W.; Vander Wal, L. J.; Ebert, S. M.; Jepperson, M. J.; Stafslien, S. J.; Pieper, R. J.; Webster, D. C.; Bahr, J., Combinatorial materials research applied to the development of new surface coatings XII: Novel, environmentally friendly antimicrobial coatings derived from biocide-functional acrylic polyols and isocyanates. *Journal of Coatings Technology and Research* **2009,** *6* (1), 107-121.

39. Stafslien, S. J.; Bahr, J. A.; Feser, J. M.; Weisz, J. C.; Chisholm, B. J.; Ready, T. E.; Boudjouk, P., Combinatorial materials research applied to the development of new surface coatings I: a multiwell plate screening method for the high-throughput assessment of bacterial biofilm retention on surfaces. *Journal of Combinatorial Chemistry* **2006,** *8* (2), 156-162.

40. Stafslien, S. J.; Bahr, J. A.; Daniels, J. W.; Vander Wal, L.; Nevins, J.; Smith, J.; Schiele, K.; Chisholm, B., Combinatorial materials research applied to the development of new surface coatings VI: an automated spinning water jet apparatus for the high-throughput characterization of fouling-release marine coatings. *Review of Scientific Instruments* **2007,** *78* (7), 072204.

41. Bell, E. C.; Gosline, J. M., Strategies for life in flow: tenacity, morphometry, and probability of dislodgment of two Mytilus species. *Marine Ecology Progress Series* **1997,** *159*, 197-208.

42. Burkett, J. R.; Wojtas, J. L.; Cloud, J. L.; Wilker, J. J., A method for measuring the adhesion strength of marine mussels. *The Journal of Adhesion* **2009,** *85* (9), 601-615.

43. Crisp, D. J.; Walker, G.; Young, G. A.; Yule, A. B., Adhesion and substrate choice in mussels and barnacles. *Journal of Colloid and Interface Science* **1985,** *104* (1), 40-50.

44. Majumdar, P.; Stafslien, S.; Daniels, J.; Webster, D. C., High throughput combinatorial characterization of thermosetting siloxane–urethane coatings having spontaneously formed microtopographical surfaces. *Journal of Coatings Technology and Research* **2007,** *4* (2), 131-138.

45. Rittschof, D.; Orihuela, B.; Stafslien, S.; Daniels, J.; Christianson, D.; Chisholm, B.; Holm, E., Barnacle reattachment: a tool for studying barnacle adhesion. *Biofouling* **2008,** *24* (1), 1-9.

CHAPTER 6. SUMMARY AND FUTURE WORK

Previously developed, self-stratified siloxane-polyurethane coatings (SiPU) were made using isocyanate, 50% acrylic polyol in toluene, 20k MW aminopropyl terminated polydimethylsiloxane (APT-PDMS), and catalyst. The amount of APT-PDMS was maintained at 20% by weight acrylic polyol. Two different Scotch Brite pads of varying roughness, SP and GP, were used to abrade the cured SiPU coatings. Number of abrasions with each pad was also varied. Evaluation of FR performance of the abraded coatings showed that FR performance against diatoms deteriorated with increasing roughness of the coatings. But interestingly, the FR performance of the coatings against biofilm, microalgae, barnacles, and mussels improved with increasing roughness. Determination of the dimensions of the abrasions or surface features showed that SiPU coatings abraded with SP resulted in formation of surface features with sizes significantly larger than the size of the fouling organisms. On the other hand, coatings abraded using GP resulted in features less than the size of the fouling organisms. Therefore, FR performance of the abraded coatings was enhanced by introduction of surface features that made the coatings potentially less conducive for growth and metamorphosis of the organisms. WCA value remained greater than 90°, indicating hydrophobic nature of the abraded coatings. XPS analysis of the abraded coatings indicated presence of APT-PDMS on the coating surfaces even after abrasions. Although smooth, unabraded standards were used to compare FR performance of the abraded SiPU coatings, future experiments can be conducted by abrading the commercial standards and studying the change in FR performance of the coatings. The commercial standards may not be able to withstand surface abrasions due to their soft, elastomeric nature. Another study involving multidirectional abrasions can be conducted to better simulate coating damage in practical applications.

In the second part, glycidyl carbamate (GC) technologies were explored as “safer” isocyanate-free alternatives for conventional polyurethanes to make self-stratified FR coatings. In this project, GC coatings with different surface chemistries were made by modifying the resin with siloxanes and polyethylene glycols. The MW, the functionality, and the amount of modifiers, along with type and amount of amine crosslinkers and curing schedules were varied to understand effect of these variables on coating properties and FR performance.

Hydrophobic GC coatings were made using dicarbinol terminated PDMS modified GC resin (IGC_PDMS), amine crosslinkers with varying structures and reactivities, and APT-PDMS. APT-PDMS content of the formulations was varied to increase hydrophobicity of the coatings. Diamines, PACM, Ancamine 2143, Ancamine 2432, Ancamide 2634, and Ancamide 2767, were used to crosslink the resin in 1:1, 1:2, and 2:1 epoxy: AHEW ratios. Results from mechanical tests showed that the coatings could be completely cured even at room temperature. Among the different amine crosslinkers, coatings cured using polyamides showed poorest overall performance and appearance. On the other hand, coatings cured at elevated temperature appeared smooth and uniform and showed the best overall performance. Results from DSC and DMA showed that Ancamine 2143 crosslinker resulted in coatings with highest T_g, while coatings cured using Ancamine 2432 exhibited the lowest T_g. Onset of degradation for all the coatings was observed between 250-265°C. Although tan delta peaks for most of the coatings appeared narrow and uniform, presence of secondary peaks in tan delta peaks of some formulations indicated formation of heterogeneous coating networks. Characterization techniques such as contact angle, ATR-FTIR, AFM, and XPS were utilized to understand the surface chemistry of the coatings after curing. Hydrophobic nature of all the coatings was observed from WCA values > 90°. Increasing APT-PDMS content in the formulations resulted in increase in WCA and drop in surface energy of the coatings. Highest WCA of 118° and lowest SE of 10.5 mN/m was obtained for PACM_1:1_F20 and PACM_1:1_F30. ATR-FTIR showed presence of PDMS on the surface of all the coatings. FTIR analysis of “oil” from the surface of the PACM cured coatings with APT-PDMS content > 15% indicated presence of unreacted APT-PDMS chains in the coatings. AFM analysis showed that although the coating surfaces smoothened with addition of APT-PDMS, increasing APT-PDMS also resulted in formation of “pores” on the coating surfaces. Analysis of coatings using XPS showed higher concentration of PDMS on surfaces of Ancamine 2432 cured coatings as compared to PACM cured coatings, probably due to movement of the unbound APT-PDMS chains at higher APT-PDMS content.

FR results for the IGC_PDMS coatings against diatoms showed that higher APT-PDMS content with PACM cured formulations facilitated diatom removal; the PACM cured coatings successfully deterred attachment of the diatoms and showed 75-90% removal with APT-PDMS content between 10-30%. But, Ancamine 2432 cured coatings showed lower removal of the diatoms with increasing APT-PDMS content.

This unusual behavior of the PACM cured coatings was attributed to presence of unbound APT-PDMS chains that may have exposed the GC matrix to the diatoms. The IGC_PDMS coatings showed poor removal of the biofilm as compared to the commercial standards. Among the IGC_PDMS coatings, Ancamine 2432 resulted in coatings with lower biofilm attachment as compared to the PACM cured coatings. In spite of the highly hydrophobic nature of the IGC_PDMS coatings, the formulations could not facilitate removal of the microalgae, with the IGC_PDMS coatings showing 5-20% removal as against 70-80% removal from 1100SR and T2 standards. The IGC_PDMS coatings showed poor overall FR performance against mussels and barnacles. Among the IGC_PDMS coatings, PACM_1:1_Fx allowed lower attachment strength of the mussels compared to 2432_1:1_Fx coatings; PACM_1:1_F10 showed the best performance, with 4 out of 6 mussels requiring removal force of ~10 N. Similarly, PACM_1:1_Fx coatings showed lower barnacle adhesion force compared to 2432_1:1_Fx coatings. For PACM_1:1_Fx coatings, barnacle adhesion strength decreased with increasing APT-PDMS content, but the reverse was true for the coatings cured using Ancamine 2432.

Isocyanate-free amphiphilic GC coatings with different molecular architectures were explored for use as FR coatings. In the first approach, amphiphilic coatings were made using difunctional PDMS and PEG components such that the resultant coatings formed ambiguous PDMS and PEG rich domains on the surfaces. Amine terminated PEGs (Jeffamines) with MW = 900 and 2003 g/mol, J900 and J2003 respectively, were incorporated as co-crosslinkers in formulations with the hydrophobic IGC_PDMS resin to impart hydrophilicity to the coatings. Formulations were made by varying the amounts of the co-crosslinkers as, 5, 10, 15, and 20% resin solids. For formulations with 15 and 20% hydrophilic co-crosslinkers, additional APT-PDMS was added to the formulations to balance amphiphilicity of the coatings. Diamines, PACM, Ancamine 2143, and Ancamine 2432, were used as primary crosslinkers in 1:1 epoxy: AHEW ratio. As compared to the hydrophobic IGC_PDMS coatings, lower solvent resistance of the Jeffamine formulations indicated interference of hydrophilic and hydrophobic components in the formulations in network formation. Among the Jeffamine formulations, coatings with PACM exhibited highest pendulum hardness, while the Ancamine 2432 cured coatings showed lowest pendulum hardness. Lower impact resistance of most of the coatings can be attributed to their high hardness. Onset of thermal degradation of all the coatings was observed between 250-265°C. Coatings with Ancamine

2143 exhibited highest T_g among all the formulations as observed from DSC. Formulations with J2003 co-crosslinker showed higher T_g compared to J900. Heterogeneity of some Jeffamine coatings was observed from presence of secondary tan delta peaks as seen from DMA. Measurement of WCA showed dynamic changes in WCA, indicating rearrangement of surface chains. ATR-FTIR showed presence of both PDMS and PEG chains on the coating surfaces. Diatom attachment on the Jeffamine coatings was higher than the commercial standards. But, formulations cured using Ancamine 2432 facilitated diatom removal as compared to PACM cured coatings. Decrease in diatom removal with increasing J900 or J2003 content may be attributed to presence of APT-PDMS in formulations with higher J900 or J2003 content. Biofilm attachment onto the Jeffamine coatings was lower than the commercial standards, but the coatings could not facilitate removal of biofilm. Although some of the coatings successfully deterred attachment of mussels, the Jeffamine coatings showed stronger attachment of mussels and barnacles as compared to the commercial standards, like 1100SR. Analysis of the coatings with XPS showed that concentration of PEG was significantly higher than PDMS, which may have resulted in poor FR performance of the Jeffamine coatings.

In the second approach, a number of amphiphilic resins were synthesized using HDI trimer, glycidol, and monofunctional and difunctional PDMS and PEG. The amount and MW of the PDMS and PEG modifiers was varied. It was anticipated that the monofunctional component will provide comb-like dangling chains, while the difunctional component will form surface domains in the final amphiphilic coatings. The resins were cured using different amine crosslinkers— Ancamine 2143, Ancamine 2432, Ancamide 2634, and Ancamide 2767— in 1:1 and 1:2 epoxy: AHEW ratios. Most of the cured coatings showed excellent solvent resistance, hardness, flexibility, and impact resistance. In spite of the presence of PDMS and PEG chains within the resins, the coatings appeared uniform and glossy even after curing under ambient conditions. All the coatings showed high T_g, as observed using DSC and DMA. Melting peaks at ~50°C were observed for coatings with 2k g/mol MW PEG, indicating formation of crystalline phases in the films during crosslinking. Similar to the other GC coatings, some of the amphiphilic coatings also showed presence of secondary phases in the matrix. Onset of thermal degradation for all coatings was observed between 120-250°C, with degradation temperature decreasing with increasing MW of PDMS chains. Similar to the Jeffamine coatings, the AMP_GC coatings also showed a dynamic change

in WCA, indicating rearrangement of PEG chains on the coating surfaces. ATR-FTIR showed presence of PEG and PDMS chains on the surface of the coatings. XPS analysis showed higher concentration of the monofunctional component (PEG or PDMS) as compared to the difunctional chains; since most formulations contained monofunctional PEG, the AMP_GC surfaces exhibited higher concentration of PEG than PDMS. FR test against biofilm showed that AMP_GC coatings with higher MW PDMS showed lowest biofilm attachment among all the coatings (the commercial standards and AMP_GC coatings). But, the AMP_GC formulations could not facilitate removal of the biofilm. AMP_GC coatings with higher MW PDMS showed lower attachment of diatoms as compared to the commercial standards and > 80% removal of diatoms. Most of the AMP_GC coatings allowed microalgae to attach strongly onto the surfaces and could facilitate more than 5-50% removal of the microalgae only. Interestingly, formulations with PDMS = 1k, 5k and PEG-2k showed lowest algal attachment among all the coatings (the commercial standards and AMP_GC coatings) and highest removal among all the coatings. Hard foulants, mussels and barnacles, attached strongly on the AMP_GC coatings as compared to the commercial standards. Coatings with 10k PDMS and 10% 1k MW PDMS showed lowest mussel attachment strength among the AMP_GC formulations. All the AMP_GC coatings caused breaking of barnacle bases, indicating strong attachment of barnacles to the coatings. Although force of barnacle removal was higher than the commercial standards, breaking of only one barnacle base and higher release of microalgae from formulations with PEG-2k as compared to other AMP_GC formulations provided insights into potentially incorporating crystalline phases in coating networks to reduce biofouling.

In spite of the subpar FR performance of the IGC_PDMS coatings as compared to the commercial standards, the coatings showed potential for use in marine applications with proper tuning of formulation variables like, MW of PDMS and PEG chains, solvent selection, and amine crosslinkers. Versatility of GC systems allows convenient combination of GC with polymer additives. As the additives diffuse to the surface over time, the change in surface chemistry of the coatings will affect the FR performance of the coatings. Different additives with different components (PDMS, PEG, zwitterionic chains), MW, and architectures can be easily synthesized using controlled radical polymerization techniques like Reversible Addition-Fragmentation Chain Transfer (RAFT) and ATRP. FR performance of the coatings can be easily altered by varying concentration of such additives in the coating formulations.